The Temporal Region of the Tetrapod Skull – Research History, Evolution, and Functional Backgrounds

Dissertation
der Mathematisch-Naturwissenschaftlichen Fakultät
der Eberhard Karls Universität Tübingen
zur Erlangung des Grades eines
Doktors der Naturwissenschaften
(Dr. rer. nat.)

vorgelegt von
Pascal Abel, M. Sc.
aus Gunzenhausen

Tübingen
2023

Gedruckt mit Genehmigung der Mathematisch-Naturwissenschaftlichen Fakultät der Eberhard Karls Universität Tübingen.

Tag der mündlichen Qualifikation: 26.10.2023
Dekan: Prof. Dr. Thilo Stehle
1. Berichterstatter/-in: PD Dr. Ingmar Werneburg
2. Berichterstatter/-in: Prof. Dr. Madelaine Böhme

"Es ist die Arbeit unserer und der folgenden Generationen, die durch die thierischen Bildungen gehenden Gesetze immer deutlicher und vollständiger zu entziffern. Der Codex der Natur liegt der Betrachtung jedes sinnenden Menschen aufgeschlagen."

– Eduard Hallmann (1837), *Die Vergleichende Osteologie des Schläfenbeins*.

Acknowledgements

This work would not have been possible without the support from many people. I wish to thank my supervisor PD Dr. Ingmar Werneburg for granting me the ability to perform my doctoral research in his lab as well as for the mentoring and guidance throughout the last three years. Prof. Dr. Madelaine Böhme is thanked for providing space and for the fruitful discussions.

I also want to thank my collaborators Dr. Victoria Fernandez Blanco, Dr. Neil Brocklehurst, Dr. David Ford, Dr. Michela Johnson, Prof. Dr. Daisuke Koyabu, Dr. Stephan Lautenschlager, Yannick Pommery, Sven Sachs, Dr. Mark Young, and Franziska Zepf for their irreplaceable input on the studies described herein and those yet to come. In addition to that, I want to thank Tatjana Goller and Benedikt Kaestle for assisting in data collecting. Dr. Rainer Brocke, Gunnar Riedel, Dr. Richard Cifelli, Dr. Nicholas Czaplewski, Dr. Erin Maxwell, and Prof. Dr. Oliver Rauhut kindly provided access to the paleontological collections in Frankfurt am Main, Norman, Stuttgart, and Munich, respectively. Dr. Eduardo Ascarrunz, Dr. Josep Fortuny, Prof. Dr. Michel Laurin, Dr. David Marjanović, Dr. Diego Rasskin-Gutman, and three anonymous reviewers reviewed the publications compiled in this thesis and I want to thank them for their invaluable input. Patrick Hänsel helped in translating Ancient Greek terminology. Dr. Matthew Colbert and Dr. Jessica Maisano created and prepared the microCT scan analyzed and discussed in Chapters 3 and 4. Markus Bühler drew the life reconstruction for Chapter 4. I also want to thank Dr. Evelyn Kustatscher, Prof. Dr. Wolfgang Maier, Prof. Dr. Rainer Schoch, Dr. Frederik Spindler, and Prof. Dr. Hans Sues for the scientific discussions.

I am grateful for all my current and former colleagues within and outside our lab, namely Felix Augustin, Dr. Mario Bronzati, Gustavo Darlim, Christian Dietzel, Josefina Hartung, August Ilg, Panagiotis Kampouridis, Dr. Uwe Kirscher, Christina Kyriakouli, Thomas Lechner, Tobias Massonne, Dr. Andreas Matzke, Dr. Márton Rabi, Henrik Stöhr, Adrian Tröscher, Jules Walter, and Dr. Sibylle Wolf, with special thanks to Agnes Fatz and Dr. Gabriel Ferreira for their additional technical support, Mareike Keysan for guiding me through the bureaucracy, as well as PD Dr. Haytham El Afty, Dr. Anna Ayvazyan, Dr. Chris Bauman, Dr. Gerardo Antonio Cordero, Dr. Omar Rafael Regalado Fernandez, Jordy Figueroa, Dr. Anna Krahl, Ella Reiter, Dr. William Snyder, Dr. Oleksandr Yaryhin, and Zitong Zhang for the support and beautiful times beyond office hours.

Finally, I am especially grateful for my wonderful family and friends for accompanying me on this journey, with special thanks to Marius for the consistent advice and Kim, for everything.

This thesis was funded by DFG grant WE 5440/6-1

Contents

Zusammenfassung

Die Schläfenregion der frühesten Tetrapoda und ihrer nächsten Verwandten war in den meisten Fällen komplett von einem Panzer aus Dermalknochen bedeckt. Dieser wurde im Lauf der Evolution tendenziell reduziert, was in den bekanntesten Fällen zur Ausbildung von Schläfenfenstern oder randständiger Einbuchtungen führte. Derartige Schläfenöffnungen sind heute die Regel in den meisten Tetrapoda. Dabei inspirierte besonders ihre Vielfalt innerhalb der Amniota (Säugetiere und Reptilien einschließlich der Vögel) viele frühe Arbeiten über mögliche phylogenetische und evolutionsbiologische Implikationen der Schläfenmorphologie. Im frühen 20. Jahrhundert brachte dies verschiedene Autoren zur Aufstellung neuer Taxa, die wesentlich über ihre Schläfenmorphologie definiert waren, am bekanntesten darunter Anapsida, Synapsida, Diapsida und Euryapsida. Die meisten dieser Taxa werden jedoch nicht mehr als natürliche Gruppen anerkannt und neue Erkenntnisse bekräftigten, dass sich ähnliche Typen von Öffnungen sowohl innerhalb als auch außerhalb der Amniota mehrmals unabhängig entwickelten. Das Hauptaugenmerk in der Untersuchung von Schläfenöffnungen liegt deshalb auf deren funktionsmorphologischer Relevanz. Eine wesentliche Rolle spielen dabei die Kräfte ausgehend von den äußeren Kieferadduktoren, aber unter anderem auch die Halsmechanik, Schädelform und entwicklungsbiologische Aspekte werden diskutiert.

Diese Dissertation liefert einen Einblick in die Anatomie und morphologischen Muster der Schläfenregion innerhalb der Tetrapoda und ihren nächsten Verwandten (Stegocephali). Zuerst wird die Forschungsgeschichte der Schläfenregion seit dem 19. Jahrhundert aufgearbeitet und analysiert und die verschiedenen phylogenetischen und funktionsmorphologischen Hypothesen, sowie darauf basierende Terminologie einander gegenübergestellt. Dazu werden zehn neue Morphotypen zur Kategorisierung der Schläfenmorphologie eingeführt. Im Anschluss werden die Suturen der Dermalknochen im Schädel des permischen Reptils *Captorhinus aguti* im Detail beschrieben und die Kieferadduktoren rekonstruiert, um Rückschlüsse auf die Beweglichkeit und Kräfteverteilung im Schädel eines frühen Amnioten ohne Schläfenöffnungen zu ziehen. Anhand davon werden Erklärungen zur Entstehung von Schläfenöffnungen diskutiert und inwiefern Vorstufen dazu bereits in einem vollständigen Schläfenpanzer sichtbar sein könnten. Zuletzt wird eine Anatomische Netzwerkanalyse an *C. aguti* durchgeführt, um die Integration der Knochen im Schädel eines frühen Amnioten darzustellen und zu diskutieren, inwiefern die gefundenen Module mit Hypothesen zum Ursprung in Einklang gebracht werden können. Die für diese Analyse erstellte Matrix wird außerdem modifiziert, um die zuvor beschriebenen zehn Morphotypen zu simulieren und auszuwerten welche Einflüsse verschiedene Schläfenöffnungen auf die Integration des Modellschädels hätten und wie das mit Beobachtungen an tatsächlichen Arten übereinstimmt.

Summary

The temporal region of the earliest Tetrapoda and their closest relatives was, in most cases, completely covered by an armor of dermal bones. This armor has been successively reduced over time, leading most famously to the evolution of temporal fenestrae and marginal excavations. Such temporal openings are widespread in extant Tetrapoda, but especially their great diversity within Amniota (mammals and reptiles, including birds) inspired many early studies on the potential phylogenetic and evolutionary implications of temporal openings. In the early 20th century, this led to various researchers naming new taxa that were mainly defined by their temporal morphology, with Anapsida, Synapsida, Diapsida, and Euryapsida being the most known. Most of these taxa are not considered to represent natural groupings anymore; instead, new fossil findings and analyses confirmed that similar types of temporal openings independently evolved several times within, as well as outside of Amniota. Thus, the main focus of temporal region research has been on their functional morphology. The forces generated by the external jaw adductors hereby play an essential role, but additionally the impact of neck mechanics, skull shape, developmental biology, and others are being discussed.

This thesis provides an insight to the anatomy and morphological patterns of the temporal region in Tetrapoda and their closest relatives (Stegocephali). The first part focuses on reviewing and analyzing the research history of the temporal region, starting in the early 19th century discussing the various phylogenetic and functional hypotheses, as well as comparisons of previous terminologies. Additionally, ten new morphotypes for the categorization of temporal morphology are introduced. In the subsequent chapter, sutures of the dermal bones in the skull of the Permian reptile *Captorhinus aguti* are described in detail and its jaw adductors are reconstructed. This is important to draw inferences on the intracranial mobility and stress distribution in an early amniote skull without temporal openings. Relating thereto, previous explanations on the formation of temporal openings alongside the presence of potential pre-stages for such in a fully roofed dermal temporal region are debated. Lastly, an Anatomical Network Analysis is performed on the skull of *C. aguti* to illustrate and consider the bone integration in an early amniote skull and whether the observed modules correspond to previous hypotheses on the origin of temporal openings. The matrix generated for this analysis is then modified to simulate the ten morphotypes mentioned above, but also to evaluate the influences of various temporal openings on the integration of the respective model skull and its correspondence to observations on actual taxa.

Deep into the past
Follow the aeon path
Greet a blade of grass
Every endless form most beautiful
Alive, aware, in awe
Before the grandeur of it all
Our floating pale blue ark
Of endless forms most beautiful

Tuomas Holopainen, *Endless Forms Most Beautiful*

Chapter 1

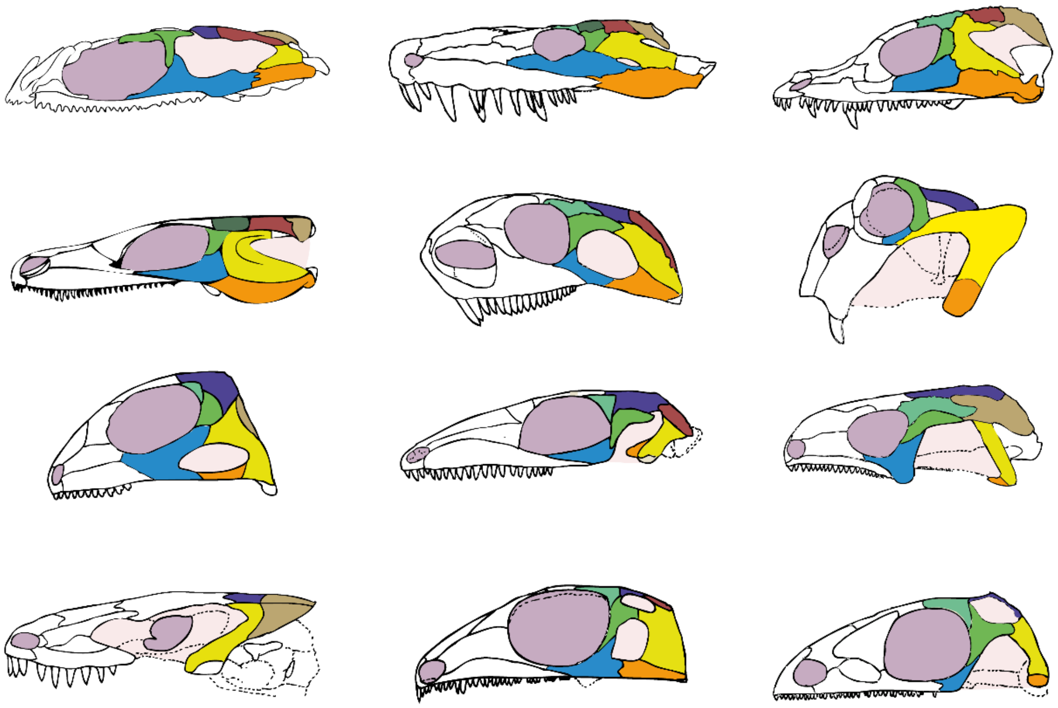

Introduction

A modified version of this chapter has been published as:

Abel, P., and Werneburg, I. (2024). The temporal region of the tetrapod skull: a textbook example on integrative morphology. *Revue de Paléobiologie* 43(1).

Author contributions:

Author	**Concept [%]**	**Writing [%]**	**Illustrations [%]**	**Providing of funding [%]**
Abel, P.	60	90	90	0
Werneburg, I.	40	10	10	100

1. Introduction

1.1. Anatomical overview

The temporal region comprises the area of the vertebrate skull between the orbits and the occiput. It borders the cranial jaw joint and auditory apparatus and serves as the cranial attachment site for most jaw muscles, the anterior portion of the neck musculature, and ultimately covers the braincase. Accordingly, the morphology of the temporal region is greatly related to the lifestyle of a species and varies based on different functional adaptations.

In most vertebrates, the temporal region is externally covered by dermal bones. This dermal armor may be generally subdivided into a lateral "cheek" and a dorsal skull roof. In tetrapods and early limbed vertebrates (i.e., Stegocephali *sensu* Laurin 2020a; Fig. 1) the "cheek" ancestrally consisted of the jugal, postorbital, squamosal, and quadratojugal. Often, the maxilla extended posteriorly to form the ventral "cheek" margin as well (e.g., Clack 1997; Holmes et al. 1998; Sigurdsen & Bolt 2010; Porro et al. 2015), which can be observed similarly in anurans (e.g., Wild 1997; Paluh et al. 2020). The ancestral skull roof incorporated the parietal, postfrontal, supratemporal, postparietal, tabular, and – in some groups – the intertemporal. Many of these temporal bones were lost in various later groups or fused with other parts of the temporal dermatocranium. Such later fusions include the frontoparietal in anurans (e.g., Čihák et al. 2003; Roček et al. 2015), the postorbitofrontal (e.g., in squamates and thalattosaurs: Lee & Caldwell 1998; Nicholls 1999; Jimenez-Huidobro & Caldwell 2016), or the mammalian interparietal, which might be the result of a postparietal and tabular fusion (Koyabu et al. 2012).

To the author's knowledge, the parietal is present in all known stegocephalians. In most cases, the same applies to the squamosal; however, in some mammals, this bone is fused with various enchondral bones to form the temporal bone (e.g., Boot 1910; Khatra 1980; Arnaudo et al. 2014). The jugal is absent in lissamphibians (Carroll 2007) and some "microsaurs" (Pardo et al. 2016; Mann et al. 2019), but otherwise present in the majority of all taxa. The quadratojugal independently disappears in various groups like mammals, squamates, urodelans, and caecilians (Carroll 2007; Evans 2008; Luo 2011). Likewise, the postorbital disappears, among other taxa, towards the origins of mammals, birds, lissamphibians, as well as in various squamates (Jollie 1957; Kemp 1984; Carroll 2007; Evans 2008). The postfrontal is absent in the majority of extant tetrapods but is still present in tuatara and some squamates (Evans 2008; Jones et al. 2011). The intertemporal is known only from Paleozoic taxa (e.g., Panchen 1964; Klembara et al. 2006, 2014; Rawson et al. 2021) and is absent in amniotes and lissamphibians. The supratemporal can be commonly observed in early amniotes but is restricted to squamates among extant taxa (e.g., Romer & Price 1940;

Fox & Bowman 1966; Maisch & Hungerbühler 2001; Evans 2008). A separate tabular becomes rare in post-Paleozoic taxa (e.g., Kuhn-Schnyder 1967; Sues 1986) and is unknown for extant tetrapods. Likewise, the paired postparietal is restricted to only a few post-Paleozoic groups (e.g., Witzmann & Schoch 2018). In some extinct therapsids an unpaired preparietal was formed (Maisch & Gebauer 2005; Sullivan & Reisz 2005; Gebauer 2007).

In addition to the presence or absence of specific bones, the osteology of the temporal region can vary in the arrangement of the dermal armor and the sets of bones directly suturing each other. Enlargements and/or reduction of individual bones can shift the arrangement within the dermatocranium and may generally lead to a simplification of the dermal armor (Williston 1914). An example for this is the reduction of the quadratojugal in synapsids (Kemp 1984). Additionally, bone contacts can be disjoined by forming an opening within their sutural area. The evolutionary origins, functional backgrounds, and probable phylogenetic implications of such temporal openings have been widely discussed in vertebrate paleontology and neontology (see Chapter 2 – Abel & Werneburg 2021) and will be reassessed in the following chapters.

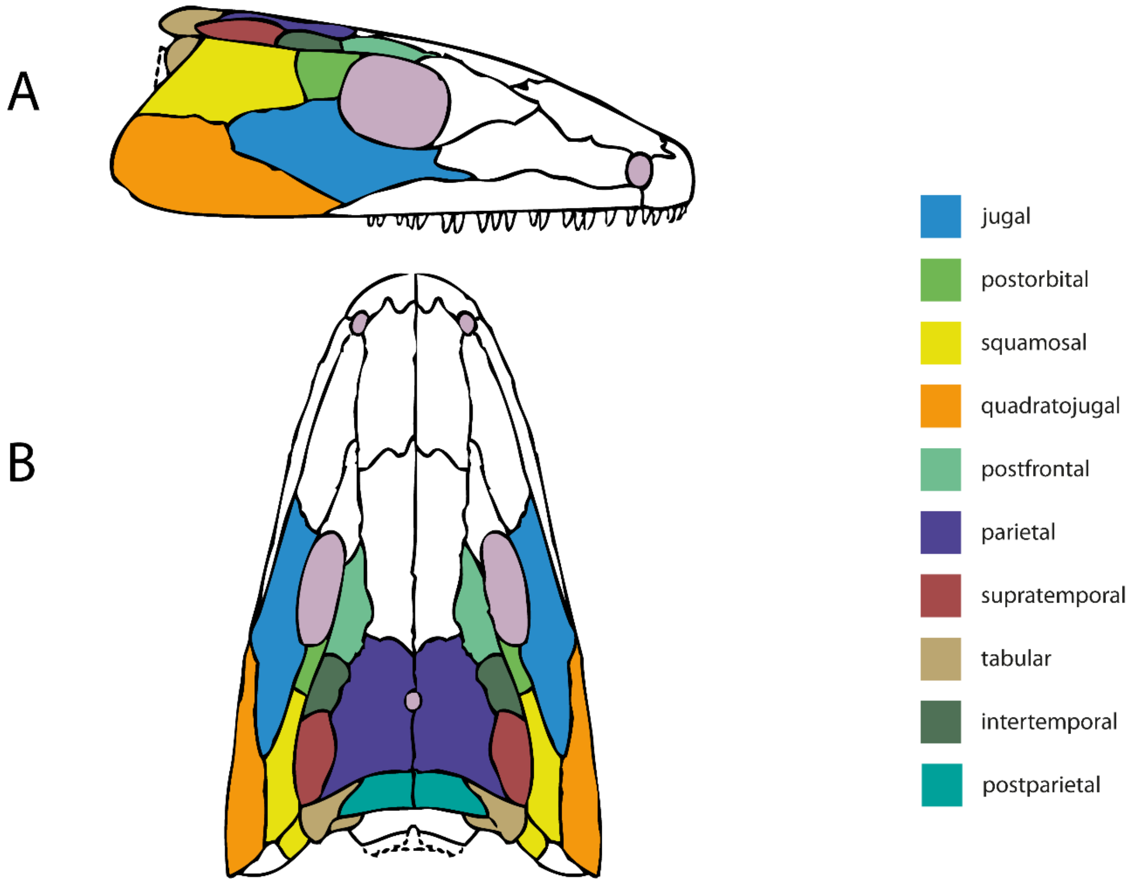

Fig. 1 Skull drawing of the Carboniferous stegocephalian *Eoherpeton watsoni* in (A) lateral and (B) dorsal view, highlighting the dermal bones of the temporal region. After Smithson (1985).

1.2. Temporal openings

Temporal openings can be subdivided into two main types (Tab. 1). If a temporal opening is fully surrounded by dermal bones, it is called a temporal fenestra (Fig. 2A, C). Such temporal fenestrae may be further subdivided based on their relative position in the temporal region. If a fenestra forms in the cheek region, it is called an infratemporal fenestra. If it instead forms in the skull roof, it is referred to as a supratemporal fenestra. Sometimes, an additional unpaired or even complete second pair of infratemporal fenestrae can develop (Romer & Price 1940; Berman et al. 1995; Weinbaum 2011; Haridy et al. 2016). The distinction between the subtypes of temporal fenestrae is not always straightforward, especially in various therapsids in which the ancestral infratemporal fenestra mediolaterally expanded and often resembled the supratemporal fenestra as described for many diapsids and some lissamphibians (see Chapter 2). It should be noted that this terminology is independent of which set of bones contribute to the margin of a temporal opening.

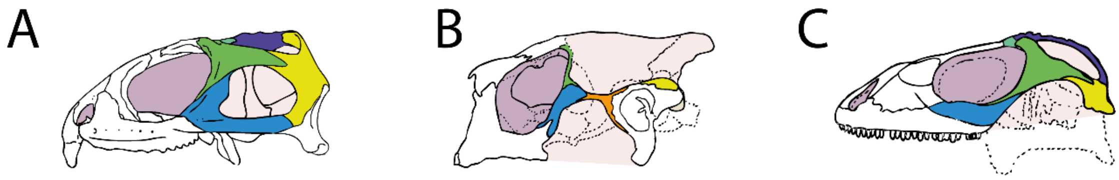

Fig. 2 Different types of temporal openings as exemplified by (A), tuatara (*Sphenodon punctatus*), exhibiting temporal fenestrae; (B) Greek tortoise (*Testudo graeca*), exhibiting marginal excavations; as well as (C), green iguana (*Iguana iguana*), exhibiting both fenestrae and excavations. Drawings from left to right after Jones et al. (2009), Gaffney (1979), and Conrad & Norell (2010). Colors as used in Fig. 1.

The infratemporal fenestra is usually bordered by the squamosal and jugal; however, in anurans the jugal is missing. Other bones usually contributing are the postorbital, quadratojugal, and – rather rarely – the supratemporal (Ford 2018; Ford & Benson 2020). Especially in synapsids, the parietal can additionally contribute to the margin of the infratemporal fenestra (e.g., Boonstra 1952; Modesto 1995). The supratemporal fenestra is always bordered by the parietal and usually by the squamosal. If present, the postorbital often contributes to the supratemporal fenestra as well. Sometimes, the supratemporal, postfrontal, or frontal are incorporated to the border of this opening, too (Carroll 1981; Nicholls 1999; Maisch & Hungerbühler 2001).

The second major type of temporal openings are temporal excavations (Fig. 2B, C). These differ from fenestrae by their incomplete bony margin, resulting in a distinct marginal embayment in the temporal dermatocranium. Most temporal excavations form at the ventral margin of the cheek, usually between the jugal and the quadratojugal and/or quadrate (Rieppel & Gronowski 1991; Evans 2008). Such a ventrolateral excavation can extend dorsally to the skull roof and incorporate other bones of the temporal dermatocranium. A posterodorsal excavation forms mostly in turtles (Werneburg 2012) but can be present in caecilians as well (Kleinteich et al. 2012).

In many species, different combinations of these types or subtypes of temporal openings occur simultaneously (see Chapter 2 for a detailed overview). These include a cooccurrence of infratemporal and supratemporal fenestrae (Fig. 2A); a ventrolateral excavation together with the supratemporal fenestra (Fig. 2C); a ventrolateral excavation together with the infratemporal fenestra (e.g., Modesto 1995; Norman et al. 2011); and lastly a cooccurrence of ventrolateral and posterodorsal excavation, so far only known from testudines (Fig. 2B).

This high variance of morphotypes within the temporal region inspired several workers to introduce a large array of descriptive terminology (see Chapter 2) and greatly influenced early hypotheses on tetrapod phylogeny, notably within amniotes.

1.3. Temporal openings and their role in phylogeny

By the late 19th century, it had been repeatedly suggested that these different temporal morphotypes may reflect phylogenetic patterns and that amniotes may be broadly classified based on their type and number of temporal openings (Günther 1867; Baur 1889, 1894; Cope 1892; Case 1898; Osborn 1903; Williston 1917; Broom 1922; Colbert 1945; Boettger 1952; see Chapter 2 for a detailed review). While opinions on content of and interrelationships between these phylogenetic groupings varied, it was generally agreed on that all amniotes with temporal openings derived from an ancestor with a fully covered temporal dermatocranium as it can be found in the majority of early stegocephalians (Baur 1889, 1894; Cope 1892; Gaupp 1895b; Gegenbaur 1898; Williston 1917; Versluys 1919).

Most influential in this regard has been the work of Osborn (1903), who subdivided "reptiles", in line with contemporary knowledge, into Synapsida and Diapsida, primarily based on the amount of bony "temporal arches" in the skull. Synapsida would therefore contain all "reptiles" that were thought to be close to mammals, which, back then, also included turtles and sauropterygians. Whereas Diapsida would consist of all "reptiles" closer to birds, including squamates, rhynchocephalians, and crocodylians. Later authors adapted Osborn's scheme by suggesting more subdivisions, most famously "Anapsida" (Williston 1917), "Parapsida" (Williston 1917), and "Euryapsida" (Colbert 1945). "Anapsida" has been usually thought of as containing turtles and an ancestral stock of "stem-reptiles" without temporal openings like diadectomorphs or captorhinids (e.g., Williston 1917, 1925; Colbert 1945; Boettger 1952; Gauthier et al. 1988). "Euryapsida" contained "protorosaurs", as well as plesiosaurs and other sauropterygians that developed a large supratemporal fenestra (Colbert 1945). "Parapsida" summarized other "aberrant" groups like mesosaurs, ichthyosaurs, but in earlier versions also squamates (Williston 1917, 1925; Colbert 1945).

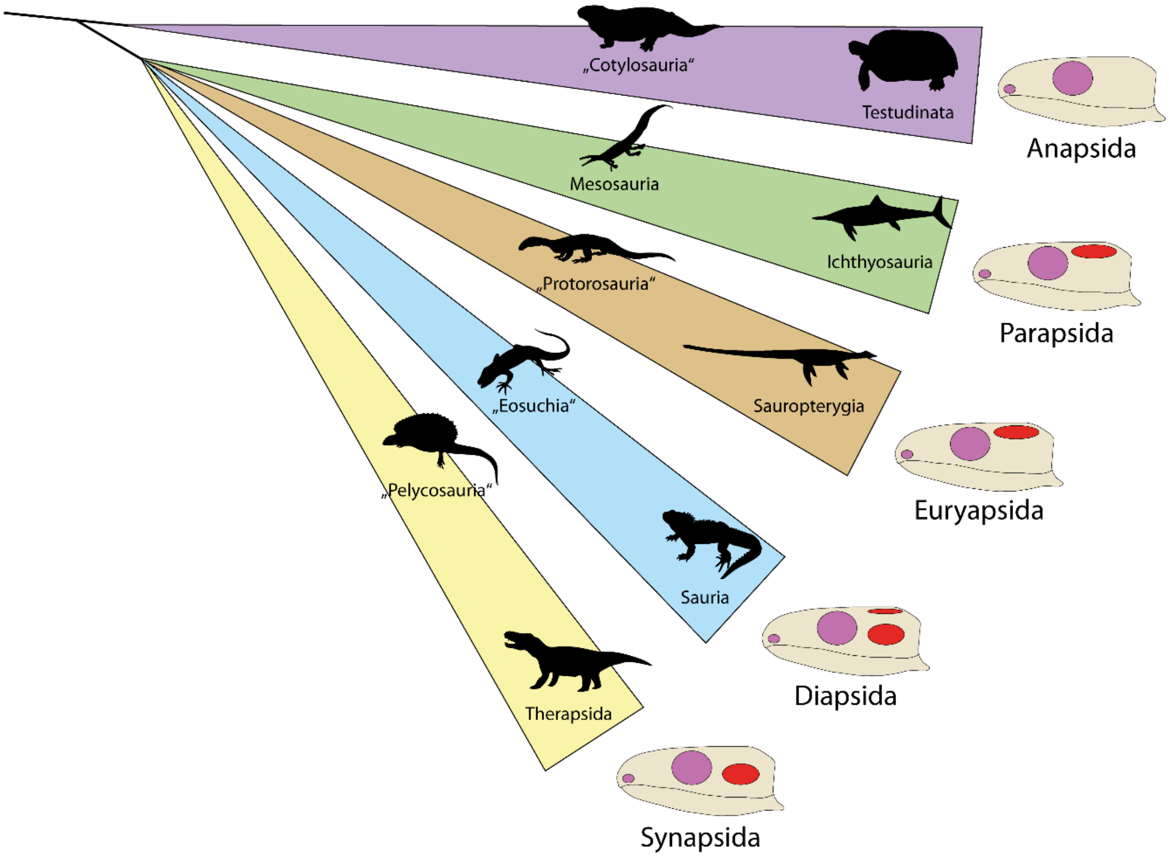

Fig. 3 Traditional subdivision of amniotes based on their temporal morphology after Colbert (1945). Skull outlines based on Fox & Bowman (1966) with modifications by Abel & Werneburg (2021). Silhouettes of "Cotylosauria" by Dmitry Bogdanov/Roberto Díaz Sibaja (CC BY 3.0); Testudinata by Christoph Schomburg; Mesosauria by Nobu Tamura/A. Verriére (CC BY-NC-SA 3.0); Ichthyosauria by Gareth Monger (CC BY 3.0); "Protorosauria" by T. Michael Keesey; Sauropterygia by Frank Denota; "Eosuchia" by Brad McFeeters/T. Michael Keesey; Sauria by Steven Traver; "Pelycosauria" by Dmitry Bogdanov (CC BY 3.0); Therapsida by Nobu Tamura/T. Michael Keesey (CC BY-SA 3.0).

Nevertheless, classifying amniotes based on their temporal openings has been criticized quite early on (Fuchs 1909; Goodrich 1916) and the concept has been further reassessed in the second half of the 20th century with notable works by Kuhn-Schnyder (1954, 1963, 1967, 1980). Furthermore, new fossil finds, the widespread application of genetics as well as morphological phylogenetic analyses challenged our understanding of amniote interrelationships (e.g., Rieppel & deBraga 1996; deBraga & Rieppel 1997; Lyson et al. 2012; Crawford et al. 2012, 2015; Field et al. 2014; Schoch & Sues 2015; Mann et al. 2019, 2021; Ford & Benson 2020). While there is still a consensus on a rough subdivision of amniotes into a branch leading to mammals (Synapsida) and one leading to birds and other extant reptiles (Diapsida), it is now generally agreed on that similar types of temporal openings appeared several times independently within Amniota (Ford 2018; Ford & Benson 2020) but also within Stegocephali (Gaupp 1985*b*; Panchen 1967; Pardo et al. 2017) and that the traditional "Anapsida", "Parapsida", and "Euryapsida" only represent para- or polyphyletic groupings.

1.4. Evolutionary distributions of temporal openings within the tetrapod tree

Temporal openings evolved early in various amniote clades with the oldest known examples postdating the oldest unambiguous amniotes by just a few million years (Reisz 1972, 1977; Modesto & Reisz 1990; Reisz & Dilkes 2003; Reisz & Fröbisch 2014). This implies a rapid emergence and diversification of temporal openings in amniotes compared to other early stegocephalians. However, amniotes might not have been the first stegocephalian lineage to reduce their temporal dermal armor (Fig. 4).

The oldest known occurrence of temporal openings can be found in Mississippian aistopods (Fig. 5A), which formed a large infratemporal fenestra or ventrolateral excavation (Milner 1993; Pardo et al. 2017). A small infratemporal fenestra is also known from the early Pennsylvanian embolomere *Anthracosaurus russelli* Huxley, 1863 (Panchen 1977; Fig. 5B); however, this appears to be an exception among Anthracosauria (Panchen 1964, 1972; Holmes 1984; Smithson 1985). Large ventrolateral excavations evolved further in various recumbirostran “microsaurs” (Pardo et al. 2016, 2017; Gee et al. 2019; Fig. 5I, J). Often assumed to nest outside of Amniota or even within Amphibia *sensu* Laurin et al. (2020*b*) (Marjanović & Laurin 2019), several recent studies argue for a reptilian affinity of recumbirostrans (Pardo et al. 2017; Mann et al. 2019, 2021), adding another branch of taxa with temporal openings to the early amniote radiation (Fig. 4). Arguably, large otic notches like they occur in seymouriamorphs, or some temnospondyls (Fig. 5C, D) might also be described as temporal excavations (Klembara et al. 2006; Reisz et al. 2009).

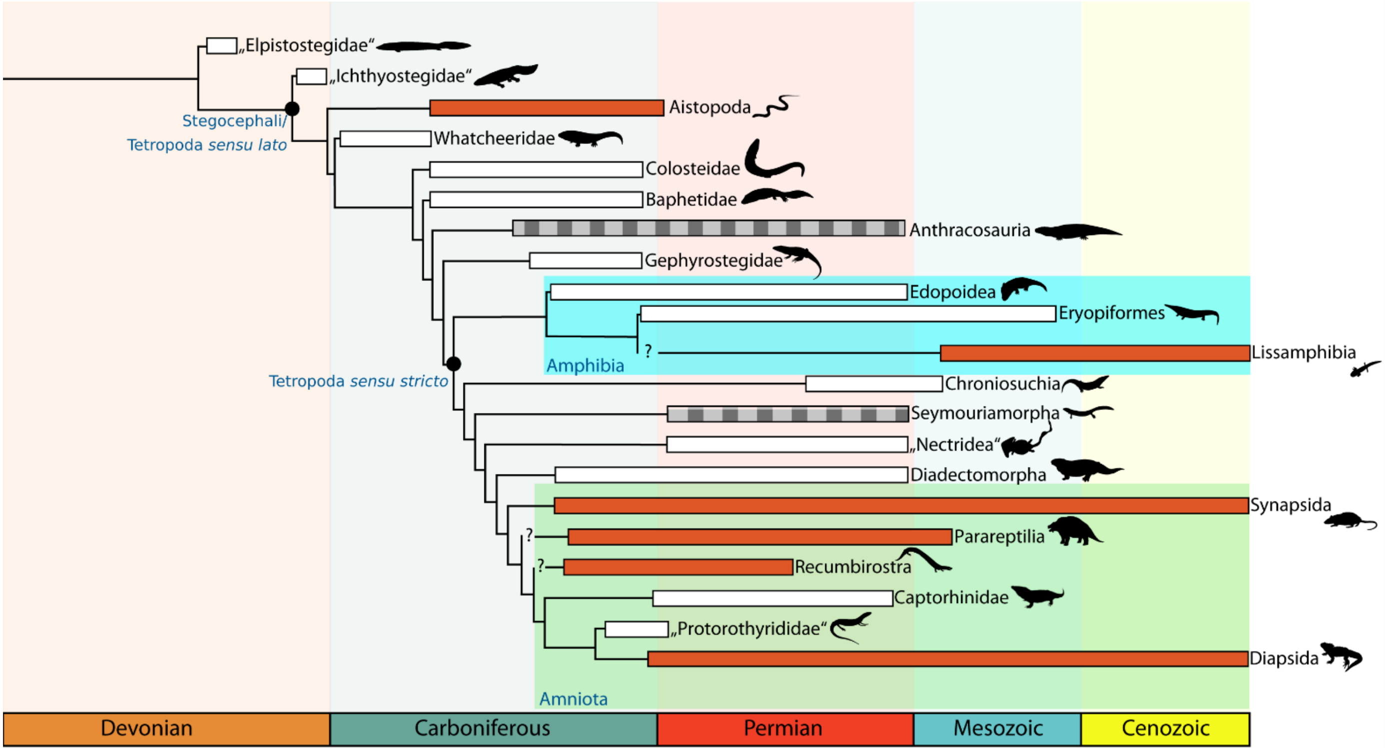

Fig. 4 Simplified phylogenetic tree of early limbed vertebrates based mostly on Pardo et al. (2017) and Marjanović & Laurin (2019), highlighting groups in which temporal openings are common (red), and in which temporal openings are rare or their presence debatable (shaded). Duration of Mesozoic and Cenozoic not to scale. Note that there are alternative hypotheses on the nesting of some groups like lissamphibians, diadectomorphs, parareptiles or various “lepospondyls” (i.e., aistopods, “nectrideans”, recumbirostrans) as outlined in Subchapter 2.3.1. Silhouettes of "Elpistostegidae" by T. Michael Keesey; "Ichthyostegidae" by Nobu Tamura/T. Michael Keesey (CC BY-SA 3.0); Aistopoda by Nobu Tamura (CC BY 2.5, edited); Whatcheeridae, Baphetidae, Chroniosuchia, and Captorhinidae by Dmitry Bogdanov (CC BY-SA 3.0, edited); Colosteidae by Dmitry Bogdanov (edited); Anthracosauria by Nobu Tamura/Andrew A. Farke (CC BY 3.0); Gephyrostegidae, and Edopoidea by Dmitry Bogdanov/T. Michael Keesey (CC BY-SA 3.0); Eryopiformes by Dmitry Bogdanov/T. Michael Keesey; Lissamphibia by Jake Warner; Seymouriamorpha and Diadectomorpha by Dmitry Bogdanov/T. Michael Keesey (CC BY 3.0); "Nectridea" by DataBase Center for Life Science (CC BY 4.0); Synapsida by Ferran Sayol; Parareptilia by Chris Jennings/A. Verrière; Recumbirostra and "Protorothyrididae" by Smokeybjb (CC BY-SA 3.0); Diapsida by Steven Traver.

Like in amniotes, temporal openings are widespread in lissamphibians. While the temporal dermatocranium of caecilians is often fully closed (Kleinteich et al. 2012), most batrachians possess a distinctly reduced dermatocranium (Carroll 2007). However, cases of secondary hyperossifications of the skull bones are known from various anurans (Paluh et al. 2020), where the latter can result in a fully closed temporal region. Nonetheless, in many taxa an infratemporal fenestra is present, and sometimes a supratemporal fenestra appears (Boas 1915; Wild 1997; AmphibiaTree & Gosselin-Ildari 2008; Paluh et al. 2020).

Apart from recumbirostrans, all of these stegocephalian groups evolved their temporal openings independently from amniotes. A detailed overview on the evolution of temporal openings within Stegocephali is provided in Chapter 2.3.1d.

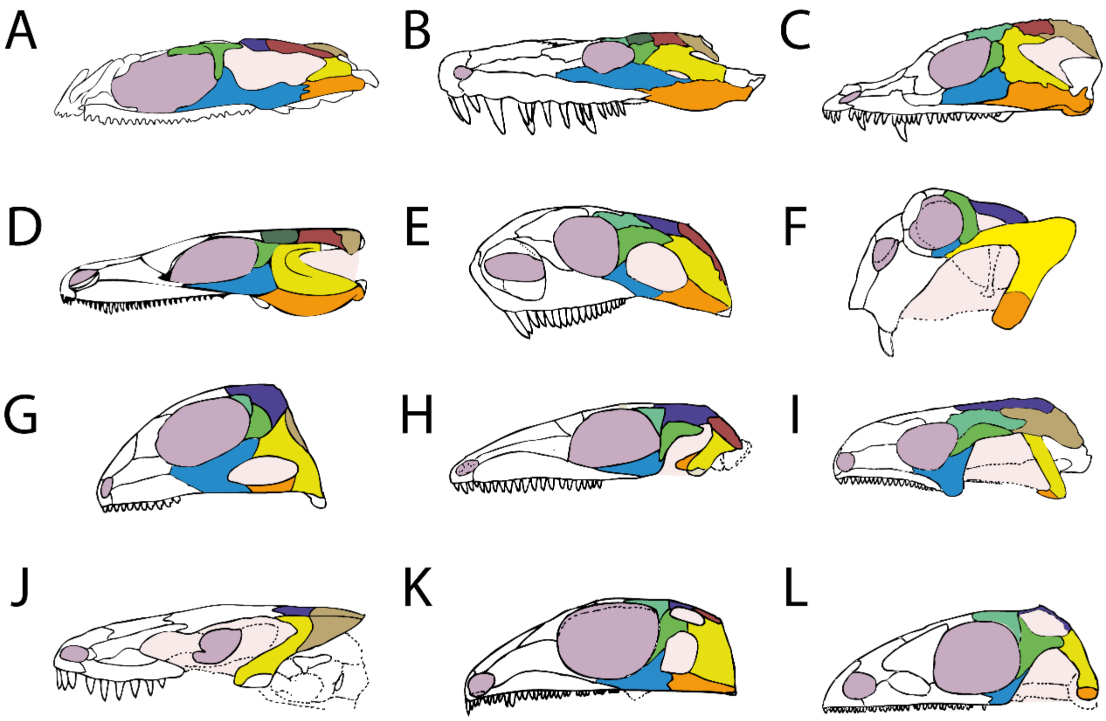

Fig. 5 Diversity of temporal openings and similar reductions of the dermatocranium among early stegocephalians. (A) *Lethiscus stocki* (Aistopoda; after Pardo et al. 2017); (B) *Anthracosaurus russelli* (Anthracosauria; after Panchen 1977); (C) *Cacops morrisi* (Temnospondyli; after Reisz et al. 2009); (D) *Seymouria sanjuanensis* (Seymouriamorpha; after Klembara et al. 2007); (E) *Cotylorhynchus romeri* (Synapsida; after Romer & Price 1940); (F) *Lystrosaurus murrayi* (Therapsida; after Ray 2005); (G) *Bolosaurus striatus* (Parareptilia; after Broom 1913); (H) *Milleropsis pricei* (Parareptilia; after Gow 1972); (I) *Llistrofus pricei* (Recumbirostra; after Bolt & Rieppel 2009); (J) *Brachydectes newberryi* (Recumbirostra; after Pardo et al. 2016); (K) *Petrolacosaurus kansensis* (Diapsida; after Reisz 1977); (L) *Claudiosaurus germaini* (Diapsida; after Carroll 1981).

1.5. Intraspecific variations

In addition to the disparity of the temporal dermatocranium found among Stegocephali, variation in the number and type of temporal openings can also appear intraspecifically (Mook 1921; Romer & Price 1940; Gow 1972; Berman et al. 1995; Cisneros 2008; Ezcurra & Butler 2015; Haridy et al. 2016).

Relative size and shape of temporal openings can shift during ontogeny (e.g., Westphal 1962; Blanco et al. 2018) or vary across populations (Escobedo-Galván et al. 2015).

Moreover, openings might disappear during life as observed in old individuals of the spectacled caiman (Mook 1921). A similar case has been suggested for the infratemporal fenestra in the parareptile *Milleretta rubidgei* Broom, 1938 (Gow 1972) and the supratemporal fenestra in *Eunotosaurus africanus* Seeley, 1892 (Bever et al. 2015; however, see Subchapter 2.3.1.e for a different interpretation on the latter). In more mature individuals of the parareptile *Delorhynchus ciffelii*, a posterior process of the jugal likely grew into the area of the infratemporal fenestra (Haridy et al. 2016).

There are further examples of likely more random variations. In some instances, a variation might be due to the occasional lack of suture closure in already thin areas of the temporal dermatocranium (see also Chapter 3 – Abel et al. 2022*a*). This includes the presence of an additional infratemporal fenestra at the jugal-squamosal-quadratojugal intersection in some specimens of the early synapsid *Ophiacodon retroversus* Cope, 1878 (Romer & Price 1940). In at least one specimen of *Varanosaurus acutirostris* Broili, 1904–05, another ophiacodontid, a similar second infratemporal fenestra formed between the jugal and squamosal, directly dorsal to the intersection with the quadratojugal (Berman et al. 1995; Ford 2018). This is reminiscent of the small fenestra observed in *Anthracosaurus russelli* (see previous subchapter; Fig. 5B). Similarly, an infratemporal fenestra can appear in the usually non-fenestrated "cheek" of the parareptile *Procolophon trigoniceps* Owen, 1876 (Cisneros 2008). In the archosauriform *Proterosuchus fergusi* Broom, 1903, the lower temporal bar apparently does not fully close in all individuals (Ezcurra & Butler 2015). These examples are likely not size- or ontogeny-dependent (Cisneros 2008; Ezcurra & Butler 2015). In fact, there can be further variation among such individuals as it is the case in the different sets of bones bordering the infratemporal fenestra in *P. trigoniceps* and by the second infratemporal fenestra of *O. retroversus*. The latter can be restricted to just one side of the skull, suggesting an interpretation as pathologies or, perhaps harmless, anomalies (Romer & Price 1940; Cisneros 2008).

1.6. Functional morphology

The high diversity of temporal morphotypes among tetrapods, as well as the repeated independent evolution of temporal openings, suggests mostly functional causes for the emergence of temporal openings with similar morphotypes evolving due to similar ecological or biomechanical adaptations. Many if not most explanations for the evolution of temporal openings are related to biting mechanics (e.g., Dollo 1884; Gregory & Adams 1915; Versluys 1919; Case 1924; Lakjer 1926; Olson 1961; Fox 1964; Frazzetta 1968; Carroll 1982; Whiteside 1986; Tarsitano et al. 2001; Kleinteich et al. 2012; Werneburg 2013*b*; Schoch

2014*b*). Other explanations include the influence of the neck (e.g., Zdansky 1923–1925; Kilias 1957; Kuhn-Schnyder 1980; Werneburg 2012, 2015; Ferreira et al. 2020), or an aquatic or fossorial lifestyle (Gaupp 1895*b*; Olson 1961; Sherratt et al. 2014; Bardua et al. 2019). Overall, the causes may be expected to be multidimensional, and the relative role of single factors will vary among taxa (see also Subchapter 2.3.3.).

1.6.1. Jaw adductors and stress network

Considering biting mechanics to be the main driver behind the evolution of temporal openings, a high emphasis must be set on the role of the external jaw adductor musculature (*musculus adductor mandibulae externus*, AME; Fig. 6), which – in most amniotes – is the main driver in jaw adduction (e.g., Fox 1964; Bramble 1978; Wittorski et al. 2016) and, hence, produces the main force during biting. The AME originates in the temporal region from where it inserts on the posterior mandible (Holliday & Witmer 2007; Diogo & Abdala 2010; Werneburg 2011, 2013*a*; Ziermann et al. 2018; Ferreira & Werneburg 2019).

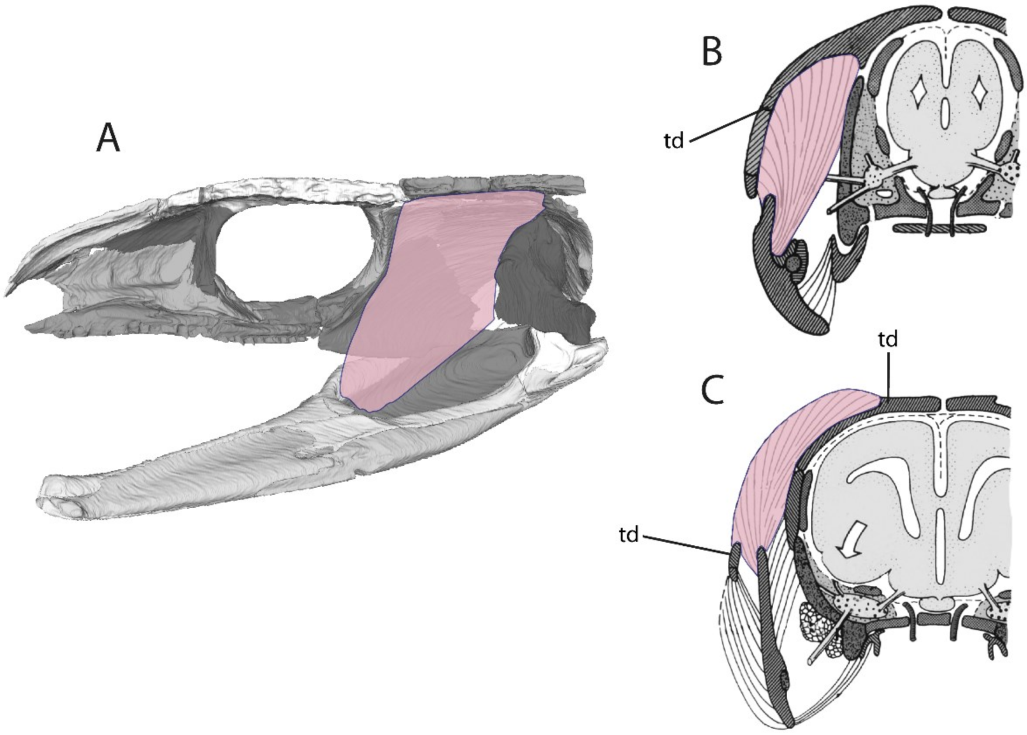

Fig. 6 Simplified depiction of the arrangement of the external jaw adductors (pink) in skulls with a fully covered temporal region (A, B) and with a distinctly reduced dermatocranium (C). (A) Skull of the early amniote *Captorhinus aguti* in internal view (after Abel et al. 2022*a*; see also Fig. 26). (B) Illustration of a skull lacking temporal openings in posterior view; (C) illustration of an extant mammalian skull in posterior view. (B) and (C) after Maier (2018). td = temporal dermatocranium.

In extant vertebrates with a fully covered temporal region, the origination sites of the AME usually lie internally to the dermal armor (Diogo 2008; Jones et al. 2012; Kleinteich et al. 2012; Fig. 6A, B). The same may be also expected for early stegocephalians and other extinct taxa that lacked openings (e.g., Adams 1919; Olson 1961; Fox 1964; Werneburg 2013*a*, 2019; see also Chapters 3, as well as 4 – Werneburg & Abel 2022). This arrangement might restrict movement or further enlargement of the AME for expansion beyond the dermatocranium, which could have been solved by reducing the dermatocranial coverage and, therefore, could have been a driver for the evolution of temporal openings (Dollo 1884; Gregory & Adams 1915; Versluys 1919; Lakjer 1926; Kleinteich et al. 2012). Nevertheless, while larger temporal openings can certainly be correlated with an equally large AME (e.g., Lautenschlager et al. 2017; Johnson et al. 2020), size of the AME can also distinctly increase without the formation of temporal openings as evident by the enlarged adductor chambers in groups that retained or re-evolved a non-fenestrated skull (Sues & Reisz 1998).

The emergence of temporal openings could also have been related to a generally more domed skull in early amniotes relative to most other early stegocephalians (Olson 1961; Frazzetta 1968; Tarsitano et al. 2001). In taxa with a comparatively flat skull, the main force during biting usually is produced by the internal jaw adductors (Olson 1961; Frazzetta 1968; Erickson et al. 2013 and references therein). A flat skull outline is widespread among the majority of early stegocephalians and might as well be related to their predominantly aquatic lifestyle. Once amniotes and their relatives became more terrestrial, a relative increase in their temporal height can be observed (Olson 1961; Frazzetta 1968). This likely enlarged their AME and steepened the angle by which it would have inserted on the mandible, increasing the amount of perpendicular forces acting on the temporal dermatocranium (Frazzetta 1968; Tarsitano et al. 2001). These changes probably correspond to adaptations of feeding outside of the aquatic realm and the change from a "kinetic-inertial" to a more complex "static-pressure" jaw adduction system (Olson 1961).

It is these higher and, due to the derived jaw adduction, more complex forces acting on the temporal dermatocranium that might have triggered the evolution of temporal openings. While it can be assumed that the AME internally attached to a large area of the temporal dermatocranium in taxa without temporal openings (Schumacher 1973; Jones et al. 2012), stress during biting was heterogeneously distributed leading to a "network of lines of stress" (Olson 1961). Bony areas that sustained higher stresses generally thickened or formed crests for stronger muscle attachments (Gegenbaur 1898; Case 1924; Fox 1964), developed external ornamentations (Fox 1964), or tightened bone sutures (Herring 1972; Rafferty & Herring 1999; see Chapter 3). These highly stressed areas might be the predecessors of temporal bars, whereas bony areas that were less affected by stress remained less ossified and were subsequently lost, forming temporal openings (Case 1924; Fox 1964; Fig. 7).

Evidence for this may be seen in the accessory infratemporal fenestra that can form in the thin jugal-squamosal-quadratojugal intersection of *Ophiacodon retroversus* (see Subchapter 1.5). In addition to that, "weak" areas that correspond to the position of temporal fenestrae in early fenestrated amniote can also be observed in the Permian reptile *Captorhinus aguti* Cope, 1882 (Fox 1964; see Chapter 3) or probably in even more rootward species (Jaekel 1902). However, whether there is a significant relationship between skull proportions and the evolution of temporal openings remains to be tested (see Chapter 5). Large temporal openings can indeed evolve in taxa with a flat skull outline (Ogushi 1911; Mook 1921; Schoch 2014*b*; Young et al. 2014; Hinz et al. 2019) and a domed skull with large adductor chambers does not necessarily lead to the formation of temporal openings (Clark & Carroll 1983; Gaffney 1990; Sues & Reisz 1998).

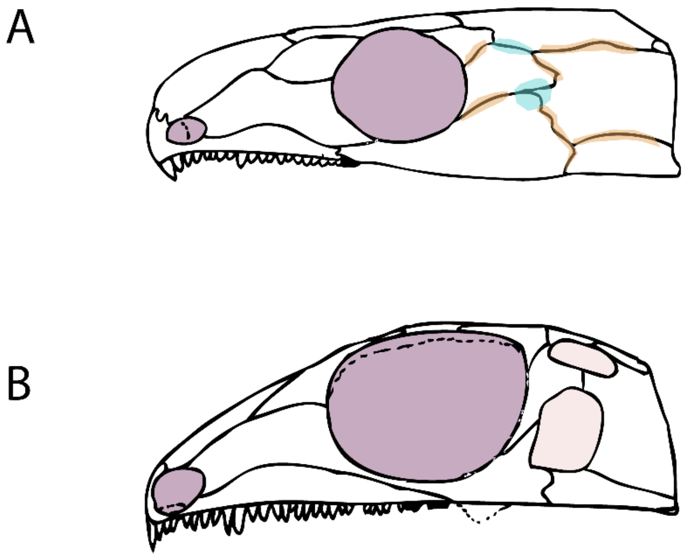

Fig. 7 (A) Skull of the early amniote *Captorhinus aguti* highlighting potentially weak (blue) and strengthened sutures (orange) in the temporal dermatocranium as described in Chapter 3. (B) Skull of the early diapsid *Petrolacosaurus kansensis* with the temporal fenestrae corresponding to the thin bony areas found in *C. aguti*. Drawings after Fox & Bowman (1966) and Reisz (1977).

1.6.2. Neck mechanics

While temporal openings have been commonly associated with adaptations of the jaw musculature, changes in neck mechanics might have equally affected the evolution of the temporal region. A differentiated neck is considered to be a key evolution in the terrestrialization of early stegocephalians (Laurin 2010; Heiss et al. 2018) and a highly mobile atlanto-occipital joint appeared the latest in amniotes, suggesting the need of a light and narrow skull in terrestrial forms, hence, a reduction of the dermal armor (Versluys 1919; Kuhn-Schnyder 1980).

Irrespective of this, neck mechanics likely play a major role in the temporal morphology of turtles (Hay 1908; Zdansky 1923–25; Kilias 1957; Werneburg 2012, 2015; Werneburg et al. 2015*c*; Ferreira et al. 2020). To date, it is mostly agreed on that turtles (i.e., Testudinata) evolved from diapsid ancestors with temporal openings (e.g., Rieppel & deBraga 1996; deBraga & Rieppel 1997; Bever et al. 2015; Schoch & Sues 2015, 2018; Li et al. 2018; Gemmell et al. 2020) but these openings closed in the earliest forms (Gaffney & Jenkins 2010; Werneburg 2013*a*; Schoch & Sues 2015, 2018; Werneburg et al. 2015*a*). In later turtles, ventrolateral and/or posterodorsal excavation formed in the temporal region but occasionally closed again (Gaffney 1979; Jones et al. 2012; Werneburg 2012; see Subchapter 1.2.)

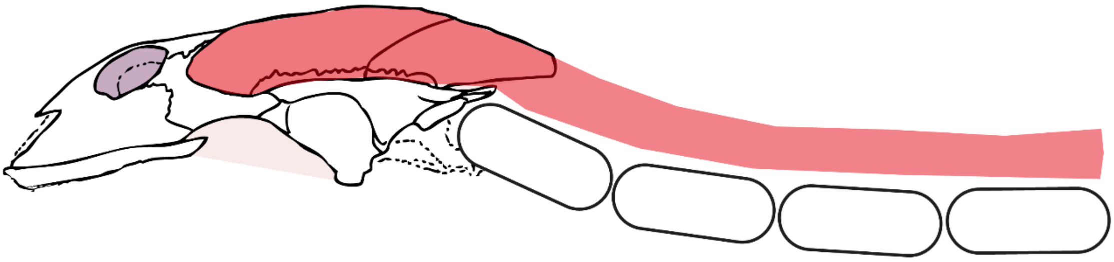

Fig. 8 Skull of the Chinese softshell turtle (*Pelodiscus sinensis*) with a schematic illustration of the neck and the cryptodiran trapezius muscle (red), attaching anteriorly to the posterodorsal excavation of the temporal region. Based on Ferreira & Werneburg (2019). Skull after Ogushi (1911).

Both, the ancestral closing of temporal openings in turtles, as well as the later formation of a posterodorsal and maybe also the anterolateral temporal excavation, can be associated with the evolution and further specialization of neck retraction. Earliest turtles were likely capable of a limited form of neck retraction (Werneburg et al. 2015*a*). It has been hypothesized that action of the neck musculature selected for a more robust temporal region, realized by the closure of openings and a decrease of intracranial mobility (Werneburg 2015; Ferreira & Werneburg 2019; Werneburg & Maier 2019; Werneburg et al. 2021). The subsequent formation of temporal excavations in later turtles may be related to the mode of retraction ["hidden-neck" (Cryptodira) or "side-neck" (Pleurodira)]. The widespread cryptodiran mode of retraction has been enabled by a strengthened dorsal neck musculature with the posterodorsal excavations being adaptations to stress distribution, as well as providing additional attachment sites for these muscles (Ferreira & Werneburg 2019; Fig. 8). Correspondingly, large excavations are missing in those cryptodiran turtles that lost their ability to retract their neck (Zdansky 1923–25; Kilias 1957), as well as in chelid pleurodirans (Werneburg 2012). In chelids, the ventrolateral excavation is distinctly enlarged instead, which might be related to their pleurodiran retraction mode; however, a large ventrolateral excavation can also appear in cryptodirans and may be additionally related to the arrangement of the jaw musculature and the fixation of the palatoquadrate in turtles (Werneburg 2012).

1.6.3. Other adaptations

Over decades, various other factors have been suggested to additionally affect the emergence or loss of temporal openings. Many of these play an indirect role on stress distribution within the temporal dermatocranium as they influence the arrangement and size of the jaw adductor musculature like relative positions of other skull parts (e.g., Dollo 1884; Lakjer 1926), or the type of jaw articulation and/or cranial kinesis (e.g., Romer 1956; Whiteside 1986). It has also been suggested that this might relate hearing and physiology [(Robinson 1973; Holliday et al. 2020; however, see also Evans (1980), Carr (2021), and Ramirez et al. (2022)], or defensive adaptations (Zdansky 1923–25; Kilias 1957; Paluh et al. 2020). In some instances, closure and increased robustness of the dermal armor may be related to the evolution of a fossorial lifestyle [Gower et al. 2004; Sherratt et al. 2014; Ebel et al. 2020; but see also Kleinteich et al. (2012)]. Furthermore, the non-fenestrated skulls in sea turtles and early sarcopterygians have been interpreted as adaptations to the high hydrostatic pressure acting on their skulls when submerged (Gaupp 1895*b*), but considering the often large temporal openings in various aquatic reptiles this does not seem to be a general pattern (e.g., Maisch & Hungerbühler 2001; Benson et al. 2013; Young et al. 2014) and may be dependent on different other factors.

1.7. Ontogeny

Ultimately, the evolution of various temporal morphotypes is bound to changes in developmental patterns (see Subchapter 2.3.2.e). Emergence of new types may be favored by the occasional occurrence of slight intraspecific/ontogenetic variations (see Subchapter 1.5.). In addition to this, major drivers are likely embryonal movements of the jaw and neck musculature that shape and arrange the still plastic dermatocranium (Schoch 2014*b*;

Werneburg 2019; Werneburg & Maier 2019). For example, the rapid emergence of temporal openings in early amniotes might have been enabled, because the lack of larval development extended, which the time for the dermatocranium to align before the musculature became active (Werneburg 2019). Yet, the presence of a larval stage does not exclude the evolution of temporal openings in lissamphibians (Schoch 2014*b*; Paluh et al. 2020) and the developmental backgrounds behind the formation of temporal openings in some extinct non-amniotes are hard to reconstruct (see Subchapter 2.3.2.e). Indeed, research on how various groups differ in their development of the temporal region is still in its early stages but the current theoretical framework and first embryological studies promise new insights within the upcoming years (Tarsitano et al. 2001; Tokita et al. 2013; Schoch 2014*b*; Werneburg 2019; Werneburg & Maier 2019; Werneburg et al. 2021).

1.8. Aim and overview of the following chapters

The aim of this thesis was to provide a broad perspective of the morphology of the temporal skull region in tetrapods and other stegocephalians. The emphasis was placed on the evolution and early emergence of temporal openings, especially within amniotes, and which intrinsic factors cause and affect their formation.

Chapter 2 provides an in-depth review on previous research on the topic with a special focus on how opinions and hypotheses on phylogenetic patterns and functional causes behind temporal openings changed over the last 150 years. Additionally, this chapter introduces a new comprehensive scheme to subdivide stegocephalian skulls into ten morphotypes based on their type and number of temporal openings.

In Chapter 3 a detailed description of the sutures in the dermatocranium of the early amniote *Captorhinus aguti* is given and a reconstruction of its jaw adductor musculature was modeled. This was done to discuss the intracranial mechanics in the hypothetic ancestral amniote and how they might have affected the evolution of temporal openings. It has been shown that *C. aguti* possessed potential weak areas in its temporal dermal armor that corresponds to the position of infratemporal and supratemporal fenestrae in other amniotes.

Chapter 4 presents an Anatomical Network Analysis of the skull of the same species as a model for skull bone integration in early "anapsids". It will be demonstrated that the skull of *C. aguti* can be subdivided in several functional modules with the “weak areas” described in Chapter 3 mainly lying on the contact zones of these modules. Additionally, the skull network of *C. aguti* has been modified to imitate the presence of the above described ten types of temporal openings. This leads to changes in the modular composition likely having implications for jaw adductor arrangement and intracranial mobility.

Lastly, Chapter 5 provides a conclusion and short outlook on projects that may arise from this thesis.

Chapter 2

Morphology of the temporal skull region in tetrapods: research history, functional explanations, and a new comprehensive classification scheme

A modified version of this chapter has been published as:

Abel, P., and Werneburg, I. (2021). Morphology of the temporal skull region in tetrapods: research history, functional explanations, and a new comprehensive classification scheme. *Biological Reviews* 96, 2229–2257.

Author contributions:

Author	**Concept [%]**	**Writing [%]**	**Illustrations [%]**	**Providing of funding [%]**
Abel, P.	50	80	90	0
Werneburg, I.	50	20	10	100

2. Morphology of the temporal skull region in tetrapods: research history, functional explanations, and a new comprehensive classification scheme

2.1. Introduction

The temporal region, the part of the dermatocranium between the orbits, and the occiput serves multiple purposes in the vertebrate skull: it incorporates the cranial origin sites of the jaw adductor musculature, the jaw hinge, and covers the ear and ultimately also the braincase. Accordingly, the temporal region exhibits a vast array of morphotypes, reflecting evolutionary differences in lifestyle and developmental patterns in the respective taxa. The high morphological diversity of the temporal region is most evident in the extant tetrapod main groups Lissamphibia and Amniota. While most Paleozoic non-tetrapods (*sensu* Laurin 2020*b*) had a fully closed temporal dermatocranium (e.g., Clack 1997, 2002; Blom 2005; Daeschler et al. 2006), most lissamphibians and amniotes show either a greatly reduced temporal dermatocranium or have developed a variety of temporal openings (e.g., Kleinteich et al. 2012; Werneburg 2019; Ford & Benson 2020; Paluh et al. 2020). Even in some radiations of extinct tetrapods, like "Lepospondyli", a variety of temporal morphotypes, such as large ventral excavations or overall reductions of the dermatocranium, can be observed (e.g., Bolt & Rieppel 2009; Pardo & Anderson 2016). The morphology of the temporal region in tetrapods has thus attracted much interest over the last 200 years, from paleontologists and neontologists alike (e.g., Hallmann 1837; Cope 1892; Baur 1894; Gaupp 1895*a*,*b*; Williston 1904; Fuchs 1909; Jaekel 1913; Boas 1915; Versluys 1919; Broom 1922; Fox 1964; Frazzetta 1968; Tarsitano et al. 2001; Werneburg 2019). Apart from purely morphological comparisons (Hallmann 1837), previous workers focused on the functional (e.g., Dollo 1884; Gaupp 1895*b*; Gregory & Adams 1915; Case 1924; Frazzetta 1968), developmental (e.g., Tarsitano et al. 2001; Schoch 2014*b*; Ford 2018; Werneburg 2019), and phylogenetic background (e.g., Baur 1894; Osborn 1903; Williston 1917; Broom 1922; Kuhn-Schnyder 1980; Müller 2003; MacDougall & Reisz 2014; Ford & Benson 2020) of the structural diversity in the temporal skull region. Much emphasis has been put on the phylogenetic value of temporal morphology, inspiring the naming of several higher taxa, such as "Synapsida", "Diapsida", "Anapsida", "Euryapsida", "Stegokrotaphia", and "Stegocephali" (e.g., Cope 1868; Osborn 1903; Fuchs 1909; Williston 1917; Broom 1922; Colbert 1945; Boettger 1952; Cannatella & Hillis 1993), some of them remain in use to the present day – although often with a different definition.

Yet it has been demonstrated that some morphological traits, such as an infratemporal fenestra or a fully closed temporal dermatocranium, appeared independently and repeatedly in distantly related taxa (Müller 2003; MacDougall & Reisz 2014; Ford & Benson 2020), probably not always in response to the same selective pressure (Carroll 1982; Werneburg 2012, 2015, 2019). Additionally, the temporal region can vary distinctly in morphology among closely related taxa (Gow 1972; Tsuji et al. 2012), specimens of the same species (Cisneros 2008; Ezcurra et al. 2015), or throughout ontogeny (Gow 1972; Haridy et al. 2016). This highlights the complex evolution of the temporal region in tetrapods and casts doubt on a classification of various tetrapod clades that emphasizes their temporal morphology, especially within Amniota (e.g., "Synapsida", "Diapsida", "Anapsida", "Parapsida", "Euryapsida"). It seems likely that similar temporal morphotypes evolved in different clades, either because of similar selective pressures or because different selective regimes favored the convergent evolution of similar morphotypes. Thus, to establish an understanding of the diversity of the tetrapod temporal region, a holistic approach involving phylogenetic, functional, developmental, and ecological considerations is needed.

Here, a completely new classification scheme for temporal morphology in both tetrapod groups (amphibians and reptiliomorphs) is provided, enabling the discussion on the diversity of the temporal skull region without adding confusion by expanding or modifying the vast number of previous perspectives. Afterwards, an overview on the research history of temporal morphology in Tetrapoda and their extinct relatives follows. This chapter illustrates the different approaches used by previous, sometimes rarely cited, researchers to investigate the high disparity of the tetrapod temporal region, and discusses which functional, developmental, and evolutionary factors they considered as fundamental to changes in temporal morphology.

2.2.1. Morphological and taxonomic definitions

2.2.1.a) *Morphology*

Morphological terms for the temporal region have been used differently by previous researchers. This applies especially to the question of whether excavations in the temporal region (e.g., ventrally in the “cheek” of most squamates or the posterodorsal and ventral excavations observed in most turtles) should be described as temporal fenestrae or not. For clarification on morphotypes as used in this thesis, definitions are provided in Tab. 1 that are mostly based on Werneburg (2013*b*, 2019).

2.2.1.a) *Taxonomy*

In the works discussed in this chapter, taxonomic names often were used in a non-cladistic sense or differed in their taxonomic content from their modern usage [e.g., “Synapsida”, which also incorporated “cotylosaurs”, placodonts, plesiosaurs, and turtles when Osborn (1903) first introduced the name]. Additionally, even in recent decades, the definitions of some commonly used taxa have been extensively discussed (e.g., Laurin & Anderson 2004; Modesto & Anderson 2004). Hence, to avoid confusion, definitions on some of these names are presented in Tab. 2. As it will be shown in this chapter, an apomorphy-based definition of clades using temporal morphology can be ambiguous, thus the application of such definitions is avoided here. This applies especially to Diapsida, which generally has been used as the amniote clade possessing both an infratemporal and a supratemporal fenestra; a presumed apomorphy inherited by the extant tuatara (Gauthier & de Queiroz 2020). However, whether this trait appeared only once or arose several times independently in early reptiles is hard to determine (Ford & Benson 2020; see Subchapter 2.3.1e). In fact, the morphotype of the tuatara may have evolved secondarily (e.g., Müller 2003; Evans 2008). Therefore, Diapsida is used herein with a node-based definition as has been applied in previous publications (e.g., Laurin, 1991; Laurin & Reisz, 1995).

Tab 1. Morphological terms used in this thesis.

Term	Definition
Temporal opening	Temporal openings are reductions of the temporal dermatocranium that are either formed within the suture of two or more bones (temporal fenestra) or by excavations in the dermal armor in a ventrolateral or posterodorsal direction.
Temporal fenestra	Temporal fenestrae are temporal openings that are completely surrounded by bone. They always form within the sutural contact of two or more temporal bones. An infratemporal fenestra forms in the "cheek" region of the skull and is ventrally always bordered by a lower temporal bar (i.e., zygomatic arch). A supratemporal fenestra forms in the skull roof and is medially always bordered by the parietal. In some cases, the temporal fenestra is confluent with the orbit (e.g., many Mammalia), or the orbit extends distinctly into the temporal region (e.g., Procolophonidae). Both conditions are referred to as an orbitotemporal opening, however, they have different developmental and evolutionary origins.
Temporal excavation	Temporal excavations are ventrolateral or posterodorsal excavations of the dermal armor, formed either by the reduction of a temporal bar (squamates, birds), loss of bones (lissamphibians), or by an embayment of the dermal armor (mammals, turtles). The otic notch is not a temporal excavation.
Temporal bar	Temporal bars are bony arches that border temporal fenestrae. The lower temporal bar (or zygomatic arch) is the bony arch that ventrally borders the infratemporal fenestra. The upper temporal bar borders the infratemporal fenestra dorsally, or the supratemporal fenestra laterally. The arch bordering the infratemporal fenestra anteriorly is the postorbital bar. The posterior equivalent is the posttemporal bar.
Temporal bridge	Temporal bridges are remnants of the temporal dermal armor in-between two temporal excavations. They are mostly found in turtles but are also present in other taxa such as Recumbirostra (early Tetrapoda).

2.2. An updated morphological classification scheme

The history of research on the tetrapod temporal region involved the introduction of several classification schemes for the different temporal morphotypes and sometimes the erection of new taxa based on these morphotypes. While systems following Osborn (1903; see Subchapter 2.3.1.c) and Gaupp (1895*b*; see Subchapter 2.3.1.b) are in common use in comparative anatomy, there are currently two challenges.

Tab. 2 Definitions of taxonomic names used in this thesis.

Taxon	Definition
Stegocephali	Used mostly *sensu* Laurin (2020*a*) as the clade containing Tetrapoda, but not *Panderichthys rhombolepis* and *Tiktaalik roseae*.
Tetrapoda	Used *sensu* Laurin (2020*b*) as the least inclusive clade containing Amniota and Lissamphibia.
Amphibia	Used *sensu* Laurin et al. (2020*a*) as the clade containing Lissamphibia and all taxa closer to Lissamphibia than to Amniota.
Lissamphibia	Used *sensu* Laurin et al. (2020*b*) as the least-inclusive clade containing Anura (frogs), Caudata (salamanders), and Gymnophiona (caecilians).
Reptilia	Used mostly *sensu* Modesto & Anderson (2004) as the clade containing Lepidosauria (squamates and tuatara), Archosauria (crocodiles and birds), Testudines (turtles), and all taxa closer to these than to Mammalia.
Diapsida	Used mostly *sensu* Laurin (1991) and Laurin & Reisz (1995) as the least-inclusive clade containing Lepidosauria, Archosauria, *Youngina capensis*, and *Araeoscelis gracilis*.
Synapsida	Used mostly *sensu* Laurin & Reisz (2020) as the clade containing Therapsida (mammals and their relatives) but not Reptilia after Modesto & Anderson (2004).

First, amniote and amphibian researchers apply two different classification schemes to describe the temporal morphology of their studied species. Amniote researchers usually prefer the scheme initiated by Osborn (1903) (which uses "synapsid", "anapsid", "diapsid", "euryapsid", and so forth), whereas in the amphibian literature the terms of Gaupp (1895*b*) ("stegokrotaphic", "zygokrotaphic", "gymnokrotaphic") prevail. It may be argued that this can be justified by the evolutionary distance and developmental/morphological differences between these groups. Yet, as demonstrated herein, developmental or functional reasons for temporal openings may even vary within amniotes and lissamphibians, and similar factors might invoke their convergent development.

Second, in the scheme used for amniotes, the commonly used terms are based on formally erected taxa. However, of these taxa only Synapsida and Diapsida are still considered to be monophyletic (e.g., Benton 1985; Gauthier & de Queiroz 2020; Laurin & Reisz 2020), although with ongoing controversies on their actual taxonomic composition (e.g., Berman 2013; Schoch & Sues 2015; Laurin & Piñeiro 2017, 2018; Ford & Benson 2020). In fact, even the current consensus differs markedly from the point of view when these taxa were first introduced (Osborn 1903; Williston 1917) and the original terms are now often used to describe the morphology of species that were previously not considered to belong to one of these taxa (e.g., Nussbaum 1983; Tarsitano 1983; Carroll 1988; Heckert et al. 2012). Hence, instead of further modifying one of the traditional schemes, especially by adding a new array of "-apsid" types, here a new and comprehensive classification scheme for the tetrapod temporal region is introduced that is neither based on phylogeny nor on assumed functional backgrounds or homology criteria (Fig. 9).

The main goal for the new terms to be (1) short and coherent in their phrasing, and (2) descriptively distinct but still generally applicable to a high number of clades. This classification scheme introduces ten distinct morphotypes applicable to Tetrapoda and other Stegocephali (Fig. 10). Some skulls may not be unambiguously assignable to a single one of these morphotypes. This is as expected: naturally occurring morphological variation may never fit an artificial scheme perfectly. Yet, it is expected that the majority of tetrapod skulls can be assigned to one of these types. This scheme is not based on homology criteria, but rather on the presence, configuration, and number of temporal openings. Hence, it does not consider the exact suturing between the temporal bones, the presence or absence of a specific bone, the presence of a posttemporal fenestra, skull proportions, or muscle arrangements. The relative size of a temporal opening is only considered for temporal excavations, whereas the relative size of a temporal fenestra has no implications for morphological assignment herein. This approach thus carries the risk of integrating only superficially similar temporal skull conditions within the same morphotype. Nevertheless, this scheme also retains independence from taxonomic and functional interpretations. Ordering the tetrapod temporal region by a simple morphological scheme should ensure a better comprehension of the complexity and functional adaptations in this large area of the cranium and provides a basis for future quantitative studies that examine the underlying developmental patterns and structural homology of the temporal dermatocranium.

A scutal

No temporal openings are present

Synonyms

- **stegokrotaphic** (after Gaupp, 1895*b*)
- holo-stegocrotaph (Gaupp, 1895*a*)
- **stegal** (Jaekel, 1909*a*)
- *pars* tegal (Jaekel, 1909*a*)
- **anapsid** (after Williston, 1917)
- akeiroid/euanapsid (Smith *et al.*, 1983)

B nudital

Temporal bars or bridges are absent

Synonyms

- **gymnokrotaphic** (after Gaupp, 1895*b*)
- Untergruppe A (Fuchs, 1909)
- *pars* saurocrotaphic (Williston, 1912)
- *pars* **parapsid** (after Williston, 1917)
- 1. Typus (Versluys, 1919)
- anadiapsid (Smith *et al.*, 1983)
- anasynapsid (Smith *et al.*, 1983)
- hyperpleurokeiroid (Smith *et al.*, 1983)
- *pars* excavation (Werneburg 2019)

C infrafenestral

Infratemporal fenestra as the only temporal opening

Synonyms

- **zygokrotaphic** (after Gaupp, 1895*b*)
- mono-zygocrotaph (Gaupp, 1895*b*)
- anazygocrotaph (Fürbringer, 1900)
- *pars* **synapsid** (after Osborn, 1903)
- *pars* **zygal** (Jaekel, 1909*a*)
- *pars* monozygal (Jaekel, 1909*a*)
- *pars* Untergruppe B (Fuchs, 1909)
- *pars* therocrotaphic (Williston, 1912)
- 2. Typus/Typus A (Versluys, 1919)
- *pars* eusynapsid (Smith *et al.*, 1983)
- monapsid (Werneburg 2019)

D infrafossal

Ventral excavation as the only temporal opening

Synonyms

- *pars* **stegokrotaphic** (after Gaupp, 1895*b*)
- hemi-stegocrotaph (Gaupp, 1895*a*)
- *pars* tegal (Jaekel, 1909*a*)
- Zweite Reihe (Fuchs, 1909)
- *pars* **anapsid** (after Williston, 1917)
- 4. Typus (Versluys, 1919)
- pleurokeiroid (Smith *et al.*, 1983)
- *pars* excavation (Werneburg, 2019)

E suprafenestral

Supratemporal fenestra as the only temporal opening

Synonyms

- **zygokrotaphic** (after Gaupp, 1985*b*)
- *pars* mono-zygocrotaph (Gaupp, 1895*b*)
- katazygocrotaph (Fürbringer, 1900)
- *pars* **synapsid** (after Osborn, 1903)
- *pars* **zygal** (Jaekel, 1909*a*)
- *pars* monozygal (Jaekel, 1909*a*)
- Untergruppe B (Fuchs, 1909)
- *pars* therocrotaphic (Williston, 1912)
- *pars* **parapsid** (after Williston, 1917)
- 3. Typus/Typus B (Versluys, 1919)
- **euryapsid** (after Colbert, 1945)
- **metapsid** (after Boettger, 1952)
- *pars* hemidiapsid (Smith *et al.*, 1983)
- *pars* excavation (Werneburg, 2019)

F suprafossal

Posterodorsal excavation as the only temporal opening

Synonyms

- **zygokrotaphic** (after Gaupp, 1895*b*)
- *pars* tegal (Jaekel, 1909*a*)
- Erste Reihe (Fuchs, 1909)
- *pars* **anapsid** (after Williston, 1917)
- *pars* 4. Typus (Versluys, 1919)
- opisthokeiroid (Smith *et al.*, 1983)
- *pars* excavation (Werneburg, 2019)

G bifenestral

Infratemporal and supratemporal fenestrae are present

Synonyms

- **zygokrotaphic** (after Gaupp, 1895*b*)
- di-zygocrotaph (Gaupp, 1895*b*)
- **diapsid** (after Osborn, 1903)
- *pars* **zygal** (Jaekel, 1909*a*)
- dizygal (Jaekel, 1909*a*)
- Untergruppe A (Fuchs, 1909)
- *pars* saurocrotaphic (Williston, 1912)
- 1. Typus (Versluys, 1919)
- eudiapsid (Smith *et al.*, 1983)
- diplapsid (Werneburg, 2019)

H bifossal

Ventral and posterodorsal excavations are present

Synonyms

- **zygokrotaphic** (after Gaupp, 1895*b*)
- *pars* tegal (Jaekel, 1909*a*)
- *pars* **anapsid** (after Williston, 1917)
- 4. Typus (Versluys, 1919)
- *pars* opisthokeiroid (Smith *et al.*, 1983)
- *pars* pleurokeiroid (Smith *et al.*, 1983)
- *pars* excavation (Werneburg, 2019)

I additofenestral

Two pairs of infratemporal fenestrae are present, often with a supratemporal fenestra

Synonyms

- *pars* **diapsid** (after Osborn, 1903)

J fossafenestral

Ventral excavation and supratemporal fenestra are present

Synonyms

- **zygokrotaphic** (after Gaupp, 1895*b*)
- *pars* mono-zygocrotaph (Gaupp, 1895*b*)
- katazygocrotaph (Fürbringer, 1900)
- *pars* **diapsid** (after Osborn, 1903)
- *pars* **zygal** (Jaekel, 1909*a*)
- *pars* monozygal (Jaekel, 1909*a*)
- Untergruppe A (Fuchs, 1909)
- *pars* saurocrotaphic (Williston, 1912)
- *pars* **parapsid** (after Williston, 1917)
- 1. Typus (Versluys, 1919)
- **katapsid** (after Boettger, 1952)
- hemidiapsid (Smith *et al.*, 1983)
- *pars* excavation (Werneburg 2019)

[Figure caption on the following page]

Fig. 9 Novel comprehensive classification scheme for the arrangement of temporal openings in Tetrapoda. (A) Scutal, (B) nudital, (C) infrafenestral, (D) infrafossal, (E) suprafenestral, (F) suprafossal, (G) bifenestral, (H) bifossal, (I) additofenestral, (J) fossafenestral. Red = temporal fenestra; light pink = temporal excavation; dark pink = other skull openings. Skull outlines are generalized after the early reptile *Captorhinus* from Fox & Bowman (1966). Widely used synonyms are highlighted in blue.

2.2.1. Scutal

From Latin *scutum* = "shield", scutal describes skulls with a fully roofed temporal region, i.e. a temporal dermatocranium lacking fenestrations or distinct temporal excavations (Fig. 9A). It corresponds, among others, to "anapsid" (after Williston 1917), "stegokrotaphic" (after Gaupp 1895*b*), and "stegal" (Jaekel 1909*a*; see also Fig. 9A for further synonyms). It is the ancestral condition in Tetrapodomorpha and is mostly retained, with a reduced number of dermal bones, in several extinct relatives of Lissamphibia and Amniota, and likely as a symplesiomorphy in early Amniota and Gymnophiona (for further details of the taxa and literature mentioned in the skull type descriptions, see Subchapter 2.3.1.d). It reappeared likely secondarily in Pareiasauromorpha, early Testudinata and a number of Testudines, as well as in some hyperossified Anura. The skulls of various Mammalia may be referred to this type.

2.2.2. Nudital

From Latin *nuditas* = "bareness", nudital describes skulls that lack temporal bars or bridges due to a heavily reduced temporal dermatocranium (Fig. 9B). Usually only the parietal region still retains dermal bones. This morphotype corresponds with "gymnokrotaphic" (after Gaupp 1895b). It is widespread in Batrachia and Ophidia, but occurs also in a number of other Squamata, as well as some Testudines.

2.2.3. Infrafenestral

From Latin *infra* = "below" and *fenestra* = "window", infrafenestral describes skulls that possess an infratemporal fenestra as their only temporal opening (Fig. 9C). This morphotype corresponds mainly to "synapsid" (after Osborn 1903), but also partly to "zygokrotaphic" (after Gaupp 1895*b*) or "zygal" (Jaekel 1909*a*). It occurs most notably in the majority of non-neotherapsidan Synapsida, Gorgonopsia, and many Parareptilia. It can be also found in the embolomere *Anthracosaurus russelli* and some the caimans, some Ankylosauria, and a number of Anura. The size of the fenestra varies distinctly among taxa, ranging from miniscule to large openings that occupy most of the "cheek". The infrafenestral type may have arisen independently in Synapsida and Parareptilia, or may represent a synapomorphy of Amniota (see Subchapter 2.3.1.e). In caimans and ankylosaurs, this morphotype emerged by secondary closure of the supratemporal fenestra.

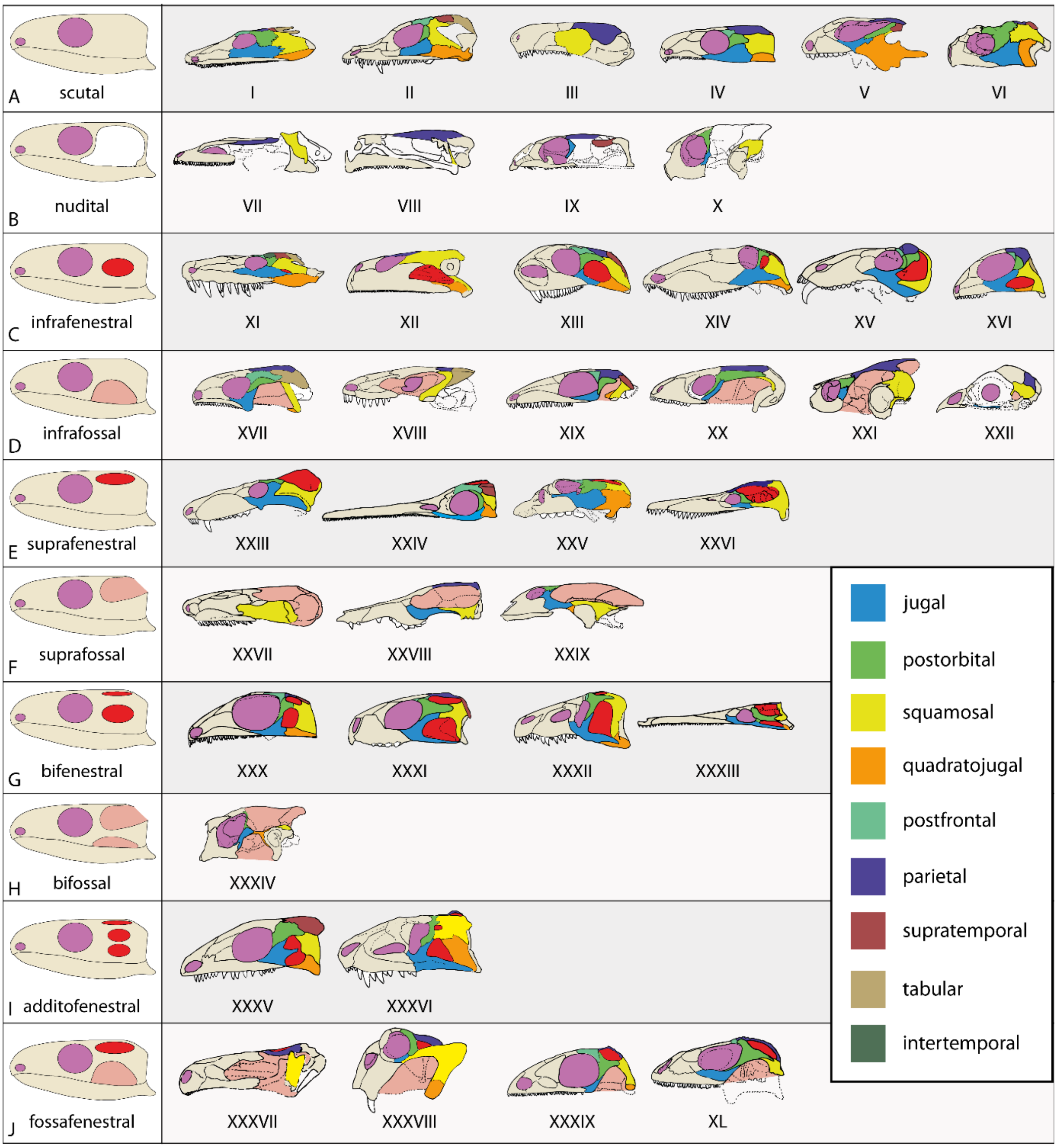

[Figure caption on the following page]

Fig. 10 The ten morphotypes proposed by the novel classification scheme (see Fig. 9), with examples of taxa to show the potential variation. (I) *Acanthostega gunnari* (early Stegocephali; after Clack 2002); (II) *Cacops morrisi* (Temnospondyli; after Reisz et al. 2009); (III) *Microcaecilia iwokramae* (Gymnophiona; after Wake & Donnelly 2012); (IV) *Captorhinus aguti* (early Reptilia; after Fox & Bowman 1966); (V) *Kapes bentoni* (Parareptilia; after Zaher et al. 2019); (VI) *Proganochelys quenstedti* (early Testudinata; after Gaffney 1990); (VII) *Cryptobranchus alleganiensis* (Caudata; after Carroll & Holmes 1980); (VIII) *Bombina orientalis* (Anura; after AmphibiaTree 2004); (IX) *Argyrogena fasciolata* (Squamata; after Das et al. 2019); (X) *Terrapene ornata* (Testudines; after Gaffney 1979); (XI) *Anthracosarus russelli* (Embolomeri; after Panchen 1977); (XII) *Calyptocephalella gayi* (Anura; after Boas 1915); (XIII) *Cotylorhynchus romeri* (early Synapsida; after Romer & Price 1940); (XIV) *Ophiacodon uniformis* (early Synapsida; after Romer & Price 1940); (XV) *Syodon biarmicum* (Dinocephalia; after Kammerer 2011); (XVI) *Bolosaurus striatus* (early Parareptilia; after Broom 1913); (XVII) *Llistrofus pricei* ("Lepospondyli"; after Bolt & Rieppel 2009); (XVIII) *Brachydectes newberryi* ("Lepospondyli"; after Pardo & Anderson 2016); (XIX) *Milleropsis pricei* (Parareptilia; after Gow 1972); (XX) *Cricosaura typica* (Squamata; after Maisano 2003); (XXI) *Emydura maquarii* (Testudines; after Gaffney 1979); (XXII) *Gallus gallus* (Avialae; after Jollie 1957); (XXIII) *Cynognathus platyceps* (early Eutheriodontia; after Broom 1911); (XXIV) *Temnodontosaurus trigonodon* (Ichthyosauria; after Maisch & Hungerbühler 2001); (XXV) *Placodus gigas* (Placodontia; after Sues 1987); (XXVI) *Pliosaurus kevani* (Plesiosauria; after Benson et al. 2013); (XXVII) *Scolecomorphus* sp. (Gymnophiona; after DigiMorph Staff 2002); (XXVIII) *Zalambdalestes lechei* (Mammalia; after Wible et al. 2004); (XXIX) *Pelodiscus sinensis* (Testudines; after Ogushi 1911); (XXX) *Petrolacosaurus kansensis* (early Diapsida; after Reisz 1977); (XXXI) *Clevosaurus hudsoni* (Rhynchocephalia; after Fraser 1988); (XXXII) *Erythrosuchus africanus* (early Archosauriformes; after Nesbitt 2011); (XXXIII) *Thalattosuchus superciliosus* (Thalattosuchia; after Andrews 1913); (XXXIV) *Testudo graeca* (Testudines; after Gaffney 1979); (XXXV) *Delorhynchus cifellii* (Parareptilia; after Haridy et al. 2016); (XXXVI) *Postosuchus kirkpatricki* (early Pseudosuchia; after Weinbaum 2011); (XXXVII) *Pleurodeles walti* (Caudata; after AmphibiaTree & Gosselin-Ildari 2008); (XXXVIII) *Lystrosaurus murrayi* (Anomodontia; after Ray 2005); (XXXIX) *Claudiosaurus germaini* (early Diapsida; after Carroll 1981); (XL) *Iguana iguana* (Squamata; after Conrad & Norell 2010).

2.2.4. Infrafossal

From Latin *infra* = "below" and *fossa* = "cavity", infrafossal describes skulls with a large ventral excavation in the "cheek" as the only temporal opening, with this excavation occupying more than 30% of the temporal height (Fig. 9D). Smaller excavations are not considered for classification. Skulls of this type have been sometimes referred to as "anapsid", but the best historical analogues may be "hemi-stegokrotaph" (Gaupp 1895*a*), "second series" (Fuchs 1909), and "pleurokeiroid" (Smith et al. 1983). The morphotype occurs most notably in Pleurodira, but also in *Eunotosaurus africanus*, Scincoidea, some Parareptilia, and some "Lepospondyli".

2.2.5. Suprafenestral

From Latin *supra* = "above" and *fenestra* = "window", suprafenestral describes skulls that possess a supratemporal fenestra as the only temporal opening (Fig. 9E). This morphotype corresponds mostly to "euryapsid" (after Colbert 1945), but also "parapsid" (after Williston 1917), and "metapsid" (after Boettger 1952). It occurs especially in various Sauropterygia and Ichthyosauromorpha, as well as in non-mammalian Eutheriodontia. It is also present in the early diapsid *Araeoscelis gracilis* Williston, 1910, a few Archosauriformes, and some Choristodera. In all reptiles with a suprafenestral skull, this morphotype likely evolved due to closure of the infratemporal fenestra. In Eutheriodontia, however, the suprafenestral type evolved by a lateromedial widening of the infratemporal fenestra.

2.2.6. Suprafossal

From Latin *supra* = "above" and *fossa* = "cavity", suprafossal describes skulls with a large posterodorsal excavation in the skull roof as their only temporal opening, with this excavation occupying more than 30% of the temporal length (Fig. 9F). Skulls of this type have been sometimes referred to as "anapsid". The best historic analogues may be "first series" (Fuchs 1909) and "opisthokeiroid" (Smith et al. 1983). This morphotype occurs most notably in Cryptodira, but also in several Gymnophiona. Arguably may also be referred to Mammalia.

2.2.7. Bifenestral

From Latin *bis* = "two" and *fenestra* = "window", bifenestral describes skulls that possess an infratemporal and a supratemporal fenestra (Fig. 9G). This morphotype corresponds mainly to "diapsid" (after Osborn 1903). Occurs mostly in non-avialian Archosauriformes, but also in some early Diapsida, several Lepidosauria, and late Rhynchosauria. Arguably also present in some Anura, but overall restricted to reptiles. May be the ancestral condition in Diapsida, however, the bifenestral morphotype in many Sauria is likely a secondary condition that emerged through the development of a lower temporal bar. The shape and proportions of both fenestrae can vary drastically.

2.2.8. Bifossal

From Latin *bis* = "two" and *fossa* = "cavity", bifossal describes skulls that possess a large posterodorsal and ventral excavation as temporal openings, occupying more than 30 % of the temporal height or temporal length, respectively (Fig. 9H). There is no perfectly fitting historical analogue. Overall restricted to Testudines. Arguably, most mammal skulls fall under this type, however, in their case the posterodorsal excavation is a drastically widened infratemporal fenestra, and both excavations are separated by the former lower temporal bar (i.e., zygomatic arch), whereas in turtles the excavations are secondary reductions of a formal scutal skull.

2.2.9. Additofenestral

From Latin *additus* = "additional" and *fenestra* = "window", additofenestral describes skulls that possess two pairs of infratemporal fenestrae often in addition to a supratemporal fenestra (Fig. 9I). There is no perfectly fitting historical analogue, but skulls of this type are often referred to as "diapsid". The second pair of infratemporal fenestrae can emerge by the subdivision of a large infratemporal fenestra by a bony process or within another suture of the temporal dermatocranium. Occurs in Tyrannosauridae, several early Loricata, and some Parareptilia. Infrafenestral types with an "auxiliary" fenestra on one side of the skull (as in some early synapsids) may, arguably, be referred to this type.

2.2.10. Fossafenestral

From Latin *fossa* = "cavity" and *fenestra* = "window", fossafenestral describes skulls that possess a supratemporal fenestra together with a large ventral excavation in the "cheek" that occupies at least 30% of the temporal height (Fig. 9J). Corresponds mainly to "parapsid" (after Williston 1917) and "katapsid" (after Boettger 1952). Widespread in Diapsida, especially within Lepidosauria, in most Anomodontia and some Salamandridae. However, in Anomodontia the supratemporal fenestra is evolutionary derived from a widened infratemporal fenestra. The size of the supratemporal fenestra can differ markedly. This morphotype is often associated with a streptostylic jaw.

2.3. Research history of the temporal skull region

2.3.1. Temporal skull diversity as a classification tool

Comparative studies of the vertebrate skull, including differences in the temporal region, predate Darwin with a notable contribution by Cuvier (1829). The first detailed monograph on the temporal skull region was by Hallmann (1837). He described the osteology and myology of the temporal region as well as the associated neurobiology, and the auditory system mainly of extant vertebrates. Hallmann (1837) did not examine the skull under a phylogenetic perspective, but focused particularly on embryological differences among vertebrates and how the various morphotypes formed during prehatching/prenatal ontogeny.

2.3.1.a) *Early phylogenetic inferences*

Scientific interest in the morphology of the temporal skull region increased by the end of the 19th century (Fig. 11). Due to increasing attempts to understand evolutionary changes metaphorically as a "tree" (Tassy 2011), together with the growing acceptance of Darwinian theories of evolution (Darwin 1859) and better availability of paleontological data, morphological differences were increasingly viewed in terms of phylogenetic relationships. The early phylogenetic discussions were mostly focused on the homology of particular temporal bones (mainly the squamosal and quadratojugal). The first attempt explicitly to discuss phylogenetic aspects of temporal anatomy likely was Günther (1867), who highlighted similarities in the temporal region between the tuatara (*Sphenodon punctatus* Gray, 1842) and crocodiles, contrasting these with the morphology of squamates and turtles. Baur (1889) was probably the first to describe the evolution of the "temporal arches" (i.e., temporal bars) in different tetrapods from early stegocephalians and their assumed gar-like ancestors with a complete dermal covering of the temporal region.

Cope (1892), who argued for homology of the temporal arches among reptiles, further distinguished between a "Series I", "Series II", and "Series III" in the evolution of reptiles with respect to the formation of temporal bars (Fig. 11). Like Baur (1889), Cope (1892) considered a closed dermatocranium as the ancestral condition from which the reduced dermatocranium of turtles (Series I), the supratemporal fenestra ["supramastoid foramen" in Cope (1892)] of Ichthyopterygia (Series II), as well as different appearances and losses of temporal bars in various other amniotes (Series III) evolved.

Baur (1895) discussed the works of Cope (1892) and Gaupp (1895*a*,*b*; see Subchapter 2.3.1.b) with regard to homologies of the temporal bones among different taxa. Case (1898) argued that the non-fenestrated Pareiasauria were the ancestral "reptilian" group, of which, first, the "Proganosauria" (= Mesosauridae) with an infratemporal and supratemporal fenestra arose, followed by branches leading to extant reptiles ("saurocephalous group") and mammals ("mastocephalous group"; Fig. 11).

Gegenbaur (1898) postulated that taxa with several "Spangen" ("clasps", meaning temporal bars and bridges) like rhynchocephalians or crocodiles represent the condition that arose first from taxa with a fully roofed dermatocranium, from which taxa with only one "clasp" (turtles, "enaliosaurs", and "theromeres") and also the morphotypes of squamates evolved.

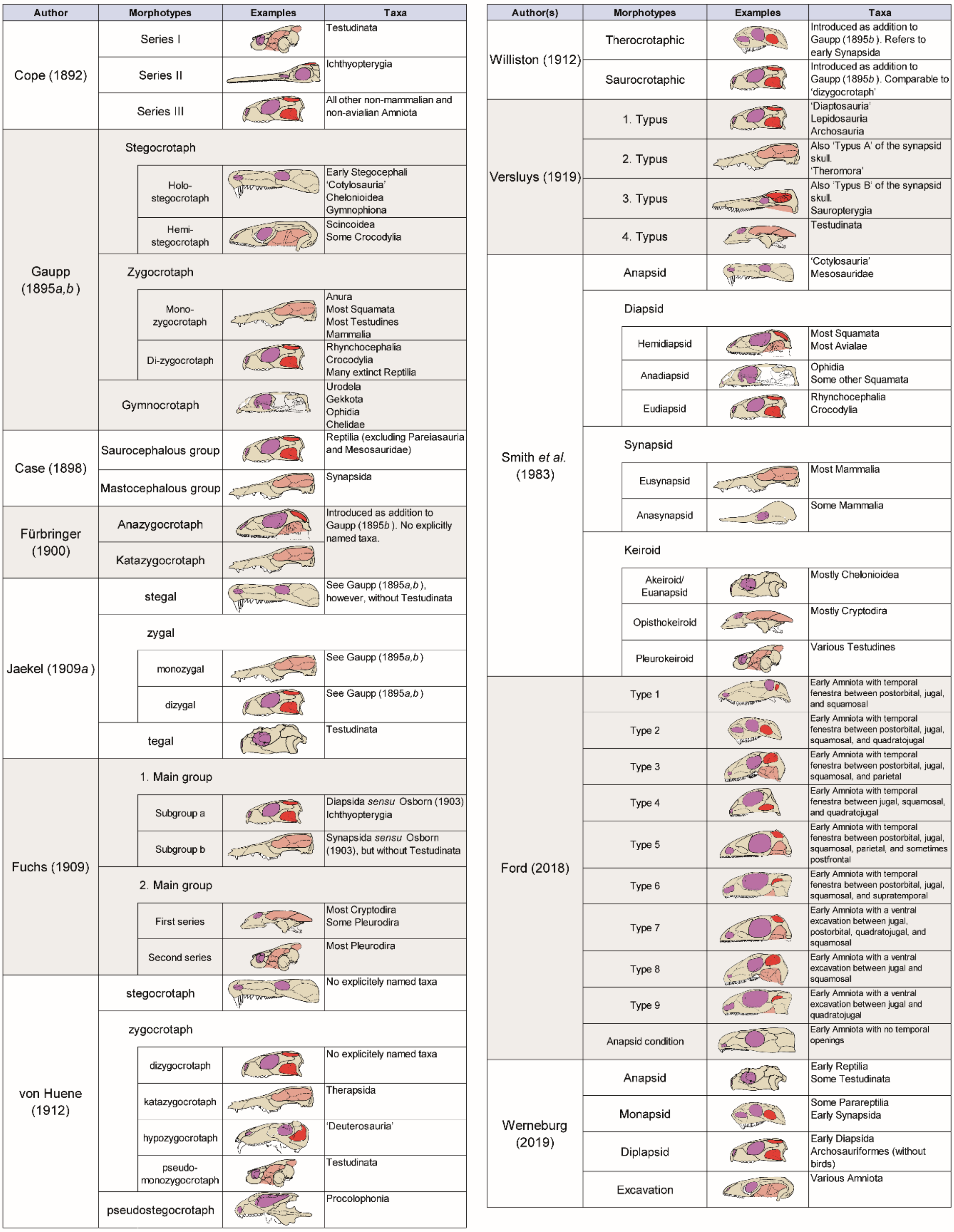

Author	Morphotypes	Examples	Taxa
Cope (1892)	Series I		Testudinata
	Series II		Ichthyopterygia
	Series III		All other non-mammalian and non-avialian Amniota
Gaupp (1895*a*,*b*)	Stegocrotaph		
	Holo-stegocrotaph		Early Stegocephali 'Cotylosauria' Chelonioidea Gymnophiona
	Hemi-stegocrotaph		Scincoidea Some Crocodylia
	Zygocrotaph		
	Mono-zygocrotaph		Anura Most Squamata Most Testudines Mammalia
	Di-zygocrotaph		Rhynchocephalia Crocodylia Many extinct Reptilia
	Gymnocrotaph		Urodela Gekkota Ophidia Chelidae
Case (1898)	Saurocephalous group		Reptilia (excluding Pareiasauria and Mesosauridae)
	Mastocephalous group		Synapsida
Fürbringer (1900)	Anazygocrotaph		Introduced as addition to Gaupp (1895*b*). No explicitly named taxa.
	Katazygocrotaph		
Jaekel (1909*a*)	stegal		See Gaupp (1895*a*,*b*), however, without Testudinata
	zygal		
	monozygal		See Gaupp (1895*a*,*b*)
	dizygal		See Gaupp (1895*a*,*b*)
	tegal		Testudinata
Fuchs (1909)	1. Main group		
	Subgroup a		Diapsida *sensu* Osborn (1903) Ichthyopterygia
	Subgroup b		Synapsida *sensu* Osborn (1903), but without Testudinata
	2. Main group		
	First series		Most Cryptodira Some Pleurodira
	Second series		Most Pleurodira
von Huene (1912)	stegocrotaph		No explicitely named taxa
	zygocrotaph		
	dizygocrotaph		No explicitely named taxa
	katazygocrotaph		Therapsida
	hypozygocrotaph		'Deuterosauria'
	pseudo-monozygocrotaph		Testudinata
	pseudostegocrotaph		Procolophonia

Author(s)	Morphotypes	Examples	Taxa
Williston (1912)	Therocrotaphic		Introduced as addition to Gaupp (1895*b*). Refers to early Synapsida
	Saurocrotaphic		Introduced as addition to Gaupp (1895*b*). Comparable to 'dizygocrotaph'
Versluys (1919)	1. Typus		'Diaptosauria' Lepidosauria Archosauria
	2. Typus		Also 'Typus A' of the synapsid skull. 'Theromora'
	3. Typus		Also 'Typus B' of the synapsid skull. Sauropterygia
	4. Typus		Testudinata
Smith *et al.* (1983)	Anapsid		'Cotylosauria' Mesosauridae
	Diapsid		
	Hemidiapsid		Most Squamata Most Avialae
	Anadiapsid		Ophidia Some other Squamata
	Eudiapsid		Rhynchocephalia Crocodylia
	Synapsid		
	Eusynapsid		Most Mammalia
	Anasynapsid		Some Mammalia
	Keiroid		
	Akeiroid/ Euanapsid		Mostly Chelonioidea
	Opisthokeiroid		Mostly Cryptodira
	Pleurokeiroid		Various Testudines
Ford (2018)	Type 1		Early Amniota with temporal fenestra between postorbital, jugal, and squamosal
	Type 2		Early Amniota with temporal fenestra between postorbital, jugal, squamosal, and quadratojugal
	Type 3		Early Amniota with temporal fenestra between postorbital, jugal, squamosal, and parietal
	Type 4		Early Amniota with temporal fenestra between jugal, squamosal, and quadratojugal
	Type 5		Early Amniota with temporal fenestra between postorbital, jugal, squamosal, parietal, and sometimes postfrontal
	Type 6		Early Amniota with temporal fenestra between postorbital, jugal, squamosal, and supratemporal
	Type 7		Early Amniota with a ventral excavation between jugal, postorbital, quadratojugal, and squamosal
	Type 8		Early Amniota with a ventral excavation between jugal and squamosal
	Type 9		Early Amniota with a ventral excavation between jugal and quadratojugal
	Anapsid condition		Early Amniota with no temporal openings
Werneburg (2019)	Anapsid		Early Reptilia Some Testudinata
	Monapsid		Some Parareptilia Early Synapsida
	Diplapsid		Early Diapsida Archosauriformes (without birds)
	Excavation		Various Amniota

Fig. 11 Overview of previous descriptive classification schemes based on the morphology of the temporal skull region. Skulls are as listed in legend to Fig. 10 with the addition of "Holo-stegocrotaph": *Limnoscelis paludis* after Romer (1946); "Anasynapsid": *Tachyglossus aculeatus* after Macrini (2004); "Type 3", "Type 8": *Edaphosaurus boanerges* after Modesto (1995); "Type 6", "Type 9": *Candelaria barbouri* after Cisneros et al. (2004).

2.3.1.b) *Handling morphological diversity*

Gaupp (1895*a*,*b*) was the first to introduce anatomical terms for different temporal morphotypes, coining the terms "stegocrotaph", "zygocrotaph", and "gymnocrotaph" (Fig. 11). With reference to the taxon Stegocephali, he adopted the term "stegocrotaph" [from Ancient Greek *στέγος* (*stégos*) = "roof" and *κρόταφος* (*krótaphos*) = "temple"] for species with a fully closed dermatocranium in their temporal region, including early stegocephalians, marine turtles, and "Cotylosauria". In fact, Stegocephali [from Ancient Greek *στέγος* (see above) and *κεφαλή* (*kephalé*) = "skull"], which was introduced by Cope (1868) for a set of Paleozoic tetrapods, may be the first time a taxon was named based on its temporal morphotype. Gaupp (1895*a*) proposed a further subdivision of "stegocrotaph" skulls into "holo-stegocrotaph" and "hemi-stegocrotaph" types. He used "holo-stegocrotaph" [from Ancient Greek *ὅλος* (*hólos*) = "complete"] for skulls that possess a fully enclosed temporal region, whereas "hemi-stegocrotaph" skulls [from Ancient Greek *ἥμισυς* (*hḗmisys*) = "half"] have a completely ossified skull roof but a ventrally emarginated "cheek" region like that found in scincoids. "Zygocrotaph" [from Ancient Greek *ζύγωμα* (*zýgōma*) = "bar"], which Gaupp (1895*b*) subdivided into "mono-zygocrotaph" and "di-zygocrotaph", was used for skulls with one or two fully formed temporal bars. Gaupp (1895*b*) defined a "mono-zygocrotaph" condition [from Ancient Greek *μόνος* (*mónos*) = "single"] to be present in anurans, mammals, birds, the majority of turtles, and non-ophidian squamates, whereas a "di-zygocrotaph" cranium [from Ancient Greek *δίς* (*dís*) = "double")] is found in rhynchocephalians, crocodiles, and some fossil taxa like non-avian dinosaurs. "Gymnocrotaph" [from Ancient Greek *γυμνός* (*gymnós*) = "naked"] referred to crania missing most of the dermal bones in the temporal region, which Gaupp (1895*b*) used for most urodeles, snakes, gekkotans, and chelid turtles ["Chelydae" in Gaupp (1895*a*,*b*)]. Gaupp (1895*b*) also postulated the "stegocrotaph" skull to be the ancestral condition from which first the "zygocrotaph" morphology, and from this the "gymnocrotaph" morphology evolved. Fürbringer (1900) suggested an extension of Gaupp"s (1895*a*,*b*) scheme with the terms "anazygocrotaph" [from Ancient Greek *ἀνα* (*ána*) = "up"] and "katazygocrotaph" [from Ancient Greek *κατά* (*katá*) = "downward"], depending on a ventral or dorsal position of the temporal bar, respectively (Fig. 11).

Jaekel (1909*a*) criticized the terms introduced by Gaupp (1895*b*), not only because he considered them to be "almost unpronounceable" ("fast unaussprechlich"), but also because he emphasized the distinct osteological differences present, for example between early Stegocephali and turtles. Jaekel (1909*a*) suggested as an alternative the similarly defined terms "stegal" and "zygal", with the latter also subdivided into "monozygal" and "dizygal" (Fig. 11). The "stegal"-like type in extant turtles, he considered to be a specialised condition derived from a "zygal" skull, hence he referred to them as "tegal" [from Ancient Greek *τέγος* (*tégos*), also meaning "roof"]. Jaekel (1909*a*) also highlighted differences among the "stegal" skulls of early stegocephalians, "placoderms" and other "fishes" with fully roofed dermal armor in their skull, arguing for a need for similar rigorous comparison as already performed for fenestrated skulls in reptiles.

Fuchs (1909) also described the development and evolution of the temporal region in tetrapods ("Quadrupeda"). He demonstrated a trend for simplification of the temporal dermatocranium during tetrapod evolution [see also "Williston's law", *sensu* Williston (1914)] and highlighted its unique position covering the large jaw adductor musculature. He ordered skulls with temporal openings using a new morphological classification system that partly considered phylogeny. He erected two "main groups" ("Hauptgruppen"), subdivided into "subgroups" ("Untergruppen") or "series" ("Reihen"; Fig. 11). Fuchs (1909) first main group incorporated all skulls with temporal fenestrae ("zentral gelegener Reduktion"), his second main group included skulls with temporal excavations ("randständiger Reduktion"). Fuchs (1909) adopted Jaekel"s (1909*a*) terms "stegal" and "zygal", but ordered his first main group mostly in the sense of Osborn (1903; see Section III.1*c*). Accordingly, his "subgroup a" of the "first main group" contained all skulls with two temporal fenestrae, which he identified with Osborn"s (1903) "Diapsida", and all skulls that Fuchs (1909) thought were derived from them (i.e. squamates, birds, "pelycosaurs"). "Subgroup b" of this "first main group" contained all skulls with only a dorsally open temporal fenestra, which the author described as present in most early Synapsida, Sauropterygia, and Ichthyopterygia. Fuchs (1909) restricted his "second main group" to Testudinata: the "first series" of this group contained turtle skulls predominantly with a large posterior excavation in the skull roof; his "second series" incorporated skulls with a large ventral excavation in the "cheek" region (Fig. 3).

Discussing the evolutionary origins of procolophonian reptiles, von Huene (1912; Fig. 11) described amniote skulls using a scheme derived from Gaupp (1895*a*,*b*) and Fürbringer (1900). He hypothesized that from the "stegocrotaph" "cotylosaurs", five amniote radiations with convergent temporal openings emerged: "dizygocrotaph" forms (he presumably meant forms like tuatara, although not named explicitly), "katazygocrotaph" therapsids, "pseudo-monozygocrotaph" turtles [from Ancient Greek *ψευδής* (*pseudes*) = "false"], "hypozygocrotaph" "deuterosaurs" [from Ancient Greek *ὑπό* (*hỳpó*) = "under"], as well as ichthyosaurs together with mesosaurids, which von Huene (1912) apparently also counted as "zygocrotaph". Von Huene (1912) interpreted procolophonians as late-surviving "cotylosaurs" and the only such taxon to evolve temporal openings. However, he distinguished them from "normal zygocrotaph" taxa by their evolution of an orbitotemporal opening, suggesting the term "pseudostegocrotaph". Note that von Huene (1912) did not include the "stegocrotaph" Pareiasauromorpha inside Procolophonia, contrasting to more recent analyses (e.g., MacDougall & Reisz 2014). The "deuterosaurs" mentioned by von Huene (1912) as examples of the "hypozygocrotaph" type are now nested within Dinocephalia (Kammerer 2011). As they had a large infratemporal fenestra in their "cheek", it could be argued that von Huene (1912) understood hypozygocrotaph as similar to Fürbringer's (1900) term "katazygocrotaph" (Fig. 11), although von Huene (1912) used katazygocrotaph to refer to taxa that he considered to be therapsids.

Williston (1912) modified the terms of Gaupp (1895*b*), referring to them as "stegocrotaphic" and "zygocrotaphic". Additionally, for the type found in "Theromorpha" he coined the term "therocrotaphic" [from Ancient Greek *θηρίον* (*thēríon*) = "beast"] and for the condition in Diapsida with two temporal bars he used "saurocrotaphic" [from Ancient Greek *σαῦρος* (*saûros*) = "lizard"; Fig. 11].

Versluys (1919) summarized the temporal region in terms of the then-understood phylogeny of Reptilia. Like previous authors, he interpreted the fully roofed condition as the ancestral state. From this he derived four "types" (Fig. 11): the first type ("1. Typus") referred to a skull with infra- and supratemporal fenestrae, as found in Diapsida; a second type (which he also called "type A" when it appears in synapsid skulls) was used for skulls with only the infratemporal fenestra present; a third type (or "type B" in the synapsid skull) had only the supratemporal fenestra present, as found in Sauropterygia and Ichthyosauria; and, lastly, a fourth type applied to skulls with marginal reductions as found in turtles. Versluys (1919) argued that phylogenetic relevance ("genetische Bedeutung") was present only in the second and fourth "Typus", whereas the third and probably the first could have developed more than once or have been derived from each other (in case of Ichthyosauria).

In 2018, Ford introduced a new scheme to classify the temporal morphology of early amniotes based on the suturing of the dermal bones and their contribution to the temporal openings (Fig. 11). In addition to the "anapsid" condition [see Williston (1917) in Subchapter 2.3.1.c], Ford (2018) distinguished nine different morphotypes, taking both temporal fenestrae and temporal excavations, as well as co-occurences of both opening types into account.

Gaupp"s (1895*b*) original terms (rephrased as "stegokrotaphic", "zygokrotaphic", and "gymnokrotaphic") have remained relevant in the comparative anatomy of non-amniote tetrapods, most notably in the study of caecilians (e.g., Nussbaum 1983; Anderson 2008; Kleinteich et al. 2012; Schoch 2014*b*; Bardua et al. 2019). Similarly, Jaekel"s (1909*a*) terms have remained in use (e.g., Jaekel 1913, 1922, 1927; Zdansky 1923–25; Dombrowski 1924; Kilias 1957; Vorobyeva 2007; von Huene 1954, 1956; Iordansky 1990), although far less frequently than terms introduced by Osborn (1903; see Subchapter 2.3.1.c).

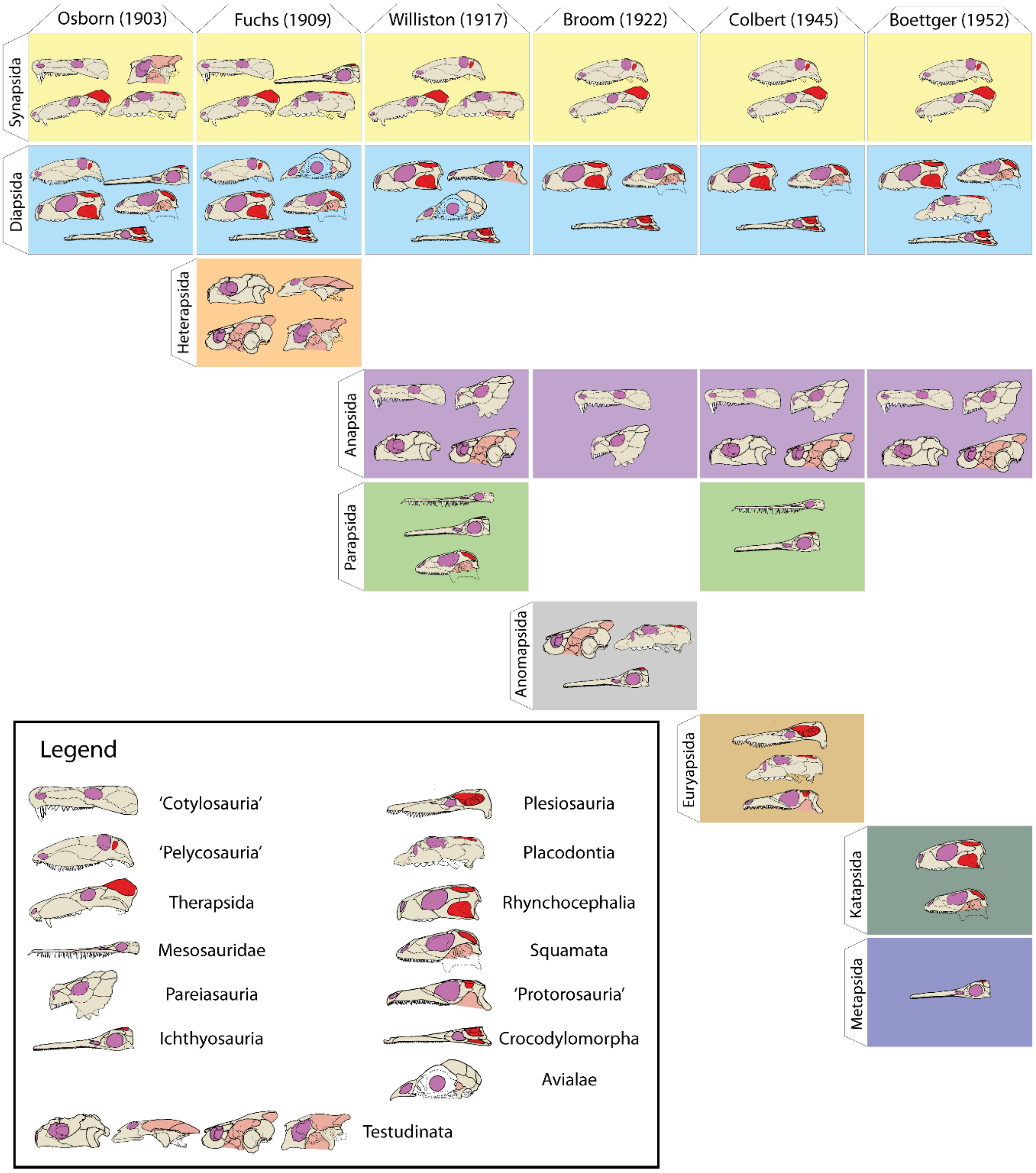

Fig. 12 Overview of amniote systematics as proposed by different authors based on the temporal region. Skulls are as listed in legend to Fig. 10 with the addition of Pareiasauria: *Scutosaurus karpinskii* after Lee (2000); "Protorosauria": *Prolacerta broomi* after Nesbitt (2011); Mesosauridae: *Mesosaurus tenuidens* after Modesto (2006).

2.3.1.c) *Formal taxa based on temporal morphology – the beginning of a taxonomic and nomenclatural tradition*

Simultaneously with the introduction of morphological terminology, other researchers used differences in temporal morphology formally to erect new taxa. This led to the start of a taxonomic and nomenclatural tradition, which resulted in the introduction of at least nine etymologically similarly named taxa during the first half of the 20th century (i.e., "Synapsida", "Diapsida", "Heterapsida", "Anapsida", "Parapsida", "Anomapsida", "Euryapsida", "Metapsida", "Katapsida"). Most of these taxa have since been revised following the rise of large-scale phylogenetic analyses (see Subchapter 2.3.1.d) or in some cases never received widespread acceptance in the contemporary scientific literature.

The initiator of this tradition was Osborn (1903), who subdivided the Reptilia, as then understood, into the taxa "Synapsida" [from Ancient Greek *σύν* (*sýn*) = "with" and *άψίς* (ápsís) = "arch"] and "Diapsida" (from Ancient Greek *δύο* (*dýo*) = "two"], mainly based on the osteology of their temporal region (Fig. 12). Osborn (1903) summarized under his "Synapsida" species with skulls having “primarily […] single, or united temporal arches”, whereas the "Diapsida" possess “primarily […] double, or separated temporal arches” (Osborn 1903: p. 276). While still regarded as a monophyletic taxon (with a different delimitation) (e.g., Ford & Benson 2020), Osborn"s (1903) original "Synapsida" also incorporated Placodontia, Plesiosauria, Testudinata, and "Cotylosauria".

Instead of using his own terms from Jaekel (1909*a*), Jaekel (1909*b*) referred to temporal morphotypes using the terms of Osborn (1903): "diapsid" and "synapsid". Due to his opinion that Sauropterygia should be classified as Diapsida instead of Synapsida (as done by Osborn 1903), he coined the term "pseudosynapsid" with regard to their morphology.

Williston (1917) elaborated Osborn"s (1903) classification by coining the names "Anapsida" [from Ancient Greek *ἄνευ* (*áneu*)= "without"] and "Parapsida" (from Ancient Greek *παρά* (*pará*) = "near"]. Containing "cotylosaurs" and turtles, Williston"s (1917) "Anapsida" corresponded basically to "stegocrotaph/stegal" reptiles. "Parapsida" incorporated, among others, Ichthyosauria and Squamata, with Williston (1917) arguing that their fenestrated morphotype evolved separately from this morphology in Synapsida and Diapsida (Fig. 12).

Contrary to Osborn (1903) but like Williston (1917), Fuchs (1909) considered turtles not to be assignable to Synapsida with confidence but also neither to Diapsida (Fig. 12). Hence, he erected the new taxon "Heterapsida" [from Ancient Greek *ἕτερος* (*héteros*) = "different"].

Broom (1922) raised doubts regarding homology of the temporal arches in Ichthyosauria, Plesiosauria, and Placodontia with those of "mammal-like reptiles". Broom (1922) also highlighted similarities of turtles with plesiosaurs and placodonts, arguing that the turtle skull likely derived from an ancestor with a supratemporal fenestra. Subsequently, Broom (1922) distinguished between four taxa of Reptilia, partly defined by their temporal region: Anapsida, Diapsida, Synapsida, and a new taxon he named "Anomapsida" [from Ancient Greek *ἀνώμαλος* (*anómalos*) = "irregular"], which comprised ichthyosaurs, plesiosaurs, placodonts, and turtles (Fig. 12).

Colbert (1945) classified Sauroptergyia, Placodontia, and Protorosauria into "Euryapsida" [from Ancient Greek *εὖρύς* (*eurús*) = "broad"], identifying them by the presence of a supratemporal fenestra only, laterally bounded by the postorbital and squamosal bones (Fig. 12). Colbert's (1945) subdivision of reptiles into Anapsida, Synapsida, Diapsida, Parapsida, and Euryapsida was later popularized by Romer (1956). In fact, the term "Euryapsida" was originally suggested by Romer in a personal correnspondence as indicated by a footnote in Colbert (1945).

Kilias (1957) argued for phylogenetic relevance of the temporal excavations ("Hiatus") in the turtle skull, at least regarding differentiation between Pleurodira and Cryptodira. Additionally, and contrasting with some previous studies (e.g., Jaekel 1909*a*; Versluys 1919; Zdansky 1923–25), he interpreted the fully roofed temporal region in sea turtles as the retention of an ancestral condition due to their highly aquatic lifestyle.

The final author to name new amniote taxa based on their temporal morphology was Boettger (1952), who coined the terms "Metapsida" [from Ancient Greek *μέτα* (*méta*) = "between"] and "Katapsida" [from Ancient Greek *κατά* (*kata*) = "downward"]. He chose the name Katapsida to reflect his belief that there was a loss (or at least a tendency to lose) of the lower temporal bar in these taxa. "Katapsida" comprises Rhynchocephalia (with choristoderes), Squamata, and Thalattosauria. "Metapsida" incorporates only Ichthyosauria, justified by Boettger (1952) on the grounds that ichthyosaurs appear to possess a temporal fenestra only between the postfrontal and supratemporal bone (Fig. 12).

Criticism of phylogenies based on temporal morphology was present long before large-scale cladistic analyses became possible. Fuchs (1909) had already highlighted that differences in temporal morphology may not necessarily be of high phylogenetic value as similar arrangements could be seen in distantly related taxa. Goodrich (1916), while accepting the existence of a "reptile" branch leading to mammals ("theropsidan") and one leading to birds ("sauropsidan"), cautioned against the use of temporal morphology as a phylogenetic trait, as an appearance of a temporal opening could not be distinguished properly from disappearance of the same in extinct taxa.

In the second half of the 20th century, Kuhn-Schnyder (1954, 1963, 1967, 1980) worked extensively on the phylogenetic implications of temporal openings, especially in regard to sauropterygians and squamates. Kuhn-Schnyder (1954) discussed the ancestry of lizards ("Lacertilia") mostly with respect to their temporal morphology, although he highlighted that similar structures may be the result of convergent evolution. Kuhn-Schnyder (1963) provided a literature review on reptile systematics, especially with regards to previous interpretations of temporal morphotypes. Regarding the ancestry of lizards, Kuhn-Schnyder (1963) reinterated his earlier arguments and highlighted the many routes for the formation of a supratemporal fenestra. He also explicitly used temporal anatomy as an argument against a close relationship between placodonts and other sauropterygians. He argued that the ancestors of placodonts never possessed an infratemporal fenestra, in contrast to the assumed "diapsid" ancestors of Nothosauria and Plesiosauria. Consequently, Kuhn-Schnyder (1963, 1967) considered placodonts to be part of Synapsida and the only large taxon representing Colbert's (1945) "Euryapsida", with other sauropterygians classified as Diapsida. Kuhn-Schnyder (1980) again reviewed the association between temporal fenestration and reptilian phylogeny. While accepting there may be temporal morphotypes unique to the respective reptilian clades, he cautioned that the assumed biomechanical factors leading to temporal fenestration could argue against the use of temporal morphology as a reliable phylogenetic trait.

Nevertheless, new terms in the tradition of Osborn (1903) have been coined occasionally in recent decades. These were explicitly introduced as descriptive terms to order the vast diversity of temporal morphotypes, as originally done by Gaupp (1895*a*,*b*) and Jaekel (1909*a*), and not to describe novel taxa. Smith et al. (1983), for example (Fig. 11), introduced a large number of morphological terms applying to the amniote temporal region, partly based on what was interpreted to be a secondary or derived condition, such as "eusynapsid" [from Ancient Greek *εῦ̃* (*eû*) = "good"] for most mammal skulls and "hemidiapsid" for the skulls of most squamates. Smith et al. (1983) introduced a novel "keiroid" type [from Ancient Greek *κεὶρειν* (*keírein*) = "to cut"] based on the position of excavations in the turtle skull ["opisthokeiroid", from Ancient Greek *όπισθεν* (*ópisthen*) = "backwards"; "pleurokeiroid", from Ancient Greek *πλευρά* (*pleurá*) = "flank"] and how much space these occupy in the temporal region [e.g. "meiopisthokeiroid", from Ancient Greek *μείων* (*meíos*) = "less"; or "metapleurokeiroid" from Ancient Greek *μετά* (*metá*) = "in-between"].

Being aware of cranial plasticity during evolution, Werneburg (2019) took a simplified approach, subdividing the morphology of the amniote temporal region into "anapsid" (no temporal openings), "monapsid" [infratemporal fenestra present; from Ancient Greek *μόνος* (*mónos*) = "single"], "diplapsid" [infratemporal and supratemporal fenestrae present; from Ancient Greek *διπλοῦς* (*diploûs*) = "double"], and "excavation" types [all skulls with any kind of temporal emargination or embayment (Fig. 11)] and illustrated the diverse phylogenetic shifts among morphotypes.

The descriptive terminology introduced by Gaupp (1895*b*) occasionally inspired researchers to allocate names to new formal taxa. Based on their often "stegokrotaphic" skulls, Cannatella & Hillis (1993) erected the clade "Stegokrotaphia" for all non-rhinatrematid caecilians.

There are additional descriptive terms in the tradition of Osborn (1903), mostly used in educational material, that sometimes include the morphology of the preorbital skull. As I was unable to find scientific literature that officially introduced this terminology, these terms will not be discussed herein.

2.3.1.d) *Modern phylogeny and morphological patterns*

With the rise of cladistics and large-scale morphological and molecular phylogenetic analyses in the second half of the 20th century, as well as many new fossil finds, especially of parareptiles (e.g., deBraga & Reisz 1996; Tsuji 2006; Modesto et al. 2009; Tsuji & Müller 2009; MacDougall & Reisz 2014) and potential turtle relatives (Bever et al. 2015; Schoch & Sues 2015, 2017), phylogenies based on temporal fenestration fell out of favor. It can be demonstrated that various temporal morphotypes evolved convergently, repeatedly, and can vary intraspecifically (e.g., deBraga & Rieppel 1997; Cisneros 2008; MacDougall & Reisz 2014; Ford 2018; Ford & Benson 2020; see Chapter 1). Many taxa erected in the tradition of Osborn (1903) have been shown to be para- or polyphyletic and are only used now in a descriptive sense. These include "Anapsida" of Williston (1917) and "Euryapsida" of Colbert (1945), and to a lesser extent "Parapsida" (Williston 1917), "Katapsida" (Boettger 1952), and "Metapsida" (Boettger 1952). "Heterapsida" (Fuchs 1909) and "Anomapsida" (Broom 1922) are now mostly forgotten. Only Osborn"s (1903) original Synapsida and Diapsida are still used as monophyletic taxa, although in a more delimited way. Nevertheless, phylogenetic trends may be feasible when the actual configuration of the temporal dermatocranium is considered (MacDougall & Reisz 2014; Ford 2018), instead of the sole presence or absence of temporal openings. In fact, even under the recent perspective, some morphological patterns can be observed in the temporal skull region.

The ancestral condition in Tetrapodomorpha and Tetrapoda is scutal (1 and 2 in Fig. 13) with a temporal region roofed completely by dermal bones (e.g., Sawin 1941; Clack 1997, 2002; Blom 2005; Daeschler et al. 2006; Sigurdsen & Bolt 2010). Some extinct tipward groups had evolved small temporal fenestrae (3 in Fig. 13; Panchen 1977; Clack 1987), or distinct excavations (4 in Fig. 13), sometimes accompanied by drastic reduction of their dermal armor (Bolt & Rieppel 2015; Pardo & Anderson 2016).

The scutal type (Fig. 9) is likely also the ancestral state in Gymnophiona (5 in Fig. 13; Maddin et al. 2012) and is present in the caecilian clade Stegokrotaphia (6 in Fig. 13; Cannatella & Hillis 1993). Yet, even within stegokrotaphians a suprafossal skull evolved several times independently (7 in Fig. 13; Kleinteich et al. 2012). In Batrachia, the temporal dermatocranium is distinctly reduced. Consequently, the great majority of batrachians possesses a nudital skull (8 and 10 in Fig. 13). Usually, only the frontal, parietal (or frontoparietal), squamosal, and quadratojugal are present (Schoch 2014*b*). However, especially within Salamandridae (9 in Fig. 13), a supratemporal fenestra can be present between the squamosal, parietal, and frontal, leading to a fossafenestral skull (AmphibiaTree & Gosselin-Ildari 2008), whereas in hyperossified Anura scutal (12 in Fig. 13), infrafenestral (11 in Fig. 13), or even bifenestral forms can appear (Evans et al. 2008; Paluh et al. 2020). Due to the loss of the jugal and postorbital in anurans, the infratemporal fenestra in such hyperossified taxa is anteriorly bordered by the maxilla (e.g., Wild 1997).

The ancestral morphotype of Amniota is ambiguous (Piñeiro et al. 2012) and highly dependent on the nesting of certain key clades (see Subchapter 2.3.1.e). The ancestral amniote could have possessed a scutal skull (13 in Fig. 13), as traditionally assumed, or an infrafenestral as seen in early Synapsida and Parareptilia (e.g., Romer & Price 1940; Cisneros et al. 2004, 2021). Synapsida share ancestrally an infratemporal fenestra (infrafenestral morphotype; 14 in Fig. 13) that enlarged during early therapsid evolution (e.g., Kemp 1984). In most non-therapsidan synapsids, the infratemporal fenestra is usually bordered by the jugal, postorbital, quadratojugal, and squamosal (e.g., Romer & Price 1940). The contribution of the quadratojugal declines in Metopophora (e.g., Ophiacodontidae, Edaphosauridae, Sphenacodontidae; Romer & Price 1940). In many Therapsida, but also in some metopophorans, the parietal contributes to the infratemporal fenestra (e.g., Boonstra 1936; Modesto 1995; Kammerer 2011).

In most Anomodontia (15 in Fig. 13), the infratemporal fenestra lateromedially expanded and a distinct ventral excavation formed in the cheek region, overall resulting in a fossafenestral morphotype (e.g., Ray 2005; Sullivan & Reisz 2005). Unlike to a "true" supratemporal fenestra, the jugal still contributes to the temporal fenestra. The fenestra is further bordered by the postorbital, squamosal, and parietal (Sullivan & Reisz 2005). The infratemporal fenestra in early Eutheriodontia (16 in Fig. 13) expanded in a similar manner (e.g., Kemp 1984), leading to a suprafenestral morphotype. However, the non-expanded fenestra in early anomodontians (Angielczyk 2004; Cisneros et al. 2015), as well as in the possible Eutheriodontia sister-clade Gorgonopsia (Gebauer 2007), argue for an independent evolution of the lateromedially expanded fenestra.

Tipward, the temporal fenestra often became confluent with the orbit by loss of the postorbital (e.g., Kemp 1984). Consequently, this orbitotemporal opening in most mammals and their nearest relatives is bordered by the jugal, squamosal, parietal, and frontal. Arguably, this orbitotemporal opening may be referred to as a temporal excavation, making this a suprafossal morphotype (17 in Fig. 13), or even bifossal if the zygomatic arch is distinctly dorsally bended to form a ventral excavation that occupies more than 30 % of the temporal height (see Subchapter 2.2.8.). In some mammals, the zygomatic arch became confluent with the braincase (18 in Fig. 13), effectively forming a scutal morphology (Macrini 2004), although functionally with little similarity to other scutal tetrapods (Murray 1981).

The ancestral condition in reptiles may have been scutal (e.g., Müller & Reisz 2006; Ford & Benson 2020); however, this is highly dependent on the nesting and intrarelationships of Parareptilia (Piñeiro et al. 2012; Cisneros et al. 2021). The earliest parareptiles were likely infrafenestral (20 in Fig. 13; Cisneros et al. 2021; but see the controversy surrounding Mesosauridae in Subchapter 2.3.1.e). Later, also infrafossal (19 in Fig. 13; Gow 1972; Tsuji et al. 2010), scutal (21 in Fig. 13; Lee 1997), and additofenestral (Haridy et al. 2016) forms appeared. In contrast to synapsids and later reptiles, the infratemporal fenestra in infrafenestral parareptiles often forms between the jugal, squamosal, and quadratojugal (Broom 1913; deBraga & Reisz 1996; Tsuji 2006), probably indicating independent evolution of this temporal opening. Procolophonoids have large orbitotemporal openings (Colbert 1946; Zaher et al. 2019). In some procolophonoids, the infratemporal fenestra can co-occur with a ventral excavation in the "cheek" (Cisneros et al. 2004).

Independent of the current hypotheses on parareptile interrelationships, Diapsida likely emerged from a scutal ancestor (22 in Fig. 13; Müller & Reisz 2006; Ford & Benson 2020). The ancestral condition of diapsids may have been bifenestral (23 in Fig. 13; Reisz 1977; Ford & Benson 2020). However, the fossafenestral condition in several other early diapsids (Carroll 1981; Bickelmann et al. 2009), as well as the different bone configuration in later bifenestral taxa (Müller 2003), could also argue for an ancestrally fossafenestral condition in Diapsida (Evans 2008) or would at least imply secondary evolution of the bifenestral morphotype in these forms (26, 36, 38 in Fig. 13). In fact, Ichthyosauromorpha, Lepidosauromorpha, Sauropterygia, Archosauromorpha, and Pantestudines likely were all ancestrally fossafenestral (Waldman & Evans 1994; Evans & Borsuk-Białynicka 2009; Nesbitt 2011; Neenan et al. 2013; Motani et al. 2015; Zhou et al. 2017) or at least infrafossal in the case of pantestudines (Li et al. 2008; Bever et al. 2015). Nevertheless, the supratemporal fenestra would have been ancestrally present in either scenario (Müller 2003; Evans 2008; Ford & Benson 2020), originally likely bordered by the postorbital, squamosal, parietal, and supratemporal (Reisz 1977). Its size (e.g., Nicholls 1999; Benson et al. 2013), as well as the contributions of the supratemporal, frontal, and postfrontal varied in later representatives (e.g., Müller 2003). Additionally, the temporal opening in the "cheek" is closed in several extinct diapsids (Kuhn-Schnyder 1967; Tarsitano 1983; Reisz et al. 1984), most notably in Ichthyosauria (25 in Fig. 13) and various Sauropterygia (31 in Fig. 13), leading to a suprafenestral morphotype.

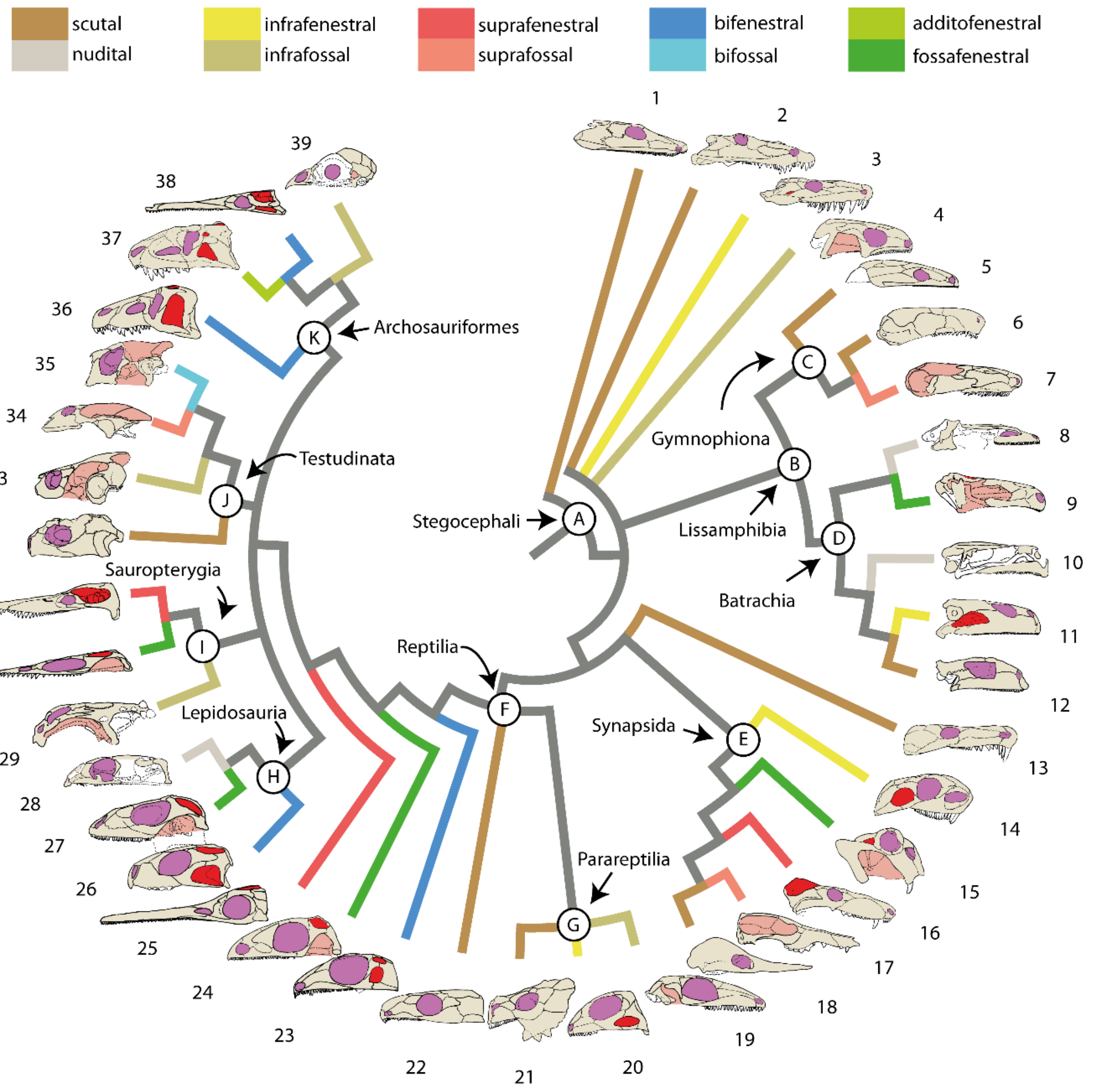

Fig. 13 Composed and simplified phylogenetic tree of Tetrapoda, depicting the distribution of the temporal morphotypes proposed in this review. Relationships that are currently controversial (early Tetrapoda, early Amniota, Parareptilia, late Diapsida) are depicted as polytomies. Note that the colors depict the presence of one representative morphotype within a clade but do not indicate its relative abundance within the respective clade. Skulls are listed as in legend to Fig. 11, unless otherwise indicated below. (1) *Acanthostega gunnari*; (2) *Eryops megacephalus* (after Sawin 1941); (3) *Anthracosaurus russelli*; (4) *Llistrofus pricei*; (5) *Eocaecilia macropodia* (after Jenkins et al. 2007); (6) *Microcaecilia iwokramae*; (7) *Scolecomorphus* sp.; (8) *Cryptobranchus alleganiensis*; (9) *Pleurodeles walti*; (10) *Bombina orientalis*; (11) *Calyptocephalella gayi*; (12) *Gastrotheca galeata* (after Paluh et al. 2020); (13) *Limnoscelis paludis;* (14) *Cotylorhynchus romeri*; (15) *Lystrosaurus murrayi*; (16) *Cynognathus platyceps*; (17) *Zalambdalestes lechei*; (18) *Tachyglossus aculeatus*; (19) *Milleropsis pricei*; (20) *Bolosaurus striatus*; (21) *Scutosaurus karpinskii*; (22) *Captorhinus aguti*; (23) *Petrolacosaurus kansensis*; (24) *Claudiosaurus germaini*; (25) *Temnodontosaurus trigonodon*; (26) *Clevosaurus hudsoni*; (27) *Iguana iguana*; (28) *Argyrogena fasciolata*; (29) *Henodus chelyops* (after Rieppel, 2001); (30) *Keichousaurus hui* (after Holmes *et al*., 2008); (31) *Pliosaurus kevani*; (32) *Proganochelys quenstedti*; (33) *Emydura maquarii*; (34) *Pelodiscus sinensis*; (35) *Testudo graeca*; (36) *Erythrosuchus africanus*; (37) *Postosuchus kirkpatricki*; (38) *Thalattosuchus superciliosus*; (39) *Gallus gallus*.

The fossafenestral state was retained in most Lepidosauria (27 in Fig. 13; Evans 2008), although in Rhynchocephalia (26 in Fig. 13; Whiteside 1986; Jones 2004), as well as a few Squamata (Mo et al. 2010), the bifenestral state reappeared. In Scincoidea, the supratemporal fenestra is closed (infrafossal; Gaupp 1895*a*), whereas in Ophidia (28 in Fig. 13) and some other squamate clades, large portions of the temporal dermatocranium have been reduced, forming a nudital morphotype (e.g., Das et al. 2019).

Testudinata are ancestrally scutal (32 in Fig. 13); however, with morphological differences from the scutal ancestors of diapsids (e.g., Jaekel 1909*a*; Rieppel & deBraga 1996; Müller 2003; Werneburg 2012). This condition formed likely by closure of the supratemporal fenestra, followed by closure of the ventral excavation (Werneburg 2015; Schoch & Sues 2018). In Testudines, distinct ventral and posterodorsal excavations formed in the temporal dermatocranium (Gaffney 1979; Werneburg 2012). Pleurodira usually possess a large ventral opening (infrafossal; 33 in Fig. 13), whereas in Cryptodira the posterodorsal opening is often dominant (suprafossal; 34 in Fig. 13). Sometimes both the ventral and posterodorsal excavations can be enlarged, leaving only a narrow temporal bridge between them (bifossal; Gaffney 1979) or even become entirely confluent (nudital; Gaffney 1979). The set of dermal bones that contribute to the testudine temporal bridges varies considerably (Werneburg 2012). Notably, the scutal morphotype reappeared in Testudines, especially in Chelonioidea (Jones et al. 2012).

The ancestral fossafenestral state in Archosauromorpha evolved twice independently into a bifenestral condition by closure of the lower temporal bar: in late Rhynchosauria (Benton 1983), as well as in Archosauriformes (36 and 38 in Fig. 13), where it became the dominant morphotype in all non-avialian taxa (Nesbitt 2011). In some early archosauriforms, the infratemporal fenestra was closed again (suprafenestral; Heckert et al. 2012), whereas in some Caimaninae the supratemporal fenestra is closed instead (infrafenestral; Mook 1921). In some early Pseudosuchia (37 in Fig. 13), an additional pair of infratemporal fenestrae even appeared (additofenestral; Sulej 2005; Weinbaum 2011). A similar arrangement formed in Tyrannosauridae by subdivision of the previous infratemporal fenestra by a bony process (e.g., Carr 1999). Finally, within Ornithothoraces, the supratemporal fenestra was closed and the lower temporal bar disappeared (e.g., Jollie 1957; O'Connor & Chiappe 2011; Field et al. 2018), leading to the typical infrafossal morphotype of birds (39 in Fig. 13). Within Neognathae, the upper temporal bar reformed several times independently (fossafenestral; Elzanowski & Mayr 2017).

2.3.1.e) *Unresolved controversies*

In spite of moving away from using temporal morphology as a major trait in phylogenies, ongoing debates remain regarding the temporal morphology of phylogenetically unstable taxa and on the ancestral condition for some radiations. As indicated in Subchapter 2.3.1.d, such debates surround the ancestral condition in early amniotes, as well as the evolution of the turtle skull.

While there is mostly a consensus on the content of early Synapsida and early Reptilia (e.g., Müller & Reisz 2006; Benson 2012; MacDougall et al. 2018; Spindler et al. 2018; but see also Laurin & Piñeiro 2017, 2018; Ford & Benson 2020), the relationships of some Paleozoic tetrapod groups relative to Amniota are subject to debate. For example, the Diadectomorpha, traditionally seen as the sister taxon to Amniota (e.g., Laurin & Reisz 1995, 1997; Lee & Spencer 1997; Reisz 1997; Laurin & Piñeiro 2017; Ford & Benson 2020), also have been repeatedly argued to nest within Amniota as sister to synapsids (e.g., Berman et al. 1992; Sumida et al. 1992; Berman 2000, 2013; Marjanović & Laurin 2019; Klembara et al. 2019). Similarly, Recumbirostra, a potential clade of "microsaurs" and some other ""lepospondyls"" has been proposed actually to represent one of the earliest reptilian radiations (Pardo et al. 2017; Mann et al. 2019). In fact, the monophyly and phylogenetic position of "lepospondyls" within Tetrapoda is still controversial (e.g., Marjanović & Laurin 2019). The potential nesting of diadectomorphs and recumbirostrans within Amniota would have implications for the ancestral condition and early evolution of the temporal region in the amniotes. Like many other Paleozoic tetrapods, diadectomorphs typically had a fully roofed dermatocranium (Kissel 2010). If they are indeed the sister-clade to synapsids, the infratemporal fenestra in synapsids could have evolved later, after the split of the synapsid-diadectomorph clade from Reptilia, or the fully roofed (scutal) morphotype in diadectomorphs could have been a derived condition from a fenestrated ancestor. Piñeiro et al. (2012) argued that the possession of an infratemporal fenestra could be the ancestral condition in amniotes. However, this would be dependent on the phylogenetic position and temporal morphology in Mesosauridae (see below). Lastly, nesting recumbirostrans within reptiles would add another set of temporal morphotypes to the early morphological diversity of Reptilia, including excavations and distinct reductions of the dermatocranium (e.g., Pardo & Anderson 2016; Mann et al. 2019).

A second major discussion relates to the presence of an infratemporal fenestra in the Permian reptile taxon Mesosauridae. Despite an uncertain phylogenetic history [see Modesto (2006) and references therein], mesosaurids are usually seen as an early-diverging branch of parareptiles (e.g., Tsuji & Müller 2009; Ford & Benson 2020), or taking an even more rootward position within reptiles (e.g., Laurin & Piñeiro 2017). Thus, they could be a key to reconstructing the ancestral temporal morphotype for Parareptilia, and potentially also for Reptilia or Amniota as a whole (Piñeiro et al. 2012). Previously interpreted to possess both an infratemporal and supratemporal fenestra (MacGregor 1908), later work (von Huene 1941) led to a new consensus that only the infratemporal fenestra was present. This changed with Modesto (2006), who redescribed the cranial anatomy of mesosaurids, interpreting them to possess a fully roofed temporal region. By contrast, Piñeiro et al. (2012) reported the infratemporal fenestra to be present in the specimens they described and even to be demonstrable in disarticulated remains due to the shape of the jugal and postorbital. Their interpretation has since been disputed [MacDougall & Reisz 2014; MacDougall et al. 2018; but see Laurin & Piñeiro (2018) for a response]. It has been also suggested that the infratemporal fenestra may have been ontogenetically (MacDougall et al. 2018) or intraspecifically variable, given that both scenarios have been demonstrated for other parareptiles (Gow 1972; Cisneros 2008; Haridy et al. 2016). Despite being able to examine the mesosaurid material of the Senckenberg collections in Tübingen and Frankfurt am Main, Germany, I remain unable to agree confidently with either hypothesis. At present, there seems to be no consensus on mesosaurid phylogeny and temporal morphology. Their highly aquatic lifestyle (Silva et al. 2017) may also mean that their morphology is too derived to be able to draw conclusions regarding the ancestral cranial morphotype in amniotes.

Another controversial topic in terms of the evolution of the temporal region remains the ancestry and phylogenetic position of turtles. Traditionally depicted as possessing an ancestral fully roofed temporal region (e.g., Cope 1892; Williston 1917; Boettger 1952; Kilias 1957), many early researchers highlighted the derived morphology of the turtle skull relative to the condition in early tetrapods (e.g., Baur 1889; Fuchs 1909; Jaekel 1909*a*; Zdansky 1923–25). Different phylogenetic analyses have nested turtles deep within Diapsida and, hence, implied their descent from ancestors with a fenestrated temporal region (e.g., Rieppel & deBraga 1996; deBraga & Rieppel 1997; Bhullar & Bever 2009; Schoch & Sues 2015). An example of a close fenestrated turtle relative possibly has been found: the description of the Triassic diapsid *Pappochelys rosinae* suggests that it had a supratemporal fenestra and distinct ventral excavation in the "cheek" region (Schoch & Sues 2015, 2017). An even more rootward relative may be the Permian *Eunotosaurus africanus* (Lyson et al. 2010; Bever et al. 2015; Schoch & Sues 2015). Bever et al. (2015) argued that in juvenile specimens of *E. africanus*, in addition to the distinct ventral excavation observed for assumed adults, a supratemporal fenestra was present. The supratemporal fenestra would have been closed during ontogeny by the extreme anterior, autapomorphic expansion of the supratemporal and hence may perhaps represent an early stage of the condition in turtles. However, this scenario appears to be unlikely, because such an extraordinary bone growth in post-hatching ontogeny is extremely rare among amniotes and if present, it usually concerns multiple bones aligning to each other (e.g., Hall 2014). For closure, even separate ossification inside the upper temporal opening may occur (Klembara et al. 2017). However, it might be argued that the juvenile presented by Bever et al. (2015) rather shows a taphonomic disruption than a preservation of an early ontogenetic state of fenestral development. Compared to the adult condition, the jugal is broken off the postorbital and unnaturally reaches into the ventral temporal excavation in the juvenile suggesting that some pressure on the snout travelled along the maxilla to break the jugal. Before breakage, the force was likely further transmitted via the postorbital towards the dorsal temporal region and the scute-like supratemporal (Bever et al. 2015) was likely spalled off. A precise description and reconstruction of the juvenile bones, by which a premature and unbroken supratemporal could be discovered would, however, support the hypothesis of Bever et al. (2015).

It is worth noting that *E. africanus* could also represent a species of parareptile or synapsid, not closely related to turtles (Lee 1995, 2013; Tsuji & Müller 2009; MacDougall & Reisz 2014; Lichtig & Lucas 2021); correspondingly, *P. rosinae* has been also argued by some to be not closely related to turtles (Lichtig & Lucas 2021).

Ford & Benson (2020) provided the most recent assessment of the phylogenetic implications of temporal fenestrations on the relationships of early amniotes. In contrast to most previous workers (although see Laurin & Piñeiro 2017), they found parareptiles as well as the traditional synapsid group Varanopidae to nest within Diapsida. This would have major implications for the ancestral condition in diapsids as, if varanopids and parareptiles are early-branching diapsids, the infrafenestral morphotype could either have been the ancestral state of all diapsids (similar to synapsids) or evolved secondarily by closure of the supratemporal fenestra. This would mean there could have been diverse temporal morphotypes around the base of Diapsida with taxa possessing both temporal fenestrae (Reisz 1977; Müller 2003; Ford & Benson 2019), with a secondarily closed infratemporal fenestra (Reisz et al. 1984), with a secondarily closed or never evolved supratemporal fenestra (Tsuji & Müller 2009; Piñeiro et al. 2012; MacDougall & Reisz 2014), with a supratemporal fenestra and distinct ventral excavation (Carroll 1981; Modesto & Reisz 2003), or with a ventral excavation alone (Tsuji et al. 2010; MacDougall & Reisz 2014).

2.3.2. Understanding the functional origins of temporal openings

Early in the research history of the temporal region, investigators not only described the morphological patterns they observed, but also attempted to explain how the vast structural diversity in lissamphibian and especially in amniote skulls had arisen. For example, Hallmann (1837) already emphasized the functional background to the observed temporal anatomy.

2.3.2.a) *Comprehending diversity (1880s–1900s)*

Dollo (1884) compared the temporal anatomy of non-avian dinosaurs and other extinct taxa with extant groups to predict the size of different jaw adductor muscles. He argued that dominance of either the internal or external jaw musculature would affect the feeding mode of a taxon. Dollo (1884) also argued that dominance of internal jaw adductors in crocodylians and sauropods was related to the posterior movement of the choanae or external nares, respectively, enabling more space for these muscles in the anterior palate. Dollo (1884) saw this as the reason for the small size of the supratemporal fenestra in crocodylians compared with the enlarged fenestra in extinct marine crocodiles, with the latter having their choanae positioned more anteriorly.

Gaupp (1895*b*) related the transition of a closed, "stegocrotaph" dermatocranium to a fenestrated, "zygocrotaph" appearance to the presence of hydrostatic forces acting on the skull. According to Gaupp (1895*b*), the lack of external hydrostatic forces in terrestrial vertebrates as well as the increased need to counter gravitational forces, favored a reduction of skull mass. The remaining temporal bars in the "zygocrotaph" skull would then be aligned and strengthened or weakened depending on the forces applied by the jaw musculature. Gaupp (1895*b*) interpreted the "gymnocrotaph" morphology (i.e., a temporal region, in which the temporal bars are reduced) as the result of limited forces acting on the temporal bones.

Gegenbaur (1898) also provided an in-depth discussion of the relationships between jaw musculature and temporal morphology. He was probably the first explicitly to interpret the evolution of temporal openings as an adaptation to provide attachment sites for the jaw muscles. Particularly with reference to mammals, Gegenbaur (1898) made a connection between a more "massive" dentition and stronger jaw musculature, which would influence the morphology of the zygomatic arch and parietal crests relative to the feeding strategy of any taxon. By contrast, a reduction of the dentition in insectivorous taxa like *Tachyglossus* Illiger, 1811 would allow a corresponding reduction of the zygomatic arch and parietal crest.

Fuchs (1909) argued that simplification of the dermal covering of the temporal region would not inevitably lead to the evolution of temporal openings. Fuchs (1909) postulated that the relative proportions of the braincase and otic capsules as well as the evolution of a streptostylic jaw (i.e., with a mobile quadrate) were major factors explaining the observed variations in the temporal region. Fuchs (1909) described how the dermal bones of the temporal region can extend internally to the jaw adductor musculature (internal lamella) with the potential to replace the primary cartilaginous braincase of the embryonic skull (as seen in mammals and turtles; Werneburg & Maier 2019). With changes in the size of the braincase, the size of the internal lamellae and hence temporal anatomy would also have been affected.

Also affecting the size of the internal lamellae would be the size of the otic capsules, which Fuchs (1909) argued would ancestrally have been large but occupied less space in the interior cranium in later taxa. Lastly, Fuchs (1909) correlated the presence of "monimostyly" *versus* "streptostyly" with the extent of the temporal dermatocranium. A fully closed temporal region or rigidly sutured temporal bars would create a fixed quadrate and, hence, monimostylic jaw, whereas a reduction of a rigid temporal coverage would have enabled the evolution of a streptostylic jaw.

2.3.2.b) *The interplay between muscle and bone (1910s–1950s)*

Gregory & Adams (1915) considered the relationship between temporal morphology and jaw musculature. They observed that in extant taxa like *Sphenodon* Gray, 1831a and turtles the jaw adductor musculature is attached to the sagittal crest and/or to temporal bars. Gregory & Adams (1915) argued that the temporal openings provide more space for action of the temporal musculature and concluded that in extinct taxa with a closed dermatocranium the temporal musculature had to be positioned medially to the dermal bones. Stresses induced by the jaw and neck musculature were thus partly responsible for modifications of temporal osteology in later taxa. Adams (1919) extended these ideas to the relationships between osteology, diet, and myology, using evidence from numerous extant taxa and embryology.

Versluys (1919) discussed in detail how different actions of the internal and external jaw adductor musculature could be related to the evolution of different temporal morphotypes. Versluys (1919) argued that in early aquatic vertebrates with a fully closed temporal region, greater muscle movement could be achieved by simply enlarging the jaw adductor chamber. Further evolution of the neck and increased mobility of the tetrapod skull would have favored the evolution of a lighter and narrower skull. This would have restricted the possible action of the jaw adductor musculature, which could have been offset by opening the temporal dermatocranium. Versluys (1919) argued that the best way to create temporal fenestrae would have been the loss of the intertemporal bone in amniotes or degeneration between the sutures of the jugal, squamosal, and quadratojugal. Depending on the taxon, the temporal fenestrae also could have developed at other sites in the temporal region. Versluys (1919) interpreted the selection pressure involved to be differences in feeding mode, which would require different proportions of internal and external adductor musculature, depending on whether a high biting force or rapid closure of the jaw was required.

Zdansky (1923–25) was interested in the temporal morphology of turtles, which he considered to be more diverse than in other vertebrates. Similar to Jaekel (1909*a*, 1916), Zdansky (1923–25) interpreted the fully roofed temporal dermatocranium of modern turtles to have evolved secondarily in forms that could not, or could only partly, retract their head under the shell (e.g., in the sea turtles, *Platysternon* Gray, 1831b, *Macrochelys* Gray, 1856, and *Podocnemis* Wagler, 1830). A similar conclusion had been drawn by Hay (1908). Zdansky (1923–25) interpreted the return to a fully roofed dermatocranium in these taxa as a defensive adaptation to compensate for the lack of a retractable neck.

Inspired by observations on postcranial bones, Case (1924) investigated the role of muscle action on the formation of temporal openings. In the postcranial bones of humans, such as the scapula or ilium, the associated muscles are attached to thickened margins of the respective bones, whereas the centres of the bones, which experience little direct loading, are distinctly thinned. According to Case (1924), this pattern represented an adaptation to greater muscle force acting on the marginal regions of the bones, triggering the development of additional trabecular bone in these areas. Applying this logic to the temporal region, Case (1924) argued that in forms with a closed dermatocranium, the load would have been concentrated on marginal sections of the temporal bones, which would thicken in response, whereas sections subject to less loading could be thinner and subsequently reduced, forming a skull with temporal fenestrae and thickened temporal bars.

Lakjer (1926) considered in depth the functional differences in the jaw muscles, the associated bones, and skull kinesis of reptiles ("Sauropsida") and other vertebrates. Lakjer (1926) particularly highlighted the relationship between muscle size and bite force for non-ophidian squamates ["Sauria" in Lakjer (1926)], including taxa that were herbivores, omnivores, or predators of large prey. He also observed a relationship between muscle size and temporal dermal armor in lissamphibians, as demonstrated in the difference in size of the jaw muscles between fully roofed caecilians and batrachians with heavily reduced temporal dermal armor. He hypothesized that the fully roofed condition of some anurans had evolved secondarily.

To explain the different temporal morphotypes present in turtles, Kilias (1957) also argued that the load acting on the cranial bones could explain the formation of temporal excavations. He suggested that turtles lost the functional requirement for a roofed dermatocranium following the rigid attachment of the quadrate to the palate and braincase. Kilias (1957) interpreted the temporal bridges as remnants of the dermatocranium that functioned as attachment sites for the external jaw musculature. In agreement with Zdansky (1923–25), Kilias (1957) argued that the evolution of neck retraction was another important factor in turtle skull evolution. He described a trend of decreasing size of the anterior aperture of the shell as an anti-predation adaptation, which simultaneously would have required a decrease in size of the skull which he suggested was achieved by reduction of the parts of the skull with the least functional importance. The hypotheses of Zdansky (1923–25) and Kilias (1957) have recently inspired a number of modern analyses (Werneburg 2012, 2015; Ferreira et al. 2020).

2.3.2.c) *Biomechanical studies (1960s–1980s)*

Olson (1961) analysed the morphofunctional differences within the sarcopterygian jaw system and how these relate to skull morphology. Olson (1961) proposed that the different jaw systems can be broadly divided into a "kinetic inertial system" (K–I) and a "static pressure system" (S–P). In the K–I system, force is mostly applied by the kinetic energy generated by rapid and vertical jaw closing. In the S–P system, the highest force is applied when the jaws are almost closed and involves a multidimensional array of jaw movements. According to Olson (1961), non-tetrapod Sarcopterygia as well as early Tetrapoda ancestrally possessed a simple K–I system that only enabled vertical movement of the mandible. The jaw adductor musculature would have been positioned medially to the dermatocranium. While adaptations to the neck, torso, and gill apparatus in early Stegocephali could have led to rearrangement of the posterior skull region, Olson (1961) did not find evidence for major changes in the jaw musculature in these forms; however, Olson (1961) postulated that with the rise of Tetrapoda, the evolution of several modifications of the K–I and S–P systems. While early Amphibia and predominantly aquatic Amniota evolved only a derived K–I system, Olson (1961) associated the evolution of the S–P system in amniotes with doming of the skull and a tendency to develop temporal openings as well as other osteological adaptations for muscle attachments. Comparable to the conclusions of Versluys (1919) and Case (1924), Olson (1961) argued that the terrestrial lifestyle of early amniotes would have been accompanied by higher mobility of the head and changes in feeding habits, which influenced the origin sites of the jaw musculature: dermatocranium strengthening was concentrated on the few functional attachment sites for muscles, whereas the regions of the dermal roof without a function in muscle attachment were reduced. This morphology, Olson (1961) described as a "network of lines of stress".

The notion of "lines of stress" to explain the evolution of temporal openings was developed further by Fox (1964), who observed that in the early Permian reptile *Captorhinus*, the centre of the fully covered "cheek" region was thinned. Similar observations had been made by Jaekel (1902) for the possible reptiliomorph *Gephyrostegus bohemicus* Jaekel, 1902, who proposed that they represented an early stage in the evolution of fenestrated morphotypes. Fox (1964) also interpreted this morphology to result from lower levels of stress in the cheek centre. As these areas apparently did not function as muscle attachment sites, and additionally were not needed as sources of calcium for attached muscles, there would be no selection against reduction of the bone. Fox (1964) considered all possible stresses affecting the "cheek" region, including forces arising from the weight of the anterior part of the cranium, jaw articulation, and muscle action. Fox (1964) also highlighted that selective pressures leading to the development and enlargement of temporal openings were likely to be multidimensional and to differ among various clades. For the further enlargement of temporal openings in later amniotes, Fox (1964) proposed that additional space for the jaw adductor muscles and a reduction in weight of the skull were likely to be the main factors involved.

Frazzetta (1968) also argued that selection for the initial development of a temporal opening could differ from selection for retaining or enlarging it in later forms. Nevertheless, Frazzetta (1968) considered it likely that there was a common adaptive reason for the development of temporal openings in all clades. Frazzetta (1968) suggested that the lack of temporal openings in early tetrapods and their ancestors could be explained by their plesiomorphically flat skull. The main jaw action in these skulls would involve the pterygoid musculature, which would create a predominantly tangential force affecting the temporal region [i.e., the K–I system introduced by Olson (1961)]. In most amniotes and other tetrapods with a more domed skull, the main jaw action instead would arise from the jaw adductor musculature attached to the skull roof, creating predominantly perpendicular forces. Frazzetta (1968) emphasized the restricted attachment site of these muscles, which correlated with the development of medial bony ridges as described by Fox (1964) for *Captorhinus*. These ridges, representing the previously described "network of lines of stress", thus functioned to strengthen the skull at the muscle attachment sites. Another factor affecting the restricted attachment area of the jaw musculature within the adductor chamber might be the pennate structure of the jaw adductors, which is related to more efficient adduction of the mandible. Frazzetta (1968) saw the restricted attachment of the jaw adductors as a reason for the development of fenestrae in less-loaded areas of the skull. Frazzetta (1968) supported this argument with skulls of the early synapsid *Ophiacodon retroversus*, in which some specimens have a second pair of infratemporal fenestrae between the jugal, squamosal, and quadratojugal (i.e., additofenestral). When this "accessory temporal opening" was not present, or was present on only one site of the cranium, the area between the three bones was still "paper thin". Romer & Price (1940) had argued there would have been no disadvantage to leaving this suture open, indeed jaw adductor action may even have benefited from the additional free space, and that the development of large fenestrae with thickened margins (i.e., bony ridges) would provide sites for a more concentrated attachment of the jaw adductor musculature. Frazzetta (1968) further suggested that the meeting points of three dermal bones would favor the development of fenestrae where they were not subjected to loading. Finally, Frazzetta (1968) argued that, in flat-skulled tetrapods like temnospondyls, the low vertical resistance and muscle attachment without the development of bony ridges would oppose the formation of temporal fenestrae. Even in more domed tetrapods without temporal fenestration, the skull roof was only connected to the cheek region by the remnant of an intracranial joint.

Development of fenestrae in these taxa, according to Frazzetta (1968), would have significantly weakened the skull. Yet, Frazzetta (1968) did acknowledge that this condition may be present in some fenestrated amniotes such as the early synapsid *Varanosaurus* Broili, 1904. In contrast with both Gregory & Adams (1915) and Fox (1964), Frazzetta (1968) disagreed that bulging of the jaw musculature or conservation of structural materials could explain the formation of temporal openings, as the earliest temporal fenestrae would have been too small to function in this way.

Like previous authors (Fuchs 1909; Kuhn-Schnyder 1954, 1963), Gow (1972) noted that similar traits may have evolved independently in far-related taxa, even though for similar reasons. He disagreed with Fox (1964) that the weak zone in the "cheek" of *Captorhinus* could be the predecessor of a temporal fenestra. Instead, he argued that the Permian parareptilian group Millerettidae may be key to understanding the evolution of temporal fenestration in reptiles. Gow (1972) demonstrated that in juveniles of *Milleretta rubidgei* a small infratemporal fenestra was present that disappeared completely in adults, mostly due to an anterior extension of the squamosal. He explained this by contraction/expansion in the "cheek" induced by expansion of the palate at the basicranial articulation (i.e., the articulation between the pterygoid and braincase). According to Gow (1972), this could represent a condition derived from the intracranial kinetics of anthracosaurs, which could likely move their braincase and skull roof relative to their palate and "cheek" (Thomson 1967). In contrast to the typical sarcopterygian intracranial joint between "cheek" and skull roof found in the putatively reptiliomorph anthracosaurs, the squamosal of *M. rubidgei* was firmly attached to the skull roof. This would result in a "line of weakness" between the jugal, squamosal, and quadratojugal on whose dorsal termination the temporal fenestra was formed. Gow (1972) noted that widening of the temporal region would have been a significant precondition to allow such a development in *M. rubidgei*. Further reductions of the temporal dermatocranium (i.e., the formation of a ventral excavation) in other milleretids, especially *Milleropsis* Gow, 1972, would have resulted in even greater intracranial mobility. Notably, Gow (1972) highlighted that temporal fenestrae in the Permian *Youngina* Broom, 1914 and later diapsids were likely to have different causes.

Over the course of the 20th century, a growing consensus on the relationship between temporal openings and jaw adductor musculature inspired several studies on jaw biomechanics in extinct and extant taxa (e.g., Crompton 1963; Barghusen 1973; Kemp 1969, 1980, 1984; Rieppel & Gronowski 1981). The notion that temporal fenestrae functioned as an adaptation to allow bulging of the jaw musculature (see Gregory & Adams 1915) fell out of favor.

Kemp (1980) proposed that the infratemporal fenestra in early synapsids did not evolve from a skull similar to that of early Eureptilia ("Romeriidae"), but instead from a type more similar to the diadectomorph *Limnoscelis* Williston, 1911. Kemp (1980) highlighted that the appearance of supratemporal and tabular bones in synapsids is comparable to the condition in Limnoscelidae. Like other early tetrapods, *Limnoscelis* retained a loose connection between "cheek" and skull roof as a remnant of the sarcopterygian skull with its intracranial joint. According to Kemp (1980), the synapsid infratemporal fenestra could have formed by the jaw adductor musculature attaching to the bony margins of the intracranial joint, which was then strengthened by the processes described above. The fenestra would subsequently form in the connecting area between the "cheek" bones and skull roof.

Kuhn-Schnyder (1980), agreeing with Frazzetta (1968) that temporal fenestrae predominantly form in the sutures between three bones, identified the jugal–squamosal–quadratojugal and postorbital–squamosal–parietal contacts as key regions. While apparently considering muscle action as the main selective force underlying fenestration, Kuhn-Schnyder (1980) also argued for a role of the atlanto-occipital joint (see also Versluys 1919). Elongation of the neck and higher mobility of the head would require a lighter skull and hence favor the formation of fenestrae. He cautioned that such biomechanical causes would make taxonomic classifications based on temporal morphology less reliable, but he considered temporal morphotypes to be mostly constant within single reptilian groups.

Carroll (1982) interpreted early synapsids predominantly as macropredators with the relatively short jaw adductor chamber enabling a wider jaw gap, whereas early diapsids were insectivores in which the presence of temporal fenestrae would have created a lighter skull and the temporal bars formed as areas of maximal resistance against forces generated during feeding (see also Evans 2008). Similar ideas had been proposed by Versluys (1919), who interpreted temporal differences between early Synapsida and Diapsida in terms of their different feeding ecology requiring a different arrangement of the jaw musculature. Despite the presence of two pairs of temporal fenestrae in early diapsids, Carroll (1982) argued that their jaw mechanics and muscle distribution would have been similar to their non-fenestrated reptilian ancestors.

The loss of the lower temporal bar in Lepidosauria and a variety of other fossil taxa was discussed by several researchers (Robinson 1973; Evans 1980; Rieppel & Gronowski 1981; Whiteside 1986). They generally disagreed that this loss had a functional relationship with the evolution of streptostyly as proposed by previous researchers (Fuchs 1909; Romer 1956). Based on an incomplete lower temporal bar and fixated quadrate in the early rhynchocephalian *Clevosaurus hudsoni* Swinton, 1939, Robinson (1973) argued that this may be an auditory adaptation, separating the quadrate from the lower temporal bar to reduce interference with the ears during feeding. Evans (1980) disagreed with this interpretation, because action of the dentulous palatine and stretching of the post-quadrate tympanic membrane by the mandible would still affect hearing ability during feeding, making any effect of a jugal–quadrate separation negligible. She also suggested that this and similar excavations of the "cheek" bones were not related to quadrate movement and that skulls with a mobile quadrate represented a derived condition relative to skulls lacking the lower temporal bar (in squamates) or in which the lower temporal bar was present (in birds). Evans (1980) favored a relationship with the size and attachment sites of the jaw adductor musculature, probably making the lower temporal bar unnecessary for muscle attachment. Rieppel & Gronowski (1981) also did not support a relationship with streptostyly, instead postulating that loss of the lower temporal bar was a consequence of differentiation of the external jaw adductor musculature: a newly developed muscle unit extended posteroventrally from the posterior temporal region to the lateral mandible. Whiteside (1986) drew connections between the weak but rapid bite that would have accompanied the punctuating dentition in these taxa and interpreted the reappearance of the lower temporal bar in the extant tuatara as an adaptation to ensure precise occlusion of the jaws in taxa with a more powerful bite.

In a study on turtles, Lakjer (1926) interpreted a ligament between the quadrate and jugal as the retention of a lower temporal arch from diapsid ancestors. Werneburg (2013*b*), however, demonstrated that this ligament was likely derived from a superficial craniocervical aponeurosis and argued that adjacent bones could not develop histologically into one consistent ligament. The quadratojugal ligament would serve in turtles as tension cord (*sensu* Klenner et al. 2015) to buffer bite forces (Werneburg 2013*b*; see also Jones et al. 2012). In other amniotes, this ligament is either detached from the quadrate in mammals (i.e., as the external masseter fascia) or from the jugal in non-turtle reptiles (i.e., as the quadrate ligament; compare to Iordansky 1996) and serves as a morphogenetic structure to differentiate the external jaw musculature in these taxa (Werneburg 2013*b*).

2.3.2.d) *Quantitative modeling and other recent approaches (1990s–present)*

The recent increase in computational power has enabled researchers to perform quantitative analyses on the functional morphology of tetrapod skulls. In addition to large-scale statistical analyses of diversity patterns (e.g., Jones 2008; Young et al. 2010; Ferreira et al. 2020; Paluh et al. 2020), these include muscle reconstructions and finite element analyses of the skull, and modelling of strain distributions along the temporal bones (e.g., Hylander & Johnson 1997; Holliday & Witmer 2007; Lautenschlager, 2015; Lautenschlager et al. 2017; Ferreira et al. 2020; Nabavizadeh 2020). An in-depth discussion of this literature is outside the scope of this review, but these studies provide a valuable basis for future large-scale studies on the comparative functional morphology of the tetrapod temporal region.

Of particular interest are the functional causes underlying the temporal morphology of caecilians (Gymnophiona). Extant caecilians either possess a distinct posterodorsal excavation between the parietal and squamosal ("zygokrotaphic") or a fully roofed dermatocranium ("stegokrotaphic"; e.g., Kleinteich et al. 2012; Sherrat et al. 2014). In contrast to earlier interpretations (Nussbaum 1983), the ancestral morphology of caecilians was likely "stegokrotaphic" (i.e., scutal) and probably symplesiomorphic with the condition in dissorophoid temnospondyls, the putative sister-clade to lissamphibians (Maddin et al. 2012; see Subchapter 2.3.1.d) with "zygokrotaphic" (i.e., suprafossal in caecilians) forms having evolved several times independently in later forms (Kleinteich et al. 2012). "Stegokrotaphy", together with eyes covered by bone and a subterminal mouth, has been interpreted as an adaptation to a fossorial lifestyle including head-first burrowing (Sherratt et al. 2014; Bardua et al. 2019). "Stegokrotaphic" forms differ in their fossorial behaviour from "zygokrotaphic" taxa, as they are apparently better adapted to burrow in more compact soil (Gower et al. 2004). However, Kleinteich et al. (2012) demonstrated that the temporal bones are relatively unaffected by forces assumed to act during head-first burrowing. They postulated instead that "zygokrotaphy" evolved in caecilians to provide more space for the jaw adductor musculature. Nevertheless, even among "zygokrotaphic" caecilians, the alignment of the jaw adductors can vary (Nussbaum 1983). The influence of the neck musculature might be relevant if head mobility varies among taxa (sensu Werneburg 2015).

In another group of lissamphibians, namely anurans, Paluh et al. (2020) inferred a relationship between a hyperossified cranium and dietary or defense adaptations. In anurans, the temporal region is usually reduced to the frontoparietal, squamosal, and quadratojugal (e.g., Schoch 2014*b*). In several lineages, hyperossification of the frontoparietal, squamosal, as well as the maxilla led independently to secondary closure of the temporal region, sometimes with formation of an infratemporal fenestra in the "cheek" (e.g., *Ceratophrys* Wied-Neuwied, 1824, *Calyptocephalella* Strand, 1928) or a casque-like cranium (e.g., *Hemisus* Günther, 1858, *Myobatrachus* Schlegel, 1850) (Paluh et al. 2020). In a large-scale quantitative analysis, the authors reported that such hyperossification occurs in hypercarnivorous taxa adapted to feed on other large vertebrates and is correlated with high and wide skulls that are also anteroposteriorly short. Paluh et al. (2020) further argued that this may represent an adaptation to the high forces acting on the skull during feeding. The casque-like cranium was found in taxa capable of phragmotic behavior, i.e., the ability to retract the eyes within the orbital cavity, which is likely a defensive strategy, protects the eyes during feeding, or prevents water loss through evaporation.

Holliday et al. (2020) showed that, at least in archosaurs, only part of the supratemporal fenestra serves as an attachment site for the jaw adductor musculature. Small excavations adjacent to the supratemporal fenestra, which they referred to as the "frontoparietal fossa", may instead have contained vascular and adipose structures. Holliday et al. (2020) argued that these structures could have functioned in thermoregulation, especially of the eyes and/or brain, or they may have supplied integumentary structures used in display [see Carr (2020) for a discussion on Holliday *et al.*'s (2020) interpretation of the frontoparietal fossa].

Werneburg (2012, 2013*a*, 2015, 2019) and Werneburg et al. (2015*a*,*b*) reported a series of studies focussing on the temporal region of turtles. Werneburg (2012) reviewed the morphological, evolutionary, and ecological factors potentially influencing temporal morphology in turtles and other amniotes. Werneburg (2015) identified a correlation between neck retraction in cryptodiran turtles and the formation of posterior excavations in their temporal region. He postulated that the tensile forces generated during neck retraction would require the skull to form deep posterodorsal emarginations for better stress distribution. If the original state in the ancestors of turtles was indeed a fenestrated skull, this would have also resulted in closing of the temporal fenestrae to produce the non-fenestrated condition seen in Testudinata. Indeed, the turtle skull may have evolved in response to a complex set of adaptations initiated by an increase in neck mobility and the evolution of the turtle shell (Ferreira et al. 2020; Werneburg, 2020). The loss, reduction, or absence of the ability to retract the neck could also explain the distinct reduction in temporal excavations in many extant taxa like sea turtles, *Platysternon*, or the recently extinct meiolaniids, a conclusion also drawn in some previous publications (Zdansky 1923–25; Gaffney 1983; Jones et al. 2012).

2.3.2.e) *Developmental studies*

The field of evo-devo has grown considerably in recent decades (Olsson et al. 2006), offering a perspective on macroevolutionary patterns often not feasible using anatomy alone. Considering embryology, ontogenetic changes, and the genetic mechanisms behind skull development may be key to understanding the evolution of temporal openings in tetrapods.

Tarsitano et al. (2001) considered mineralization of the jaw muscle tendons as a main driver behind the evolution of temporal fenestrae in amniotes. They proposed that the evolution of temporal fenestrae allowed a size increase in jaw musculature while ensuring a low angle of bone attachment. For muscles originally attaching to the sutures of temporal bones, incomplete closure of these sutures would enlarge the available attachment area for the jaw muscles (as already argued by previous authors) while maintaining a low angle of attachment. Over time, the developmental relationship between bone and jaw muscles would select for a more circular shape of the fenestrae as this would maximize the available surface for muscle attachment. A low angle of attachment between muscle and bone is not only optimal for biomechanical reasons but also would be beneficial during prenatal ontogeny due to the physiological need to maintain a large attachment area for the transport of biomolecules from bone to tendon.

Tokita et al. (2013) identified a possible relationship between temporal morphology in reptiles and the distribution of mesenchymal cells expressing *Runx2* and *Msx2* genes. They reported a higher distribution of *Runx2* and *Msx2* expression in the lateral skull of turtle embryos relative to a focal distribution on regions forming the temporal bars in a crocodile embryo, and a distribution restricted to the precursor of the braincase in a snake embryo. Tokita et al. (2013) interpreted these distribution patterns of *Runx2* and *Msx2* expression as a key element in the diversity of the temporal region of amniotes.

Schoch (2014*b*) provided a hypothesis for the origin of emarginated "gymnokrotaphic" (i.e., nudital) skulls in batrachians (frogs and salamanders). He argued that the cranial osteology of adult batrachians can be compared to the larvae of branchiosaurid temnospondyls but with a trend for successive flattening of the skull that led to the

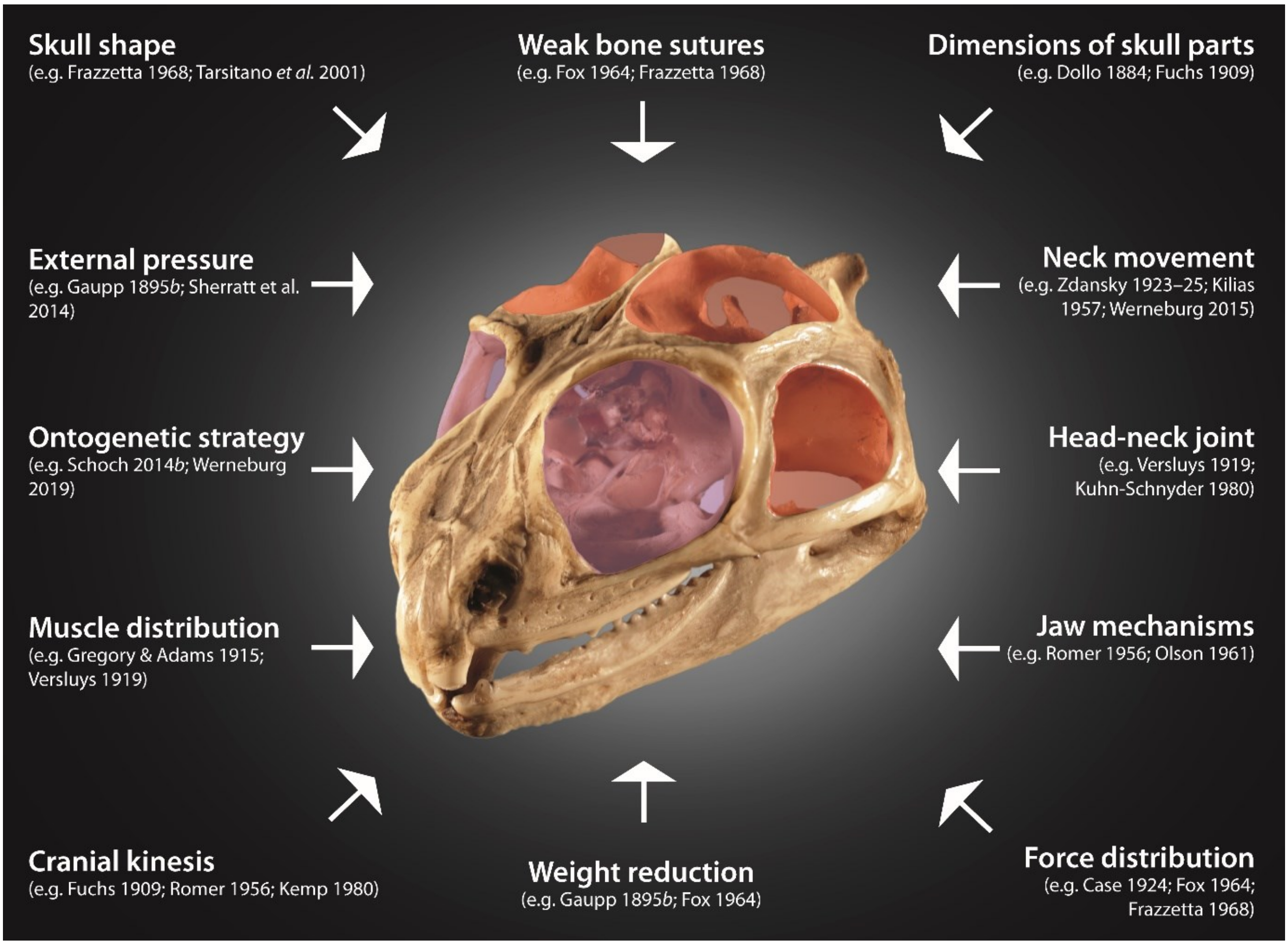

Fig. 14 Summary of the different factors proposed to affect the morphology of the temporal skull region in tetrapods. The relative importance of these factors differs among taxa. For some taxa, specific factors may be not applicable; additionally, factors not mentioned in this figure may also play a relevant role in some case.

"gymnokrotaphic" morphotype. According to Schoch (2014*b*), this skull flattening made it necessary for the jaw musculature to increase in length [see also Frazzetta (1968); Subchapter 2.3.2.c], which would require a reduction of the ancestrally fully roofed dermal armor. This was achieved both by a lack of ossification in some of the dermal bones present in their presumed temnospondylian ancestors and by early fusion of primordial bones. The latter enabled the jaw adductors to attach dorsally to the frontal and parietal primordia before other dermal bones were formed. A dorsal attachment of the jaw adductors has been also reported for suprafossal caecilians (Nussbaum 1983; Kleinteich et al. 2012). However, note that lissamphibian origins, as well as their temnospondylian affinities are still debated [Schoch (2014*a*) and references therein; Laurin et al. 2019; Marjanović & Laurin 2019), and the ossification sequences of branchiosaurids may be different to those of extant amphibians (Laurin et al. 2019).

Werneburg (2019) postulated ontogenetic plasticity as an underlying cause for the high diversity in amniote temporal anatomy. He argued that the absence of a larval stage in amniotes enabled the jaw musculature to attach directly to the developing temporal dermatocranium. Whereas in larvae the dermal bones are not fully differentiated and jaw musculature has to attach to the primordial skull to be functional (Ziermann et al. 2018), in the direct development of amniotes, the jaw musculature is not restricted to an insertion onto the chondro- respectively neurocranium, and has more freedom to respond to the functional requirements of the hatchling/newborn.

The scenarios proposed by Schoch (2014*b*) and Werneburg (2019) may explain how both tetrapod main groups could reduce their temporal dermatocranium despite different developmental strategies. Yet, these developmental strategies are derived relative to those of extinct tetrapod groups (e.g., Packard & Seymour 1997; Schoch 2014*a*; Laurin et al. 2019). The lack of temporal openings in most other Paleozoic tetrapods must be explained by selective forces that prevented the development of temporal openings in these taxa. While the developmental strategies of several Paleozoic tetrapod groups were strikingly diverse [Schoch (2014*a*) and references therein], especially in groups that possessed temporal openings such as the embolomere *Anthracosaurus russelli* (Panchen 1977; Clack 1987) or some "lepospondyls" (e.g., Bolt & Rieppel 2015; Pardo & Anderson 2016), their ontogenetic trajectories are not understood in detail (Schoch 2014*a*; Laurin et al. 2019). Nevertheless, many "lepospondyls" apparently had an uniphasic life cycle, possibly comparable to amniotes or terrestrial salamanders (Schoch 2014*a*). Hence, the development of temporal openings in some "lepospondyls" may be explained in the same way (Werneburg 2019). In fact, several "lepospondyls" with distinctly reduced regions of the dermatocranium recently have been proposed to nest within Amniota (Mann et al. 2019; see Subchapter 2.3.1.e). However, the proposed absence of larvae in "lepospondyls" could be also explained by a preservation bias

(Michel Laurin, personal communication 2021) and the absence of a consensus on early tetrapod interrelationships complicates any attempt to make developmental inferences regarding this essential period of skull evolution.

2.3.3. Summary on the origins of temporal openings

The majority of researchers have made a connection between jaw muscular arrangement and the presence and morphology of temporal openings. Yet, the evolution of the temporal region is likely to be multidimensional (e.g., Fox 1964; Kuhn-Schnyder 1980; Ferreira et al. 2020). Temporal openings seem predominantly to form in weak areas of the dermatocranium, characterized by relatively thin bone (Jaekel 1902; Romer & Price 1940; Fox, 1964) and along the sutures of three or more bones (Frazzetta 1968; Kuhn-Schnyder 1980) or at intracranial joints (Kemp 1980). These "weak" areas may be more likely to form temporal openings due to a lack of ossification (Romer & Price 1940; Cisneros 2008), as an adaptation to reduce skull weight (Gaupp 1895*b*; Fox 1964), or to reduce bone volume in functionally less important areas (Case 1924; Olson 1961; Fox 1964; Frazzetta 1968) to provide more space for the jaw adductors (Dollo 1884; Gregory & Adams 1915; Versluys 1919; Lakjer 1926; Kleinteich et al. 2012). The arrangement of the latter determines the force distribution on the temporal dermatocranium, thereby favoring the development of bony ridges along 'networks of lines of stress' for attachment of the musculature. This could subsequently facilitate reduction of areas subject to lower applied forces and the formation of strong temporal bars in high-stress regions (Gaupp 1895*b*; Gegenbaur 1898; Case 1924; Kilias 1957; Olson 1961; Fox 1964; Frazzetta 1968; Carroll 1982; Tarsitano et al. 2001).

The arrangement of the jaw adductors is then dependent on the shape of the skull (Olson 1961; Frazzetta 1968; Tarsitano et al. 2001; Schoch 2014*b*), the relative dimensions and positions of different skull regions like the choanae, otic capsules, braincase, and orbits (Dollo 1884; Fuchs 1909; Lakjer 1926), and on the ontogenetic strategy (Schoch 2014*b*; Werneburg 2019). Temporal morphology will be further related to aspects of feeding mechanics like jaw movement (Dollo 1884; Versluys 1919; Olson 1961; Whiteside 1986), jaw articulation, and cranial kinesis (Fuchs 1909; Romer 1956; Kilias 1957). Temporal morphology may be also dependent on neck anatomy, including the mobility of the head-neck joint (Versluys 1919; Olson 1961; Kuhn-Schnyder 1980; Werneburg 2015) and the ability to retract the head (Zdansky 1923–1925; Kilias 1957; Werneburg 2012, 2015; Ferreira et al. 2020). Finally, external mechanical stresses during an aquatic or fossorial lifestyle may also be related to a reduction in the temporal region (Gaupp 1895*b*; Olson 1961; Sherratt et al. 2014; Bardua et al. 2019).

There is obviously no universal answer explaining the formation of temporal openings in Tetrapoda, with selective regimes varying according to taxon (Fig. 14). For example, the ability to retract the head arguably plays an important role for the turtle skull, but is unlikely to be able to explain the presence of temporal openings in lepidosaurs or lissamphibians. Temporal morphology will be a compromise of the various factors that act on the skull, including potential phylogenetic constraints. Nevertheless, examples of independent evolution of similar temporal morphotypes (e.g., MacDougall & Reisz 2014; Ford & Benson 2020) suggest that in some cases we will be able to uncover general patterns of selection leading to a particular temporal morphology.

2.4. Conclusions

(1) Here a novel morphological classification scheme is introduced that subdivides tetrapod temporal morphology into ten morphotypes: scutal, infrafenestral, suprafenestral, bifenestral, additofenestral, fossafenestral, infrafossal, suprafossal, bifossal, and nudital. This scheme represents an alternative to traditional classification schemes in being independent of phylogeny, homology criteria, and functional interpretations. Plotting these ten morphotypes onto a phylogenetic tree illustrates the broad range of character distributions among taxa. The ancestral condition of major clades remains uncertain – including those of Amniota, Reptilia, and Synapsida – because many morphotypes evolved in parallel in the early members of these groups. Future research should focus on obtaining a detailed and homology-based character definition of the temporal region, including bone-to-bone contacts, suture anatomy, and suitable metrics to understand the detailed pathways of evolution of the temporal region. This will allow to clarify how similar morphotypes evolved in different taxa in response to (potentially different) selective forces.

(2) Research on the tetrapod temporal region has a long history, extending back to the early 19th century. The morphological differences observed comparatively early in this field of research were placed into an evolutionary context by the late 19th and early 20th century. Within this period, several authors independently devised naming conventions for the different temporal configurations, and for taxa based on the latter, with several of these terms still in common use.

(3) A relationship between jaw musculature and the formation of temporal openings was proposed early on and was generally accepted during the last century. Temporal openings appear to form predominantly in relatively weak areas of the dermal armor, such as in the contact zone of three or more bones or at the intracranial joint between the parietal and "cheek". Many researchers interpreted the formation of temporal openings, or more precisely the associated temporal bars and thickened bony margins, as an adaptation to force distribution and muscle size. The development of temporal openings has been considered in the context of tetrapod terrestrialisation and postulated to be favored by the absence of

external hydrostatic pressure, weight reduction, evolution of the head–neck joint, doming of the skull, but also skull flattening (in batrachians), changes in the jaw hinge and cranial kinesis, evolution of the otic capsules and auditory apparatus, or by the absence of a larval stage in early ontogeny. Postulated selective pressures include changes in feeding mechanics, enlarging of the braincase, evolution of neck retraction, fossoriality, and differentiation of the jaw adductor musculature.

Chapter 3

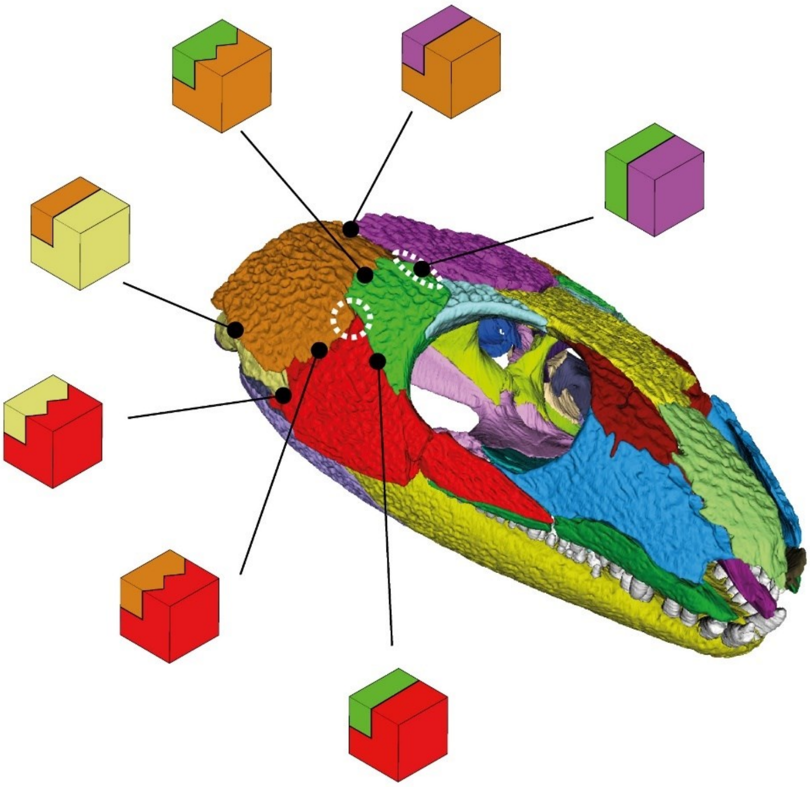

Skull sutures and cranial mechanics in the Permian reptile *Captorhinus aguti* and the evolution of the temporal region in early amniotes

A modified version of this chapter has been published as:

Abel, P., Pommery, Y., Ford, D.P., Koyabu, D., and Werneburg, I. (2022). Skull sutures and cranial mechanics in the Permian reptile *Captorhinus aguti* and the evolution of the temporal region in early amniotes. *Frontiers in Ecology and Evolution* 10, 841784.

Author contributions:

Author	**Concept [%]**	**Providing of data [%]**	**Segmentation/ modelling [%]**	**Analysis [%]**	**Illustrations [%]**	**Writing [%]**	**Providing of funding [%]**
Abel, P.	45	0	20	40	45	65	0
Pommery, Y.	0	0	80	25	45	5	0
Ford, D.P.	5	100	0	10	0	5	0
Koyabu, D.	5	0	0	0	0	5	0
Werneburg, I.	45	0	0	25	10	20	100

3. Skull sutures and cranial mechanics in the Permian reptile *Captorhinus aguti* and the evolution of the temporal region in early amniotes

3.1. Introduction

Amniota, the clade comprising mammals, turtles, lepidosaurs, crocodylians, birds, and their extinct relatives, emerged no later than the early Pennsylvanian (ca. 319 Ma ago; Ford & Benson 2020). In contrast to the majority of coeval limbed vertebrates, the earliest amniotes and their closest extinct relatives adopted a predominantly or even exclusively terrestrial lifestyle (Sumida 1997; Nyakatura et al. 2019; Buchwitz et al. 2021). This ecological shift had been accomplished by innovations in their developmental strategies (e.g., Packard and Seymour 1997; Werneburg 2019; Blackburn & Stewart 2021) and was accompanied by further changes in their general anatomy, involving the appendicular skeleton and vertebral column (Sumida 1997), as well as the skull (Bramble & Wake 1985; Iordansky 1990). Especially, the adaptations in the skull are an essential aspect of amniote terrestrialization, as life outside of the aquatic realm makes specific demands on sensorial abilities, respiration, and feeding (Olson 1961; Lauder & Gillis 1997; Laurin 2010).

One of the most recurrent differences in the skull morphology between early amniotes and most other Paleozoic limbed vertebrates are the reductions of the dermatocranium in the temporal region, leading to the formation of temporal fenestrae or marginal excavations (Werneburg 2012, 2019; Abel & Werneburg 2021). Such temporal openings evolved at least twice independently in early amniotes (Ford & Benson 2020), corroborating the notion that they were a response to new functional demands (e.g., Case 1924; Fox 1964; Frazzetta 1968; for a review see Chapter 2), likely caused by a greater role of the external jaw adductor musculature and corresponding changes in force distribution (e.g., Versluys 1919; Case 1924; Lakjer 1926; Frazzetta 1968). Initially, this might have been also bound to amniote terrestrialization and accompanied adaptations like weight reduction, higher mobility of the atlanto-occipital joint, and change from a kinetic-inertial to a static-pressure biting system (Gaupp 1895; Versluys 1919; Olson 1961; Fox 1964; Kuhn-Schnyder 1980). Overall, temporal openings have been hypothesized to form especially within "weak" regions of the dermatocranium that could easily have been reduced. Those include generally thin areas (e.g., Case 1924; Romer & Price 1940; Fox 1964), intersections of more than two bones (Frazzetta 1968; Kuhn-Schnyder 1980), and bone articulations (Kemp 1980).

Yet, the ancestral configuration without temporal openings (*scutal sensu* Abel & Werneburg 2021) was retained in many Paleozoic amniotes ("Anapsida"; e.g., Carroll & Baird 1972; Clark & Carroll 1973), and also secondarily reevolved in groups like the Permian pareiasauromorphs (MacDougall & Reisz 2014) and turtles (Gaffney 1990; Jones et al. 2012). However, no ancestrally scutal amniote is known from post-Paleozoic strata and even extant turtles may not be a good analog due to their unique cranial adaptations (e.g., Kilias 1957; Werneburg 2011, 2012, 2013*a*, 2015; Ferreira & Werneburg 2019; Werneburg & Maier 2019). Consequently, any hypothesis regarding the functional morphology in the ancestral scutal skull and its role in the evolution of temporal openings is dependent upon the assessment of fossil material.

Here, the skull of the Permian reptile (*sensu* Modesto & Anderson 2004) *Captorhinus aguti* Cope, 1882 (Amniota, Captorhinidae) is used as a model for the cranial functional morphology in an early “anapsid”. *Captorhinus* Cope, 1896 was chosen, because species of this genus represent some of the best documented early scutal reptiles with easily accessible articulated skull material and a wealth of literature on their cranial anatomy (e.g., Branson 1911; Case 1911; Sushkin 1928; Price 1935; Romer 1956; Fox & Bowman 1966; Heaton 1979; Modesto 1998; Kissel et al. 2002; Egberts 2008), including discussions on their jaw musculature, cranial kinesis, and its relevance in understanding the origin of temporal fenestration (Warren 1961; Fox 1964; Fox & Bowman 1966; Bolt 1974; Heaton 1979; Jones & Zikmund 2012; Werneburg & Abel 2022).

It is worth mentioning that *C. aguti* postdated the oldest known amniotes by ca. 30 Ma (Woodhead et al. 2010; Ford & Benson 2020) and already exhibited some adaptations that might be considered derived relative to earlier anapsids, especially in its dentition, feeding mechanics, and skull proportions (Heaton 1979; Dodick & Modesto 1995; Hotton et al. 1997; Modesto et al. 2007). Nevertheless, *C. aguti* appears to be still rather generalized in its overall cranial morphology in relation to some other contemporary taxa with a scutal temporal region (e.g., *Labidosaurus* Cope, 1896, moradisaurine captorhinids, and probably *Mesosaurus* Gervais, 1865; Dodick & Modesto 1995; Modesto 2006; Modesto et al. 2007) and its temporal morphology is overall similar to other early scutal reptiles (Carroll & Baird 1972; Clark & Carroll 1973; Heaton 1979), among them the oldest known unambiguous amniotes (e.g., *Hylonomus lyelli* Dawson, 1860; *Paleothyris acadiana* Carroll, 1969*b*). Notable differences in its temporal region, especially to non-captorhinid taxa, are the distinctly reduced supratemporals and absent tabulars (Fox & Bowman 1966; Heaton 1979; compare to Koyabu et al. 2012).

A detailed description of the suture morphology within the dermatocranium of *C. aguti* and its adjacent contacts with the viscero- and neurocranium is provided to better understand the general stability and integrity of the hypothetical ancestral amniote skull. Possible “weak” regions in the dermatocranium are described and their implications for strain distribution are discussed. Using a conservative reconstruction of the jaw adductor musculature, the possibilities of cranial kinesis and elastic bone movements in the temporal region of C. aguti will further be discussed, and how the here presented interpretation compares to previous studies involving this taxon. Lastly, it is outlined how the cranial mechanics in the ancestral amniote probably differed from other Paleozoic limbed vertebrates and how they might have provided preconditions for the evolution of temporal openings.

3.2. Material and methods

For this study, an almost complete, three-dimensionally preserved skull of *Captorhinus aguti*, housed at the Sam Noble Oklahoma Museum of Natural History (OMNH 44816; Fig. 15), has been used. As documented by the OMNH, the specimen derives from an unspecified Cisuralian fissure filling in Comanche County, Oklahoma. It is likely that this refers to the well-documented Richards Spur speleothem, which is Artinskian in age (ca. 289 Ma; Woodhead et al. 2010). OMNH 44816 is missing bones especially in the left half of the skull, namely the left nasal and jugal. The left prefrontal and squamosal, the parabasisphenoid and supraoccipital, as well as the left dentary, angular, and surangular are incomplete. The right septomaxilla is probably present but metallic inclusions precluded a proper segmentation. Completely missing in the skull are the premaxillae, prootics, basioccipital, and exoccipitals. Some bones are broken, but nevertheless completely preserved, these are most notably the right palatine, left postorbital, right maxilla and jugal, and both parietals.

OMNH 44816 was scanned by Matthew Colbert with an NSI scanner at the University of Texas High-Resolution X-ray Computed Tomography Facility (UTCT), Austin, United States, in February 2017. The scanner is powered by a Fein Focus High Power source with 180 kV and 0.15 mA. It uses an aluminum filter and a Perkin Elmer detector. The scan has a voxel size of 33.5 mm and consists of 1897 single slices. Further corrections were performed by Jessica Maisano. MicroCT images are deposited in MorphoSource (morphosource.org/concern/media/000439915).

Each bone was virtually extracted using manual segmentation in Avizo 8.13D renderings of the external surface of the bones and the teeth were generated and converted into meshes. Meshes were saved as PLY-files and were projected as 3D models in MorphoDig 1.5 (Lebrun 2018; Fig. 15, 17–23). Renderings are available in Abel et al. (2022*b*).

The thickness of the sutures of the dermatocranium was measured using the 2D Length Tool in Avizo 8.1. The measurements were taken in the orientation in which the suture was most complete and visible. Not being homogeneous over the entire suture length, the suture thickness was measured in five different spots. These spots are quite regularly distributed along the whole suture to obtain an accurate and well-representative mean. All measurements and means of the suture thickness are listed in Suppl. Tab. 2.

For this chapter, the term “suture” is generally applied for the contact of two bones, including their non-preserved soft-tissue components. The bone areas that articulate with each other are referred to as “articulation facets,” the externally visible area incorporating the suture is the “external surface” (Fig. 16).

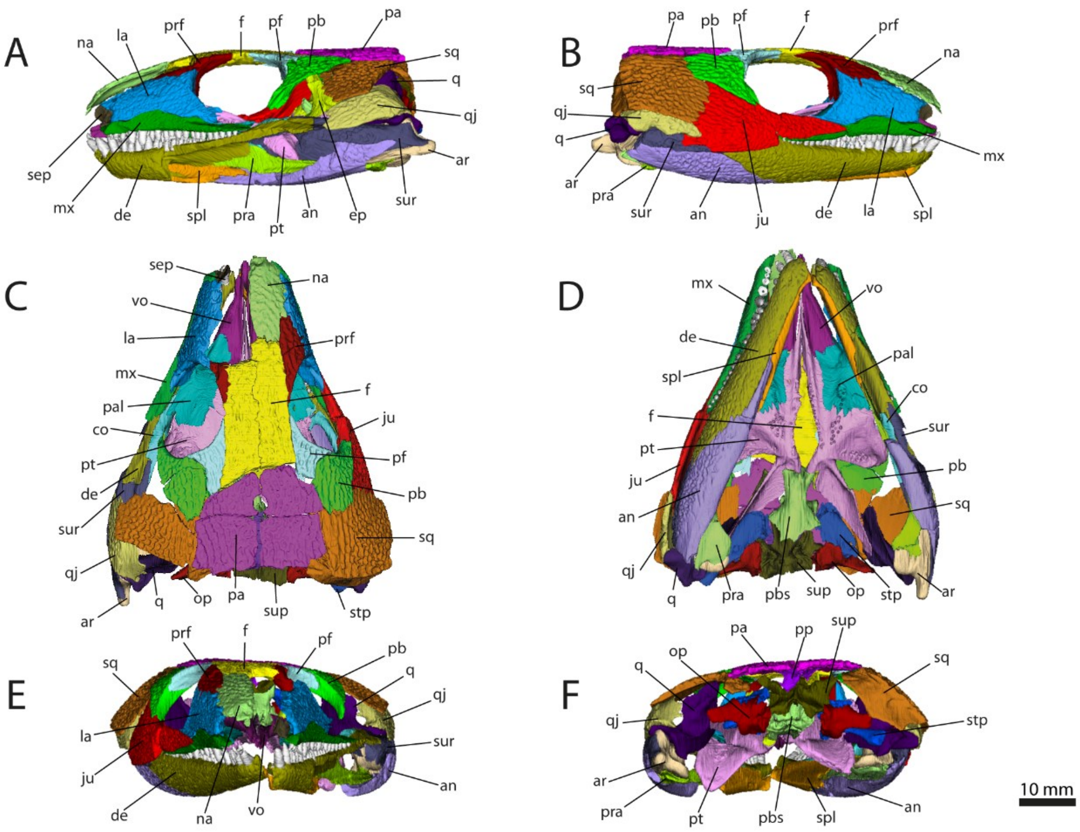

Fig. 15 3D model generated from the scan of OMNH 44816 in left lateral (A), right lateral (B), dorsal (C), ventral (D), anterior (E), and posterior view (F). Abbreviations: an, angular; ar, articular; co, coronoid; de, dentary; ep, epipterygoid; f, frontal; ju, jugal; la, lacrimal; mx, maxilla; na, nasal; op, opisthotic; pa, parietal; pal, palatine; pb, postorbital; pf, postfrontal; pp, postparietal; pra, prearticular; prf, prefrontal; pbs, parabasisphenoid; pt, pterygoid; q, quadrate; qj, quadratojugal; sep, septomaxilla; spl, splenial; sq, squamosal; stp, stapes; sup, supraoccipital; sur, surangular; vo, vomer.

3.3. Results

Eight different suture types in the dermatocranium of *Captorhinus aguti* could be identified and defined (Fig. 24). Most used suture type terminology follows Jones et al. (2011). The type “stepped interdigitation” (8 in Fig. 24) is a combination of “stepped joint” (7 in Fig. 24) and “Type-B interdigitation” (5 in Fig. 24) *sensu* Jones et al. (2011). Sutures can vary in the presence and type of interdigitations as well as in the presence of a bony lamina that extends from one of the suturing bones medially to its respective contralateral neighbor, forming an additional medial contact. Like observed for other taxa (e.g., Clack 2002; Rayfield 2005), sutures also can vary in suture type and thickness along the contact of two bones. In some cases, the type of suturing could not be directly observed, because the relevant bones were missing in OMNH 44816 or had been disarticulated. Articulations between dermal bones and those of the neuro- and viscerocranium are briefly described but not categorized after the scheme in Fig. 24, because they fall out of the research question tested herein and have a very different, enchondral type of ossification (Koyabu et al. 2014) and related suture formation. Likewise, contacts between such non-dermal bones were also not described.

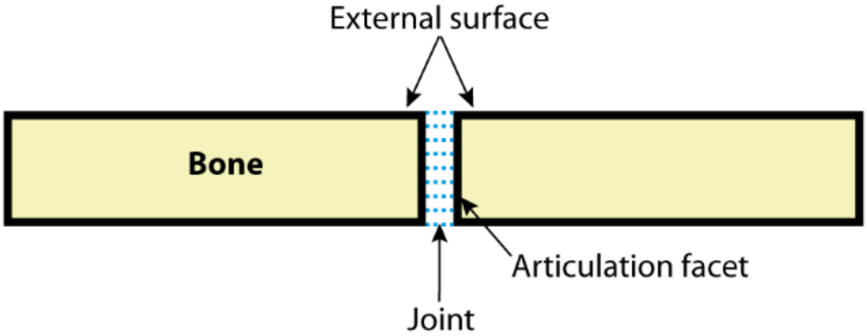

Fig. 16 Simplified cross section of a skull suture, illustrating the terminology used in this manuscript.
sep, septomaxilla; spl, splenial; sq, squamosal; stp, stapes; sup, supraoccipital; sur, surangular; vo, vomer.

3.3.1. Preorbital region

The preorbital region of *C. aguti* consists of the premaxilla, septomaxilla, maxilla, nasal, lacrimal, prefrontal, as well as of the anterior portions of the frontal and jugal. Only some preorbital sutures exhibit a simple structure. Interdigitating contacts appear especially close to the orbits.

The maxilla (Fig. 18) forms laterally a facial lamina that fits into a ventral notch of the lacrimal (“tongue-and-groove joint”; 2 in Fig. 24). The posterior half of the maxilla is overlapped by the jugal by a “stepped joint” (7 in Fig. 24). The palatine contacts the maxilla laterally by what may be referred to as a low “slot joint” (3 in Fig. 24). Anteriorly, the maxilla would have overlapped the non-preserved premaxilla (Fox & Bowman 1966; Heaton 1979).

The ventral margin of the lacrimal (Fig. 19) is concave to house the facial lamina of the maxilla. Overall, the ventral margin forms a medially expanded rim that forms the external surface with the maxilla. On its dorsal margin, it underlies the nasal, the bones interdigitate externally (“stepped interdigitation”; 8 in Fig. 24). Posteriorly to the lacrimal-nasal contact, the lacrimal exhibits a similar contact with the prefrontal, the latter underlies the lacrimal. Posteroventrally, it sutures with the jugal by a stepped joint. At its anterior end, the lacrimal is slightly overlapping the septomaxilla laterally. The lacrimal section of the orbital rim medially overlaps a dorsal ridge of the palatine, forming a slot joint.

Excluding its lateral contact with the prefrontal, the nasal (Fig. 19) interdigitates with all its preserved neighboring bones. Its anterior tip would have underlain the premaxilla. Posterior to the nasal-lacrimal contact, the nasal forms a “butt joint” with the prefrontal (1 in Fig. 24). The remainder of the nasal-prefrontal contact can be described as a stepped interdigitation. A stepped interdigitation can be also observed at the posterior end of the nasal for its contact with the frontal, where the frontal underlies the nasal.

Apart from its already described sutures with the lacrimal and nasal, the prefrontal (Fig. 20) medially contacts the frontal by a stepped joint posterior to the prefrontal-nasal contact.

The posterior suture of the frontal (Fig. 20) with the parietal is overall similar to the frontal-nasal contact. Posterolaterally, the frontal forms a “Type-A interdigitation” (4 in Fig. 24) with the postfrontal. Additionally, a complex inter-frontal suture is present (“Type-C interdigitation”; 6 in Fig. 24). Only the posterior end of the frontal that contacts the postfrontal and parietal contributes to the temporal region.

3.3.2. Temporal region

The temporal part of the dermatocranium in *C. aguti* consists of the posterior portion of the jugal and frontal, as well as the postfrontal, postorbital, squamosal, quadratojugal, parietal, postparietal, and supratemporal. Interdigitating contacts are especially formed on the external surfaces in the “cheeks” (i.e., jugal, squamosal, postorbital, and quadratojugal).

The posterior jugal (Fig. 21) dorsally underlies the postorbital, forming a stepped joint (7 in Fig. 24). At its posterior end, the jugal also underlies the squamosal; both bones form a stepped interdigitation (8 in Fig. 24). The jugal is similarly contacted by the quadratojugal at its posteroventral edge, although the interdigitation sequence is short. A medial contact with the pterygoid has been reported for *Captorhinus* and other captorhinids (Fox & Bowman 1966; Heaton 1979; Dodick & Modesto 1995; Modesto et al. 2007). However, such a contact is not preserved in OMNH 44816. This is likely due to the loss of the anteromedial process that would have connected the jugal to the pterygoid and a slight displacement of the palate.

The postorbital (Fig. 22) anterodorsally underlies the postfrontal (stepped joint). Dorsally, the postorbital is simply contacted by the parietal (butt joint; 1 in Fig. 24). Posteriorly, the postorbital is underlain by the squamosal, and like between the squamosal and the jugal, both contacts interdigitate externally (stepped interdigitation).

Next to its sutures with the postorbital and frontal, the postfrontal (Fig. 22) likewise contacts the parietal posteriorly by a stepped interdigitation.

The squamosal (Fig. 23) underlies the parietal dorsally, forming together another stepped joint. Ventrally, the squamosal itself is underlain by the quadratojugal in a similar manner. Posterodorsally, it would have also sutured to the supratemporal; however, it was not possible to reconstruct the latter for OMNH 44816. Similarly, both postparietals are too badly preserved to make any judgment about their contact to the squamosal. Medially, the squamosal is contacted by the quadrate. At the medial margin of its occipital flange, the squamosal forms a short contact with the opisthotic. It was not possible to unambiguously confirm a contact with the supraoccipital.

In addition to the contacts with the squamosal and jugal, the quadratojugal (Fig. 21) is underlain posteriorly by the quadrate.

Other sutures with the parietal (Fig. 22) include the contact with the postparietal, which it overlaps posteriorly (stepped joint). Posterolaterally, it would have contacted the supratemporal. Both parietals suture each other medially by a butt joint. The supraoccipital would have sutured with the parietals posteroventrally.

The left and right postparietal (Fig. 22) are sutured to each other medially by a thin Type-C interdigitation (6 in Fig. 24). Ventrally, they overlap the supraoccipital.

3.3.3. Palatal region

The dermal palate consists of three bones: the vomer, palatine, and pterygoid. All three bones are rigidly connected by interdigitating sutures.

Both vomers (Fig. 18) contact each other medially at their anterior end by a butt joint (1 in Fig. 24). Posteriorly, the vomer interdigitates with the palatine by a Type-C interdigitation (6 in Fig. 24). A shorter interdigitation with the pterygoid can be observed at its posteromedial edge (“Type-B interdigitation”; 5 in Fig. 24). Additionally, the rod-shaped anterior extension of the pterygoid is on much of its lateral margin contacted with the vomer by a butt joint. Anteriorly, the vomer would have contacted the premaxilla.

The palatine (Fig. 21) interdigitates further with the pterygoid at its posterior and medial margins (Type-C interdigitation). Anteromedially, the palatine-pterygoid contact develops into simple a butt joint. As described above for the preorbital region, the palatine laterally contacts the maxilla and lacrimal.

At their anterior extremity, both pterygoids (Fig. 21) contact each other medially by a short butt joint. In the anteromedial section of the quadrate process, the pterygoid is overlapped by the epipterygoid. The pterygoid does not contact the parabasisphenoid. Posterolaterally, the quadrate broadly contacts the quadrate process of the pterygoid. Posteromedially, the same process is abutted by the stapes.

3.3.4. Mandible

The bones of the mandible comprise the dentary, angular, surangular, coronoid, splenial, prearticular, and articular. The mandibular symphysis is restricted to the anterior tip of the mandible. In most cases, the bones of the lower jaw have simple contacts with each other. Interdigitating sutures appear only on the external surface.

Both dentaries (Fig. 17) are sutured to each other on their anteromedial end by a butt joint (1 in Fig. 24). On its external surface, the dentary interdigitates posteriorly with the angular by a Type-B interdigitation (5 in Fig. 24). Medially, the two bones contact each other along the posterior half of the dentary by what may be referred to as a butt joint. A similar arrangement exists between dentary and surangular; the latter borders the dentary posterodorsally. Medially, the splenial also contacts the dentary both dorsally and ventrally to the Meckelian groove. The dorsal contact is similar to the medial contacts with the angular and surangular described above, however, ventrally, the splenial slightly underlies the dentary by a stepped joint (7 in Fig. 24). Posterior to the dorsal dentary-splenial suture, the dentary contacts the anterior end of the prearticular by another butt joint. The medial portion of the dentary, dorsally to the other mandibular bones, is mostly covered by the coronoid.

Next to its already described contact with the dentary, the midsection of the coronoid (Fig. 17) overlaps the anterior prearticular by a butt joint. Anteriorly, the coronoid tapers between the dentary and splenial. Posteriorly, a large wedge of the surangular protrudes to the coronoid, forming a short interdigitating sequence.

At their anterior ends, both splenials (Fig. 18) contact each other medially by a butt joint as part of the mandibular symphysis. Posterodorsally, the prearticular tapers in-between the dentary-splenial contact. Posterolaterally, the angular contacts the splenial by a butt joint; posteroventrally, it also overlies the splenial by a stepped joint.

Like described above, the surangular interdigitates anteriorly with the dentary and coronoid by a Type-B interdigitation. On its external surface, it is ventrally overlapped by the angular by a stepped joint. On their internal surface, both bones exhibit a Type-B interdigitation. The prearticular simply sutures the surangular by a butt joint at its posteroventral extremity. Posteromedially, the surangular is wedged into the articular.

Apart from its sutures mentioned above, the angular (Fig. 17) is dorsally overlain by the prearticular medially to the Meckelian groove. The latter widens medially at its posterior end to surround the ventral portion of the articular.

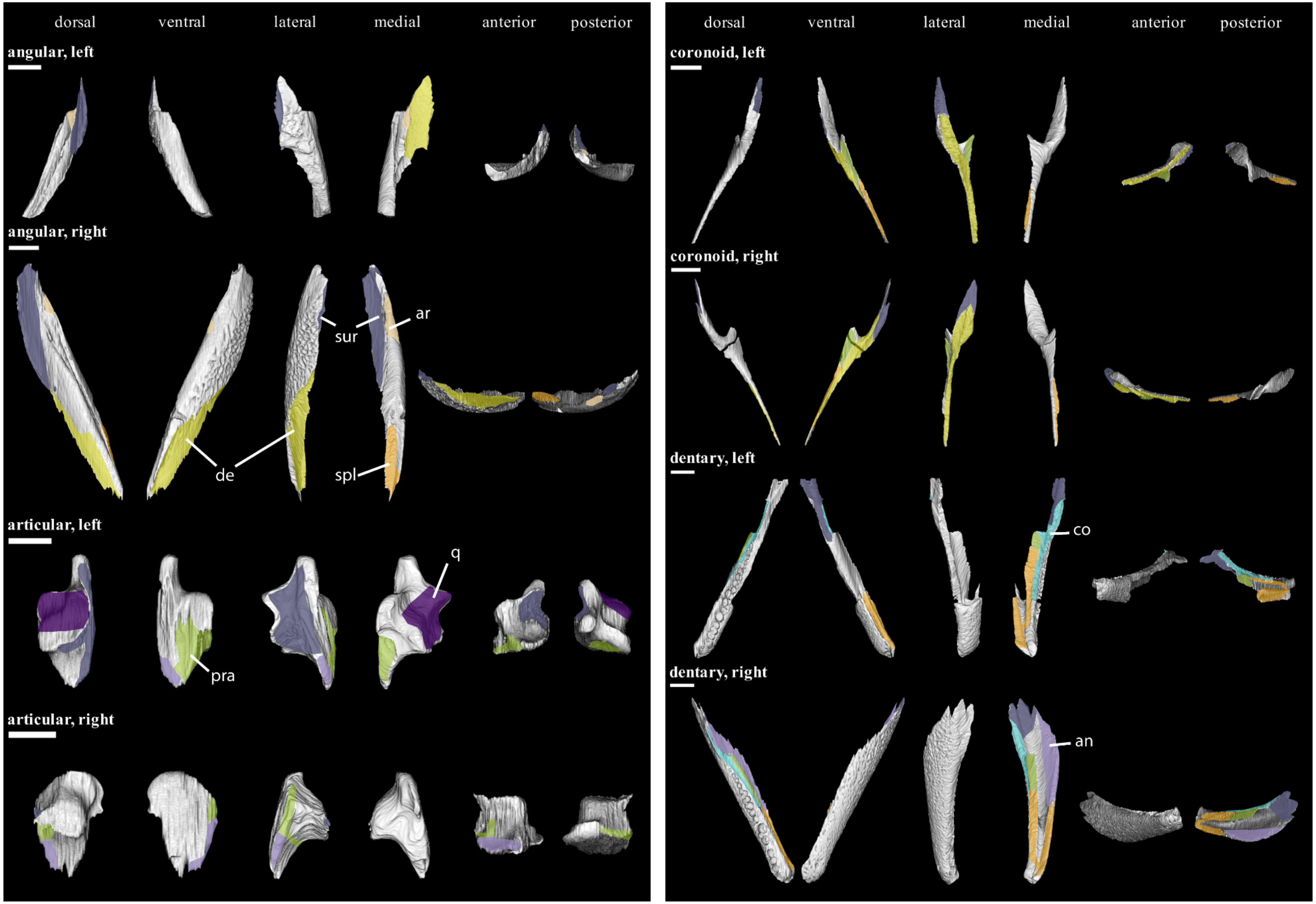

Fig. 17 Isolated bones in dorsal, ventral, lateral, medial, anterior and posterior views. Articulation areas with other bones are colored. Left and right angular, left and right articular, left and right coronoid, and left and right dentary are shown. Scale bar = 10 mm. For abbreviations see caption to Fig. 15.

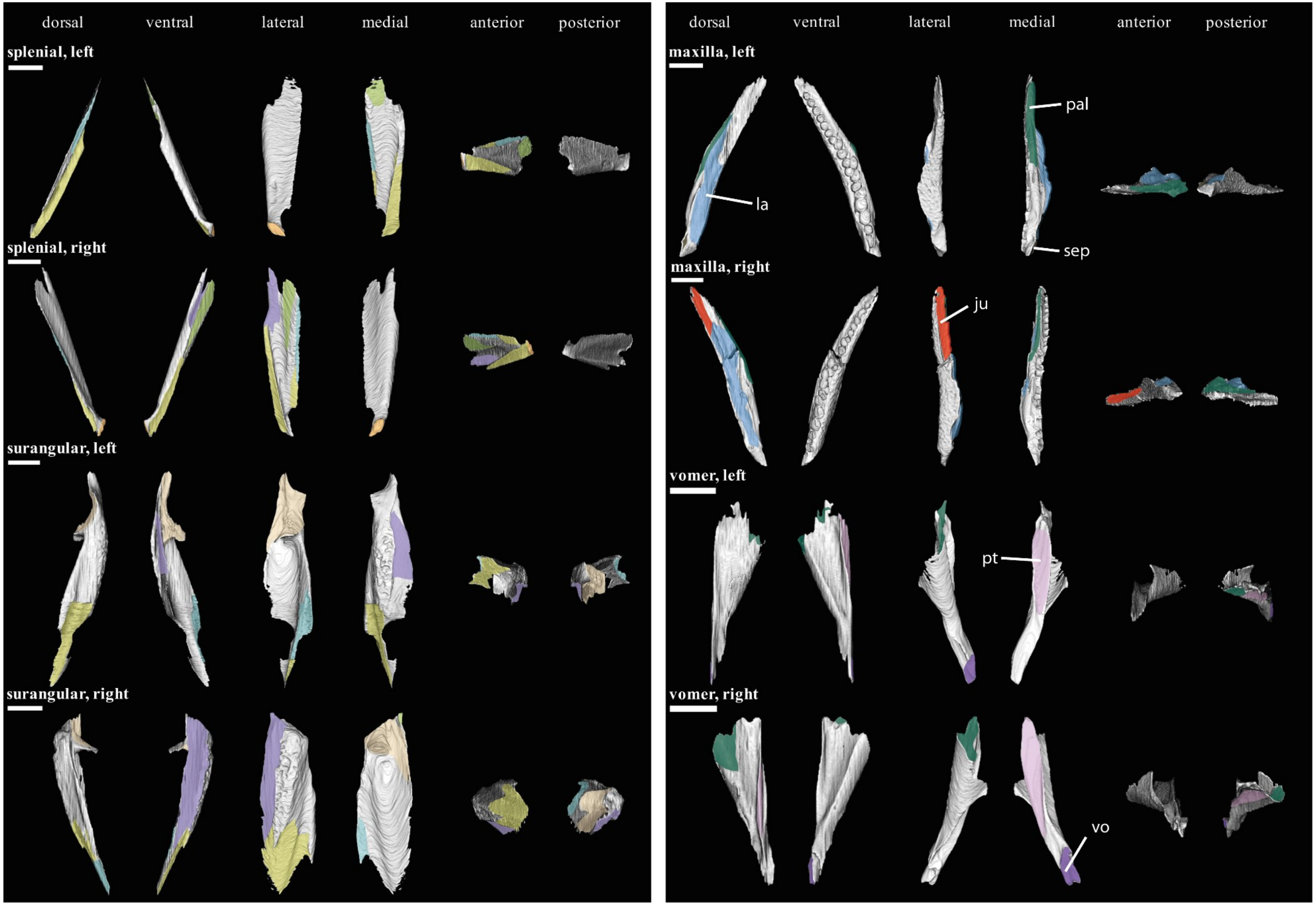

Fig. 18 Isolated bones in dorsal, ventral, lateral, medial, anterior and posterior views. Articulation areas with other bones are colored. Left and right splenial, left and right surangular, left and right maxilla, and left and right vomer are shown. .Scale bar = 10 mm. For abbreviations see caption to Fig. 15.

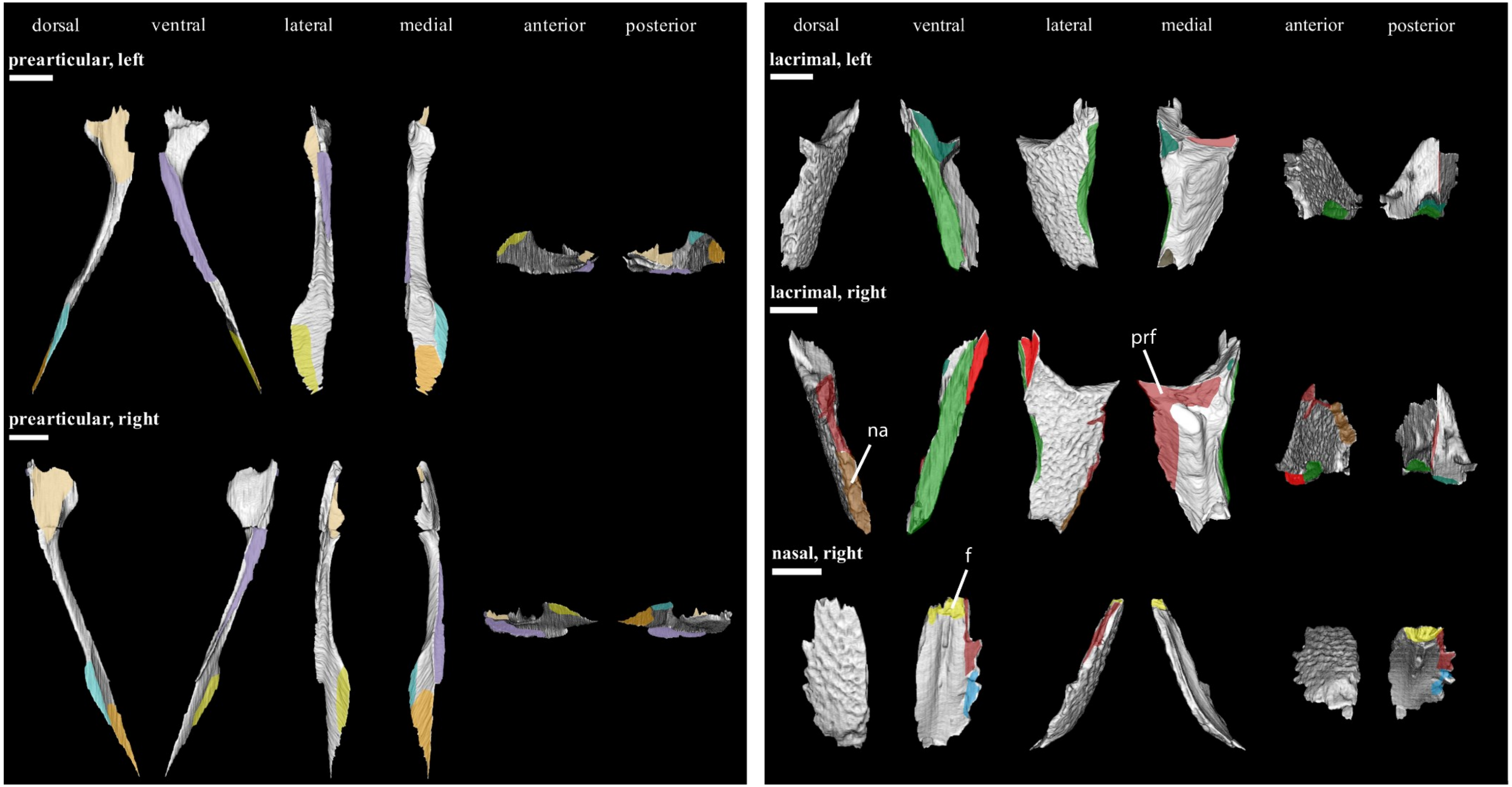

Fig. 19 Isolated bones in dorsal, ventral, lateral, medial, anterior and posterior views. Articulation areas with other bones are colored. Left and right prearticular, left and right lacrimal, and right nasal are shown. Scale bar = 10 mm. For abbreviations see caption to Fig. 15.

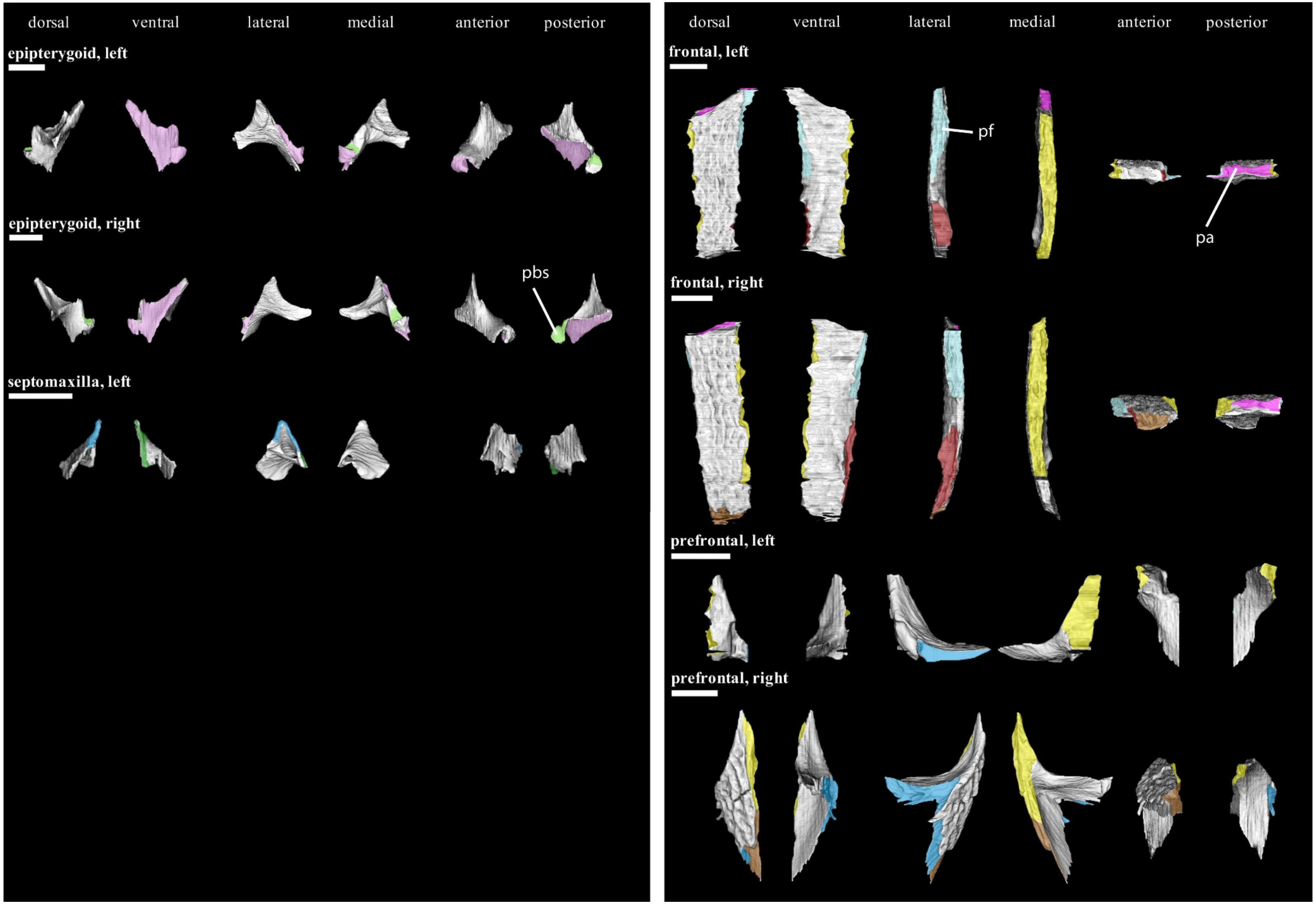

Fig. 20 Isolated bones in dorsal, ventral, lateral, medial, anterior and posterior views. Articulation areas with other bones are colored. Left and right epipterygoid, left septomaxilla, left and right frontal, and left and right prefrontal are shown. Scale bar = 10 mm. For abbreviations see caption to Fig. 15.

Fig. 21 Isolated bones in dorsal, ventral, lateral, medial, anterior and posterior views. Articulation areas with other bones are colored. Left and right pterygoid, left and right palatine, right jugal, and left and right quadratojugal are shown. Scale bar = 10 mm. For abbreviations see caption to Fig. 15.

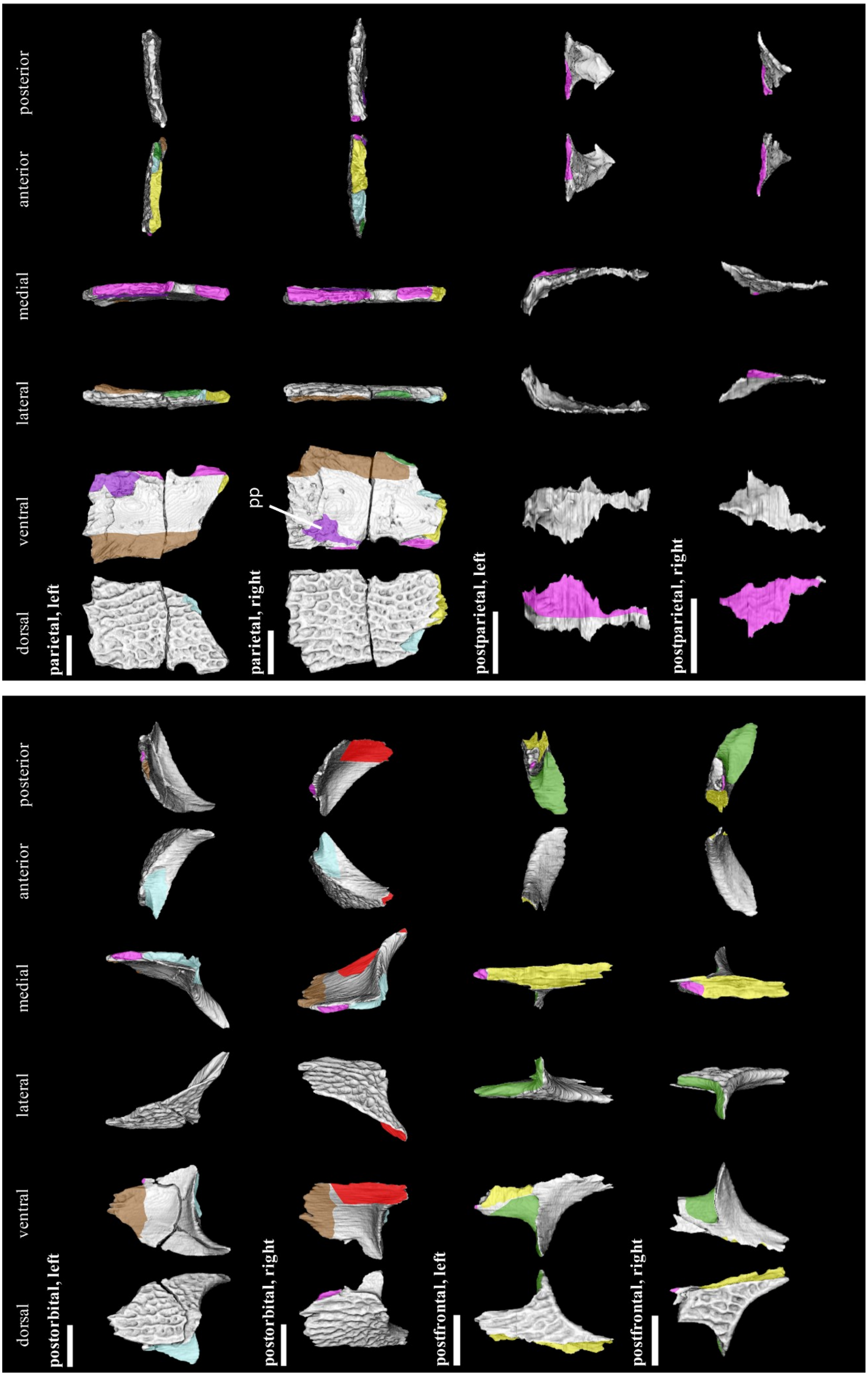

Fig. 22 Isolated bones in dorsal, ventral, lateral, medial, anterior and posterior views. Articulation areas with other bones are colored. Left and right postorbital, left and right postfrontal, left and right parietal, and left and right postparietal are shown. Scale bar = 10 mm. For abbreviations see caption to Fig. 15.

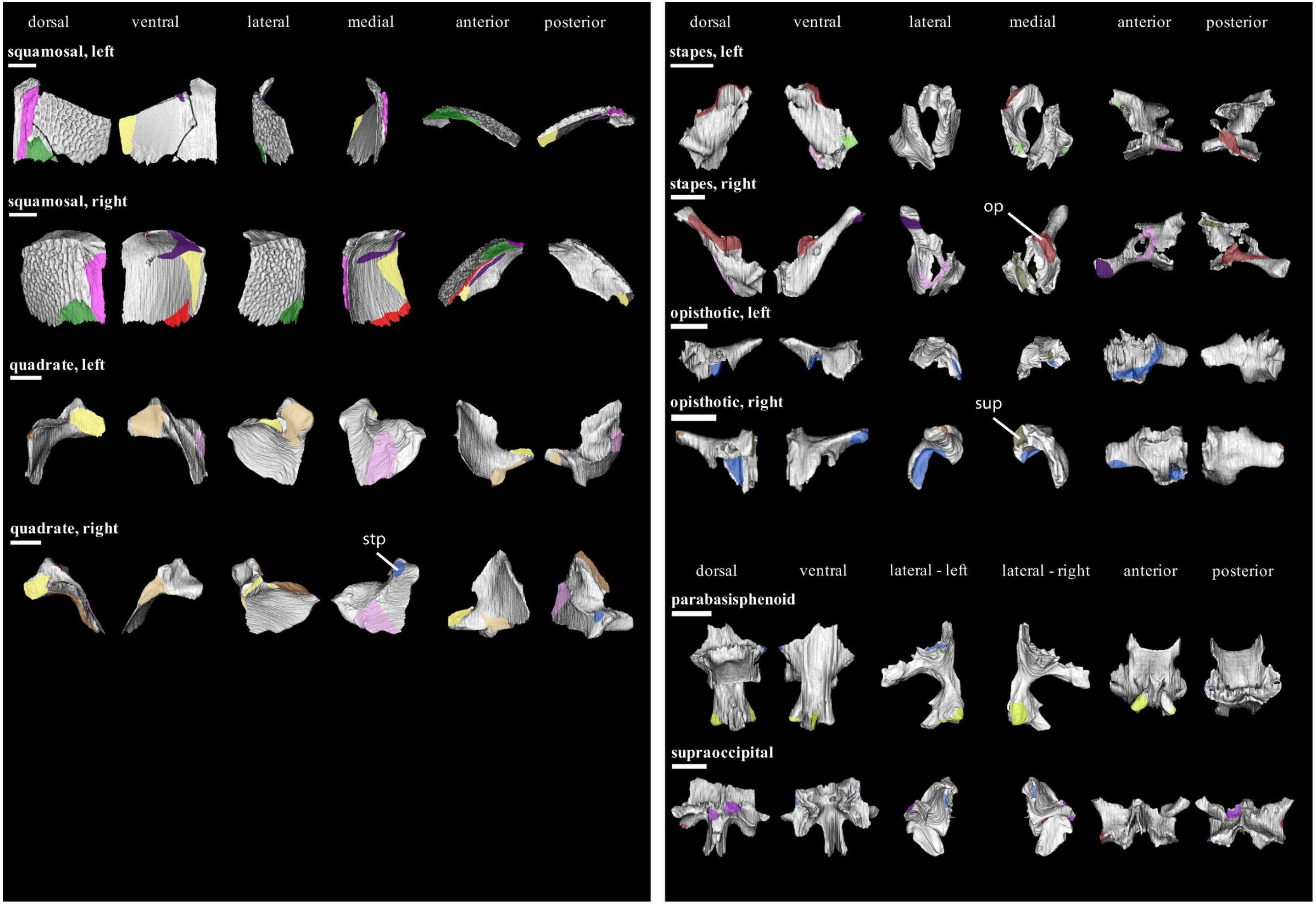

Fig. 23 Isolated bones in dorsal, ventral, lateral, medial, anterior and posterior views. Articulation areas with other bones are colored. Left and right squamosal, Left and right quadrate, Left and right stapes, Left and right opisthotic, parabasisphenoid, and supraoccipital are shown.Scale bar = 10 mm. For abbreviations see caption to Fig. 15.

3.3.5. Suture thickness

The thickness of bones at their sutures varies greatly in the dermatocranium of OMNH 44816 (Suppl. Tab. 2 and Fig. 25). Overall, the thinnest sutural areas in the skull are the anterior palate (0.52–0.79 mm), the intersection of jugal, squamosal, and postorbital (0.46–1.33 mm), the interparietal contact (0.36–1.34 mm) as well as the dorsolateral rostrum (0.78–1.12 mm). The thickest areas are located close to the maxilla (max. 2.93 mm), in the anterior "cheek" (max. 3.56 mm), at the lacrimal-palatine contact (max. 3.55 mm), and between both pterygoids (max. 2.32 mm). Noteworthy trends include a thinning of the jugal-squamosal, jugal-postorbital, and squamosal-postorbital sutures toward the jugal-squamosal-postorbital intersection, as well as a thinning in anterior direction along the sutures between parietal and "cheek."

3.4. Discussion

3.4.1. Suture morphology and strain transmission in OMNH 44816

Sutures connect neighboring skull bones by differently arranged viscoelastic fibers (Herring 2008). In addition to providing sites for bone growth, the main function of sutures is likely the absorption and transmission of strain (e.g., Herring et al. 1996; Herring & Teng 2000; Herring 2008; Moazen et al. 2009; Curtis et al. 2013; even though some theoretical approaches showed only little effect of sutures on strain distribution: see Ferreira et al. 2020). Moreover, soft- and hard-tissue suture morphology is dependent on the presence and, probably, also on the type of strain (e.g., Moss 1957; Herring 1972, 2008; Herring & Mucci 1991). However, osteological evidence alone is not suitable to unambiguously determine the main type of strain affecting a suture (Herring & Mucci 1991; Rayfield 2005). Overall, suture morphology may be used to roughly infer the distribution of strain within the skull and jaw adductor action even when *in vivo* observations are not possible (Herring, 1972).

The eight identified suture types can be broadly subdivided based on their complexity and, hence, their assumed robustness (Herring 2008). Simple butt joints (1 in Fig. 24) like they occur especially in the anterior palate, but also at the prefrontal-nasal and postorbital-parietal contacts, as well as between the parietals, could be interpreted as regions little affected by mechanical stimuli (Moss 1957). Butt joints have been associated with both compressional and tensile strain (Herring & Mucci 1991; Rayfield 2005; Porro et al. 2015), making a more detailed interpretation for OMNH44816 difficult. Compared to other suture morphotypes, butt joints might be least resistant toward stress and strain due to less available attachment area for the fibers (Jones et al. 2011). The slot and tongue-and-groove joints (2 and 3 in Fig. 24) only occur in the preorbital region and adjacent palatal contacts. Tongue-and-groove joints

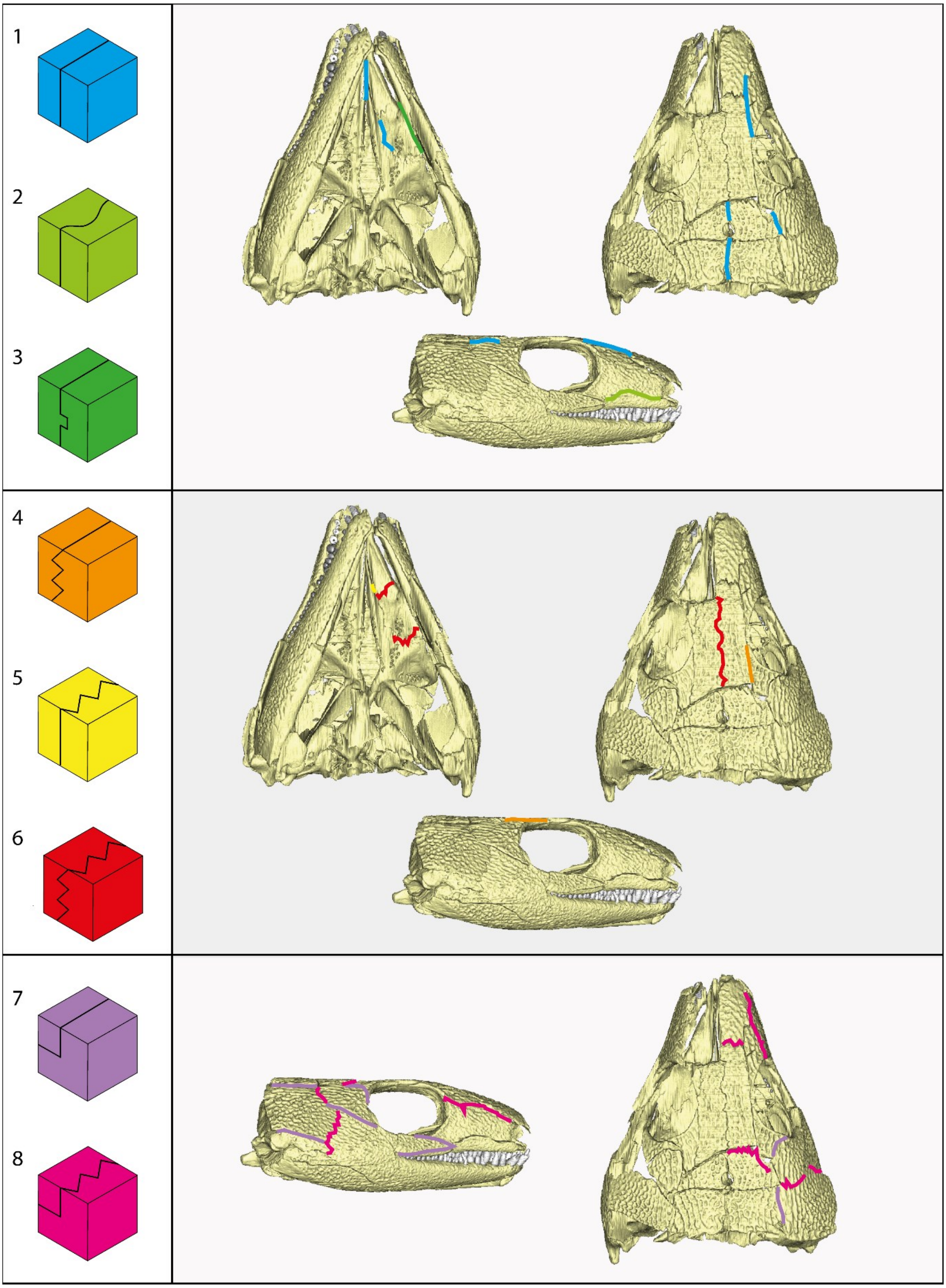

Fig. 24 Suture types observed in the dermatocranium of OMNH 44816 and their position in the skull. 1, butt joint; 2, tongue-and-groove joint; 3, slot joint; 4, Type-A interdigitation; 5, Type-B interdigitation; 6, Type-C interdigitation; 7, stepped joint; 8, stepped interdigitation. Terminology mostly after Jones et al. (2011).

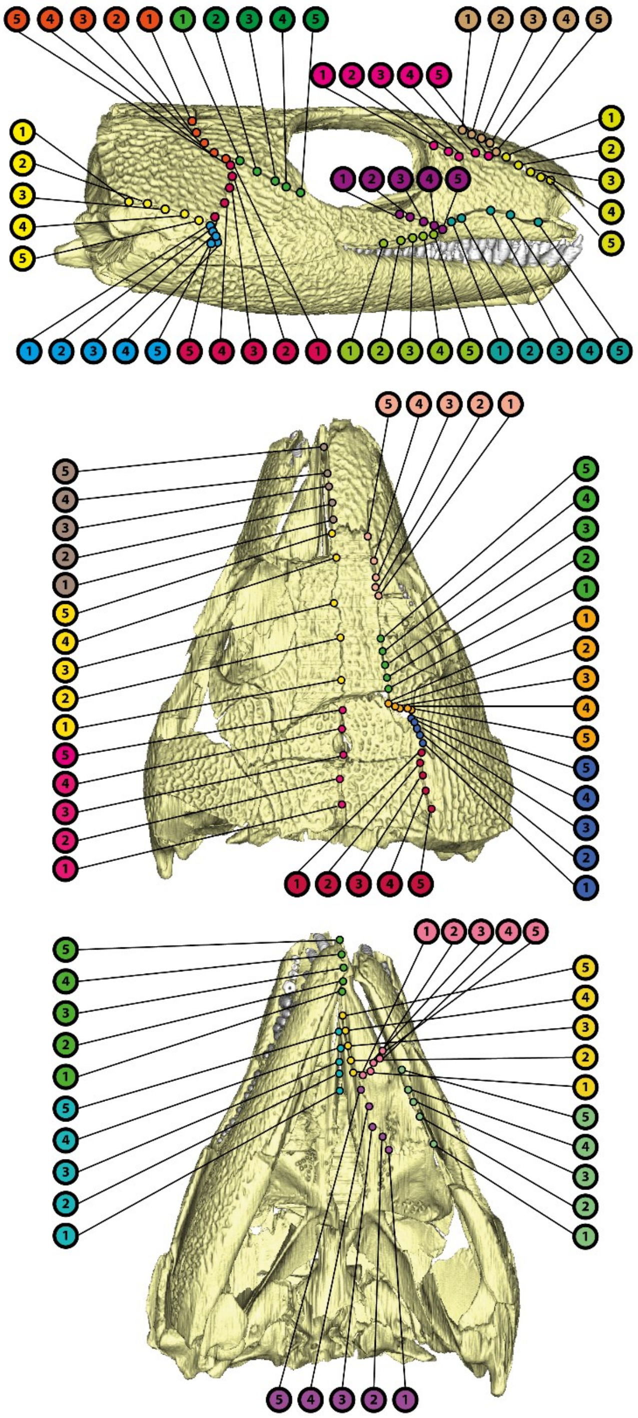

Fig. 25 Points of measurements for suture thickness in OMNH 44816 as indicated in Suppl. Tab. 2.

had been previously interpreted as an adaptation toward tensile strains (Herring & Mucci 1991; Porro et al. 2015; Rawson et al. 2021). Based on their horizontally intercalated geometry, the author would tentatively argue that slot joints are more resistant to compressive than to tensile strains. The majority of the dermal bones in *C. aguti* are connected by stepped joints or stepped interdigitations [7 and 8 in Fig. 24; see also Jones and Zikmund (2012)]. Other types of interdigitations (4, 5, and 6 in Fig. 24) are restricted to the frontal and palatal region. The role of stepped joints appears to be more complex (Rayfield 2005; Porro et al. 2015; Rawson et al. 2021). They might act as a response to shear (Bolt 1974), torsion (Busbey 1995; Clack 2002), or to a combination of tension and compression (Gans 1960; Markey et al. 2006). Robustness of stepped joints might have been higher when the respective bones were additionally connected by external interdigitations (8 in Fig. 24). Generally, interdigitations have been shown to be an adaptation to compression and overall high strains (e.g., Herring 1972; Rafferty & Herring 1999; Rayfield 2005; Markey et al. 2006).

Additionally, suture robustness may be also controlled by interdigitation type. Bones that are only interdigitated at their articulation facet (5 in Fig. 24) may be less resistant to forces acting longitudinally to the suture than bones that are additionally interdigitated at their external surfaces (6 in Fig. 24). Comparably, a lack of interdigitations at the articulation facet may also reduce the resistance to vertical forces (4 in Fig. 24). Overall, a higher degree of interdigitation leads to more available fiber attachment area and thus to a higher resistance toward strain than simpler suture morphotypes (Herring 1972). Also considering thickness measurements, potentially weak areas might have been at the jugal-squamosal-postorbital intersection, at the parietal-postorbital suture, between both parietals, at the dorsolateral rostrum, and in the anterior palate.

These assumptions also allow direct comparisons with the suture morphology described for several Paleozoic non-amniotes (e.g., Klembara 1994; Kathe 1995, 1999; Berman et al. 2010; Porro et al. 2015; Gruntmejer et al. 2019; Rawson et al. 2021), especially when focusing on the temporal region. Interdigitations can be seen in a wide array of taxa, and often developed for more sutures than found in the skull of OMNH 44816 (Porro et al. 2015; Gruntmejer et al. 2019; Rawson et al. 2021); however, there are also numerous examples with less pronounced or absent interdigitations in this part of the skull.

In many cases, morphotypes corresponding to the herein used butt and stepped joints prevail (Klembara 1994; Kathe 1995), arguing that compressional strain on the temporal region was comparatively low. This highlights that strain distribution in the temporal region could differ markedly among Paleozoic limbed vertebrates. Considering that the formation of temporal openings is due to specific distributions of strain within the temporal region (Abel & Werneburg 2021), this might explain why temporal openings occur mainly in amniotes and only in few other clades in which these preconditions are met (see Subchapter 3.4.4.).

The main source of strain within the temporal region is likely related to the action of the jaw musculature (Jones et al. 2011). Indeed, it has been demonstrated that attachment of the jaw adductors is directly related to suture morphology (Herring & Mucci 1991; Herring & Teng 2000). More precisely, forces that are applied onto the cranium by muscle action cause the bony coverage to respond by a strengthening of the affected bones and sutures (e.g., Case 1924; Herring & Mucci 1991; Rayfield 2005; Jones et al. 2011); with stronger sutures inevitably reducing the intracranial mobility in the respective skull areas (Clack 2002). Such forces are expected to be applied especially by direct or indirect action of the jaw adductors (Herring & Mucci 1991; Herring et al. 1996; Rafferty et al. 2000); hence, the focus is on this set of muscles herein. It is appreciated, however, that also neck muscles, related to the posture and movement of the head and being relevant for feeding biology when pulling food items, play a role for the biomechanics of the temporal region (*sensu* Werneburg 2015; Werneburg et al. 2015). As no radical differences in neck mobility are expected among most early amniotes, this is considered as a stable condition among most clades and neck musculature is not discussed any further.

3.4.2. Jaw musculature in *Captorhinus aguti*

3.4.2.a) Challenges of cranial muscle reconstruction

Direct evidence for muscle is usually not preserved in the fossil record. While specific morphological features of bones like processes, ridges, or scars can be used to deduce former muscle attachment sites (e.g., Fox 1964; Heaton 1979; Witzmann & Werneburg 2017), there are also some limitations to a purely osteological approach as muscles may also attach to cartilage or other soft tissue like skin and usually do not leave any trace on the bones (e.g., Romer 1927; Schumacher 1973; Werneburg 2011; Wilken et al. 2019). The development of osteological correlates may be dependent on the type of attaching tissue [fleshy or tendinous; Bryant & Seymour (1990) and references therein; Werneburg 2011, 2013*a*,*b*] and may vary within a species or even between both sides of the skull (Poglayen-Neuwall 1953; Witzmann & Werneburg 2017). Such uncertainties could be met by taking the known myology of comparable taxa into account.

3.4.2.b) Analogs to reconstruct fossil musculature

Comparative anatomical studies show that in tetrapods the jaw adductors generally can be subdivided into an external, internal, and posterior compartment based on their respective position relative to the divisions of the trigeminal nerve (e.g., Luther 1914; Barghusen 1973; Holliday & Witmer 2007; Diogo et al. 2008; Witzmann & Werneburg 2017; Ferreira & Werneburg 2019). Within reptiles, the external jaw adductors [“adductor mandibulae externus” (AME)] usually originate from the dermal bones of the skull roof and “cheek,” and sometimes also from the quadrate or neurocranium. The internal adductors [“adductor mandibulae internus” (AMI)] originate mostly from the palate and the lateral braincase wall. The posterior jaw adductor [“adductor mandibulae posterior” (AMP)] arises from the quadrate. All jaw adductors insert onto the posterior portion of the mandible (Holliday & Witmer 2007; Diogo & Abdala 2010; Werneburg 2011, 2013*a*; Ziermann et al. 2018; Ferreira & Werneburg 2019).

In reptiles, the external adductor (AME) can be usually further subdivided into a lateral [“adductor mandibulae externus superficialis” (AMES)], a deep [“adductor mandibulae externus profundus” (AMEP)], and a medial muscle portion [“adductor mandibulae externus medialis” (AMEM)]; the internal adductors can be subdivided into the pterygoideus (PT), pseudotemporalis (PST), and constrictor internus dorsalis (CID) muscles (Holliday & Witmer 2007; Werneburg 2011; Ferreira & Werneburg 2019; and references in these works). However, variation to this pattern can be observed widely across various taxa (Holliday & Witmer 2007; Daza et al. 2011; Werneburg 2013*a*). Nevertheless, assuming these subdivisions to represent the plesiomorphic condition of extant reptiles, it may be inferred that it also represented the condition in an early-diverging taxon like *C. aguti*. The condition found in mammals is highly derived with a masseter muscle first evolving in Cynodontia (Barghusen 1973; Abdala & Damiani 2004; Werneburg 2013*b*). Homologizations of reptilian to lissamphibian muscles are possible (Diogo & Abdala 2010). Therefore, the ancestral reptilian condition is herein considered as also being ancestral to Amniota as a whole.

Most extant amniotes possess temporal fenestrae, and at least the external jaw adductors are usually associated with the surrounding temporal bars (e.g., Holliday & Witmer 2007; Jones et al. 2009; Werneburg 2019). Consequently, the muscle attachment sites for an extinct taxon with a scutal temporal region like *C. aguti* may not be fully predictable based on these taxa. Considering the shared trait of a skull without temporal fenestrae, turtles instead might be an intuitively fitting extant analog for *C. aguti*. Whereas the majority of extant turtles also possess a distinctly reduced dermal armor in the form of a highly emarginated temporal region (Gaffney 1979; Jones et al. 2012; Werneburg 2012; Abel & Werneburg 2021), some groups like sea turtles as well as the earliest known Testudinata exhibit, like *C. aguti*, a scutal morphology without distinct temporal openings (Gaffney 1990; Jones et al. 2012). However, most current phylogenetic placements of turtles (e.g., Rieppel & deBraga 1996; deBraga & Rieppel 1997; Crawford et al. 2012, 2015; Lyson et al. 2012; Field et al. 2014; Schoch & Sues 2015; Irisarri et al. 2017; Li et al. 2018; Gemmell et al. 2020; but see also Lichtig & Lucas 2021) indicate that they are deeply nested within Diapsida and the scutal morphology in early Testudinata likely derived from a fenestrated ancestor due to selective pressures specific to the turtle skull (Zdansky 1923–1925; Kilias 1957; Werneburg 2015), which also involved a comprehensive rearrangement of soft tissue (Werneburg 2013*a*,*b*) and the suturing of the quadrate to the braincase (Werneburg & Maier 2019). Additionally, the scutal sea turtle skull likely represents a secondary evolution within Testudines and its jaw muscle arrangement is probably different from the one in early Testudinata (Jones et al. 2012; Werneburg, 2013*a*; Ferreira & Werneburg 2019; Werneburg et al. 2019). Hence, while extant turtles can help to predict how the jaw adductors would attach in a scutal skull in general, their derived morphology would limit their applicability for the reconstruction of the jaw musculature in an ancestral “anapsid”.

Yet, comparisons with taxa outside of Reptilia might be even less adequate. As mentioned above, mammalian jaw adductors are distinctly derived from the assumed condition in their early synapsid ancestors and cannot be directly homologized with the reptilian condition (Barghusen 1973; Diogo et al. 2008). Likewise, the specifics of lissamphibian anatomy are largely influenced by metamorphotic developmental events (Haas 2001, 2003; Iordansky 2010; Kleinteich & Haas 2011; Ziermann 2019), and the nearest extant non-tetrapod relatives, Dipnoi, are argumentatively too distantly related to reptiles to provide a good bracketing taxon (but see Werneburg 2019). Taking all into account, the jaw adductors of *C. aguti* may be best inferred from the assumed myology in the last common ancestor of all extant reptiles in the context of a scutal temporal region with respect to the osteological peculiarities of *C. aguti*.

3.4.2.c) Previous reconstructions of captorhinid jaw musculature

Reconstructions and suggestions regarding the jaw musculature of *C. aguti* and other captorhinids have been already provided by previous authors (Adams 1919; Fox 1964; Fox & Bowman 1966; Heaton 1979; Dodick & Modesto 1995). Fox (1964) subdivided the external adductors of *Captorhinus* [“capitimandibularis” in Fox (1964)] into two main sections, the lateral “masseter” (i.e., AMES) and the medial “temporal” (i.e., AMEP) section. Additionally, he discussed also the presence of a third section between the AMES and AMEP, which would likely correspond to the AMEM of diapsids. Fox (1964) argued that the AMEP would have been the largest section and attached to the parietal, postfrontal, postorbital, and squamosal. The AMES would have been sheet-like and originated from the jugal, quadratojugal, and squamosal from where it inserted onto the coronoid process (Fox 1964; Fox & Bowman 1966). If the AMEM was present, Fox (1964) argued it would have been sheet-like and extend from the skull roof onto a bony “knob” anterodorsally to the Meckelian fossa, as observed for extant tuatara [however, this is likely more complicated, see Jones et al. (2009), given also the fact that tuatara has a *bifenestral* skull morphotype with specifically derived muscle arrangements]. In regard of the internal jaw adductors [“pterygoideus” in Fox (1964)], he suggested a subdivision into an anterior (i.e., PT) and a posterior section (i.e., AMP). Fox (1964) let the PT occupy large portions of the dorsal pterygoid surface as well as the lateral surface of the pterygoid flange. He argued it would have extended in a posteroventral direction, medially to the AMEP, and inserted medially inside the Meckelian fossa. The AMP would have been of limited size and attached to the quadrate from where it would have inserted onto the mandible between the jaw joint and Meckelian fossa. Lastly, Fox (1964) also discussed the presence of a pseudotemporalis muscle (i.e., PST), but he argued that if it would have been present, the relative position of the pterygoid would prohibit an arrangement as observed for extant taxa.

Fox (1964) and Fox & Bowman (1966) partly provided osteological arguments for their suggested muscle arrangements. However, in some cases they also argued for particular muscle attachment sites without describing a clear reasoning, or despite the lack of osteological evidence like muscle scars. Nevertheless, the latter is per se legitimated as discussed above as the authors indeed highlighted the impact of different attaching tissues on the presence of osteological correlates. Fox & Bowman (1966) described distinct striae on the medial portion of the parietals close to the suture between these bones, which would likely indicate a tendinous attachment of the AMEP there [however, see Heaton (1979) below for a different interpretation]. Likewise, they interpreted distinct concavities occupying most of the medial parietal surface as likely fleshy attachment sites of the AMEP, because no structures were visible on the internal bone surface. A bony ridge which ran close to the squamosal-parietal suture probably separated the AMEP from the AMES (Fox 1964; Fox & Bowman 1966). Apparently, Fox (1964) also assumed the attachment of the AMES onto the jugal and quadratojugal to be fleshy as he highlighted the smooth medial surfaces of these bones. In the mandible, the AMES would insert onto the surangular portion of the coronoid process at a vertical flange of the surangular that bore two concavities (Fox 1964; Fox & Bowman 1966).

Fox (1964) further argued for a tendinous attachment of the PT onto the lateral pterygoid flange as evident by its size, which he also compared to the condition in crocodiles. According to him, too, the attachment to the dorsal pterygoid surface was likely fleshy. The PT could have inserted onto the ventral and medial surfaces of the angular. A medial groove on the prearticular, bearing pits and striae, might have been another insertion site of the PT (Fox & Bowman 1966). These latter authors suggested that the AMP could have inserted onto a medial ridge formed by the articular and prearticular and a small concavity dorsal to that ridge as indicated by probable muscle scars on both structures. Lastly, based on comparison with tuatara, Fox (1964) suggested that an AMEM with uncertain origin on the skull roof (see above) might have inserted onto a “knob” anterior to the Meckelian fossa.

Heaton (1979) discussed the cranial musculature in the related species *Captorhinus laticeps* Williston, 1909 [“*Eocaptorhinus*” in Heaton (1979)] and other material referred to the genus. In fact, some of the material described by Heaton (1979) and used for his illustrations might be actually referable to *C. aguti*, namely the specimens found at the Dolese Brothers Quarry (Robert Reisz, personal communication, 2021).

Heaton (1979) disagreed with Fox & Bowman (1966) on the interpretation of the medial striae in the parietals of *Captorhinus* being remnants of a tendinous attachment of the jaw adductors. Instead, he argued they were due to attachment of meninx and taenia marginalis. The bony ridge that runs parallel to the parietosquamosal suture identified by Fox (1964) and Fox & Bowman (1966) as the border between AMES and AMEP was recognized by Heaton (1979) as an attachment site solely for the AMES. Other sections of the AMES might have attached to the mediodorsal portion of the squamosal. Also, the ventral concavities of the parietals already reported by Fox & Bowman (1966) as likely attachment sites for the AMEP are, according to Heaton (1979), muscle scars from the AMEM. He argued that the AMEM was further divided into an “adductor mandibulae externus 2 c (pars media C)” and “adductor mandibulae externus 2 a (pars media A)” muscle head (*sensu* Lakjer 1926). The two muscle heads would have been subdivided by the temporal artery, evident by a distinct foramen in the proximity of the mentioned parietal concavity. The “adductor mandibulae externus 2 b (pars media B)" is said to have been attached anteriorly to the concavity, where it left an additional number of muscle scars. A more posterior section of the AMEM would have attached to the quadrate, together with the AMP. Heaton (1979) considered the AMEP to be present; however, he only stated that it would have inserted ventrally to the coronoid like in Fox (1964). For the AMES and AMEM, Heaton (1979) argued that they would have inserted by a joint tendon onto the lateral surface of the surangular.

In addition to the already mentioned AMP, Heaton (1979) identified the PT and PST for the internal jaw adductors. He distinguished between an "anterior" and "posterior" muscle head of the PT [apparently synonymous with "pterygoideus lateralis" and "pterygoideus medius" of Heaton (1979, Figure 24)]. Overall, the PT originated, according to Heaton (1979), from the mediodorsal surface of the pterygoid, including the anterior section of the quadrate process. The PST, subdivided into "pseudotemporalis superficialis" and "pseudotemporalis profundus" after Heaton (1979), originated from the epipterygoid. Heaton (1979) reconstructed a mostly tendinous insertion of the internal jaw adductors onto the mandibular fossa, coronoid, medioposterior prearticular, and onto the medial articular.

The reconstructions of Fox (1964) and Heaton (1979) differ markedly from an earlier proposal of Adams (1919) on the jaw muscles of the captorhinid *Labidosaurus*. Like Fox (1964), Adams (1919) argued that the AMES would attach to the jugal and squamosal, but also to the quadrate instead of the quadratojugal. The AMEP instead would have not been attached to the skull roof, but only to the pterygoid and epipterygoid ["alisphenoid" in Adams (1919)]. He further reconstructed the AMEM as attaching mostly to the parietal and squamosal, which resembles the reconstruction by Heaton (1979) and effectively may be the attachment sites Fox (1964) suggested for the AMEP in *Captorhinus*. Adams (1919) suggested that the external adductors would insert onto the suprameckelian fossa, the PT ventrally onto the retroarticular process. The cranial attachment sites proposed by Adams (1919) for the PT are similar to the ones by Fox (1964) and Heaton (1979); i.e., attaching to the pterygoid]. Adams (1919) did not discuss the AMP and PST. None of the cited references discussed the CID.

3.4.2.d) Reassessment of the jaw adductors in *Captorhinus aguti*

Based on the observations on bone structure and comparisons with published extant amniote jaw muscle anatomy (e.g., Diogo et al., 2008; Daza et al., 2011; Ziermann et al., 2018), the models of Fox (1964) and Heaton (1979) are herein modified and expanded as follows: In model presented herein, the external section consists of a medial (AMEP) and lateral muscle portion. In lateral view, the lateral portion occupies most of the "cheek" region (Fig. 26A). It attaches to the jugal and quadratojugal, and it extends dorsally to the squamosal until it meets the ventral bony ridge of the parietal that runs roughly parallel to the parietosquamosal suture (Fig. 26C).

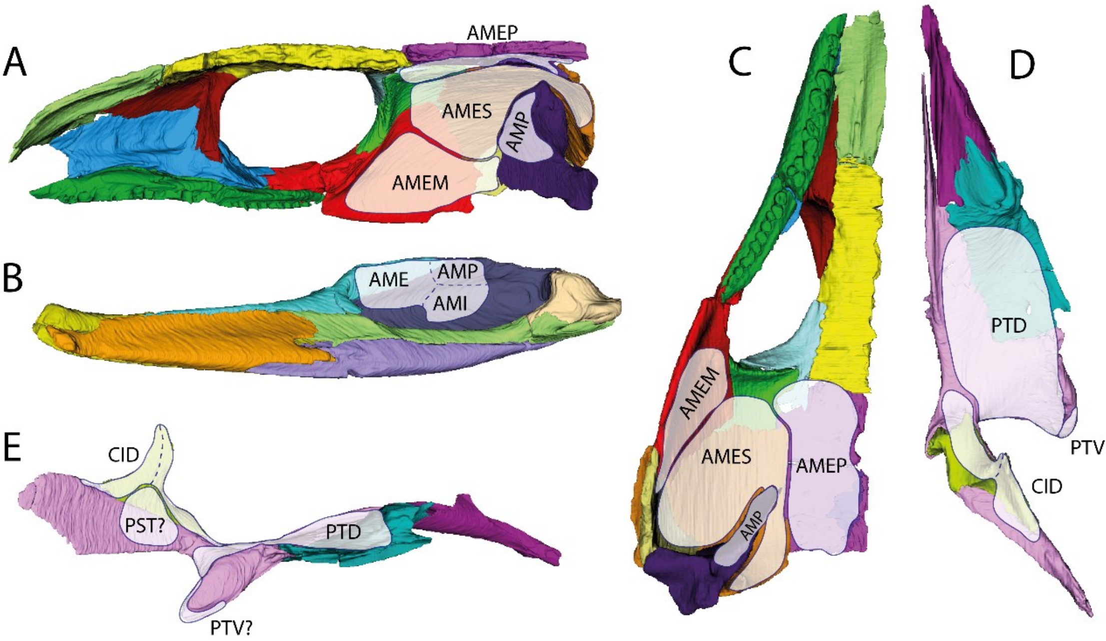

Fig. 26 Rough position of the jaw adductor musculature in the temporal dermatocranium of OMNH 44816 in medial (A) and ventral view (C); as well as of the internal adductor and constrictor musculature in the palate and epipterygoid in dorsal (D) and lateral view (E), and the insertion of all named muscles onto the mandible in medial view (B). AME, adductor mandibulae externus; AMEM, adductor mandibulae externus medialis; AMEP, adductor mandibulae externus profundus; AMES, adductor mandibulae externus superficialis; AMI, adductor mandibulae internus; AMP, adductor mandibulae posterior; CID, constrictor internus dorsalis; PST, pseudotemporalis; PTD, pterygoideus dorsalis; PTV, pterygoideus ventralis.

It is known for marine turtles that the AMES may separate a distinct lateral muscle portion inserting to the broadly armored “cheek” region (Werneburg 2011; Jones et al. 2012). When present, AMEM is known to attach anterolaterally to the quadrate and medially to the quadratojugal in many turtles (Schumacher 1973). As highlighted by Werneburg (2011, 2013*a*), jaw musculature is highly plastic in its anatomy and basically “follows” the arrangements of the temporal skull bones. In this regard, AMEM, which is relatively well-defined in reptiles with temporal fenestration and placed between AMEP and AMES (Holliday & Witmer 2007; Jones et al. 2009), is considered to exhibit a more fluent nature in non-fenestrated forms. That said, the homology of particular muscle portions and muscle heads among reptiles is debatable (Rieppel 1987; Werneburg 2013*a*). By positional criteria, AMES of turtles might be homologous to AMEM in other reptiles, and the AMEM of turtles might be identical with AMES of other reptiles. However, as musculature develops from a consistent cell mass in early ontogeny and differentiates based on perinatal requirements of the respective animal (Werneburg 2019), the developmental fate and differentiation of muscle portions might actually be unique to each individual taxon. Medially to the AMES, in the assessment herein, the AMEP would attach to the postfrontal, postorbital, and parietal (Fig. 26C). Both external adductors would fuse at the height of the squamosal and insert onto the coronoid process of the mandible (Fig. 26B).

The internal adductor section would comprise an anterior (PT) and posterior (AMP) muscle portion, an intercalated pseudotemporalis (PST), and a constrictor internus dorsalis (CID) part. The PT would cover the dorsal face of the dermal palate and reach anteriorly to the palatine as indicated by the smooth transition between palatine and pterygoid (Fig. 26D,E). The PST would attach to the lateral face of the posterior process of the pterygoid, to the (mainly cartilaginous) lateral braincase wall, and maybe with a few fibers to the epipterygoid (*sensu* Heaton 1979; Fig. 26E). The AMP would attach to the anterolateral surface of the quadrate (Fig. 26A). All three muscle portions of the internal adductor section would insert onto the posterior part of the mandibular fossa (Fig. 26B). The CID is here considered to have been present around the epipterygoid, with an anterior and a posterior part, and attach to the pterygoid dorsally (Fig. 26E). It is difficult to reconstruct levator arcus palatini, which would dorsally connect to the skull roof and/or the lateral wall of the braincase and might help to position the palate. Other muscles of the head were not considered for this assessment. Heaton (1979) provided reconstructions of several muscle heads for different muscles, which might be too speculative to discern given the rather unspecific osteological correlates in this fossil.

3.4.3. Cranial kinesis and elasticity in *Captorhinus aguti*

These assessments on suture morphology and jaw adductors allow further inferences on cranial kinesis and elasticity. Cranial kinesis describes the movement of one or more bones relative to other bones or set of bones along intracranial sutures. Among extant tetrapods, it is present in various squamates, birds, and lissamphibians, but effectively absent in mammals, crocodylians, turtles, and tuatara (e.g., Versluys 1910; Frazzetta 1962; Bock 1964; Iordansky 1990; Metzger 2002; Holliday & Witmer 2008; Jones et al. 2011; Natchev et al. 2016; Werneburg & Maier 2019; Yaryhin & Werneburg 2019). The presence and evolution of cranial kinesis has been also discussed for various extinct clades (e.g., Versluys 1910, 1912; Carroll 1969*a*; Bramble & Wake 1985; Iordansky 1990; Clack 2002; Holliday & Witmer 2008; Cost et al. 2020), even though the inapplicability of *in vivo* studies represents a considerable limitation. In fact, intracranial mobility observed in prepared specimens does not necessarily correspond to movements actually exhibited by the living animal [Evans 2008; Holliday & Witmer 2008; however, see also Iordansky (2011)]. Cranial kinesis proper, which describes active movements of skull parts due to muscle action, should further be distinguished from passive elastic/flexible movements of bone and cartilage due to applied strain (Fracasso 1983;

Rayfield 2005; Moazen et al. 2009). Indeed, all skulls require at least some degree of elasticity/flexibility to avoid breakage; hence, “passive kinesis” is also present in skulls that might usually be considered akinetic in terms of cranial kinesis proper (Thomson 1967; Beaumont 1977; Kathe 1999; Herring 2008; Natchev et al. 2016). It is expected that even “stepped joints” and distinctly interdigitated sutures still react elastically to mechanical stimuli, especially when the respective bones are thin in the sutural area (Beaumont 1977; Clack 2002; Natchev et al. 2016). The relationship between elasticity at intracranial sutures and the evolution of cranial kinesis proper is uncertain (Moazen et al. 2009).

Using the examples of lepidosaurs and bird-line archosaurs, Holliday and Witmer (2008) provided a list of criteria that need to be fulfilled to allow cranial kinesis proper. In the following, these criteria are discussed based on observations on OMNH 44816 and whether previously defined types of cranial kinesis (i.e., at the basicranial joint; otic joint; pleurokinesis; metakinesis; mesokinesis; prokinesis; rhynchokinesis) were present in *C. aguti*.

For the condylar basicranial joint (i.e., between the palate and neurocranium), previous observations in other *Captorhinus* specimens (Warren 1961; Heaton 1979; however, see also Olson 1951; Fox & Bowman 1966) that the pterygoid does not directly contact the parabasisphenoid can be confirmed. Instead, the joint is formed only between parabasisphenoid and epipterygoid (see Werneburg & Maier 2019). The basicranial joint is plesiomorphic in tetrapods (Thomson 1967; Beaumon, 1977; Iordansky 1990; Porro et al. 2015) and notably immobilized in extant turtles (e.g., Gaffney 1979; Werneburg & Maier 2019; Ferreira et al. 2020), further highlighting their more derived state relative to early scutal reptiles. Presence of a synovial basicranial joint is the first criterion defined for cranial kinesis (“basipterygopterygoid joint” in Holliday & Witmer 2008); however, whether a condylar joint was indeed synovial is hard to determine for fossil specimens (Bailleul & Holliday 2017) and even if present, it might not necessarily imply any form of cranial kinesis proper (Holliday & Witmer 2008; Johnston 2010; Payne et al. 2011). Nevertheless, using a modularity approach of skull network integrity, a clear distinction between the palate and epipterygoid on one side and the braincase on the other side suggesting the presence of ancestral basicranial mobility in *C. aguti* can be reconstructed (see Chapter 4). This methodology might be understood as additional line of evidence to understand intracranial mobility (Werneburg & Abel 2022).

Iordansky (1990, 2011, 2015) considered pleurokinesis (i.e., mediolateral movement of the quadrate together with other “maxillobuccal” segments relative to the axial parts of the skull) to be present in the earliest amniotes [“reptiles” in Iordansky (1990, 2011, 2015)]. Indeed, the butting contact of the quadrate with the quadrate wing of the pterygoid as well as the probable attachment site of the AMP suggest that some degree of mediolateral movement could have been possible in the quadrate of *C. aguti*. Yet, this was certainly restricted by the contact of the quadrate with the quadratojugal and squamosal. In fact, a condylar and, therefore, potentially synovial otic joint like it can be observed in many later diverging taxa is not observable in OMNH 44816, *C. aguti* thereby lacked an important criterion for cranial kinesis *sensu* Holliday & Witmer (2008). Similar to the basicranial joint, pleurokinesis has been considered to be the plesiomorphic condition in tetrapods (Iordansky 1990) and proposed for various extant and extinct taxa like lissamphibians (e.g., Iordansky 2000; Natchev et al. 2016), squamates (e.g., Iordansky 2004, 2015), or ornithopod dinosaurs (e.g., Norman & Weishampel 1985); however, unambiguous evidence for active pleurokinesis in any of these taxa is rare at best, if present at all (Evans 2008; Holliday & Witmer 2008; Cuthbertson et al., 2012; Heiss & Grell 2019; but see also Chapter 4).

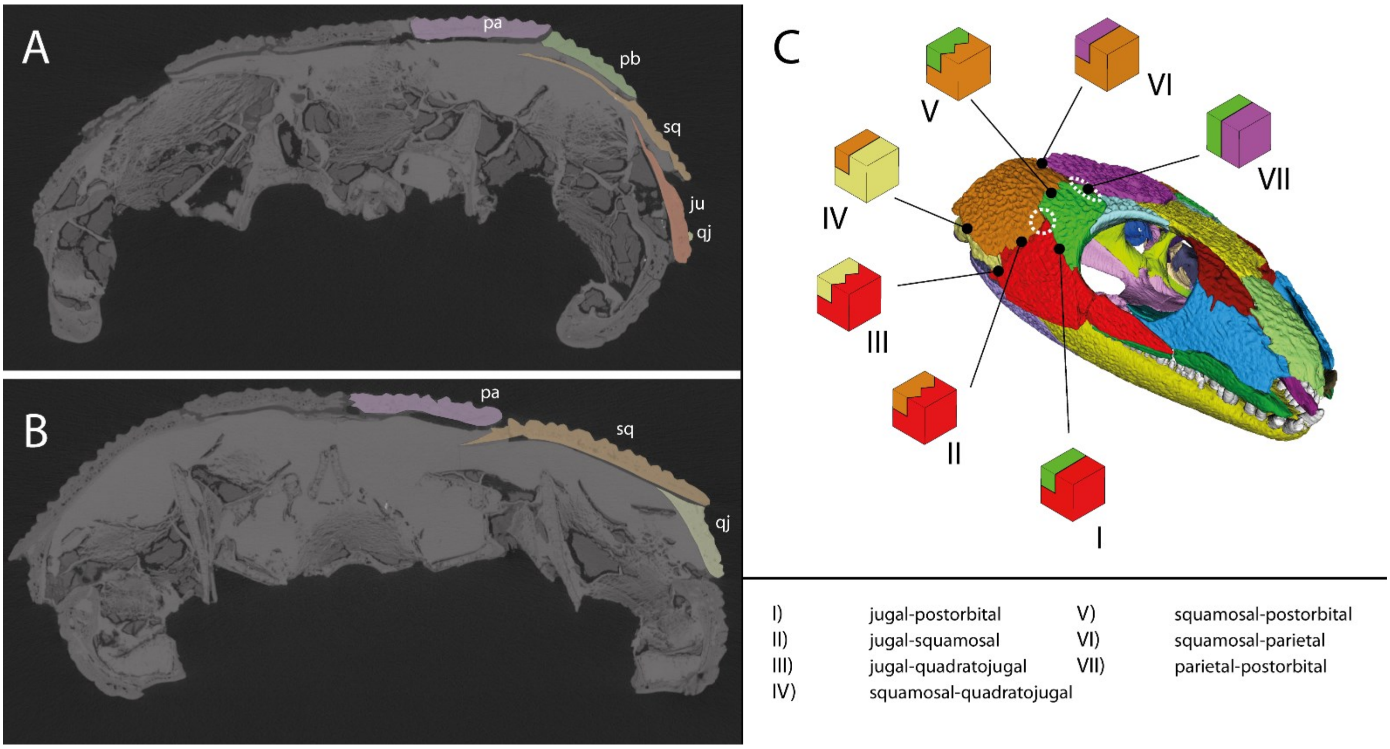

Fig. 27 Cross section through the temporal region of OMNH 44816 in posterior view highlighting the internal contacts of the dermal bones. (A) Anterior temporal region; (B) posterior temporal region. (C) 3D view on the dermal sutures in the temporal region of OMNH 44816. Dashed lines indicate potentially weak areas that could correspond to temporal openings in other early amniotes.

A metakinetic joint (i.e., movement of the temporal dermatocranium, together with the snout, relative to the occiput; Frazzetta 1962) has been repeatedly described for early amniotes (e.g., Versluys 1912; Carroll 1969*a*; Gow 1972; Bramble & Wake 1985; Iordansky 1990), even though its nature in extant taxa has remained barely understood until recently (Mezzasalma et al. 2014; Handschuh et al. 2019), where it is mainly present in squamates (Evans 2008; Jones et al. 2011), but maybe also in some other tetrapods (Natchev et al. 2016). In OMNH 44816, bony contacts between the temporal dermatocranium and the braincase are only present between the postparietal and supraoccipital, as well as between squamosal and opisthotic. Based on other *Captorhinus* specimens, the supraoccipital was also dorsally sutured to the parietal by a bony process (Fox & Bowman 1966; Heaton 1979) and might have been also sutured to the squamosals (Price 1935). Even though captorhinids shared with later-diverging taxa the loss of the tabulars (e.g., Modesto et al. 2007), especially the retained contact between postparietals and supraoccipital argues against any major mobility in the metakinetic axis of *C. aguti* (Evans 2008). Werneburg & Abel (2022) found the braincase to form a separate functional module in *C. aguti*, which would argue for some form of metakinesis or for a weaker connection at the metakinetic axis at least that could serve as a precondition to establish metakinesis later in evolution (see Chapter 4).

Mesokinesis (*sensu* Frazzetta 1962; i.e., active movements of the parietals relative to the frontals) can be excluded for *C. aguti* based on the stepped interdigitation between the respective bones. In fact, mesokinesis can be considered a highly derived condition mostly restricted to squamates and some caudates (Frazzetta 1962; Bramble & Wake 1985; Natchev et al. 2016). However, this does not necessarily exclude any form of elasticity in the frontoparietal region (Natchev et al. 2016; Werneburg & Abel 2022). When the jaw was closed in *C. aguti*, the AMEP probably exerted a pulling force on the parietals relative to the frontals, distributing force onto the frontoparietal suture, eventually triggering the development of a more complexly stepped interdigitation there. Nevertheless, the comparatively high thickness in the sutures of the frontal region in *C. aguti* (Suppl. Tab. 2) as well as the external bony ridges might additionally have decreased the degree of elastic movements. Werneburg and Abel (2022) found a modular distinction between frontals and parietals, but based on the results presented herein, they basically refuted mesokinesis in *C. aguti*. The distinction between two modules in this area of the skull might hint at functionally differentiated skull parts in *C. aguti* - that moved against each other by elasticity as assumed herein - or to an ancestral differentiation of the skull inherited from more rootward tetrapods.

Likewise, action of AMEM (of the reconstruction herein) and AMES onto the “cheek” might have also exerted pulling forces on the jugal, squamosal, and postorbital. Being overall thinner than the parietal, elasticity was probably generally higher in the “cheek” than in the skull roof. Like in the frontoparietal suture, the pulling force on the “cheek” likely selected for a similarly stepped interdigitation between these bones (Fig. 27C, sutures II, III, V). Yet, the contact of the parietals with the “cheek” is less complex and might even be considered “weak” (Frazzetta 1968). However, this area seems to be more stabilized against torsion due to the lamina extruding from the squamosal medially to meet a medioventral ridge of the parietal (Fig. 27B). Only the parietal-postorbital contact still appears to be simple (Fig. 27A). Nevertheless, the high modular integrity of the postorbital within the dermatocranium and the more complex sutures to its neighboring bones, as well as the parietal-squamosal contact, likely restricted further mobility (see Chapter 4). Yet, the simple nature of the parietal-postorbital suture could indicate that it was less affected by compressional forces than the other sutures in the temporal region (Fig. 27C).

A joint between the snout and more posterior parts of the skull, as it occurs in most batrachians, snakes, and birds (prokinesis, rhynchokinesis; Bock 1964; Iordansky 1990), can be excluded for *C. aguti*. The frequently stepped interdigitations in the snout likely evolved to withstand the forces generated from the interaction between the tooth-bearing maxilla and food items (Jones & Zikmund 2012). This is further evident by the relatively thick sutures between the maxilla, lacrimal, and jugal. The force was probably absorbed by the thinner and, hence, more elastic sutures in more dorsal areas of the snout (between lacrimal, nasal, and prefrontal). Analogous to the parietal-postorbital suture, the simple frontal-prefrontal suture might indicate that this skull area was less affected by compressional forces generated during biting (see also Chapter 4), but again the high integrity of the prefrontal, as well as the thicker suture, argues against any major mobility.

The derived condition and possible mobility of the palate in *Captorhinus* and other early amniotes has been highlighted by previous authors (Fox 1964; Carroll 1969*a*; Bramble & Wake 1985; however, see also Heaton 1979, for an opposing view). At the anterior end of the palate, both vomers as well as both pterygoids were likely only loosely connected to each other. Likewise, the articulation between vomer and premaxilla was likely rather simple (Fox & Bowman 1966). As described by Fox (1964) and Fox & Bowman (1966), and confirmed by the observations herein, there was a joint between the palatine and maxilla that could, on its own, have allowed some rotational movement of the palate. Yet, the author agrees with Bolt (1974) that in *C. aguti* the palatine also sutured to the lacrimal, which would have restricted rotational motion. Further restriction was likely caused by the anterolateral contact of the pterygoid with the jugal. It was not possible to confirm a contact between palatine and the ventral process of the prefrontal (see Williston 1925; Bolt 1974). While there was no true kinetic joint between the palatine, vomer, and pterygoid, the relatively thin palatines suggest that the middle palate was quite elastic and would have bent dorsally by action of the dorsally attaching PT when the jaw was closed. The epipterygoid is ancestrally not fused to the braincase (as in mammals, turtles, and crocodylians) in *C. aguti,* suggesting the presence of the epipterygoid-associated CID musculature. Together, they might have permitted a certain pro- and retraction of the palate relative to the rest of the skull. The differentiation of CID into a "protractor pterygoidei," another criterion for cranial kinesis proper in lepidosaurs and bird-line archosaurs (Holliday & Witmer 2008), cannot be confirmed for *C. aguti*.

In summary, none of the traditionally defined types of cranial kinesis can be unambiguously confirmed for *C. aguti*. While it cannot be excluded that at least some of the criteria by Holliday & Witmer (2008) could have been fulfilled by *C. aguti* (i.e., synovial basicranial joint, m. protractor pterygoideus), it might be concluded that *C. aguti*, and likely also other early scutal reptiles, were functionally akinetic in terms of cranial kinesis proper. Nevertheless, due to observed differences in suture morphology and thickness, the degree of passive elastic movements is expected to differ depending on the respective skull part and, also, between different parts of the temporal dermatocranium. It may be highlighted that the criteria of Holliday & Witmer (2008) were erected for and nicely apply to extant diapsids, but the discussion herein might motivate future studies on intracranial mobility beyond traditional perceptions and categorizations.

3.4.4. Cranial mechanics and the evolution of temporal openings

Taking the morphological considerations herein, as well as comparisons with other taxa into account, it is possible to roughly reconstruct the cranial mechanics in *C. aguti* that likely applies also to other early scutal reptiles. This may offer new insights into the evolution of the amniote temporal region and allows to infer how temporal openings might have formed in early amniotes.

It can be debated whether *C. aguti* actually represents a suitable model for this approach. As stated previously, the presence of several derived traits in the skull of *C. aguti* as well as its geological age urge to caution in using it as an analog for the condition in the hypothetical ancestral amniote. To complicate things further, interrelationships at the base of Amniota are still widely discussed (e.g., Laurin & Piñeiro 2017; MacDougall et al. 2018; Klembara et al. 2019; Mann et al. 2019, 2021; Ford & Benson 2020). Hence, the ancestral morphology of the amniote skull, and especially the point of when as well as how often temporal openings appeared, is difficult to reconstruct (Laurin & Piñeiro 2017; Ford & Benson 2020; see also Subchapter 2.3.1.e). However, due to reasons mentioned in Subchapter 3.1., *Captorhinus aguti* may well be, for now, an acceptable representative to investigate the origins of temporal fenestration in ancestral amniotes (see also Maier 1993, 1999). In this chapter, differences and similarities between *C. aguti* and other taxa, notably earlier captorhinids, "protorothyridids", and some other early potential amniotes will also be further discussed.

In case of the “cheek,” the cranial mechanics of *C. aguti* can be generally described as outlined by Fox (1964). Contraction of the AMES/AMEM (as reconstructed herein) would have exerted a ventromedial bending of the bones in the “cheek” region. Additionally, the quadrate would have directed force from posterior onto the squamosal and quadratojugal. This might explain the more stabilized squamosal-quadratojugal contact by the distinctly extruding bony lamina from the quadratojugal medial to the squamosal (Fig. 27B). The observation of Fox (1964) that there is a thin area at the intersection of jugal, squamosal, and postorbital (Suppl. Tab. 2) can be confirmed, suggesting that it was less affected by muscle forces. Appropriately, the interdigitation that runs dorsoventrally to form most of the anterior contact of the squamosal with jugal and postorbital becomes a less complex suture in the intersection area of the three bones. Fox (1964) reports further that the marginal areas of the “cheek” were strengthened in *Captorhinus* by medially aligned ridges that might have also served as muscle attachment sites (at least for the stronger tendinous attachments, see above). This is also backed up by the author's observations. According to the latter, these would also correspond to the external patterns of bone ornamentation, probably another response to force distribution. Such a “network of lines of stress” (Olson 1961) on its own might select against ossification in lesser loaded areas of the “cheek,” eventually forming an opening (e.g., Case 1924; Olson 1961; Fox 1964). Intersections between more than two bones like they occur in the “cheek” of *C. aguti* (Fig. 27C) might be especially prone to forming a temporal opening (Frazzetta 1968; Kuhn-Schnyder 1980; Werneburg & Abel 2022).

Indeed, there is more evidence for this scenario in other taxa. Next to their typical infratemporal fenestra between jugal, squamosal, and postorbital, some specimens of the early synapsids *Ophiacodon retroversus* Cope (1878) and *Varanosaurus acutirostris* Broili 1904 also exhibit an “accessory temporal fenestra” at their thinned jugal-squamosal-quadratojugal intersection; sometimes even restricted to only one side of the skull (Romer & Price 1940; Frazzetta 1968; Berman et al. 1995; Ford 2018; see Chapter 1). In the usually non-fenestrated parareptile *Procolophon trigoniceps* Owen 1876, small infratemporal fenestrae can appear in-between different sets of three to four bones (Cisneros 2008). Moving more rootward, Jaekel (1902) reported for the possible amniote-line tetrapod *Gephyrostegus bohemicus* thin regions in the “cheek” and parietal area, presumably fitting to the position of

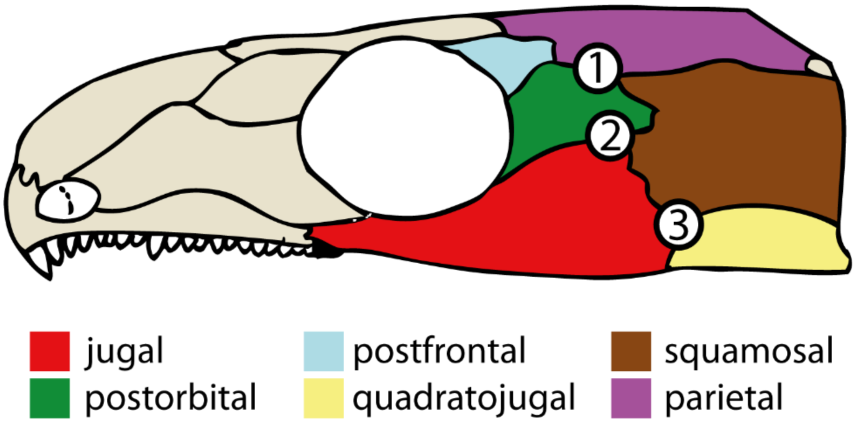

Fig. 28 Drawing of the skull of *Captorhinus aguti* after Fox and Bowman (1966) with possible origin sites for temporal openings in the hypothetical ancestral amniote. 1, squamosal-postorbital-parietal intersection; 2, jugal-squamosal-postorbital intersection; 3, jugal-squamosal-quadratojugal intersection. Sites 1 and 2 are the most likely origin sites for a taxon similar to *Captorhinus*. Site 3 occurs especially in Parareptilia. Temporal openings in early Synapsida and Diapsida formed probably by fusion of two of such origin sites (see also Werneburg & Abel, 2022).

temporal openings in later amniotes. These traits have not been mentioned in a recent reassessment of the species (Klembara et al. 2014) and so far, the author was not able to study the fossils in person to confirm or refute Jaekel's (1902) observation. Conclusively, it might be nevertheless rather easy to form small temporal openings within thin bone intersections, with their occasional presence representing no major disadvantage for the animal (Romer & Price 1940; Cisneros 2008).

While the author currently does not possess data on relative suture thickness in other early scutal tatrapods, a jugal-squamosal-postorbital intersection like observed in *C. aguti* is widespread among scutal taxa close to the amniote base (e.g., Clark & Carroll 1973; Berman et al. 1988; Boy & Martens 1991; Modesto et al. 2007; Kissel 2010). Like infratemporal fenestrae, these intersections vary in their relative position in the "cheek," probably related to differences in muscle force distribution. In fact, the latter is thought to play a significant role for the formation of temporal openings during early ontogeny (Werneburg 2019). Such variation in jaw adductor arrangement might also explain why in many parareptiles the infratemporal fenestra is located within the jugal-squamosal-quadratojugal intersection instead (MacDougall & Reisz 2014; 3 in Fig. 28), whereas in many non-sphenacodontian synapsids as well as in some early diapsids, jugal, squamosal, postorbital, and quadratojugal form the margin of the infratemporal fenestra (Romer & Price 1940; Ford & Benson 2020). In regard of the condition in non-sphenacodontian synapsids and early diapsids, the formation of the fenestra may be explained by a larger weak area in the "cheek" incorporating both discussed three-bone-intersections. Alternatively, the formation of "accessory temporal fenestrae" like observed for some ophiacodontids as mentioned above could have led to a later fusion of two separate temporal openings (see also Chapter 4).

In fact, this is congruent with the author's observations on *Protorothyris archeri* Price, 1937 (MCZ 1532, 2148; Museum of Comparative Zoology, Harvard, United States), a close relative of Diapsida, which still possessed a scutal morphology (e.g., Müller & Reisz 2006; MacDougall et al. 2018; Ford & Benson 2020). *P. archeri* is similar to *C. aguti* in regards of the jugal interdigitating with the squamosal posteriorly. Likewise, the parietal overlaps the squamosal, and there also seems to be a butt joint between parietal and postorbital. However, it differs from *C. aguti* by the lack of interdigitation in the postorbital-squamosal suture and the simpler contact between jugal and quadratojugal. These might be suitable preconditions for the formation of two pairs of temporal fenestrae in the diapsid ancestor. Yet, as the author currently has no information on relative suture thickness in *P. archeri*, segmentation of a microCT-scan like herein applied to OMNH 44816 would be needed to further elaborate on this hypothesis.

There are more reasons to assume that as a model captorhinids alone might not be able to explain the whole morphological diversity of the temporal region in early amniotes. An infratemporal fenestra corresponding to the weak area in *C. aguti* (i.e., within the jugal-squamosal-postorbital intersection; 2 in Fig. 28) occurs mostly, likely as a derived trait, in taxa with a reduced quadratojugal (e.g., Romer & Price 1940; Modesto & Reisz 1990), sometimes by also involving the parietal (Modesto 1995; Lucas et al. 2018). In fact, while especially moradisaurine captorhinids likely evolved larger external jaw adductors in context of their derived herbivorous lifestyle, neither they or any other known captorhinid evolved an infratemporal fenestra like it can be observed in coeval herbivorous synapsids, but enlarged their adductor chamber instead (Dodick & Modesto 1995; Sues & Reisz 1998). This might be due to other constraints like skull flattening during ontogeny, especially in more deeply nested captorhinids (Heaton 1979). Indeed, skull doming and accompanying changes in jaw adductor orientation has been repeatedly argued to be necessary for the initial evolution of temporal openings (Olson 1961; Frazzetta 1968; Tarsitano et al. 2001; see Chapter 2), even though it might have been the opposite in lissamphibians (Schoch 2014). There might be also a phylogenetic signal due to herbivorous synapsids retaining their fenestrae from their fenestrated non-herbivorous ancestors. Considering this and other peculiarities of the captorhinid temporal region, notably the loss of the tabular and the distinctly reduced supratemporal (e.g., Fox & Bowman 1966; Dodick & Modesto 1995), it emphasizes that even early scutal radiations like captorhinids might not offer a “perfect” analog for the ancestral amniote.

Lastly, the probably weak connection between the parietal and “cheek” (i.e., postorbital and, to a lesser degree, squamosal) could have been related to what Kemp (1980) called the “crossopterygian hinge line,” a mobile joint presumably inherited from tetrapodomorph fishes and retained as a loose contact between squamosal and supratemporal in probable amniote-line tetrapods and other early limbed vertebrates (Panchen 1964; Thomson 1967; Frazzetta 1968; Kemp 1980; Klembara et al. 2014).

In this regard, Kemp (1980) highlighted that the temporal region of early synapsids plesiomorphically bears large supratemporals and tabulars; thus, they differ from *C. aguti* and other early non-diapsid reptiles. Kemp (1980) suggested that the synapsid fenestra originated between postorbital, squamosal, and supratemporal by attaching the jaw adductors around the former “crossopterygian hinge line.” The postorbital would have later extended posteriorly along the lateroventral margin of the supratemporal. The argumentation of Kemp (1980) implies that the synapsid fenestra would have subsequently expanded to also incorporate the jugal and quadratojugal into its border. The possible role of the “crossopterygian hinge line” has been also discussed by others (Frazzetta 1968; Gow 1972; Werneburg & Abel 2022). In regard of the parareptile *Milleretta rubidgei* Broom 1938, which possessed a small opening between the jugal, squamosal, and postorbital that was presumably closed in adult specimens, Gow (1972) argued that a firm suture between squamosal and skull roof was present. This would have led to the formation of a “line of weakness” between the squamosal, jugal, and quadratojugal in *M. rubidgei* at whose dorsal end the opening formed. A similar case might have been also present in the embolomere *Anthracosaurus russelli* Huxley 1863, which differs from other anthracosaurs by interdigitation of the suture between skull roof and “cheek” as well as the formation of an infratemporal fenestra between jugal and squamosal, adjacent to the jugal-squamosal-quadratojugal intersection (Panchen 1977; Clack 1987*a*).

It is worth noting that there are several other interpretations of this presumed “hinge line,” which either has been argued to represent a taphonomic phenomenon (Reisz & Heaton 1980), a misinterpretation of the sutures (Berman et al. 2010) or, if present, to be of little functional relevance (Clack 1987*b*). Also, given that the jugal seems to be always involved in the infratemporal fenestra of early synapsids, the author considers it more parsimonious that the fenestra would form within one of the three-bone intersections discussed above. This would also apply to other taxa like diapsids or especially to those in which the postorbital does not contribute to the infratemporal fenestra like in *A. russelli* or many parareptiles. Moreover, an infratemporal fenestra bordered by the jugal might still develop if there is a weaker contact between the skull roof and “cheek” (Frazzetta 1968). Nonetheless, a contact as observed for *C. aguti* and probably other scutal non-diapsid reptiles might have implications for the formation of the diapsid supratemporal fenestra (see also Chapter 4).

When the jaw was closed in *C. aguti*, contraction of the AMEP would have exerted a pulling force with the parietals bending in ventral direction, concentrating the main forces onto the anterior and posterior ends of the parietals, while their lateral contacts to the “cheeks” would have been less affected. Like discussed in the previous subchapter, this could have maintained the plesiomorphically interdigitated suture found between parietals and frontals. Indeed, such an interdigitated frontoparietal suture can be also observed in many other species close to the amniote base, including other captorhinids; even though with a varying degree of complexity (e.g., Clark & Carroll 1973; Gaffney & McKenna 1979; Heaton 1979; Dodick & Modesto 1995; Kissel et al. 2002; Müller & Reisz 2005; Modesto et al. 2007; Kissel 2010).

The simpler contacts of the parietal to the squamosals and postorbitals fit the interpretation as less affected areas. Analogous to the formation of the infratemporal fenestra, the less loaded parietal-postorbital and parietal-squamosal contacts could be selected to form a temporal opening. Especially the simple parietal-postorbital contact would be affected by this. In moradisaurine captorhinids with their enlarged adductor chamber, the sutures between skull roof and “cheek” appear to be more strengthened than in *C. aguti* (Dodick & Modesto 1995), whereas in other early non-diapsid reptiles, including the ones closest to diapsids (e.g., *Protorothyris* Price, 1937), the parietal simply overlapped the postorbital and squamosal (Carroll 1969*b*; Carroll & Baird 1972; Clark & Carroll 1973), indicating that the ancestor of diapsids still possessed a comparatively weak suture there and, hence, the suggested precondition to form a supratemporal fenestra (1 in Figure 28). The question remains why an amniote supratemporal fenestra has only evolved in diapsids. Observation of a weaker contact between skull roof and “cheek” in some early synapsids (Frazzetta 1968) might suggest that the potential to evolve a more dorsal fenestra was also present in synapsids. Indeed, expansion of the infratemporal fenestra toward the parietals in early therapsids and other sphenacomorph synapsids (Boonstra 1936; Romer & Price 1940; Modesto 1995; Kammerer 2011) could have been enabled by a still rather weak connection in that region of the skull.

There might be other factors involved for the lack of temporal openings in most other early limbed vertebrates (see also Subchapter 1.6.). These include a less mobile head-neck joint (Panchen 1964; Kuhn-Schnyder 1980), differing jaw mechanics (Olson 1961; Clack 1987*b*) with a, hence, different role of the external jaw adductors, eventually affected by differences in ontogenetic strategies (Werneburg 2019). Studies on fenestrated lissamphibians (e.g., Paluh et al. 2020) could also provide more insights into morphological patterns underlying tetrapod temporal openings. However, more detailed data on the suture morphology of lissamphibians and other non-amniotes is needed to comprehend the biomechanical differences between fenestrated and non-fenestrated taxa.

3.5. Conclusions

The reconstruction of the likely arrangement of jaw adductors and cranial mechanics in *Captorhinus aguti* highlights the biomechanical differences between the non-fenestrated skull of an early reptile with equally non-fenestrated skulls in extant turtles and possible extinct amniote-line tetrapods. Previous observations of a comparatively thin area in the jugal-squamosal-postorbital intersection (2 in Fig. 28) could be confirmed but also another thin area for the parietal-postorbital contact (1 in Fig. 28) has been reported. These correspond to the position of temporal fenestrae in other early amniotes, corroborating the hypothesis that such openings formed due to the reduction of less loaded areas. Yet, consideration of captorhinid evolution also emphasizes that an increasing role of the external jaw adductors does not necessarily lead to the formation of temporal openings. Hence, even a generalist captorhinid like *C. aguti* might not be the best analog for the ancestor of fenestrated amniotes. Future studies on taxa closer to early fenestrated amniotes (e.g., "protorothyridids") or of different early diverging taxa (e.g., embolomeres, *G. bohemicus*, seymouriamorphs, "lepospondyls", diadectomorphs), as well as quantitative approaches, might further deepen our understanding of the early evolution of temporal openings.

Chapter 4

Modeling skull network integration at the dawn of amniote diversification with considerations on functional morphology and fossil jaw muscle reconstructions

A modified version of this chapter has been published as:

Werneburg, I., and **Abel, P.** (2022). Modelling skull network integrity at the dawn of amniote diversification with considerations on functional morphology and fossil jaw muscle reconstructions. *Frontiers in Ecology and Evolution* 9, 799637.

Author contributions:

Author	**Concept [%]**	**Script [%]**	**Analysis [%]**	**Illustrations [%]**	**Writing [%]**	**Providing of funding [%]**
Werneburg, I.	80	0	50	80	90	100
Abel, P.	20	100	50	20	10	0

4. Modeling skull network integration at the dawn of amniote diversification with considerations on functional morphology and fossil jaw muscle reconstructions

4.1. Introduction

The evolutionary transition from a mostly aquatic to a fully terrestrial life in vertebrates is associated with a number of fundamental anatomical and physiological changes (Sumida & Martin 1997; Laurin 2010; Clack 2012). These include the evolution of an encapsuled (i.e., amniotic) egg with extraembryonic membranes and the loss of a larval stage in development (Laurin 2005). As a consequence, morphological adaptative constraints to larval aquatic feeding were skipped, permitting within a few million years an enormous radiation of new feeding types with associated anatomical structures in the early amniotes (Werneburg 2019). Concurrently, a transition from a primarily suction feeding behavior (Heiss et al. 2013; Natchev et al. 2015) toward a herbivorous (Weishampel 1996; Sues & Reisz 1998) or hunting behavior with a weapon-like jaw apparatus (Hülsmann & Wahlert 1972) took place.

Feeding musculature mainly attaches to the temporal skull region behind the eye and to the posterior part of the palate (Holliday & Witmer 2007; Jones et al. 2009; Diogo & Abdala 2010; Werneburg 2011; Ziermann et al. 2019). In both skull regions, major changes emerged, easily recognizable in all amniote skulls (Lakjer 1926, 1927; Hanken & Hall 1993*a,b*; Novacek 1993; Rieppel 1993; Zusi 1993). In particular, the temporal skull region received much attention in the scientific literature, historically resulting in taxonomic groups mainly defined by the anatomy of their temporal skull region (e.g., Synapsida, Diapsida, Anapsida; Case 1898; Williston 1904; Broom 1922; Zdansky 1923–25; Frazzetta 1968; Kuhn-Schnyder 1980; Rieppel & Gronowski 1981; Smith et al. 1983; Rieppel 1984; Tarsitano et al. 2001; Müller 2003; Cisneros et al. 2004; Werneburg 2012, 2013*a*, 2015, 2019; Haridy et al. 2016; Elzanowski & Mayr 2018; Abel & Werneburg 2021) with only few of them still used today. This is because with the rise of phylogenetic systematics and the inclusion of hundreds of other anatomical characters, along with new fossil finds, a more comprehensive picture on amniote interrelationships has been developed (Abel & Werneburg 2021). Nowadays, the temporal openings are only conditionally relevant for phylogenetic reconstructions. However, they can still be informative on selected phylogenetic levels and in particular taxonomic groups (Ford 2018) and are considered as highly relevant to understand morphofunctional relationships within the skull.

Recently, Abel & Werneburg (2021) provided a comprehensive review on the diversity and the scientific history of the temporal skull region in land vertebrates (see Chapter 2). They defined ten skull morphotypes and discussed a series of potential functional factors that shape their temporal region. Proper tests to validate and quantify biomechanical parameters in temporal skull diversification, however, are still lacking.

In the present contribution, an Anatomical Network Analysis (AnNA; Rasskin-Gutman & Esteve-Altava 2014) is used to provide new insights into the complex construction of land vertebrate skulls (Werneburg et al., 2019). For this, the focus on the Permian *Captorhinus aguti* (Amniota, Captorhinidae), an early amniote that is known from a high number of three-dimensionally preserved skulls. Even though all major skull morphotypes evolved pretty early after the amniote origin, the skull of captorhinids remained ancestrally anapsid (*scutal sensu* Abel & Werneburg 2021) with no temporal openings. After analyzing the skull of *C. aguti*, it is used it as a template by removing selected connections to create different skull models in order to estimate which influence the presence of particular temporal openings has on skull integration. This, in turn, allowed first attempts to interpret alternative functionally distinct regions in the skulls and helped in understanding why these openings might have evolved. Finally, these modularity patterns and associated functional considerations are used to infer potential muscular associations in fossil skulls for which muscle reconstructions are very difficult to perform.

4.2. Material and methods

4.2.1. Anatomical framework

Skull anatomy of *C. aguti* is well-documented in the literature (Case 1911; Sushkin 1928; Warren 1961; Fox & Bowman 1966; Bolt 1974; Modesto 1998; Abel et al. 2022). For coding of bone connections, this study mainly relies on the study of Fox & Bowman (1966). Uncertainties related to the connection of the lacrimal to the palatine (Bolt 1974), which is confirmed to be present in an available µCT-scan (see Chapter 3).

4.2.2. Anatomical network analysis

Using a walktrap algorithm, an anatomical network analysis (AnNA; e.g., Rasskin-Gutman & Esteve-Altava 2014; Esteve-Altava 2017*b*; Werneburg et al. 2019; Sookias et al. 2020) was performed for the skull of *C. aguti* by applying the *igraph* 1.2.6 package (Csardi and Nepusz 2006) in R (R Core Team 2020; see also Esteve-Altava et al. 2011; Esteve-Altava 2017*b,c*). For this, an Excel sheet was created, listing the skull bones in an adjacency matrix (i.e., binary coded N × N format) with a value of 1 indicating a contact between two bones and a value of 0 for the lack of such (Tab. 3). The skull of *C. aguti* consists of 65 bones (i.e., ‘nodes’ in network terminology) and 322 bone contacts (i.e., ‘links’). The data sheet was imported into RStudio (RStudio Team, 2019) and transformed into an undirected *igraph* object to enable

Tab. 3 Anatomical network matrix of the skull of *Captorhinus aguti*. Connections (i.e., "1") are highlighted in blue. Please note that cells representing contacts between identical nodes (e.g., "Angular_left" vs. "Angular_left") are filled black for reading aid. For the analysis, such cells have to be coded as "0". Alterations of this matrix based on Fig. 29A,C can be found in Suppl. Tab. 5–14.

	Angular_left	Angular_right	Articular_left	Articular_right	Basioccipital	Coronoid_left	Coronoid_right	Dentary_left	Dentary_right	Epipterygoid_left	Epipterygoid_right	Exoccipital_left	Exoccipital_right	Frontal_left	Frontal_right	Jugal_left	Jugal_right	Lacrimal_left	Lacrimal_right	Maxilla_left	Maxilla_right	Nasal_left	Nasal_right	Opisthotic_left	Opisthotic_right	Palatine_left	Palatine_right	Parabasisphenoid	Parietal_left	Parietal_right	Postfrontal_left	Postfrontal_right	Postorbital_left	Postorbital_right	Postparietal_left	Postparietal_right	Prearticular_left	Prearticular_right	Prefrontal_left	Prefrontal_right	Premaxilla_left	Premaxilla_right	Prootic_left	Prootic_right	Pterygoid_left	Pterygoid_right	Quadrate_left	Quadrate_right	Quadratojugal_left	Quadratojugal_right	Septomaxilla_left	Septomaxilla_right	Splenial_left	Splenial_right	Squamosal_left	Squamosal_right	Stapes_left	Stapes_right	Supraoccipital	Supratemporal_left	Supratemporal_right	Surangular_left	Surangular_right	Vomer_left	Vomer_right
Angular_left	■	0	1	0	0	0	0	1	0	0	0	0	0	0	0	0	0	0	0	0	0	0	0	0	0	0	0	0	0	0	0	0	0	0	0	0	0	0	0	0	0	0	0	0	0	0	0	0	0	0	0	0	1	0	0	0	0	0	0	0	0	1	0	0	0
Angular_right	0	■	0	1	0	0	0	0	1	0	0	0	0	0	0	0	0	0	0	0	0	0	0	0	0	0	0	0	0	0	0	0	0	0	0	0	0	0	0	0	0	0	0	0	0	0	0	0	0	0	0	0	0	1	0	0	0	0	0	0	0	0	1	0	0
Articular_left	1	0	■	0	0	0	0	0	0	0	0	0	0	0	0	0	0	0	0	0	0	0	0	0	0	0	0	0	0	0	0	0	0	0	0	0	1	0	0	0	0	0	0	0	0	0	1	0	0	0	0	0	0	0	0	0	0	0	0	0	0	1	0	0	0
Articular_right	0	1	0	■	0	0	0	0	0	0	0	0	0	0	0	0	0	0	0	0	0	0	0	0	0	0	0	0	0	0	0	0	0	0	0	0	0	1	0	0	0	0	0	0	0	0	0	1	0	0	0	0	0	0	0	0	0	0	0	0	0	0	1	0	0
Basioccipital	0	0	0	0	■	0	0	0	0	0	0	1	1	0	0	0	0	0	0	0	0	0	0	1	1	0	0	1	0	0	0	0	0	0	0	0	0	0	0	0	0	0	0	0	0	0	0	0	0	0	0	0	0	0	0	0	1	1	1	0	0	0	0	0	0
Coronoid_left	0	0	0	0	0	■	0	1	0	0	0	0	0	0	0	0	0	0	0	0	0	0	0	0	0	0	0	0	0	0	0	0	0	0	0	0	1	0	0	0	0	0	0	0	0	0	0	0	0	0	0	0	1	0	0	0	0	0	0	0	0	1	0	0	0
Coronoid_right	0	0	0	0	0	0	■	0	1	0	0	0	0	0	0	0	0	0	0	0	0	0	0	0	0	0	0	0	0	0	0	0	0	0	0	0	0	1	0	0	0	0	0	0	0	0	0	0	0	0	0	0	0	1	0	0	0	0	0	0	0	0	1	0	0
Dentary_left	1	0	0	0	0	1	0	■	1	0	0	0	0	0	0	0	0	0	0	0	0	0	0	0	0	0	0	0	0	0	0	0	0	0	0	0	1	0	0	0	0	0	0	0	0	0	0	0	0	0	0	0	1	0	0	0	0	0	0	0	0	1	0	0	0
Dentary_right	0	1	0	0	0	0	1	1	■	0	0	0	0	0	0	0	0	0	0	0	0	0	0	0	0	0	0	0	0	0	0	0	0	0	0	0	0	1	0	0	0	0	0	0	0	0	0	0	0	0	0	0	0	1	0	0	0	0	0	0	0	0	1	0	0
Epipterygoid_left	0	0	0	0	0	0	0	0	0	■	0	0	0	0	0	0	0	0	0	0	0	0	0	0	0	0	0	1	0	0	0	0	0	0	0	0	0	0	0	0	0	0	0	0	1	0	0	0	0	0	0	0	0	0	0	0	0	0	0	0	0	0	0	0	0
Epipterygoid_right	0	0	0	0	0	0	0	0	0	0	■	0	0	0	0	0	0	0	0	0	0	0	0	0	0	0	0	1	0	0	0	0	0	0	0	0	0	0	0	0	0	0	0	0	0	1	0	0	0	0	0	0	0	0	0	0	0	0	0	0	0	0	0	0	0
Exoccipital_left	0	0	0	0	1	0	0	0	0	0	0	■	0	0	0	0	0	0	0	0	0	0	0	1	0	0	0	0	0	0	0	0	0	0	0	0	0	0	0	0	0	0	0	0	0	0	0	0	0	0	0	0	0	0	0	0	0	0	1	0	0	0	0	0	0
Exoccipital_right	0	0	0	0	1	0	0	0	0	0	0	0	■	0	0	0	0	0	0	0	0	0	0	0	1	0	0	0	0	0	0	0	0	0	0	0	0	0	0	0	0	0	0	0	0	0	0	0	0	0	0	0	0	0	0	0	0	0	1	0	0	0	0	0	0
Frontal_left	0	0	0	0	0	0	0	0	0	0	0	0	0	■	1	0	0	0	0	0	0	1	0	0	0	0	0	0	1	0	1	0	0	0	0	0	0	0	1	0	0	0	0	0	0	0	0	0	0	0	0	0	0	0	0	0	0	0	0	0	0	0	0	0	0
Frontal_right	0	0	0	0	0	0	0	0	0	0	0	0	0	1	■	0	0	0	0	0	0	0	1	0	0	0	0	0	0	1	0	1	0	0	0	0	0	0	0	1	0	0	0	0	0	0	0	0	0	0	0	0	0	0	0	0	0	0	0	0	0	0	0	0	0
Jugal_left	0	0	0	0	0	0	0	0	0	0	0	0	0	0	0	■	0	1	0	1	0	0	0	0	0	0	0	0	0	0	0	0	1	0	0	0	0	0	0	0	0	0	0	0	1	0	0	0	1	0	0	0	0	0	1	0	0	0	0	0	0	0	0	0	0
Jugal_right	0	0	0	0	0	0	0	0	0	0	0	0	0	0	0	0	■	0	1	0	1	0	0	0	0	0	0	0	0	0	0	0	0	0	0	0	0	0	0	0	0	0	0	0	0	1	0	0	0	1	0	0	0	0	0	1	0	0	0	0	0	0	0	0	0
Lacrimal_left	0	0	0	0	0	0	0	0	0	0	0	0	0	0	0	1	0	■	0	1	0	1	0	0	0	1	0	0	0	0	0	0	0	0	0	0	0	0	1	0	0	0	0	0	0	0	0	0	0	0	1	0	0	0	0	0	0	0	0	0	0	0	0	0	0
Lacrimal_right	0	0	0	0	0	0	0	0	0	0	0	0	0	0	0	0	1	0	■	0	1	0	1	0	0	0	1	0	0	0	0	0	0	0	0	0	0	0	0	1	0	0	0	0	0	0	0	0	0	0	0	1	0	0	0	0	0	0	0	0	0	0	0	0	0
Maxilla_left	0	0	0	0	0	0	0	0	0	0	0	0	0	0	0	1	0	1	0	■	0	0	0	0	0	1	0	0	0	0	0	0	0	0	0	0	0	0	0	0	1	0	0	0	0	0	0	0	0	0	1	0	0	0	0	0	0	0	0	0	0	0	0	0	0
Maxilla_right	0	0	0	0	0	0	0	0	0	0	0	0	0	0	0	0	1	0	1	0	■	0	0	0	0	0	1	0	0	0	0	0	0	0	0	0	0	0	0	0	0	1	0	0	0	0	0	0	0	0	0	1	0	0	0	0	0	0	0	0	0	0	0	0	0
Nasal_left	0	0	0	0	0	0	0	0	0	0	0	0	0	1	0	0	0	1	0	0	0	■	1	0	0	0	0	0	0	0	0	0	0	0	0	0	0	0	1	0	1	0	0	0	0	0	0	0	0	0	1	0	0	0	0	0	0	0	0	0	0	0	0	0	0
Nasal_right	0	0	0	0	0	0	0	0	0	0	0	0	0	0	1	0	0	0	1	0	0	1	■	0	0	0	0	0	0	0	0	0	0	0	0	0	0	0	0	1	0	1	0	0	0	0	0	0	0	0	0	1	0	0	0	0	0	0	0	0	0	0	0	0	0
Opisthotic_left	0	0	0	0	1	0	0	0	0	0	0	1	0	0	0	0	0	0	0	0	0	0	0	■	0	0	0	0	0	0	0	0	0	0	0	0	0	0	0	0	0	0	1	0	0	0	0	0	0	0	0	0	0	0	1	0	1	0	1	0	0	0	0	0	0
Opisthotic_right	0	0	0	0	1	0	0	0	0	0	0	0	1	0	0	0	0	0	0	0	0	0	0	0	■	0	0	0	0	0	0	0	0	0	0	0	0	0	0	0	0	0	0	1	0	0	0	0	0	0	0	0	0	0	0	1	0	1	1	0	0	0	0	0	0
Palatine_left	0	0	0	0	0	0	0	0	0	0	0	0	0	0	0	0	0	1	0	1	0	0	0	0	0	■	0	0	0	0	0	0	0	0	0	0	0	0	0	0	0	0	0	0	1	0	0	0	0	0	0	0	0	0	0	0	0	0	0	0	0	0	0	1	0
Palatine_right	0	0	0	0	0	0	0	0	0	0	0	0	0	0	0	0	0	0	1	0	1	0	0	0	0	0	■	0	0	0	0	0	0	0	0	0	0	0	0	0	0	0	0	0	0	1	0	0	0	0	0	0	0	0	0	0	0	0	0	0	0	0	0	0	1
Parabasisphenoid	0	0	0	0	1	0	0	0	0	1	1	0	0	0	0	0	0	0	0	0	0	0	0	0	0	0	0	■	0	0	0	0	0	0	0	0	0	0	0	0	0	0	1	1	0	0	0	0	0	0	0	0	0	0	0	0	1	1	0	0	0	0	0	0	0
Parietal_left	0	0	0	0	0	0	0	0	0	0	0	0	0	1	0	0	0	0	0	0	0	0	0	0	0	0	0	0	■	1	1	0	1	0	1	0	0	0	0	0	0	0	0	0	0	0	0	0	0	0	0	0	0	0	1	0	0	0	1	1	0	0	0	0	0
Parietal_right	0	0	0	0	0	0	0	0	0	0	0	0	0	0	1	0	0	0	0	0	0	0	0	0	0	0	0	0	1	■	0	1	0	1	0	1	0	0	0	0	0	0	0	0	0	0	0	0	0	0	0	0	0	0	0	1	0	0	1	0	1	0	0	0	0
Postfrontal_left	0	0	0	0	0	0	0	0	0	0	0	0	0	1	0	0	0	0	0	0	0	0	0	0	0	0	0	0	1	0	■	0	1	0	0	0	0	0	0	0	0	0	0	0	0	0	0	0	0	0	0	0	0	0	0	0	0	0	0	0	0	0	0	0	0
Postfrontal_right	0	0	0	0	0	0	0	0	0	0	0	0	0	0	1	0	0	0	0	0	0	0	0	0	0	0	0	0	0	1	0	■	0	1	0	0	0	0	0	0	0	0	0	0	0	0	0	0	0	0	0	0	0	0	0	0	0	0	0	0	0	0	0	0	0
Postorbital_left	0	0	0	0	0	0	0	0	0	0	0	0	0	0	0	1	0	0	0	0	0	0	0	0	0	0	0	0	1	0	1	0	■	0	0	0	0	0	0	0	0	0	0	0	0	0	0	0	0	0	0	0	0	0	1	0	0	0	0	0	0	0	0	0	0
Postorbital_right	0	0	0	0	0	0	0	0	0	0	0	0	0	0	0	0	1	0	0	0	0	0	0	0	0	0	0	0	0	1	0	1	0	■	0	0	0	0	0	0	0	0	0	0	0	0	0	0	0	0	0	0	0	0	0	1	0	0	0	0	0	0	0	0	0
Postparietal_left	0	0	0	0	0	0	0	0	0	0	0	0	0	0	0	0	0	0	0	0	0	0	0	0	0	0	0	0	1	0	0	0	0	0	■	1	0	0	0	0	0	0	0	0	0	0	0	0	0	0	0	0	0	0	1	0	0	0	1	1	0	0	0	0	0
Postparietal_right	0	0	0	0	0	0	0	0	0	0	0	0	0	0	0	0	0	0	0	0	0	0	0	0	0	0	0	0	0	1	0	0	0	0	1	■	0	0	0	0	0	0	0	0	0	0	0	0	0	0	0	0	0	0	0	1	0	0	1	0	1	0	0	0	0
Prearticular_left	0	0	1	0	0	1	0	1	0	0	0	0	0	0	0	0	0	0	0	0	0	0	0	0	0	0	0	0	0	0	0	0	0	0	0	0	■	0	0	0	0	0	0	0	0	0	0	0	0	0	0	0	1	0	0	0	0	0	0	0	0	1	0	0	0
Prearticular_right	0	0	0	1	0	0	1	0	1	0	0	0	0	0	0	0	0	0	0	0	0	0	0	0	0	0	0	0	0	0	0	0	0	0	0	0	0	■	0	0	0	0	0	0	0	0	0	0	0	0	0	0	0	1	0	0	0	0	0	0	0	0	1	0	0
Prefrontal_left	0	0	0	0	0	0	0	0	0	0	0	0	0	1	0	0	0	1	0	0	0	1	0	0	0	0	0	0	0	0	0	0	0	0	0	0	0	0	■	0	0	0	0	0	0	0	0	0	0	0	0	0	0	0	0	0	0	0	0	0	0	0	0	0	0
Prefrontal_right	0	0	0	0	0	0	0	0	0	0	0	0	0	0	1	0	0	0	1	0	0	0	1	0	0	0	0	0	0	0	0	0	0	0	0	0	0	0	0	■	0	0	0	0	0	0	0	0	0	0	0	0	0	0	0	0	0	0	0	0	0	0	0	0	0
Premaxilla_left	0	0	0	0	0	0	0	0	0	0	0	0	0	0	0	0	0	0	0	1	0	1	0	0	0	0	0	0	0	0	0	0	0	0	0	0	0	0	0	0	■	1	0	0	0	0	0	0	0	0	0	0	0	0	0	0	0	0	0	0	0	0	0	1	0
Premaxilla_right	0	0	0	0	0	0	0	0	0	0	0	0	0	0	0	0	0	0	0	0	1	0	1	0	0	0	0	0	0	0	0	0	0	0	0	0	0	0	0	0	1	■	0	0	0	0	0	0	0	0	0	0	0	0	0	0	0	0	0	0	0	0	0	0	1
Prootic_left	0	0	0	0	0	0	0	0	0	0	0	0	0	0	0	0	0	0	0	0	0	0	0	1	0	0	0	1	0	0	0	0	0	0	0	0	0	0	0	0	0	0	■	0	0	0	0	0	0	0	0	0	0	0	0	0	1	0	1	0	0	0	0	0	0
Prootic_right	0	0	0	0	0	0	0	0	0	0	0	0	0	0	0	0	0	0	0	0	0	0	0	0	1	0	0	1	0	0	0	0	0	0	0	0	0	0	0	0	0	0	0	■	0	0	0	0	0	0	0	0	0	0	0	0	0	1	1	0	0	0	0	0	0
Pterygoid_left	0	0	0	0	0	0	0	0	0	1	0	0	0	0	0	1	0	0	0	0	0	0	0	0	0	1	0	0	0	0	0	0	0	0	0	0	0	0	0	0	0	0	0	0	■	1	1	0	0	0	0	0	0	0	0	0	1	0	0	0	0	0	0	1	0
Pterygoid_right	0	0	0	0	0	0	0	0	0	0	1	0	0	0	0	0	1	0	0	0	0	0	0	0	0	0	1	0	0	0	0	0	0	0	0	0	0	0	0	0	0	0	0	0	1	■	0	1	0	0	0	0	0	0	0	0	0	1	0	0	0	0	0	0	1
Quadrate_left	0	0	1	0	0	0	0	0	0	0	0	0	0	0	0	0	0	0	0	0	0	0	0	0	0	0	0	0	0	0	0	0	0	0	0	0	0	0	0	0	0	0	0	0	1	0	■	0	1	0	0	0	0	0	1	0	1	0	0	0	0	0	0	0	0
Quadrate_right	0	0	0	1	0	0	0	0	0	0	0	0	0	0	0	0	0	0	0	0	0	0	0	0	0	0	0	0	0	0	0	0	0	0	0	0	0	0	0	0	0	0	0	0	0	1	0	■	0	1	0	0	0	0	0	1	0	1	0	0	0	0	0	0	0
Quadratojugal_left	0	0	0	0	0	0	0	0	0	0	0	0	0	0	0	1	0	0	0	0	0	0	0	0	0	0	0	0	0	0	0	0	0	0	0	0	0	0	0	0	0	0	0	0	0	0	1	0	■	0	0	0	0	0	1	0	0	0	0	0	0	0	0	0	0
Quadratojugal_right	0	0	0	0	0	0	0	0	0	0	0	0	0	0	0	0	1	0	0	0	0	0	0	0	0	0	0	0	0	0	0	0	0	0	0	0	0	0	0	0	0	0	0	0	0	0	0	1	0	■	0	0	0	0	0	1	0	0	0	0	0	0	0	0	0
Septomaxilla_left	0	0	0	0	0	0	0	0	0	0	0	0	0	0	0	0	0	1	0	1	0	1	0	0	0	0	0	0	0	0	0	0	0	0	0	0	0	0	0	0	0	0	0	0	0	0	0	0	0	0	■	0	0	0	0	0	0	0	0	0	0	0	0	0	0
Septomaxilla_right	0	0	0	0	0	0	0	0	0	0	0	0	0	0	0	0	0	0	1	0	1	0	1	0	0	0	0	0	0	0	0	0	0	0	0	0	0	0	0	0	0	0	0	0	0	0	0	0	0	0	0	■	0	0	0	0	0	0	0	0	0	0	0	0	0
Splenial_left	1	0	0	0	0	1	0	1	0	0	0	0	0	0	0	0	0	0	0	0	0	0	0	0	0	0	0	0	0	0	0	0	0	0	0	0	1	0	0	0	0	0	0	0	0	0	0	0	0	0	0	0	■	1	0	0	0	0	0	0	0	0	0	0	0
Splenial_right	0	1	0	0	0	0	1	0	1	0	0	0	0	0	0	0	0	0	0	0	0	0	0	0	0	0	0	0	0	0	0	0	0	0	0	0	0	1	0	0	0	0	0	0	0	0	0	0	0	0	0	0	1	■	0	0	0	0	0	0	0	0	0	0	0
Squamosal_left	0	0	0	0	0	0	0	0	0	0	0	0	0	0	0	1	0	0	0	0	0	0	0	1	0	0	0	0	1	0	0	0	1	0	1	0	0	0	0	0	0	0	0	0	0	0	1	0	1	0	0	0	0	0	■	0	0	0	0	1	0	0	0	0	0
Squamosal_right	0	0	0	0	0	0	0	0	0	0	0	0	0	0	0	0	1	0	0	0	0	0	0	0	1	0	0	0	0	1	0	0	0	1	0	1	0	0	0	0	0	0	0	0	0	0	0	1	0	1	0	0	0	0	0	■	0	0	0	0	1	0	0	0	0
Stapes_left	0	0	0	0	1	0	0	0	0	0	0	0	0	0	0	0	0	0	0	0	0	0	0	1	0	0	0	1	0	0	0	0	0	0	0	0	0	0	0	0	0	0	1	0	1	0	1	0	0	0	0	0	0	0	0	0	■	0	1	0	0	0	0	0	0
Stapes_right	0	0	0	0	1	0	0	0	0	0	0	0	0	0	0	0	0	0	0	0	0	0	0	0	1	0	0	1	0	0	0	0	0	0	0	0	0	0	0	0	0	0	0	1	0	1	0	1	0	0	0	0	0	0	0	0	0	■	1	0	0	0	0	0	0
Supraoccipital	0	0	0	0	1	0	0	0	0	0	0	1	1	0	0	0	0	0	0	0	0	0	0	1	1	0	0	0	1	1	0	0	0	0	1	1	0	0	0	0	0	0	1	1	0	0	0	0	0	0	0	0	0	0	0	0	1	1	■	0	0	0	0	0	0
Supratemporal_left	0	0	0	0	0	0	0	0	0	0	0	0	0	0	0	0	0	0	0	0	0	0	0	0	0	0	0	0	1	0	0	0	0	0	1	0	0	0	0	0	0	0	0	0	0	0	0	0	0	0	0	0	0	0	1	0	0	0	0	■	0	0	0	0	0
Supratemporal_right	0	0	0	0	0	0	0	0	0	0	0	0	0	0	0	0	0	0	0	0	0	0	0	0	0	0	0	0	0	1	0	0	0	0	0	1	0	0	0	0	0	0	0	0	0	0	0	0	0	0	0	0	0	0	0	1	0	0	0	0	■	0	0	0	0
Surangular_left	1	0	1	0	0	1	0	1	0	0	0	0	0	0	0	0	0	0	0	0	0	0	0	0	0	0	0	0	0	0	0	0	0	0	0	0	1	0	0	0	0	0	0	0	0	0	0	0	0	0	0	0	0	0	0	0	0	0	0	0	0	■	0	0	0
Surangular_right	0	1	0	1	0	0	1	0	1	0	0	0	0	0	0	0	0	0	0	0	0	0	0	0	0	0	0	0	0	0	0	0	0	0	0	0	0	1	0	0	0	0	0	0	0	0	0	0	0	0	0	0	0	0	0	0	0	0	0	0	0	0	■	0	0
Vomer_left	0	0	0	0	0	0	0	0	0	0	0	0	0	0	0	0	0	0	0	0	0	0	0	0	0	1	0	0	0	0	0	0	0	0	0	0	0	0	0	0	1	0	0	0	1	0	0	0	0	0	0	0	0	0	0	0	0	0	0	0	0	0	0	■	1
Vomer_right	0	0	0	0	0	0	0	0	0	0	0	0	0	0	0	0	0	0	0	0	0	0	0	0	0	0	1	0	0	0	0	0	0	0	0	0	0	0	0	0	0	1	0	0	0	1	0	0	0	0	0	0	0	0	0	0	0	0	0	0	0	0	0	1	■

network depiction and calculation of community structures. The *cluster_walktrap* function was used to find community structures based on random walks with the step number being 3 (Suppl. Tab. 3). In network analyses, the resulting community structures (i.e., modules) describe subsets that share more links with each other than with the other nodes of the network, potentially representing different functional units (see Chapter 4.4. and Werneburg et al. 2019). Additionally, the modularity-value (Q) was calculated. Q is positive when the number of contacts within the modules exceeds the expected number if all contacts were assigned randomly. Likewise, Q is negative when the number of observed contacts within a module are below the random arrangement.

Also, the number of Q-modules was calculated, which describe the best mathematical threshold (red dashed line in Fig. 29) to define a module. Depending on the algorithm used, this threshold might slightly shift. The Q-module is just a rough orientation to detect meaningful biological modules [see discussion in Werneburg et al. (2019) and Sookias et al. (2020)], and as such, the choice of the cluster optimization algorithm does not have any importance for the scope of this study (personal communication with Borja Esteve-Altava in 2021).

4.2.3. µCT-scan of *Captorhinus aguti*

For illustration of the modularity pattern (Figs. 30–36), the µCT-scan of a skull of *C. aguti* from the Sam Noble Oklahoma Museum of Natural History, University of Oklahoma, Norman, OK, United States (OMNH 44816) was used. This scan was used in a parallel study (Abel et al. 2022; see Chapter 3) in which the sutures between adjacent bones are described in detail to infer potential intracranial mobilities. In the scanned specimen, the following dermal bones are missing: left jugal, part of left prefrontal, left nasal, both premaxillae, most of the postparietals, and both supratemporals. The missing bones are indicated by semitransparent outlines in Fig. 30. In other illustrations of this specimen and in the skull models derived from it (Figs. 31–36), these missing bones were not redrawn.

4.2.4. Skull models

Skull models correspond to the temporal skull types defined in Chapter 2. For the different models of temporal skull openings, the original matrix (Tab. 3; scutal, i.e., anapsid type) was modified by removing particular bone connections (i.e., coding “1” replaced by coding “0”; see Fig. 29A,C,D; Suppl. Tabs. 5–14). The *infrafenestral*, *bifenestral*, and *fossafenestral* skull types of Abel and Werneburg (2021) were, in the present study, divided in two sub-types each. The *nudital* and *additofenestral* skull types were not modeled within the framework of this study. For a nudital model, a number of bones (not just contacts) would need to be deleted, resulting in a noncomparable network as all other models in this study have a stable bone number (N). Additofenestral refers to multiple contacts between two adjacent bones (leaving more than one opening in between) which cannot be coded using AnNA methodology.

In the infrafenestral-1 skull model (Fig. 31B), which is represented by many early Synapsida [Caseidae, Varanopidae; e.g., Romer and Price (1940)] and some Parareptilia (e.g., MacDougall and Reisz, 2014), the jugal-squamosal contacts of the original matrix were removed on both skull sides (i.e., “1” replaced by “0”), resulting in 318 remaining links.

In the infrafenestral-2 skull model (Fig. 31C), which was represented by some Edaphosauridae and early therapsids, such as Dinocephalia (Boonstra 1952; Modesto 1995; Kammerer 2011; Lucas et al. 2018), the jugal-quadratojugal and postorbital-squamosal-contacts were removed resulting in 314 remaining links. This general pattern is also developed in many lepidosauromorphs, although their fenestra has evolved from the upper instead of the lower temporal opening (see Chapter 2).

In the infrafossal skull model (Fig. 31D), jugal-squamosal and jugal-quadratojugal-contacts were removed, resulting in 314 remaining links. Early amniote taxa representing this morphotype are some millerettids, *Microleter* Tsuji et al., 2010, and *Eunotosaurus* Seeley, 1892 (Gow 1972; Keyser and Gow 1981; Tsuji et al. 2010), and some ‘microsaurs’ like *Llistrofus* Carroll & Gaskill, 1978 and related taxa that might also represent early amniotes (Bolt and Rieppel 2009; Mann et al. 2019).

In the suprafenestral skull model (Fig. 31E), which was represented by *Araeoscelis* Williston, 1910 (Reisz et al. 1984), the postorbital-parietal-contact was removed, resulting in 318 remaining links.

In the suprafossal skull model (Fig. 31F), supratemporal-parietal and squamosal/parietal-contacts were removed, resulting in 314 remaining links. Although not included as such by Abel and Werneburg (2021), this skull type mirrors a skull shape, which evolved in many non-amniote taxa (Holmes 1984; Klembara et al. 2006; Reisz et al. 2009; Klembara 2011), with the ’fossa‘ representing the otic notch.

In the bifenestral-1 skull model (Fig. 31G), which was represented by the early diapsid *Petrolacosaurus* Lane, 1945 (Reisz 1977), postorbital-parietal and jugal-squamosal-contacts were removed, resulting in 314 remaining links.

In the bifenestral-2 skull model (Fig. 31H), which was likely represented by the neodiapsid *Youngina* (Carroll 1981), postorbital-parietal, postfrontal-parietal, and jugal-squamosal-contacts were removed, resulting in 310 remaining links.

In the bifossal skull model (Fig. 31I), jugal-squamosal, jugal-quadratojugal, supratemporal-parietal, and squamosal-parietal-contacts were removed, resulting in 306 remaining links. This model represents a combination of infra- and suprafossal skull types. This is apparently not represented in any early amniote, but is a morphotype, which is well-developed in Testudines (Gaffney 1979; Werneburg 2012) and mammals (Novacek 1993). As the anatomy of these animals is highly derived compared to the ancestral amniote condition (Starck 1995; Müller 2003; Werneburg and Maier 2019), the model might have only little relevance to interpret the diverse skull construction in these groups (but see Subchapter 4.4.).

In the fossafenestral-1 skull model (Fig. 31J) which may be represented by *Claudiosaurus* Carroll, 1981 (Carroll 1981), jugal-squamosal, jugal-quadratojugal, and postorbital-parietal-contacts were removed, resulting in 306 remaining links.

In the fossafenestral-2 skull model (Fig. 31K), which may be present in the neodiapsid *Hovasaurus* Piveteau, 1926 and *Claudiosaurus* [see fossafenestral-1 type as alternative] (Currie 1981; Bickelmann et al. 2009), jugal-squamosal, jugal-quadratojugal, postorbital-parietal, and postfrontal-parietal-contacts were removed, resulting in 310 remaining links. This skull type is also visible in many squamates (Evans 2008).

4.2.5. Muscle reconstruction

An attempt to hypothetically interpret some aspects of the functional morphology of jaw musculature in the respective skull models is provided. The concept was that if muscles attach to different bones of the same skull module, they are interpreted as acting as one functional entity. It has been shown that muscles are very conservatively associated to particular bones through evolution and only rarely change their general attachment sites (Diogo and Abdala 2010; Werneburg 2013a). Skull modules have widely been interpreted in a functional manner (Esteve-Altava et al. 2015*a*,*b*,*c*; Werneburg et al. 2019; Plateau and Foth 2020). With changed osteological modularity, bone-related musculature might change its internal and external structure and functional anatomy. This could mean that the muscles could be partly or fully fused as one muscle mass and receive a common nervous signal to contract at the same time, or they could form separated muscle heads and portions with individual functional properties.

Using AnNA, Esteve-Altava et al. (2015*c*) have shown that different modules can be obtained when the skeletal and muscular components are modeled separately or together, arguing against a straightforward relationship between bone modules and functional muscle groups. Despite the fact that different node numbers in an anatomical network may result in different modular integration (see the models below), this obstacle is mainly related to the premise that, in AnNA, every anatomical element - bone and muscle alike - is treated equally as just a ‘node’ in the anatomical framework. However, bones are already very diverse in their anatomy and ontogenetic history with either their enchondral or dermal origin, resulting in altering internal structural properties (Hall 2005). Reducing them to nodes has its limitations, but it has been shown to still be informative in anatomical network studies. Muscles are more difficult in this regard.

The conservative and tendinous attachments of muscles to particular bones are derived from neural crest cells early in development (Hall 2009), making primary muscle-bone correspondences difficult to change through evolution. In contrast, muscles also possess a very plastic structure that functionally adapts - via expanded direct muscle fiber attachments to other bones - for particular biomechanical requirements. Therefore, comparing modularity of bones and modularity of muscles (Esteve-Altava et al. 2015*c*) should be taken with great care and detailed anatomical knowledge is needed to make sufficient correlations. A study in which muscles and bones are treated as equal structural entities (nodes) may result in an interesting overall network relationship, but with little functional meaning. Relative proportions, muscle vectors, and muscle fiber directions, among many other parameters, however, are imperative to make sufficient biomechanical reconstructions. Hence, muscle anatomy and not muscle network need to be discussed in relation to bone modularity for a sufficient functional interpretation. This exploratory, rough heuristic approach, of course, can only be speculative and needs to be tested with proper biomechanical methodology (e.g., finite element analyses: Lautenschlager et al. 2017; Ferreira et al. 2020). Nevertheless, comparative anatomical data already provide well founded indications on a functional relationship between bone modules and muscle morphology.

For example, Werneburg et al. (2019) discussed bone modularity of five extant species and cited muscle anatomy in clear correspondence between particular bone modules and muscles. In the alligator, an expanded snout (their ’red‘ labeled module) is related to the expanded pterygoid-musculature (Schumacher 1973). The threefold differentiation of the external adductor muscles is closely related to the encounter of three skull modules (‘green’, ’orange‘, and ’red‘) in the temporal skull region of alligator and tuatara (Holliday and Witmer 2007; Jones et al. 2009). Even the derived muscle anatomy of the leatherback turtle with straight jaw muscle orientation in the adductor chamber (Burne 1905; Schumacher 1972) directly associates with the unique skull modularity in this species (‘green’ and ‘orange‘). As differentiation of the external jaw muscles in the opossum, the mammalian temporalis musculature anatomically relates to the expanded braincase module (‘yellow’), whereas the complex masseter muscle used for chewing attaches to the jugal, which belongs to the snout module (’red‘) in this species. Even the rather simple skull modularity of the chicken corresponds to its jaw muscle anatomy (van den Heuvel 1992), taking lower level network hierarchy into account (Werneburg et al. 2019).

Based on the known extant tetrapod jaw muscle diversity (e.g., Diogo and Abdala 2010; Ziermann et al. 2019), it is hypothesized at least seven distinct major jaw muscle portions to be present in the ancestral amniote condition (Fig. 31: seven-pointed star next to each skull). These include for the external jaw adductor section: (1) *musculus (m.) adductor mandibulae externus Pars profundus* (AMEP), originating mainly from the parietal, (2) *m. adductor mandibulae externus Pars superficialis* (AMES), originating mainly from the squamosal, and (3) *m. adductor mandibulae Pars medialis* (AMEM), which is mainly associated with the jugal (see homology discussion in Abel et al. 2022; Chapter 3). The internal jaw adductor section includes the following: (4) *m. adductor mandibulae posterior*, originating mainly from the quadrate, (5) *m. pterygoideus Pars ventralis* (PTV), which is mainly associated with the posterior edge and/or ventral side of the pterygoid, (6) *m. pterygoideus Pars dorsalis* (PTD), originating dorsally from the palatine (in addition to the pterygoid), and (7) *m. constrictor internus dorsalis* (CID) mainly originating from the epipterygoid. This series of seven muscular units is obviously a simplification of the actual diversity and differentiation of jaw musculature, but this generalization was necessary to fit the focus of this article and is open to revision. Muscle terminology is based on Jones et al. (2009) and Werneburg (2011).

4.3. Results

4.3.1. Network analysis of *C. aguti* (skull type A: scutal/anapsid)

The number of contacts per bone varies from two (epipterygoid) to 13 (supraoccipital). Most bones possess three to five contacts. In the temporal region, the squamosal is the most 'integrated' bone (eight contacts). The minimum number can be observed in the postfrontal, supratemporal, and quadratojugal (three contacts). In the conceptual framework of AnNA, integration refers to the number of connections. This is related to the concept of burden (Esteve-Altava et al. 2013*a*), and it has been adapted for AnNA (see Rasskin-Gutman and Esteve-Altava 2021).

The analysis with the walktrap algorithm, which has been widely used in Anatomical Network literature before, resulted in a modularity index (Q-index) of 0.625. A Q-index > 0 means that the calculated number of contacts inside a module is higher than in a random model (Fig. 30E). Network parameters and Q-values per model are listed in Tab. 4.

4.3.2. Network description for *C. aguti* (skull type A: scutal/anapsid)

In addition to both left and right-side mandibular rami (dark blue in Figs. 29–31A), a braincase module is present (yellow), and it is separated into a left and a right submodule containing prootic-stapes and opisthotic-exoccipital on each side. The unpaired elements of the braincase (gold) - parabasisphenoid, basioccipital, and supraoccipital – randomly appear within either one of the contralateral braincase submodules in different runs of the same analysis (see Werneburg et al. 2019 for details on that phenomenon).

The remaining major modules consist of left and right dermal bones of the 'cheek', skull roof, snout, and palate regions. Inside these areas, the palate region can be divided into three modules, one left and one right-wing module (light pink), each consisting of premaxilla and palatine-vomer, and one medial palate module (dark pink). The latter plotted closer to the braincase modules (yellow) than to the palatal wing (light pink) inside the dendrogram and consists of the contralateral pterygoids and epipterygoids.

The 'cheek' region lateral and posterolateral to the orbit (orange) consists of jugal and the more integrated quadrate/quadratojugal on each side. A certain relationship exists between the ‘cheek’ and the two skull roof modules indicated by neighboring branches in the dendrogram.

The posterior roof module (red) consists of squamosal + parietal-postorbital and postparietal-supratemporal. The anterior roof module (dark green) consists of postfrontal and frontal.

In the snout, two modules can be found on each skull side. The upper snout module (dark purple) consists of prefrontal and nasal. The snout flank module (light purple) consists of maxilla and lacrimal-septomaxilla.

As for the overall network structure, the median palate modules (dark pink), together with the braincase modules (yellow), are placed in between left and right skull side modules on both skull sides functionally separating the skull in a left and right side (Fig. 30E).

Tab. 4 Network parameters of the analyzed networks based on the definitions and theoretical background as mostly summarized by Plateau & Foth (2020). For all models, N is the number of nodes (i.e., bones) and is always 65 in the analyzed models. C is the mean clustering coefficient and represents the arithmetic mean of the ratio of a node’s neighbors that connect among them in a triangular manner. D is the density of connections calculated as the number of links (K) divided by the maximum number of connections possible. L is the mean shortest path length and measures the average of the shortest path length between all pairs of bones. Q is the number of calculated Q-modules. Q_{max} evaluates whether the number of modules identified are better supported than what is expected at random.

Model	**C**	**D**	**K**	**L**	**Q**	**Q_{max}**
Scutal (*C. aguti*)	0.428	0.077	322	3.663	7	0.62
Infrafenestral-1	0.409	0.076	318	3.684	7	0.62
Infrafenestral-2	0.430	0.075	314	3.685	7	0.62
Infrafossal	0.432	0.075	314	3.697	7	0.63
Suprafenestral	0.411	0.076	318	3.674	7	0.62
Suprafossal	0.414	0.075	314	3.702	7	0.62
Bifenestral-1	0.387	0.075	314	3.702	7	0.62
Bifenestral-2	0.375	0.076	310	3.725	7	0.62
Bifossal	0.416	0.074	306	3.750	7	0.62
Fossafenestral-1	0.398	0.074	306	3.738	7	0.62
Fossafenestral-2	0.410	0.075	310	3.715	7	0.63

4.3.3. Network analyses of the skull models

All ten skull models (Figs. 31B–K, 32–36) show seven Q-modules each (Tab. 4). We found that compared to the original skull modularity of *C. aguti* (Figs. 30, 31A), the jugal, squamosal, postorbital, and postfrontal usually change their modular association when different temporal openings are modeled. Only in the original skull model, the frontal forms its own module together with postfrontal (green), but it is part of the upper snout module (dark purple) in all ten modeled skulls. Also, different to *C. aguti*, in all ten modeled skulls, the palatal wing module (light pink) plotted closer to the snout flank module (light purple) than the latter does to the upper snout module (dark purple).

As for the overall network structure, the median palate (dark pink), together with the braincase (yellow) modules, can change their relative position in relation to the palatal wings, snout, cheek, and skull roof modules in each skull model.

In the skull model dendrograms (Figs. 32–36), the original modular association of the respective bone as found in *C. aguti* is indicated by background coloration of the respective bone name embedded in a different module coloration.

In the infrafenestral-1 skull model, also different to the original scutal skull of *C. aguti* (see Figs. 29–31A vs. Figs. 31B, 32A), the cheek (orange) module plotted closer to the posterior roof module (red) than the latter does to the upper snout module (dark purple), as indicated by parallel white stripes in Figure 31B.

In the infrafenestral-2 skull model (see Figs. 29–31A vs. Figs. 31C, 32B), the cheek module split in two separated parts with the jugal integrated within the lateral snout module (light purple). A new module, the postocular module, is formed by postorbital and postfrontal (light green), and the cheek module (orange) is closer associated to the posterior roof module (red). Considering the overall network, the median palate module (dark pink) - together with the braincase module (yellow) - plotted closer to the skull roof (red and blue) and cheek (orange) modules than to the palatal wing (light pink) and the snout modules (light and dark pink) of both skull sides. Hence, the whole skull may be functionally separated into an anterior and a posterior half.

In the infrafossal skull model (see Figs. 29–31A vs. Figs. 31D, 33A), the cheek module is split with the jugal integrated in the snout flank module (light purple). Postorbital and postfrontal are part of the posterior skull roof module(red). Similar to the infrafenestral-2 model, the median palate module (dark pink), together with the braincase module (yellow), functionally separates the whole skull in an anterior and a posterior half.

In the suprafenestral skull model (see Figs. 29–31A vs. Figs. 31E, 33B), the squamosal, which originally belonged to the posterior skull roof module (red), is now part of the cheek

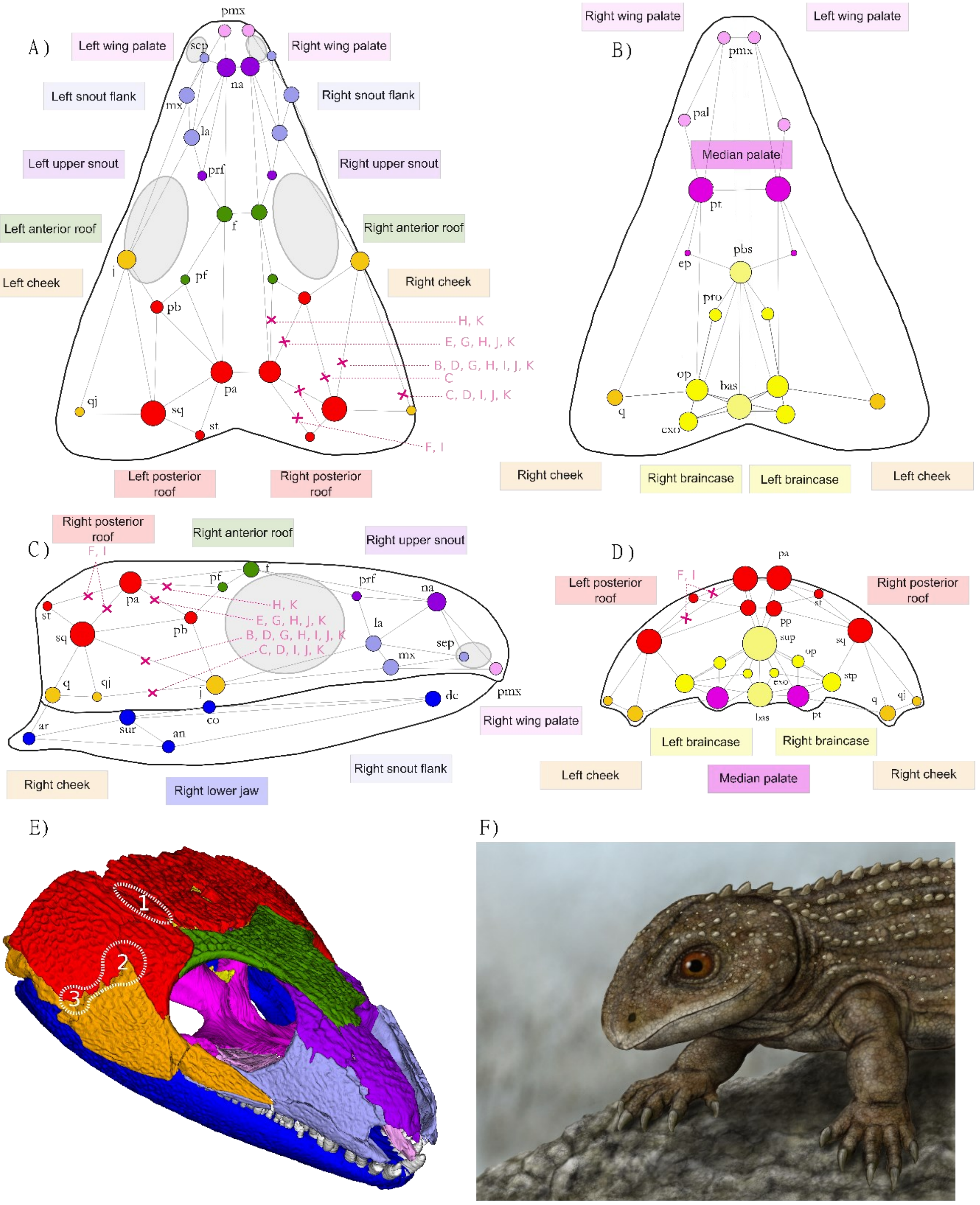

Fig. 29 Illustration of the skull network of *Captorhinus aguti* in (A) dorsal, (B) ventral, (C) lateral, and (D) posterior view. Only superficial bones and their connections to other bones (“links” in network terminology) are shown. The relative size of each circle (i.e., node) represents the number of links to the respective bone, incl. also non-illustrated ones (see legend inside Figure). Circles are colored according to the reconstructed cranial network modules (see Fig. 30E; 31). Different network models were created by cutting selected connections between particular bones, herein indicated by red “X”-symbols; letters correspond to respective models and subpanel letters in Figure 32). (E) oblique view of the 3D-reconstructed skull of *C. aguti* with colored skull modules (see Fig. 31; 32A for labeling). The potential origin sites of temporal openings among early amniotes (1–3) are indicated by dotted lines (compare to Fig. 28; 32A). (F) Digital drawing of *C. aguti* by paleoartist Markus Bühler (Balingen, Germany); Paläontologische Sammlung der Universität Tübingen, collection number of the drawing: GPIT-PV-112849. Anatomical abbreviations as in Fig. 15. Additional abbreviations: bas, basioccipital; exo, exoccipital; pmx, premaxilla; pro, prootic.

region (orange). The jugal, which originally belonged to the cheek module, is part of the snout flank module (light purple).

The suprafossal skull model (see Figs. 29–31A vs. Figs. 31F, 34A) is characterized by an expansion of the posterior skull roof module (red), which now also includes postfrontal and all three (originally orange) cheek bones: quadrate, quadratojugal, and jugal.

The bifenestral-1 skull model (see Figs. 29–31A vs. Figs. 31G, 34B) shows the same patterns as the infrafenestral-1 model (see Figs. 31B, 32A)

In the bifenestral-2 skull model (see Figs. 29–31A vs. Figs. 31H, 35A), postfrontal and postorbital form a new postocular module (light green) that is related to the cheek (orange) and to the posterior skull roof (red) modules.

In the bifossal skull model (see Figs. 29–31A vs. Figs. 31I, 35B), the jugal becomes part of the lateral snout module (light purple). The posterior skull roof module (red) has expanded and integrates the two remaining ’cheek elements‘, quadrate and quadratojugal, along with the postfrontal. Considering the overall network, the median palate module (dark pink)—together with the braincase module (yellow), are closely placed in between the posterior skull roof modules of both skull sides (red), functionally separating the whole skull in an anterior and a posterior half. The anterior half is formed by the palatal wing modules (light pink) and the snout modules (light and dark purple) of both skull sides.

In the fossafenestral-1 skull model (see Figs. 29–31A vs. Figs. 31J, 36A), postfrontal and postorbital form a new, postocular module (light green) that plotted closer to the posterior skull roof (red) module than to the cheek module (orange). The cheek module is split with the jugal, which is now integrated inside the snout flank module (light purple). Median palate modules (dark pink), together with the braincase modules (yellow), are closer related to skull roof (red and light green) and cheek (orange) modules of both skull sides than to the remaining skull modules, again functionally separating the skull in an anterior and a posterior half.

Like in the fossafenestral-1 skull model (Figs. 29J, 36A), the fossafenestral-2 skull model (see Figs. 29–31A vs. Figs. 31K, 36B) shows a postocular module. In this model, however, cheek (orange) and posterior skull roof (red) module plotted closer to each other than both do to the postocular module (light green) (see white parallel stripes in the figure). Like in the fossafenestral-1 type, the cheek module is also split with the jugal being integrated inside the snout flank module (light purple). Also, as in this skull type, the fossafenestral-2 skull is functionally separated in an anterior and a posterior half. However, the median palate module (dark pink) - together with the braincase module (yellow) - is even more strongly integrated between roof and cheek modules (red, blue, and orange) of both skull sides.

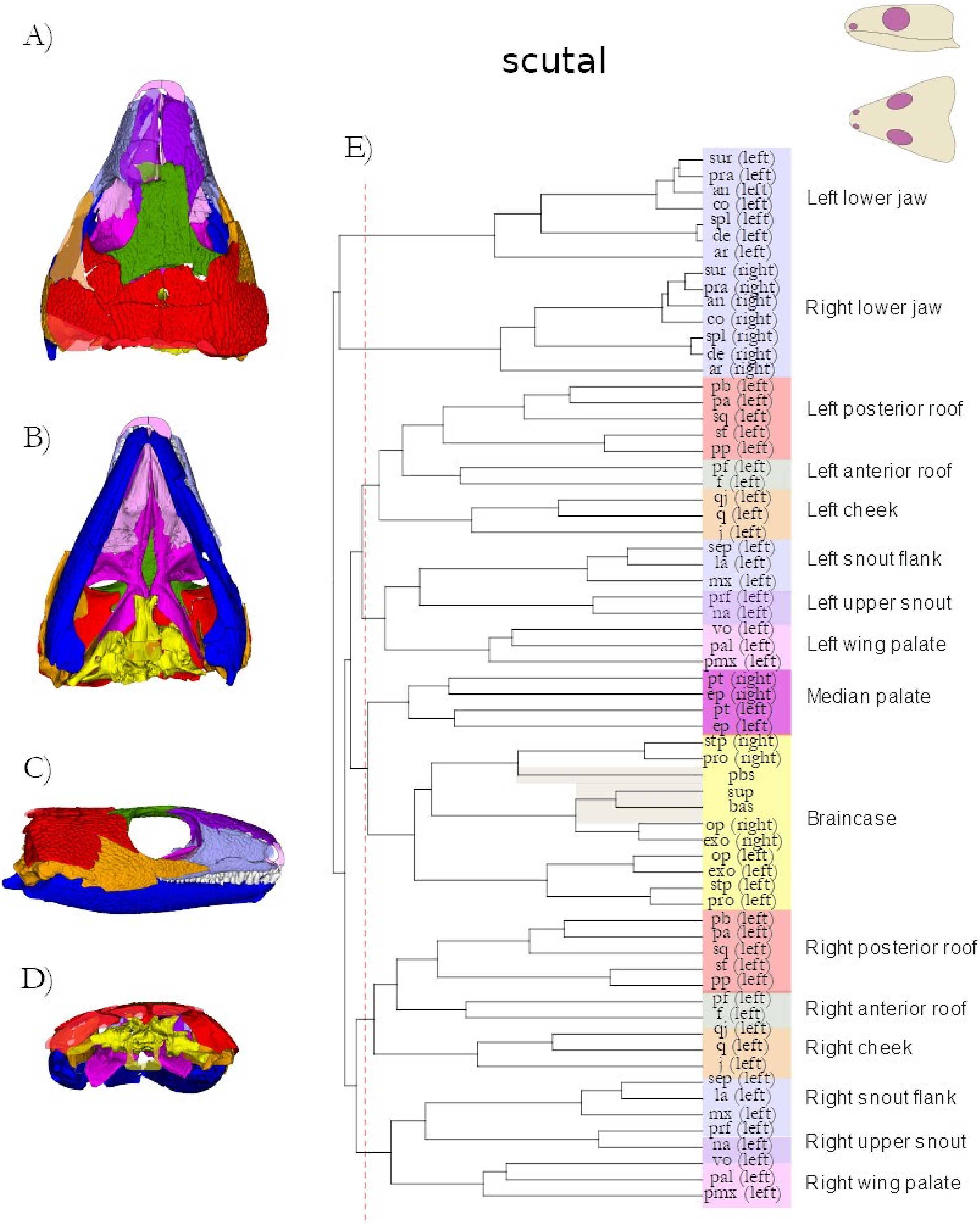

Fig. 30 Skull network of *Captorhinus aguti* in (A) dorsal, (B) ventral, (C) lateral, and (D) posterior view. Missing bones of the microCT-scanned skull are redrawn as rough semitransparent outlines. The dendrogram calculated during the network analysis is shown in (E): red dashed line indicates the threshold of the Q-modules. Biologically sound morphological modules are indicated by different colors. Unpaired bones of the (yellow) braincase have no robust position in different runs of the same analysis and are shown in gold. Sketches of the scutal skull type in the upper right corner after Abel & Werneburg (2021).

4.3.4. Muscle reconstruction

The reconstructed jaw muscle associations directly correspond to the modular pattern of each skull model (i.e., seven-pointed star in Fig. 31). In the original skull of *C. aguti* (scutal/anapsid type, Fig. 31A), the following joined muscles are reconstructed and interpreted to act as functional entity: AMEP with AMES (belonging to the red module), CID with PTV (dark purple), and AMP with AMEM (orange). The identity of AMP of either belonging to the internal or external section of the jaw musculature appears to change among taxa based on altering ontogenetic pathways (Rieppel 1987; summarized by Werneburg 2011). As such, an association of muscle portions usually assigned to the internal (AMP) or external (AMEM) section of the jaw adductor is not deceptive.

In *C. aguti*, the pterygoid teeth reach far posteriorly on the ventral surface (Fig. 30B), preventing broad insertion of PTV. Whether PTV was actually developed as a small muscle portion or whether it was just a small muscle head inserting on the posterior edge of the pterygoid cannot be determined (see Witzmann and Werneburg 2017). A PTD could have been partly associated with CID/PTV - as indicated by the half-connected points of the star in Fig. 31A - as the related bone module (light pink) was not as strongly integrated in the snout modules as both snout modules are into each other (light and dark purple: close association indicated by two parallel white lines in Fig. 31A).

Muscular associations are different in all of our skull models (Figs. 31B–K). In the infrafenestral-1 model (Fig. 31B), with the anterior expansion of the posterior skull roof module (red), the following muscular associations are hypothesized based on the modular pattern of related bones: AMES with AMEP (red), AMP with AMEM (orange), CID with PTV. AMP and AMES could had been partly connected due to the related modules showing a strong relation to each other.

In the model infrafenestral-2 (Fig. 31C), with the formation of a postocular module (light green) and the integration of the jugal into the snout flank (light purple), the following associations are hypothesized: AMES with AMEP (red), CID with PTV. Based on close modular associations, AMP could be partly related to AMES/AMAP, and AMEM to PTD.

In the infrafossal model (Fig. 31D), with the integration of the jugal into the snout flank (light purple), the following association is hypothesized: AMES with AMEP (red). Based on close modular associations, AMP could be partly related to AMES/AMAP, and AMEM to PTD. CID is considered more separate from PTV, because in the skull, which is differentiated in an anterior and a posterior part in overall network composition (Fig. 33A), the CID-associated epipterygoid might serve a key role in functional anatomy (see section 4.4.).

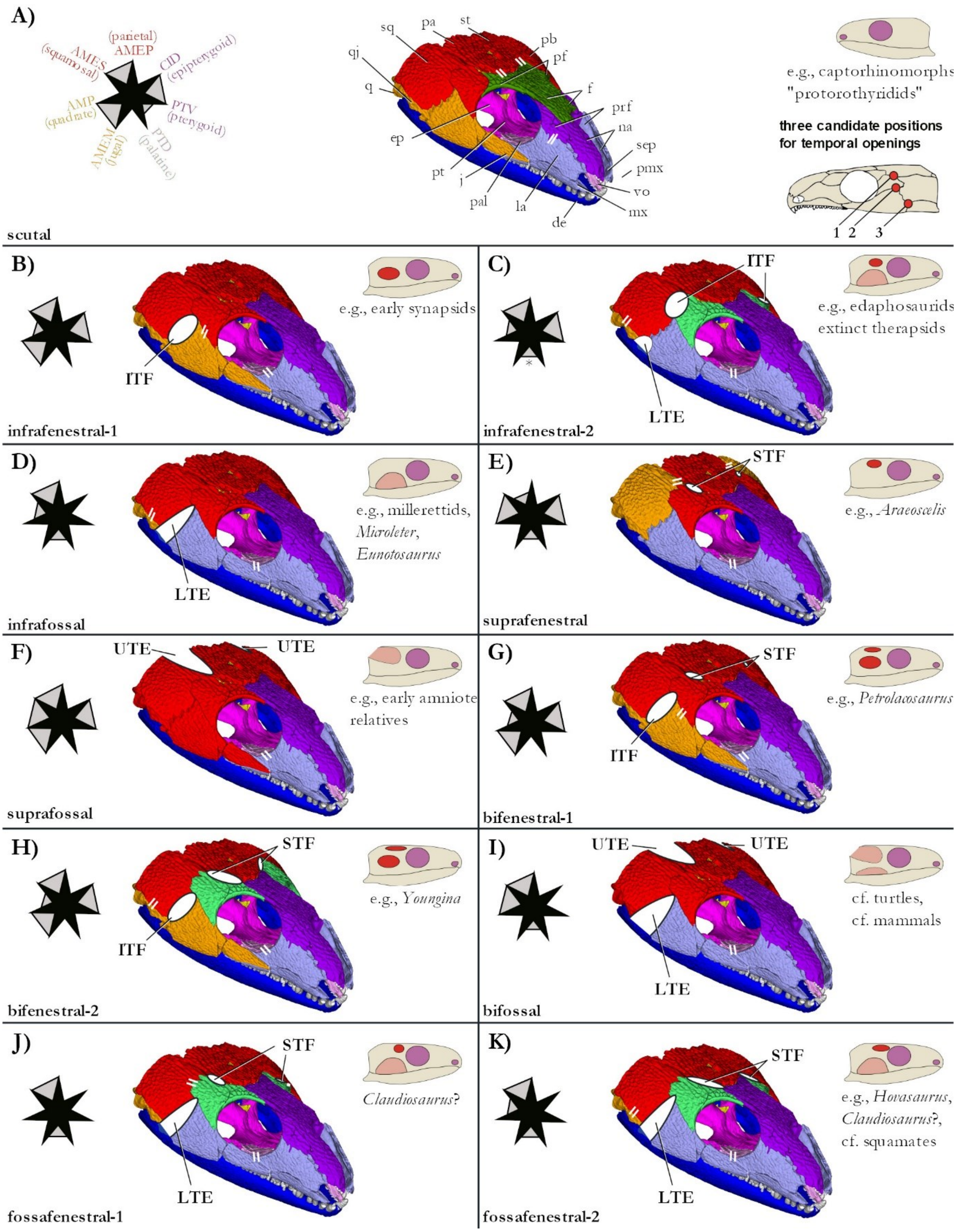

[Figure caption on the following page]

Fig. 31 Skull network illustrations of models that simulate different temporal skull morphotypes (see sketches in each subfigure) found in early amniote evolution [based on Abel and Werneburg (2021); nudital and additofenestral skull types were not possible to model, see text]. The skull of *C. aguti* (A) was used as model template. Skull models are shown in an anterior dorsolateral view (B–K). Parallel white stripes indicate a closer network relationship of the connected modules when compared to other modules in the anterior (snout) or posterior (temporal) skull half, respectively (compared to dendrograms in Figs. 31E, 33–37). Modeled temporal fenestrae are shown as white full-ellipses, temporal excavations as white half-ellipses. Star-schemes for each model indicate the differentiation of muscle inside the jaw adductor chamber [see legend in panel (A); the listed bones serve as major origin sites of these muscle portions; letter coloration based on skull modules]. Muscle portions that putatively act as a joined entity are connected by gray filling between star jags; full filling indicates that the muscles originate from the same skull module, half filling indicates that the modules, to which the muscle portions attach, are closely associated to each other in the global anatomical network (see Figs. 31E, 33–37). AMEM, musculus (m.) adductor mandibulae Pars medialis; AMEP, m. adductor mandibulae Pars profundus; AMES, m. adductor mandibulae Pars superficialis; AMP, m. adductor mandibulae posterior; ITF, infratemporal fenestra; LTE, lower temporal excavation; PTD, m. pterygoideus Pars dorsalis; PTV, m. pterygoideus Pars ventralis; STF, supratemporal fenestra; UTE, upper temporal excavation.

In the suprafenestral model (Fig. 31E), with the integration of the jugal to the snout flank (light purple) and the integration of the squamosal into the cheek module (orange), following associations are hypothesized: AMES with AMP (orange), CID with PTV (dark purple). AMEP (red) and AMES/AMP (orange) might be partly associated, similar to AMEM (light blue) and PTD (light pink) based on close relationship of the related skull modules.

In the suprafossal model (Fig. 31F), with the expansion of the posterior skull roof module above the whole temporal region (red), the following associations are hypothesized: AMEP with AMES, AMP, and AMEM (red), and CID with PTV (dark pink).

The bifenestral-1 model (Fig. 31G) shows the same patterns as the infrafenestral-1 model (Fig. 31B).

In the bifenestral-2 model (Fig. 31H), with the formation of a postocular module (light green), the following associations are hypothesized: AMEP with AMES (red), AMP with AMEM (orange), and CID with PTV (dark pink). Partial relationship might exist between AMP (orange) and AMES (red).

In the bifossal model (Fig. 31I), with the expansion of the posterior skull roof module to the cheek and postocular region (red) and with integration of the jugal to the snout flank (light purple), the following associations are hypothesized: AMEP with AMES and AMP (red). Partial relationship might exist between AMEM (light purple) and PTD (light pink).

In the fossafenestral-1 and -2 models (Figs. 31J–K), with the formation of a postocular module (light green) and the integration of the jugal into the snout flank (light pink), the following associations are hypothesized: AMEP and AMES (red), and a partial association between AMEM (light purple) and PTD (light pink).

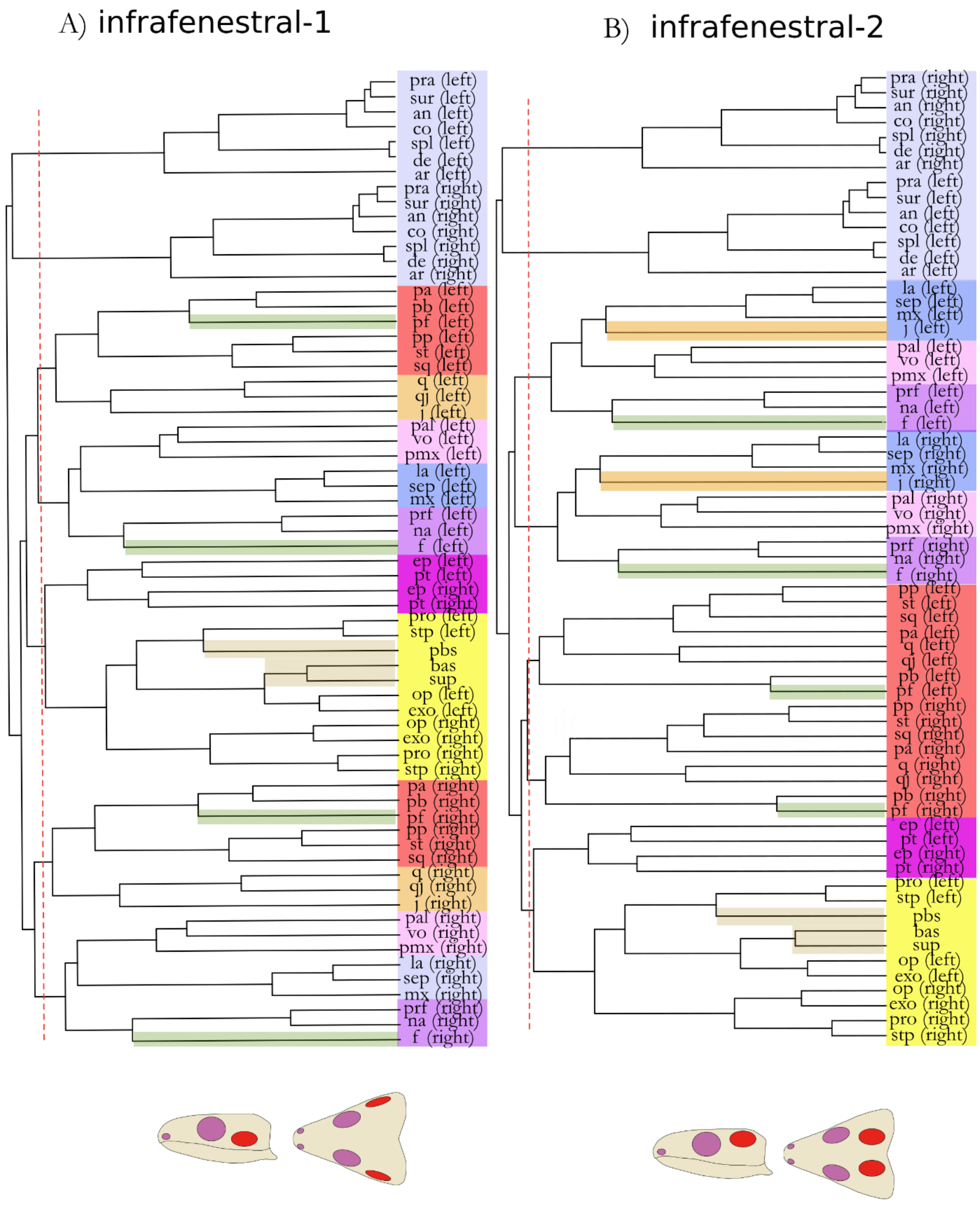

Fig. 32 Dendrogram of the skull network of (A) the infrafenestral-1 and (B) the infrafenestral-2 skull types. Compare to caption of Fig. 31E. Green- and orange-colored branches indicate that these nodes were assigned to other modules in the initial analyses (see the color code in Fig. 31E).

4.4. Discussion

4.4.1. Significance of the anatomical network approach

Using the anatomical network approach, seven distinct anatomical modules on each skull side of *C. aguti* (Figs. 29–31A) were detected. These include cheek (orange in Figures), anterior (green) and posterior (red) skull roof, palate wing (light pink), upper snout (purple), snout flank (light blue), and braincase (yellow) modules. In addition, there is a median palate module (dark pink). By modeling changes in skull network composition of *C. aguti* to mimic skull types of other early amniotes, alterations in the number and fundamental rearrangements in the respective bone composition of skull modules occur, illustrating the sensitivity of the anatomical network approach.

When trying to interpret the functional meaning of module composition, one needs to keep in mind the methodological basis of network analysis, which considers as data source just the information on presence and absence of bone connections (1/0 codification) but neglects any detailed morphological characteristic such as suture type, thickness, and gross bone anatomy. Each level of morphological organization, however, conveys different information, and to understand processes in evolution, each may first be treated separately (Rasskin-Gutman 2003) before expanding toward a more holistic view on anatomical tissue integration (Maier and Werneburg 2014). The functional meaning of skull modules, of course, has to be handled with care, and discussion always requires a thorough consideration of other morphological aspects known for the taxon in question and comparable organisms (Werneburg et al. 2019).

Functional considerations of skull anatomy cannot be performed without proper knowledge on muscle anatomy, which is usually barely described in the literature for extant taxa and usually misses relevant information of muscle fiber-compositions and orientations and tendinous components. For extinct taxa, only gross morphology of musculature can be reconstructed on a rough anatomical level, mainly based on phylogenetic bracketing and by considering indications of possible attachment sites on bones (Witzmann and Werneburg 2017). Nevertheless, anatomical network methodology has been proven to provide basis for reasonable functional conclusions and new hypotheses (Esteve-Altava et al. 2013*a*,*b*, 2015*a*; Rasskin-Gutman and Esteve-Altava 2014; Diogo et al. 2015; Molnar et al. 2017; Lee et al. 2020; Plateau and Foth 2020; Sookias et al. 2020).

Rasskin-Gutman (2003) provided a first attempt to study skull modularity in relation to temporal openings and found, by comparing nine different tetrapod skulls, that the orbit is surrounded by a rather simple modular arrangement with one element attaching to at least three other adjacent elements. In contrast, the temporal region is rather complex with bones having five or six contacts to other bones which are, eventually, surrounded by bones with triangular connections again. He also found that the snout is less variable in regard to network connections than the postorbital region, which overlaps with the known morphological and trophic diversity of extant taxa (see also Werneburg et al. 2019). As such, the complexity of the anatomy network might provide a reasonable source to understand patterns of functional morphology, in which jaw muscle anatomy is taken into account.

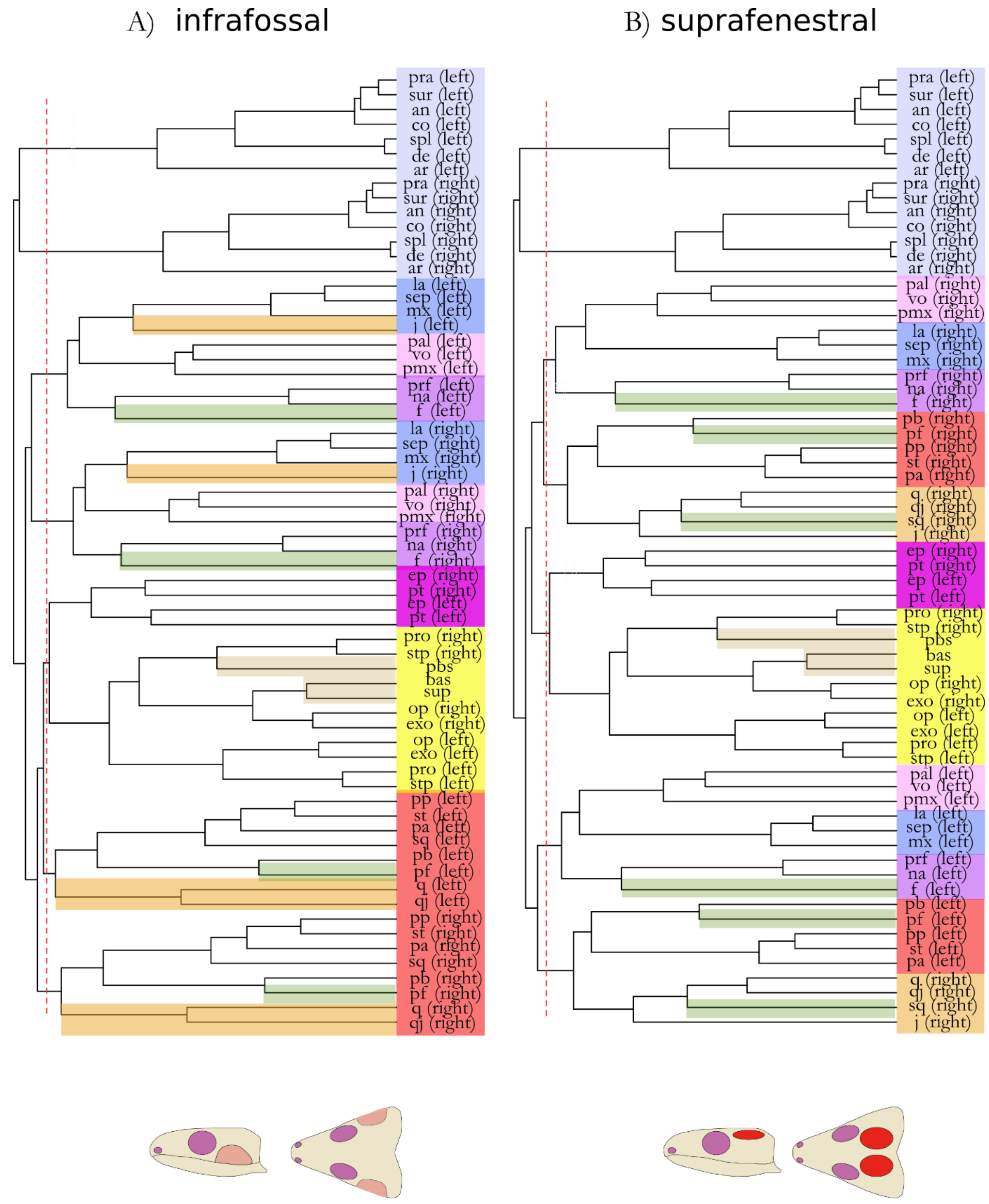

Fig. 33 Dendrogram of the skull network of (A) the infrafossal and (B) the suprafenestral skull types. Compare to caption of Fig. 31E. Green- and orange-colored branches indicate that these nodes were assigned to other modules in the initial analyses (see the color code in Fig. 31E).

4.4.2. Cranial kinesis in *C. aguti* with respect to skull modularity

Studying the suture anatomy and thickness of dermatocranial bones, Abel et al. (2022; see Chapter 3) discussed cranial kinesis in *C. aguti*. The authors discussed metakinesis - a movement of the temporal dermatocranium together with the snout relative to the braincase (Iordansky 1990) - to be present between parietal-postparietal and supraoccipital and between squamosal and opisthotic. In fact, a metakinetic joint was argued to be widespread among early amniotes (Carroll 1969*a*; Gow 1972; Bramble and Wake 1985; Iordansky 1990; however, see also Chapter 3). This could be further supported by the modularity pattern detected in the present study, in which the braincase elements (yellow) are separated from all other skull modules, including the posterior skull roof module with the squamosal (red) and the anterior skull roof module with the frontal (dark green).

Squamosal and parietal are plotted closely within the posterior skull roof module (red). Consequently, a representation of a so-called ‘crossopterygian hinge line’ (Kemp 1980) between squamosal and more dorsal bones of the skull roof, which temporarily might have been opened posteriorly as an otic notch in early tetrapods (but see Panchen 1964), cannot be postulated herein. However, the suture between both elements in *C. aguti* is not very strong (see Chapter 3), which might be mirrored in the even closer modular relationship of the parietal to the postorbital in the reconstruction herein (Fig. 30E).

Interdigitation and great thickness of the frontoparietal suture most likely prevented true joint and elasticity-based (*sensu* Natchev et al. 2016) mesokinetic movement in between the skull roof elements that otherwise could have been moved against each other by the contraction of *m. adductor mandibulae externus Pars profundus* (AMEP). Frontal (dark green) and parietal (red), however, belong to different modules in the skull illustrating that clear modular distinctions between bones must not necessarily indicate a kinetic association of them. Nevertheless, mesokinesis, as widely found in squamates (Iordansky 2011), might be an evolutionary result from the intersection between the posterior skull roof module (red) and the more anterior dorsal skull bones (dark green and dark purple) already established in an early amniote like *C. aguti*. In fact, all models with temporal openings (Figs. 31B–K) show a clear distinction between the posterior skull roof module (red) and the upper snout modules, the latter of which always includes the frontal bone (dark purple), and as such, this condition then might further favor mesokinetic evolution.

A pleurokinetic joint - a mediolateral movement of the quadrate relative to the rest of the skull (Evans 2008) – might have been present in *C. aguti* between quadrate on the one hand and pterygoid, quadratojugal, and squamosal on the other hand, being enabled by the contraction of *musculus (m.) adductor mandibulae posterior* [AMP). In the present modularity study, the quadrate of *C. aguti* belongs to the cheek module (orange), clearly separated from pterygoid (dark pink) and squamosal (red). Only the quadratojugal (in addition to the jugal) is found to share a modular identity with the quadrate. Apparently, a shared modular identity does not necessarily preclude internal kinetics within a module. The reportedly thin bones of the

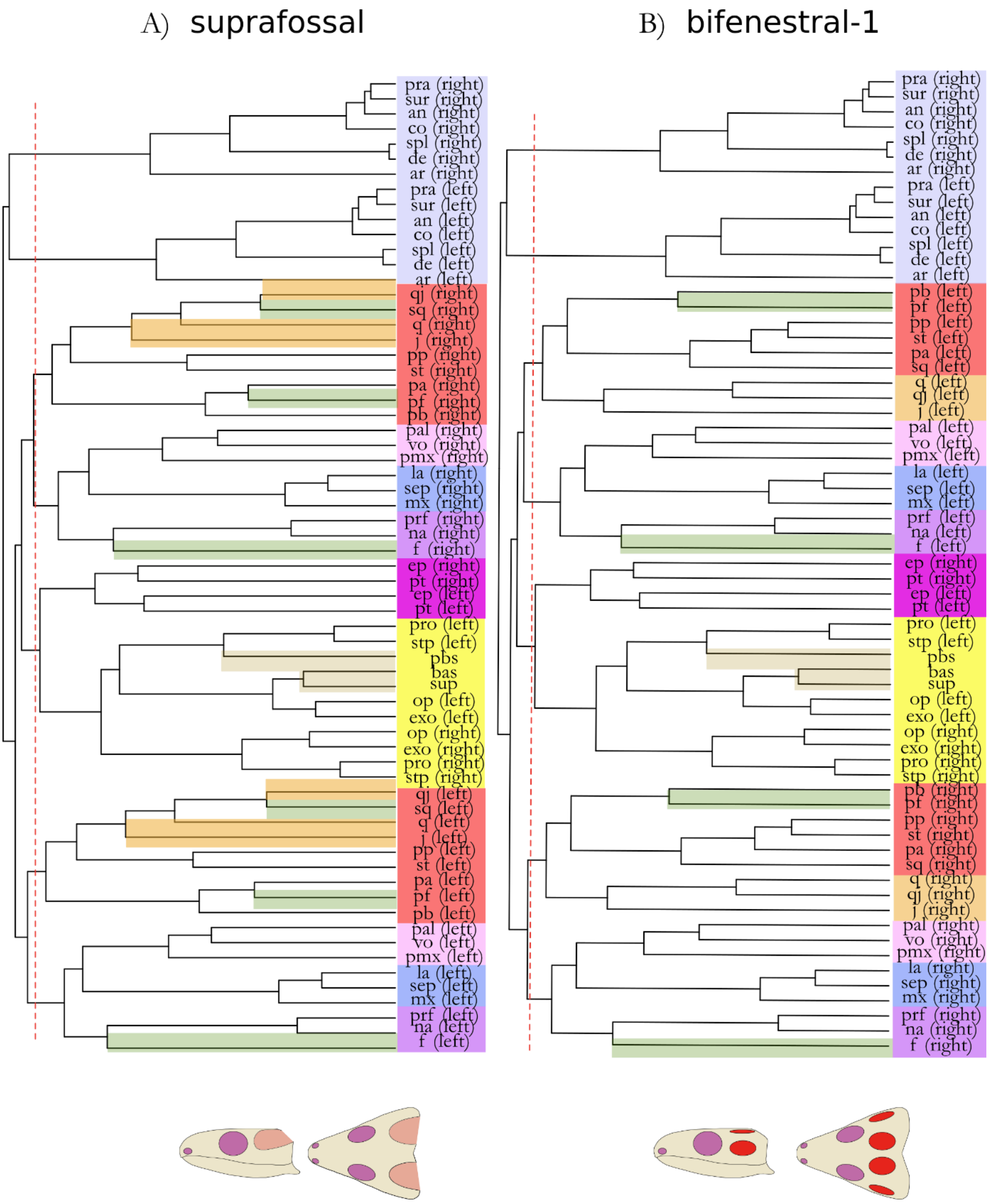

Fig. 34 Dendrogram of the skull network of (A) the suprafossal and (B) the bifenestral-1 skull types. Compare to caption of Fig. 31E. Green- and orange-colored branches indicate that these nodes were assigned to other modules in the initial analyses (see the color code in Fig. 31E).

cheek region (Fox 1964) likely permitted a certain elasticity of that region, driven by contraction of *m. adductor mandibulae Pars medialis* [(AMEM; *sensu* Abel et al. (2022)] and *Pars superficialis* (AMES).

Kinesis within the snout (prokinesis and rhynchokinesis) was certainly not possible based on the strong suturing of the snout bones (maxilla, lacrimal, and jugal). Bite forces were likely absorbed by the more elastic sutures in the more dorsal snout bones, namely, between nasal and prefrontal (Chapter 3). Herein, an absorption of biting forces in the upper snout is further supported by the presence of an upper snout module (dark purple) ventrally separated from the snout flank (light purple). The frontal and prefrontal contact is characterized by a simpler (although still thick) suture, that could indicate that this region is less effected by compressional forces (*sensu* Abel et al. 2022).

A mobility of the palate, a feature that has been suggested for the amniote base (Carroll 1969), was likely possible in *C. aguti* given the small relative thickness and simple suture types between vomer, palatine, and pterygoid. Also, a potential kinetic articulation between palatine and maxilla was present (Fox and Bowman 1966; Abel et al. 2022, see Chapter 3). The latter pattern is mirrored in the modularity of the palate with the elastic vomer and palatine forming a module together with the premaxilla, which functionally belongs to the palatal wing (light pink).

Pro- and retraction of the palate in relation to the rest of the skull might have been enabled by the pterygoid associated epipterygoid as a basicranial articulation of the epipterygoid to the braincase and a kinetic articulation between palatine and maxilla were present (Chapter 3). Pterygoid and epipterygoid together form a distinct module by their own reflecting their positional intersection between many skull modules and their various moveable and non-moveable articulations with other elements.

In sum, the observations in *C. aguti* illustrate a relatively good association of intracranial movements and skull modularity, although both relative thickness and suture type between adjacent bones require a balanced consideration of functional skull morphology (Esteve-Altava 2017*a*).

4.4.3. *C. aguti* and the origin of temporal skull openings in amniotes

It has been repeatedly discussed that particularly thin skull areas are prone to reduction as little forces are acting on these regions (e.g., Jaeckel 1902; Case 1924; Romer and Price 1940; Fox 1964). Temporal skull openings appear to develop particularly at the intersection between three adjacent bones (Frazzetta 1968; Kuhn-Schnyder 1980). As highlighted in Chapter 3, the intersections of (1) postorbital, squamosal, and parietal, of (2) jugal, squamosal, and postorbital, and of (3) jugal, squamosal, and quadratojugal may be treated candidate areas for temporal openings in early amniote evolution (see also image with numbers in Figs. 29E, 31A). In the following, the modularity pattern in *C. aguti* is used to infer potential areas for temporal openings.

(1) As mentioned above, a ’crossopterygian hinge line‘ *sensu* Kemp (1980) between squamosal and more dorsal skull roof bones could not be recovered in *C. aguti* herein, because both elements belong to one single module (red). This could indicate that the structural lability of the ’crossopterygian hinge line‘ was stabilized in early amniotes by a close integration of

both elements (however, see also other opinions on this ’hinge line‘ mentioned in Subchapter 3.4.4.). Nevertheless, like also described in Chapter 3, *C. aguti* is still characterized by weak suturing between squamosal and parietal. Therefore, this suture could have served as potential origin area of the supratemporal opening in diapsids (‘1’ in Figs. 29E, 31A), or even as an area that opened to allow dorsal expansion of the infratemporal region in therapsid synapsids.

(2) The modular distinction between jugal (orange) and postorbital/squamosal (red), together with the edge-like geometry of this intersection, makes this area a preferred candidate for the widely occurring infratemporal opening (‘2’ in Figs. 29E, 31A). Force vectors of AMEM (orange) and AMEP (red) musculature, pointing in different directions, will have further triggered the emergence of that opening.

(3) Similar to (2), the relatively rarely occurring opening between quadratojugal, jugal, and squamosal (‘3’ in Figs. 29E, 31A) might mainly result from the intersection of two modules (red and orange), specific arrangements of surrounding musculature (i.e., AMEM, AMES), plus the structural dissolution of the edge-like geometry of this intersection. This edge, however, is less pointy than in (2), which might explain the rare occurrence of this opening. Whether the infratemporal openings (2) and (3) actually have separated phylogenetic origins and whether they emerge from one unique opening or unite to one opening in the respective taxa cannot be evaluated herein. It is rather expected that the whole sutural area between squamosal and jugal serves as potential region for any infratemporal opening (Fig. 29E: indicated by white dashed line around ‘2’ and ‘3’), depending on species-specific configurations and compositions of the surrounding temporal bones. In species with a reduced quadratojugal, for example, a more dorsal position of the opening is common (Kemp 1982).

Rasskin-Gutman (2003) distinguished between ‘active and passive fenestrae’ in the vertebrate skull. Whereas ‘active’ ones between three adjacent bones (i.e., foramina) cannot close because they surround other (‘active’) tissue like nerves or vessels, the ‘passive’ ones in between four or more bones remain stable (‘passive’) along a phylogenetic lineage as long as no heterochronic event (relative growth in ontogeny) closes that opening. As such, to better understand transformations in temporal architecture, a greater focus on ontogenetic studies (Rieppel 1984; Haridy et al. 2016; Werneburg 2019; Lee et al. 2020) are urgently needed in the future.

As extensively discussed in Chapter 3, taking *C. aguti* as a model for early temporal skull evolution in amniotes has its limitations given the already derived skull anatomy of this species compared to the assumed ancestral amniote. Nevertheless, indications from this study on suture anatomy plus the support of modularity patterns provide a reasonable chain of argumentations to understand the origin of temporal openings in early amniotes. To further explore such evolutionary modifications, the modeling of different skull types, as performed in this study, provides a valuable framework to examine the complexity of cranial changes associated with temporal fenestrations.

4.4.4. Modelling temporal openings

Modeling temporal openings into the skull network of *C. aguti* of course comes with limitations. Obviously, there are no taxa in the fossil record that correspond to a fenestrated variant of *C. aguti*. Skull proportions along with bone number, suture lengths, and suture anatomy can drastically differ in early amniote species with temporal openings when compared to *C. aguti*. At this point, the above-mentioned simplification of the anatomical network methodology might actually be of a certain advantage as skull proportions and suture morphology are not considered in that approach.

In the herein used models, the number of skull bones and their general connectivity are kept stable to enable direct comparisons between the *C. aguti* network and the skull models derived from them. However, some bones, in particular the postparietal, supratemporal, and septomaxilla (Gaffney 1990; Koyabu et al. 2014; Higashiyama et al. 2021), are known to get reduced through amniote evolution (Esteve-Altava et al. 2013*b*). Nevertheless, most early amniotes, still have these bones preserved. Moreover, bones usually do not get lost as such. During ontogeny, their ossification centers generally fuse to 'larger' bones (Klembara et al. 2002; Polachowski and Werneburg 2013; Koyabu et al. 2014; Werneburg et al. 2015; Smith-Paredes et al. 2018), and coding their presence and ancestral connection to 'larger' bones may be judged as a reasonable methodological approach to retain comparability in this study.

The only major limitation of this model comparison might be the fact that some early amniotes still possess a tabular bone and an ectopterygoid. Most captorhinids, including *C. aguti*, lack those (e.g., Clack and Carroll 1973; Berman and Reisz 1986; Dodick and Modesto 1995; Müller and Reisz 2005) and they were, hence, not modeled herein.

Anatomical network analysis with actual species instead of models should be performed in the future to test and specify these initial attempts. Such species would need a comparable observation of suture anatomy (Jones et al. 2011) and muscle reconstruction before, as has been done for *C. aguti* (see Chapter 3). Fossil preservation of early amniotes, however, is poor in many cases and bone connections can be hard to reconstruct.

4.4.5. Evolutionary changes in functional skull morphology induced by temporal openings

4.4.5.a) The palate is functionally associated with changes in the temporal skull region

The modeling of temporal openings into the anapsid skull (Fig. 31A; scutal skull after Abel and Werneburg 2021) results in a number of changes in the composition of skull modules.

The most frequent skull opening in early amniotes was an infratemporal fenestra (ITF in Fig. 31), modeled as disconnection between jugal and squamosal herein (Fig. 29A,C: B-cut; intrafenestral-1 type). Whereas the modularity of the manipulated temporal skull coverage stays mainly unaltered, the snout flank (light purple) becomes more integrated with the palate wing (light pink) (Figs. 31B, 32A). This might be interpreted by a more posterior and, through a shorter lever arm, by a more powerful processing of food items in the center of the mouth. In fact, early synapsids are usually considered to have fed on hard food items associated with carnivore or herbivore feeding (Kemp 1982; Werneburg 2019). To process those, they might have been selected for a more powerful jaw adductor musculature. As illustrated herein (seven-pointed star in Fig. 31B), this might have been permitted by up to four muscle portions acting in union(i.e., AMP, AMEM, AMES, and AMEP).

A close integration of the snout flank (light purple) and the palate wing (light pink) is actually found in all modeled skulls, indicating a general adaptation to different food processing in amniotes when compared to their ancestors with further specifications by positional alteration or addition of opening(s) in the respective taxa. In therapsid synapsids, for example, a strong integration of snout and palate is related to the formation of a secondary palate introduced by neonatal lactation (Maier 1999) along with a more effective carnivore and herbivore feeding behavior, which required a strengthened palatal region. This change in therapsids was associated with a dorsal shift and expansion of the infratemporal fenestra (ITF) and a lower temporal excavation (LTE; see Chapter 2). Change in jaw muscle integration might be correlated with the observed bone modularity. With the development of a masseter muscle (i.e., AMEM-related following the argumentation Chapter 3) and an associated loss of the quadrate from the temporal region (i.e., it moves as incus to the middle ear; Werneburg 2013*b*), chewing behavior emerged in cynodont therapsids (Abdala and Damiani 2004). The adjusted side and inward movements during chewing could actually be mirrored in the postulated functional union of AMEM (masseter) and PTD musculature (asterisk in Figure 31C). The greater stability of the skull by formation of a secondary palate to withstand higher suckling and biting forces is also associated with the successive integration of the epipterygoid (as alisphenoid) to the secondary braincase wall toward Mammalia (Maier 1989, 1999). The certain independency of the median palate module (dark pink) to which the epipterygoid

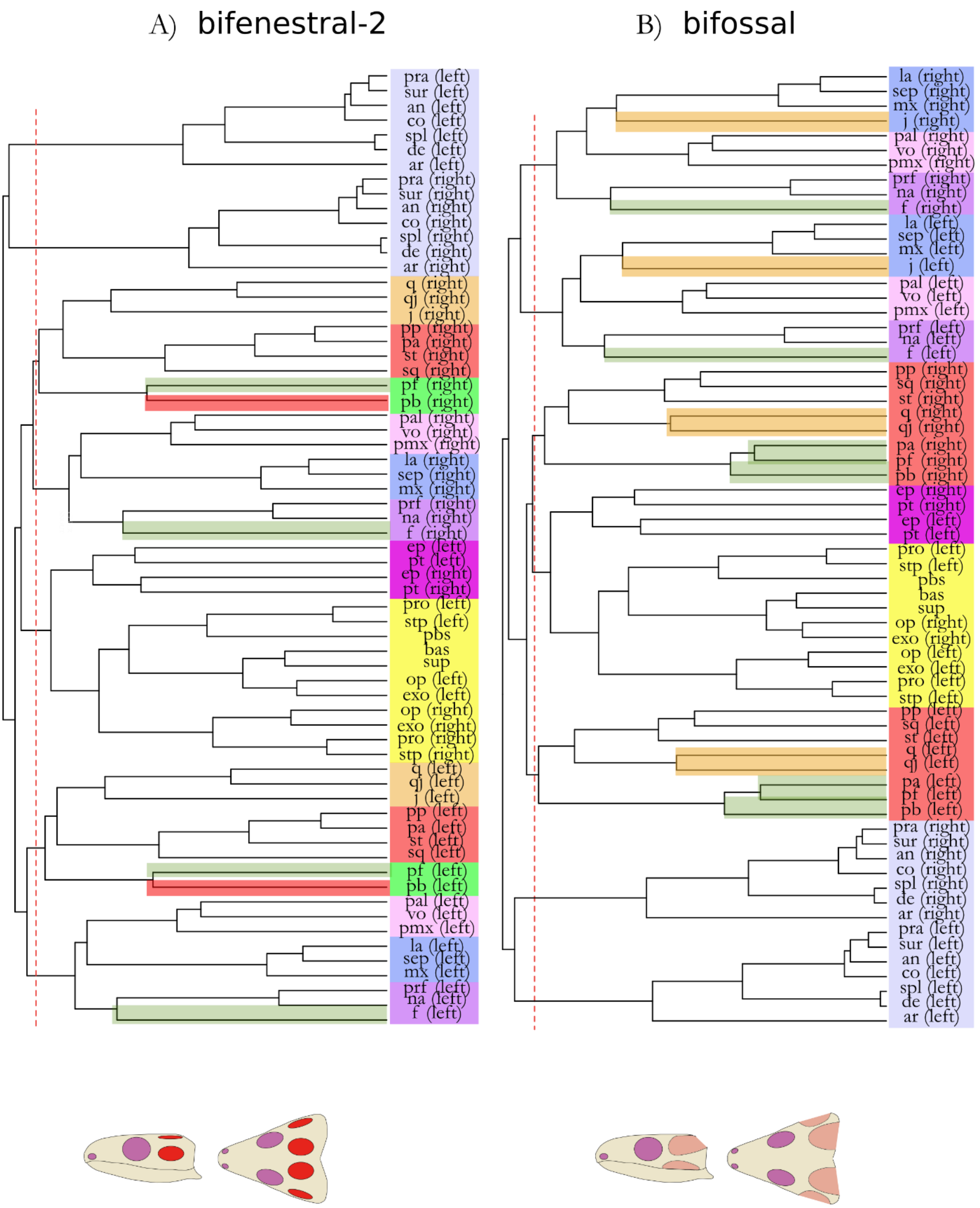

Fig. 35 Dendrogram of the skull network of (A) the bifenestral-2 and (B) the bifossal skull types. Compare to caption of Fig. 31E. Green-, orange-, and red-colored branches indicate that these nodes were assigned to other modules in the initial analyses (see the color code in Fig. 31E).

belongs in the anatomical network might have been, in this case, a precondition to uncouple this element from the palate.

The anatomical network modularity of an extant omnivorous mammal (*Didelphis virginiana* Kerr, 1792: Werneburg et al. 2019), which resembles the infratemporal-2 skull type, shows a certain similarity to the infratemporal-2 model presented herein in the way that the jugal and palatal region belong to the same module. It is worth mentioning that the fusion of the orbit with the infratemporal opening in that species has major impact on the modularity of the anterior and posterior dermal skull region. The latter is forming one consistent module with the braincase. This becomes obvious when comparing the results for *D. virginiana* to the pattern observed in primates, in which the postorbital bar is present and the frontal changes its modular association (Esteve-Altava et al. 2015*a*,*c*). Changing just one connection in the skull has major impact on general modular compositions.

4.4.5.b) Convergent evolution of stronger bite in terrestrial habitats

The modeling of a lower temporal excavation (LTE) in the skull (Fig. 31D; infrafossal type) results in the integration of the jugal into the snout flank module (light purple), suggesting a more powerful initial capture of hard food items anteriorly in a robust snout, possibly imaginable for *Eunotosaurus africanus* (Watson 1914; Keyser and Gow 1981) and other extinct taxa with similar temporal skull arrangement (e.g., *Llistrofus*, *Microleter*, *Millerosaurus* Broom, 1947, *Milleropsis*). Further food manipulation more posterior in the mouth, for instance by positioning of the food item before swallowing using pterygoid teeth (Gow 1997), might have been more complex. With the formation of a lower temporal excavation, the overall network integration falls into an anterior and a posterior skull part (double-headed arrows in Fig. 31C,D), which could hint to a more important role of the epipterygoid bone (dark pink) as pivot point between them, as indicated by a more independent related CID-musculature in the muscle reconstruction presented herein.

The presence of only a supratemporal fenestra (STF), like in the early diapsid *Araeoscelis*, resulted in a dorsal expansion of the cheek module toward squamosal (orange) (Fig. 31E; suprafenestral type). *Araeoscelis* exhibits a suite of unusual cranial features resulting in a massive, sturdily constructed skull, which is interpreted as an adaptation to a specialized diet that probably included invertebrates protected by heavy exoskeletons' (Reisz et al. 1984, p. 57). To enable this strong bite, according to the detected modularity pattern, AMES, AMP, and AMEP on the one hand, and AMEM and PTD on the other hand might have separately worked as unions. The comparison with heavy-snouted infrafossal taxa from the Permian shows that different 'experimentations' of temporal region anatomy were performed in early amniote evolution to exploit similar food resources that now became available in fully terrestrial habitats (see Chapter 2).

The presence of an upper temporal excavation (UTE) (Figure 31F; suprafossal type) results in the greatest expansion of the posterior roof module (red), suggesting high biting forces by joined action of AMEP, AMES, AMP, and AMEM. The otic notch in some potential amniote relatives like Seymouriamorpha mirrors the modeled upper temporal excavation (Klembara 1997, 2011). It is likely that these animals were already adapted to a more or less full terrestrial lifestyle with a focus on hard terrestrial food items. Also, strong biting turtles such as Chelydridae, Pelomedusidae, and Platysternidae (Herrel et al. 2002; Ferreira et al. 2020) develop deep upper temporal excavations (posterodorsal emarginations in turtle anatomical terminology *sensu* Werneburg 2012).

4.4.5.c) From robust to agile — and back to robust prey: diapsid evolution

The presence of two temporal openings (bifenestral-1 and 2) as seen in some early diapsids (Figure 31G: compare to *Petrolacosaurus*, Figure 31H: compare to *Youngina*) shows a cheek integration (orange) comparable to that of early synapsids (Figure 31B) with AMEP, AMES, AMP, and AMEM acting in union. This could highlight the generally stronger bite and, hence, better adaptation to terrestrial food in both diapsids and synapsids when compared to non-fenestrated early amniotes like *C. aguti*.

Early diapsids are thought to have been adapted to feeding on agile prey (Evans 2008), for which an increased intracranial mobility was necessary (see section 4.4.5.e). More tipward diapsids (Lee et al. 2020; Plateau and Foth 2020) differ from the modeled early diapsids. Differences are likely associated with a change to a more carnivorous feeding behavior as exemplified in archosauriform evolution with *Euparkeria capensis* Broom, 1913*b* representing a transitional form (Sookias et al. 2020) or *Tyrannosaurus rex* Osborn, 1905 showing specific snout adaptations (Werneburg et al. 2019). The relatively larger snouts, together with the orbits, increasingly restricted the space for the temporal region through archosaur evolution. Related to strong bites and long snouts, the pterygoid musculature in crocodiles dominates above the external jaw adductors with influence on bone arrangements and modularity in the respective regions as illustrated by *Alligator mississippiensis* Daudin, 1802 (Werneburg et al. 2019).

The textbook example of an extant diapsid, the tuatara *Sphenodon punctatus* (Lepidosauria), is also highly derived in its skull network modularity (Werneburg et al. 2019) when compared to the herein modeled early diapsid forms. Tuatara secondarily re-evolved the lower temporal arcade (Müller 2003) and has a number of other derived characters. The degree of its intracranial mobility is debated and seems to depend on ontogenetic changes with, likely, less mobile skulls and stronger bites in adults (Jones et al. 2011; Werneburg and Yaryhin 2019).

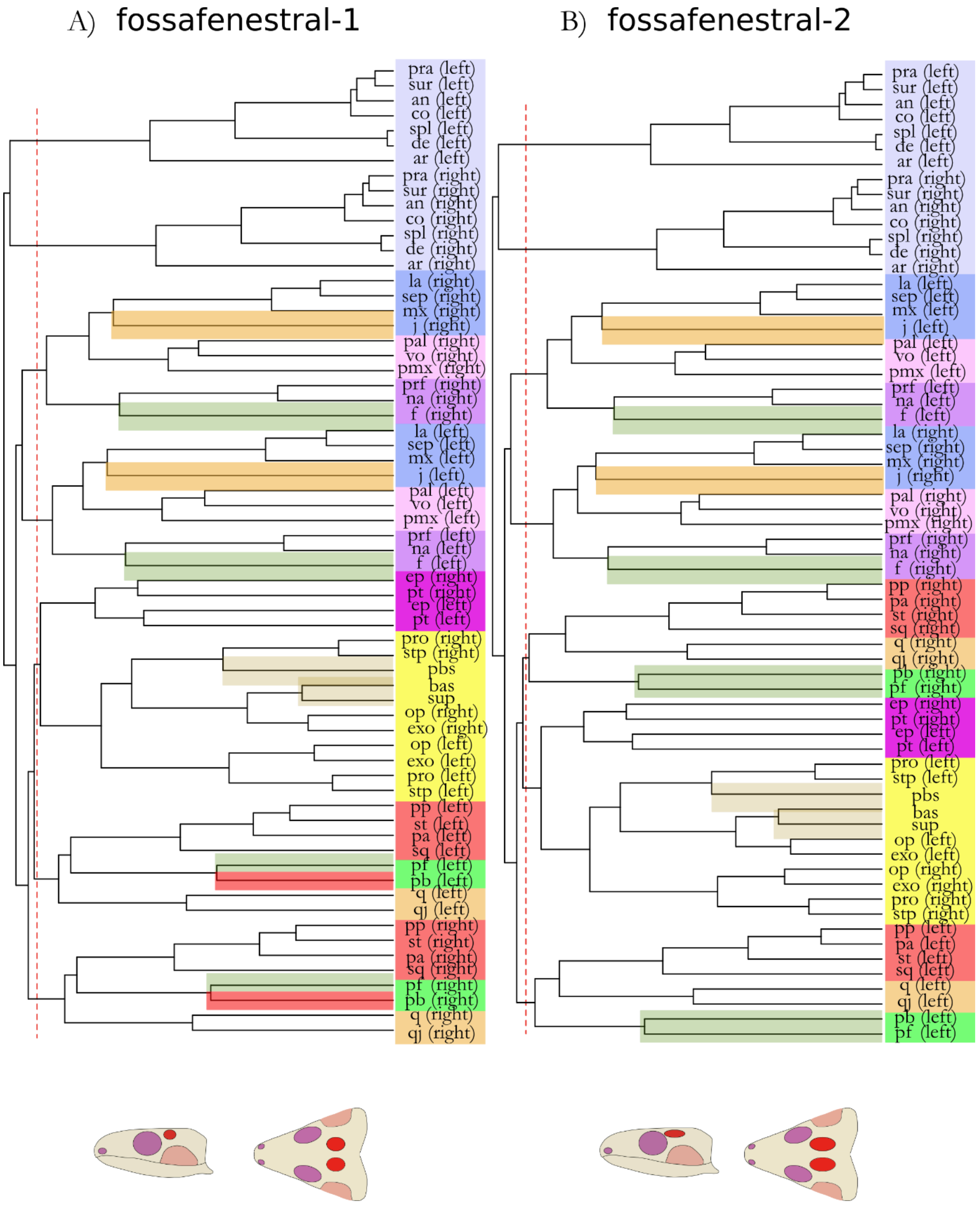

Fig. 36 Dendrogram of the skull network of (A) the fossafenestral-1 and (B) the fossafenestral-2 skull types. Compare to caption of Fig. 31E. Green-, orange-, and red-colored branches indicate that these nodes were assigned to other modules in the initial analyses (see the color code in Fig. 31E).

4.4.5.d) The never-ending turtle story

The bifossal model (Fig. 31I) resembles a morphotype that is basically established in extant turtles (Werneburg 2012), a group that reportedly shows several derived characters compared to the ancestral amniote and even to the ancestral turtle condition (Müller 2003; Joyce 2007). Hence, the limitation mentioned above for interpreting a network model also applies, particularly, when discussing the turtle skull morphotype. Nevertheless, the simplification in the network methodology permits a comparison to other models.

Compared to *C. aguti*, the jugal in the bifossal model becomes part of the snout flank module (light purple), mirrored by the general robusticity of the snout in turtles, which is ancestrally covered by an edentulous beak (Li et al. 2018). The remainder of the temporal region forms one consistent module (red) likely related to a union of AMEP, AMES, and AMP (Fig. 31I). In fact, jaw musculature in turtles is (superficially) less diverse than that of all other extant reptilian groups (Schumacher 1956; Werneburg 2011, 2013*a*,*b*).

With the formation of a deep ventral excavation, the skull network, again, separates into an anterior and a posterior skull part. Whereas this feature resulted in an apparently higher independency and mobility of the epipterygoid (dark pink) in taxa like millerettids, *Microleter*, and *Eunotosaurus* (Figure 31D), the epipterygoid is either lost (Pleurodira) or integrated (Cryptodira) into the secondary braincase wall in extant turtles (Werneburg and Maier 2019), decoupling this element from other skull modules (which is associated with the loss of CID musculature in turtles; see Werneburg 2011) and resulting in an akinetic skull (Werneburg and Maier 2019). As has been shown by Ferreira et al. (2020), the jaw muscle arrangement and the skull shape of modern turtles is associated with fundamental cranial changes related to the evolutionary increase of neck mobility. Jaw muscle functionality can be seen as a tradeoff between restrictions in space for jaw musculature in the jaw adductor chamber and the retention (but not increase) of the ancestral jaw muscle power. While the jaw musculature of turtles is rather simple in superficial view, it internally shows great tendinous differentiation, which might reflect the concealed anatomical response to that restriction (Schumacher 1956; Werneburg 2011, 2013*b*).

The expansion of the posterior skull roof module (red) in the bifossal turtle skull can be associated with a higher integration related to neck mobility. Tensional force of the retracting neck is related to enlarged temporal emarginations (Werneburg 2012, 2015) and might be buffered by a broadly integrated temporal region (Werneburg et al. 2021).

The leatherback turtle (Werneburg et al. 2019) largely reduced its ability to retract the neck and, hence, no posterodorsal emarginations are developed in the skull (*sensu* Werneburg 2015). It is noteworthy that in the anatomical network reconstructed for this species, only an integration of frontal and parietal, but not of the cheek region, is present. The close association of frontal and parietal can be interpreted by a still certain degree of embryonic neck muscle tension acting on the roof of its developing skull (Werneburg and Maier 2019; Werneburg et al. 2021). Different to the model presented herein (Figure 31I), an ancestral integration of the jugal into the cheek module (orange) is present in the leatherback turtle. This can be interpreted by the specific arrangement of bones, related to unique characters such as a truncated snout and a domed skull in this marine turtle species (Nick 1912; Schumacher 1972; Werneburg et al. 2019).

It is worth mentioning that the bifossal skull type (Figure 31I) is argumentatively also present in the akinetic mammals, although the upper temporal excavation derives from an expanded upper temporal fenestra and not by marginal bone reductions (Werneburg 2019). The convergent separation in an anterior and a posterior skull part and a related simplification of skull network composition (Werneburg et al. 2019) is striking.

4.4.5.e) Toward highly kinetic skulls

Whether a fossafenestral-1 type (Fig. 31J) was actually developed in *Claudiosaurus* is debatable based on whether and how much the postfrontal actually contributed to the upper temporal opening (Carroll 1981). Nevertheless, when compared to the fossafenestral-2 type (Fig. 31K), in which the upper temporal opening expands more anteriorly, the general size influence of an opening becomes obvious, as in this example the posterior skull roof module (red) changes its global modular association (see dendrogram in Fig. 36B and white parallel stripes in Fig. 31K).

Among early amniotes, the fossafenestral-2 type is likely present in Tangasauridae (Bickelmann et al. 2009) and basically represents the skull type found among the neodiapsid squamates. Whenever an upper temporal fenestra is formed together with a lower temporal excavation (Fig. 31C,J–K), a postocular module (light green) emerges. The same is true for the bifenestral skull, in which the supratemporal fenestra is anteriorly expanded (bifenestral-2 type; Fig. 31H) as is known for *Youngina* among early amniotes. Different muscle portions that mainly attach to other bones (see star in Fig. 31A) can partly originate or insert also to the postorbital in extant reptiles (Holliday and Witmer 2007; Werneburg 2013*a*). Possessing a postocular skull module (light green), which includes postorbital and postfrontal, could indicate to a more independent differentiation of the muscle fibers attaching there. Consequently, number and effective direction of muscle vectors will change. As virtually all external adductor muscles insert to the lower jaw, a more complex positioning of agile prey in the mouth can be assumed, as reflected by the insectivorous diet of many taxa with fossafenestral-2 skull anatomy (i.e., squamates), but also in taxa with infrafenestral-2 skulls, such as therapsids, which were ‘on their way’ to develop chewing behavior with increased jaw mobility.

The infratemporal openings of fossafenestral forms, again, split the skull in an anterior and a posterior part. The epipterygoid (dark pink), with its reconstructed independent CID musculature, could again serve as pivot point in these taxa and enable amphikinetic skull movements (Iordansky 1990, 2011). In all models described, as well as in *C. aguti*, the epipterygoids and pterygoids with their associated musculature form a single module (dark pink), suggesting that they might have acted together. Whereas the epipterygoid is originally used as lever arm to move the palate in anteroposterior direction - which might still be the case in most taxa - it appears to further act in positioning the pterygoid when handling diverse food items in bifenestral-2 and fossafenestral skulls. In this regard, the former, exemplified by *Youngina*, represents a transitional state toward the highly kinetic skull of squamate reptiles.

4.5. Conclusions

This study tackles one of the big questions in vertebrate evolutionary morphology, namely, the evolution and functional backgrounds of temporal skull openings in amniotes. Although the used anatomical network analysis has a number of limitations due to its simplifying methodology, it allows strategical comparisons among different anatomical models. A careful evaluation of the observed outcome is necessary and requires a comprehensive morphological discussion.

Here, the presence or absence of temporal openings was modeled into a given skull network to observe the effect on module composition. It has been demonstrated that changes in the number, position, and expansion of temporal openings have fundamental impact on skull modularity. This is interpreted mainly in regard to feeding behavior in amniotes, where the assumed hardness and agility of prey items are considered. Changes in temporal openings and the resulting skull modules also have impact on intracranial movements.

The present discussion is highly speculative and remains at a modeling level. It should be understood as a first attempt to interpret complex skull modularity in early amniotes. Obviously, actual skulls need to be studied and coded to get a clearer picture of network modularity in early amniote skulls. By presenting the skull network modularity of the well-known *C. aguti*, a first attempt in this direction is provided.

Lastly, a comparison with extant amniote skulls supports the basic functional assumptions that have been derived from this modeling approach. Influenced by changed feeding adaptations and associated changes in skull architecture, however, secondary alterations from the ancestral amniote skull network conditions evolved in later taxa. Detecting and describing general patterns of changes across amniote evolution is a desirable outlook on future broad scale taxonomic analysis using the anatomical network methodology.

Chapter 5

Conclusion and outlook

5. Conclusion and outlook

This thesis provides a detailed overview of the morphology and research history of the temporal region in tetrapods and their extinct relatives. The numerously suggested classifications of amniotes and other tetrapods based on their temporal morphology were described and standardized by a new purely descriptive classification system (see Chapter 2 – Abel & Werneburg 2021). This approach intentionally simplifies skull morphology and allows a broad comparison of various taxa independent of phylogeny. This can be used for future quantitative analyses on overall patterns in the evolution of the temporal region. A possible tool for this could be the methodology recently introduced by Brocklehurst et al. (2021, 2022).

In general, temporal openings might form by reduction of lesser loaded bony areas. This has been tested by examining suture morphology and reconstructing the jaw adductors in the early reptile *Captorhinus aguti* (see Chapter 3 – Abel et al. 2022*a*). It could be demonstrated that *C. aguti* exhibited two potentially lesser loaded areas in its temporal dermal armor that correspond to the loci of the infratemporal and supratemporal fenestrae in many other amniotes. Nevertheless, since *C. aguti* already possessed some derived features and captorhinids with temporal openings are unknown, future studies may further test this observation by also examining more rootward taxa or such that are closer to taxa with temporal openings. A key species for this is the diapsid-relative *Protorothyris archeri* (see Chapter 3).

Moreover, the position of the lesser loaded areas generally corresponds to the results of an Anatomical Network Analysis based on the same species (see Chapter 4 – Werneburg & Abel 2022). The latter suggests that the temporal armor can be subdivided into different functional modules that might be associated with the arrangement of the jaw adductors. Artificially modifying this network by simulating the presence of temporal openings often leads to a change in the module composition, arguing for simultaneous change in muscle arrangement and, hence, change in functional properties. This method may also be applied to analyze more skull networks of various extinct and extant species (see Esteve-Altava & Rasskin-Gutman 2014; Werneburg et al. 2019) to further test the inferences drawn from the modelled skulls.

Overall, this thesis provides an important step towards an understanding of the evolution and functional morphology of the temporal skull region. In addition to the outlook described above, further research projects could focus on the developmental aspects of temporal openings (see Schoch 2014*b*; Werneburg 2019), as well as on the temporal diversity in non-amniote groups (Kleinteich et al. 2012; Paluh et al. 2020). Lastly, further researching the temporal diversity among ecologically similar taxa, like crocodylians and specific extinct crocodylomorphs, could prove to be a meaningful endeavor (Zepf 2021).

Gedanken kommen,

Gedanken gehen,

manchmal sind sie verschwommen,

oftmals sie gleich verwehen.

Einige nur lassen sich nieder,

hämmern und pochen,

rühren sich immer wieder

und bringen mich zum kochen.

Diese jedoch lassen sich formen,

oder zu etwas gestalten

nur muß man sie normen

und abbringen vom Alten.

Hans Abel

6. References

Abdala, F., and Damiani, R. (2004). Early development of the mammalian superficial masseter muscle in cynodonts. *Palaeontologica Africana*, 40, 23–29.

Abel, P., Pommery, Y., Ford, D. P., Koyabu, D., and Werneburg, I. (2022*a*). Skull sutures and cranial mechanics in the Permian reptile *Captorhinus aguti* and the evolution of the temporal region in early amniotes. *Frontiers in Ecology and Evolution*, 10, 841784.

Abel, P., Pommery, Y., Ford, D. P., Koyabu, D., and Werneburg, I. (2022*b*). 3D models related to the publication: Skull sutures and cranial mechanics in the Permian reptile *Captorhinus aguti* and the evolution of the temporal region in early amniotes. *MorphoMuseuM*, 8(167), 1–2.

Abel, P., and Werneburg, I. (2021). Morphology of the temporal skull region in tetrapods: Research history, functional explanations, and a new comprehensive classification scheme. *Biological Reviews*, 96(5), 2229–2257.

Adams, L. A. (1919). A memoir on the phylogeny of the jaw muscles in recent and fossil vertebrates. *Annals of the New York Academy of Sciences*, 28(1), 51–166.

AmphibiaTree (2004). *Bombina orientalis*. *Digital Morphology.* http://digimorph.org/specimens/Bombina_orientalis/ (accessed on the 01.07.2022).

AmphibiaTree, and Gosselin-Ildari, A. (2008). *Pleurodeles walti*. *Digital Morphology.* http://digimorph.org/specimens/Pleurodeles_waltl/whole/ (accessed on the 01.07.2022).

Anderson, J. S. (2008). Focal review: the origin(s) of modern amphibians. *Evolutionary Biology*, 35(4), 231–247.

Andrews, C. W. (1913). *A Descriptive Catalogue of the Marine Reptiles of the Oxford Clay: Based on the Leeds Collection in the British Museum (Natural History) Library, London* (Vol. 2). London: Order of the Trustees of the British Museum.

Angielczyk, K. D. (2004). Phylogenetic evidence for and implications of a dual origin of propaliny in anomodont therapsids (Synapsida). *Paleobiology*, 30(2), 268–296.

Arnaudo, M. E., Soibelzon, L. H., Bona, P., and Schubert, B. (2014). First description of the auditory region of a Tremarctinae (Ursidae, Mammalia) bear: the case of *Arctotherium angustidens*. *Journal of Mammalian Evolution*, 21, 321–330.

Bailleul, A. M., and Holliday, C. M. (2017). Joint histology in *Alligator mississippiensis* challenges the identification of synovial joints in fossil archosaurs and inferences of cranial kinesis. *Proceedings of the Royal Society B*, 284, 20170038.

Bardua, C., Wilkinson, M., Gower, D. J., Sherratt, E., and Goswami, A. (2019). Morphological evolution and modularity of the caecilian skull. *BMC Evolutionary Biology*, 19(1), 1–23.

Barghusen, H. R. (1973). The adductor jaw musculature of *Dimetrodon* (Reptilia, Pelycosauria). *Journal of Paleontology,* 47(5), 823–834.

Baur, G. (1889). On the morphology of the vertebrate-skull. *Journal of Morphology,* 3(3), 467–474.

Baur, G. (1894). Bemerkungen über die Osteologie der Schläfengegend der höheren Wirbeltiere. *Anatomischer Anzeiger,* 10(10), 315–330.

Beaumont, E. H. (1977). Cranial morphology of the Loxommatidae (Amphibia: Labyrinthodontia). *Philosophical Transactions of the Royal Society of London,* 280(971), 29–101.

Benson, R. B. J. (2012). Interrelationships of basal synapsids: cranial and postcranial morphological partitions suggest different topologies. *Journal of Systematic Palaeontology,* 10(4), 601–624.

Benson, R. B. J., Evans, M., Smith, A. S., Sassoon, J., Moore-Faye, S., Ketchum, H. F., and Forrest, R. (2013). A giant pliosaurid skull from the Late Jurassic of England. *PLoS ONE,* 8(5), e65989.

Benton, M. J. (1983). The Triassic reptile *Hyperodapedon* from Elgin: functional morphology and relationships. *Philosophical Transactions of the Royal Society of London B, Biological Sciences,* 302(1112), 605–718.

Benton, M. J. (1985). Classification and phylogeny of the diapsid reptiles. *Zoological Journal of the Linnean Society,* 84(2), 97–164.

Berman, D. S (2000). Origin and early evolution of the amniote occiput. *Journal of Paleontology,* 74(5), 938–956.

Berman, D. S (2013). Diadectomorphs, amniotes or not? *New Mexico Museum of Natural History and Science Bulletin,* 60, 22–35.

Berman, D. S, Eberth, D. A., and Brinkman, D. B. (1988). *Stegotretus agyrus* a new genus and species of microsaur (amphibian) from the Permo-Pennsylvanian of New Mexico. *Annals of Carnegie Museum,* 57(13), 293–323.

Berman, D. S, and Reisz, R. R. (1986). Captorhinid reptiles from the Early Permian of New Mexico, with description of a new genus and species. *Annals of Carnegie Museum,* 55(1), 1–28.

Berman, D. S, Reisz, R. R., Bolt, J. R., and Scott, D. (1995). The cranial anatomy and relationships of the synapsid *Varanosaurus* (Eupelycosauria: Ophiacodontidae) from the Early Permian of Texas and Oklahoma. *Annals of Carnegie Museum,* 64(2), 99–133.

Berman, D. S, Reisz, R. R., and Scott, D. (2010). Redescription of the skull of *Limmoscelis paludis* Williston (Diadectomorpha: Limnoscelidae) from the Pennsylvanian of Cañon del Cobre, Northern New Mexico. *New Mexico Museum of Natural History and Science Bulletin,* 49, 185–210.

Berman, D. S, Sumida, S. S., and Lombard, R. E. (1992). Reinterpretation of the temporal and occipital regions in *Diadectes* and the relationships of diadectomorphs. *Journal of Paleontology,* 66(3), 481–499.

Bever, G. S., Lyson, T. R., Field, D. J., and Bhullar, B. A. (2015). Evolutionary origin of the turtle skull. *Nature,* 525(7568), 239–242.

Bhullar, B. A., and Bever, G. S. (2009). An archosaur-like laterosphenoid in early turtles (Reptilia: Pantestudines). *Breviora,* 518(1), 1–11.

Bickelmann, C., Müller, J., and Reisz, R. R. (2009). The enigmatic diapsid *Acerosodontosaurus piveteaui* (Reptilia: Neodiapsida) from the Upper Permian of Madagascar and the paraphyly of "younginiform" reptiles. *Canadian Journal of Earth Sciences,* 46(9), 651–661.

Blackburn, D. G., and Stewart, J. R. (2021). Morphological research on amniote eggs and embryos: An introduction and historical retrospective. *Journal of Morphology,* 282(7), 1–23.

Blanco, M. V. F., Cassini, G. H., and Bona, P. (2018). Skull ontogeny of extant caimans: a three-dimensional geometric morphometric approach. *Zoology,* 129, 69–81.

Blom, H. (2005). Taxonomic revision of the late Devonian tetrapod *Ichthyostega* from East Greenland. *Palaeontology,* 48(1), 111–134.

Boas, J. E. V. (1915). Die Schläfenüberdachung und das Palatoquadratum in ihrem Verhältnis zum übrigen Schädel bei den Dipnoern und den terrestren Wirbeltieren. *Gegenbaurs Morphologisches Jahrbuch,* 49(2), 229–307.

Bock, W. J. (1964). Kinetics of the avian skull. *Journal of Morphology,* 114(1), 1–42.

Boettger, C. R. (1952). Die Stämme des Tierreichs in ihrer systematischen Gliederung. *Abhandlungen der Braunschweigischen Wissenschaftlichen Gesellschaft,* 4, 238–300.

Bolt, J. R. (1974). Evolution and functional interpretation of some suture patterns in Paleozoic labyrinthodont amphibians and other lower tetrapods. *Journal of Paleontology,* 48(3), 434–458.

Bolt, J. R., and Rieppel, O. (2009). The holotype skull of *Llistrofus pricei* Carroll and Gaskill, 1978 (Microsauria: Hapsidopareiontidae). *Journal of Paleontology,* 83(3), 471–483.

Boonstra, L. D. (1936). On some features of the cranial morphology of the tapinocephalid deinocephalians. *Bulletin of the American Museum of Natural History,* 72, 75–98.

Boonstra, L. D. (1952). 'N nuwe soort van tapinocephalide deinocephalië̈r *Struthiocephalus akraalensis* sp. nov. *South African Journal of Science,* 48, 247–248.

Boot, G. W. (1910). Development of the temporal bone. *JAMA: The Journal of the American Medical Association,* 55(7), 563.

Boy, J. A., and Martens, T. (1991). Ein neues captorhinomorphes Reptil aus dem thüringischen Rotliegend (Unter-Perm; Ost-Deutschland). *Paläontologische Zeitschrift,* 65(3/4), 363–389.

Bramble, D. M. (1978). Origin of the mammalian feeding complex: models and mechanisms. *Paleobiology,* 4(3), 271–301.

Bramble, D. M., and Wake, D. B. (1985). Feeding Mechanisms of Lower Tetrapods. In M. Hildebrand, D. Bramble, K. Liem, and D. Wake (Eds.), *Functional Vertebrate Morphology* (pp. 230–261). Cambridge: Harvard University Press.

Branson, E. B. (1911). Notes on the osteology of the skull of *Pariotichus*. *The Journal of Geology,* 19(2), 135–139.

Brocklehurst, N., Ford, D. P., and Benson, R. B. J. (2022). Early origins of divergent patterns of morphological evolution on the mammal and reptile stem-lineages. *Systematic Biology, in press*.

Brocklehurst, N., Panciroli, E., Benevento, G. L., and Benson, R. B. J. (2021). Mammaliaform extinctions as a driver of the morphological radiation of Cenozoic mammals. *Current Biology,* 31, 2955–2963.

Broili, F. (1904–05). Permische Stegocephalen und Reptilien aus Texas. *Palaeontographica,* 51, 1–120.

Broom, R. (1903). On a new reptile *(Proterosuchus fergusi*) from the Karroo Beds of Tarkastad, South Africa. *Annals of the South African Museum,* 4, 161–163.

Broom, R. (1911). *On the structure of the skull in cynodont reptiles.* Paper presented at the Proceedings of the Zoological Society of London, Oxford, UK.

Broom, R. (1913a). On the structure and affinities of *Bolosaurus*. *Bulletin American Museum of Natural History,* 32(33), 509–516.

Broom, R. (1913b). Note on *Mesosuchus browni*, Watson, and on a new South African Triassic pseudosuchian (*Euparkeria capensis*). *Records of the Albany Museum,* 2, 394–396.

Broom, R. (1914). A new thecodont reptile. *Proceedings of the Zoological Society of London, 1914*, 1072–1077.

Broom, R. (1922). *On the temporal arches of the Reptilia.* Paper presented at the Proceedings of the Zoological Society of London, Oxford, UK.

Broom, R. (1938). On a new type of primitive fossil reptile from the Upper Permian of South Africa. *Proceedings of the Zoological Society of London,* B108(3), 535–542.

Broom, R. (1947). Contribution to our knowledge of the vertebrates of the Karroo Beds of South Africa. *Transactions of the Royal Society of Edinburgh,* 61(2), 577–629.

Bryant, H. N., and Seymour, K. L. (1990). Observations and comments on the reliability of muscle reconstruction in fossil vertebrates. *Journal of Morphology,* 206(1), 109–117.

Buchwitz, M., Jansen, M., Renaudie, J., Marchetti, L., and Voigt, S. (2021). Evolutionary change in locomotion close to the origin of amniotes inferred from trackway data in an ancestral state reconstruction approach. *Frontiers in Ecology and Evolution,* 9(674779), 1–24.

Burne, R. H. (1905). Notes on the muscular and visceral anatomy of the leathery turtle (*Dermochelys coriacea*). *Proceedings of the Zoological Society of London,* 75(2), 291–324.

Busbey, A. B. (1995). The structural consequences of skull flattening in crocodiles. In J. J. Thomason (Ed.), *Functional Morphology in Vertebrate Paleontology* (pp. 173–192). Cambridge: Cambridge University Press.

Cannatella, D. C., and Hillis, D. M. (1993). Amphibian relationships: phylogenetic analysis of morphology and molecules. *Herpetological Monographs,* 7, 1–7.

Carr, T. D. (1999). Craniofacial ontogeny in Tyrannosauridae (Dinosauria, Coelurosauria). *Journal of Vertebrate Paleontology,* 19(3), 497–520.

Carr, T. D. (2020). A high-resolution growth series of *Tyrannosaurus rex* obtained from multiple lines of evidence. *PeerJ,* 8, e9192.

Carroll, R. L. (1969a). Problems of the origins of reptiles. *Biological Reviews,* 44, 393–432.

Carroll, R. L. (1969b). A Middle Pennsylvanian captorhinomorph, and the interrelationships of primitive reptiles. *Journal of Paleontology,* 43(1), 151–170.

Carroll, R. L. (1981). Plesiosaur ancestors from the upper Permian of Madagascar. *Philosophical Transactions of the Royal Society of London. B, Biological Sciences,* 293(1066), 315–383.

Carroll, R. L. (1982). Early evolution of reptiles. *Annual Review of Ecology and Systematics,* 13(1), 87–109.

Carroll, R. L. (1988). *Vertebrate Paleontology and Evolution*. New York: W.H. Freeman and Company.

Carroll, R. L. (2007). The Palaeozoic ancestry of salamanders, frogs and caecilians. *Zoological Journal of the Linnean Society,* 150, 1–140.

Carroll, R. L., and Baird, D. (1972). Carboniferous stem-reptiles of the family Romeriidae. *Bulletin of the Museum of Comparative Zoology,* 143, 321–363.

Carroll, R. L., and Gaskill, P. (1978). *The Order Microsauria*. Philadelphia: The American Philosophical Society.

Carroll, R. L., and Holmes, R. (1980). The skull and jaw musculature as guides to the ancestry of salamanders. *Zoological Journal of the Linnean Society,* 68(1), 1–40.

Case, E. C. (1898). The significance of certain changes in the temporal region of the primitive Reptilia. *The American Naturalist,* 32(374), 69–74.

Case, E. C. (1911). *A Revision of the Cotylosauria of North America*. Washington, D. C.: Carnegie Institution of Washington.

Case, E. C. (1924). A possible explanation of fenestration in the primitive reptilian skull, with notes on the temporal region of the genus *Dimetrodon*. *Contributions from the Museum of Geology University of Michigan,* 2(1), 1–12.

Čihák, R., Královec, K., and Roček, Z. (2003). Developmental origin of the frontoparietal bone in *Bombina variegata* (Anura: Discoglossidae). *Journal of Morphology,* 255(1), 122–129.

Cisneros, J. C. (2008). Taxonomic status of the reptile genus *Procolophon* from the Gondwanan Triassic. *Palaeontologica Africana,* 43, 7–17.

Cisneros, J. C., Abdala, F., Jashashvili, T., de Oliveira Bueno, A., and Dentzien-Dias, P. (2015). *Tiarajudens eccentricus* and *Anomocephalus africanus,* two bizarre anomodonts (Synapsida, Therapsida) with dental occlusion from the Permian of Gondwana. *Royal Society Open Science,* 2(7), 150090.

Cisneros, J. C., Damiani, R., Schultz, C., da Rosa, A., Schwanke, C., Neto, L. W., and Aurélio, P. L. P. (2004). A procolophonoid reptile with temporal fenestration from the Middle Triassic of Brazil. *Proceedings of the Royal Society of London. Series B: Biological Sciences,* 271(1547), 1541–1546.

Cisneros, J. C., Kammerer, C. F., Angielczyk, K. D., Fröbisch, J., Marsicano, C., Smith, R. M., and Richter, M. (2021). A new reptile from the lower Permian of Brazil (*Karutia fortunata* gen. et sp. nov.) and the interrelationships of Parareptilia. *Journal of Systematic Palaeontology*, 18(23), 1939–1959.

Clack, J. A. (1987a). Two new specimens of *Anthracosaurus* (Amphibia: Anthracosauria) from the Northumberland Coal Measures. *Palaeontology,* 30(1), 15–26.

Clack, J. A. (1987b). *Pholiderpeton scutigerum* Huxley, an amphibian from the Yorkshire coal measures. *Philosophical Transactions of the Royal Society of London,* 318(1188), 1–107.

Clack, J. A. (1997). The Scottish Carboniferous tetrapod *Crassigyrinus scoticus* (Lydekker)—cranial anatomy and relationships. *Transactions of the Royal Society of Edinburgh: Earth Sciences,* 88(3), 127–142.

Clack, J. A. (2002). The dermal skull roof of *Acanthostega gunnari*, an early tetrapod from the Late Devonian. *Transactions of the Royal Society of Edinburgh: Earth Sciences,* 93(1), 17–33.

Clack, J. A. (2012). *Gaining Ground – The Origin and Evolution of Tetrapods* (2 ed.). Bloomington: Indiana University Press.

Clark, J., and Carroll, R. L. (1973). Romeriid reptiles from the Lower Permian. *Bulletin of the Museum of Comparative Zoology,* 144, 353–407.

Colbert, E. H. (1945). *The Dinosaur Book: the Ruling Reptiles and their Relatives*. New York: The American Museum of Natural History.

Colbert, E. H. (1946). *Hypsognathus*, a Triassic reptile from New Jersey. *Bulletin of the American Museum of Natural History,* 86(5), 231–274.

Conrad, J. L., and Norell, M. A. (2010). Cranial autapomorphies in two species of *Iguana* (Iguanidae: Squamata). *Journal of Herpetology,* 44(2), 307–312.

Cope, E. D. (1868). Synopsis of the extinct Batrachia of North America. *Proceedings of the Academy of Natural Sciences of Philadelphia,* 20, 208–221.

Cope, E. D. (1878). Descriptions of extinct Batrachia and Reptilia from the Permian Formation of Texas. *Proceedings of the American Philosophical Society,* 17(101), 505–530.

Cope, E. D. (1882). Third contribution to the history of the Vertebrata of the Permian formation of Texas. *Proceedings of the American Philosophical Society,* 20(112), 447–461.

Cope, E. D. (1892). On the homologies of the posterior cranial arches in the Reptilia. *Transactions of the American Philosophical Society,* 17(1), 11–26.

Cope, E. D. (1895). The reptilian order Cotylosauria. *Proceedings of the American Philosophical Society,* 34(149), 436–457.

Cope, E. D. (1896). Second contribution to the history of the Cotylosauria. *Proceedings of the American Philosophical Society,* 35(151), 122–139.

Cost, I. N., Middleton, K. M., Sellers, K. C., Echols, M. S., Witmer, L. M., Davis, J. L., and Holliday, C. M. (2020). Palatal biomechanics and its significance for cranial kinesis in *Tyrannosaurus rex*. *The Anatomical Record,* 303, 999–1017.

Crawford, N. G., Faircloth, B. C., McCormack, J. E., Brumfield, R. T., Winker, K., and Glenn, T. C. (2012). More than 1000 ultraconserved elements provide evidence that turtles are the sister group of archosaurs. *Biology Letters,* 8(5), 783–786.

Crawford, N. G., Parham, J. F., Sellas, A. B., Faircloth, B. C., Glenn, T. C., Papenfuss, T. J., Henderson, J. B., Hansen, M. H., and Simison, W. B. (2015). A phylogenomic analysis of turtles. *Molecular Phylogenetics and Evolution,* 83, 250–257.

Crompton, A. W. (1963). The evolution of the mammalian jaw. *Evolution,* 17(4), 431–439.

Csardi, G., and Nepusz, T. (2006). The *igraph* software package for complex network research. *InterJournal Complex Systems,* 1659, 1–9.

Currie, P. J. (1981). *Hovasaurus boulei*, an aquatic eosuchian from the Upper Permian of Madagascar. *Palaeontologia Africana,* 24, 99–168.

Curtis, N., Jones, M. E. H., Evans, S. E., O'Higgins, P., and Fagan, M. (2013). Cranial sutures work collectively to distribute strain throughout the reptile skull. *Journal of the Royal Society Interface,* 10(86), 1–8.

Cuthbertson, R. S., Tirabasso, A., Rybczynski, N., and Holmes, R. B. (2012). Kinetic limitations of intracranial joints in *Brachylophosaurus canadensis* and *Edmontosaurus regalis* (Dinosauria: Hadrosauridae), and their implications for the chewing mechanics of hadrosaurids. *The Anatomical Record,* 295(6), 968–979.

Cuvier, G. L. C. F. D. (1829). *Le Règne Animal Distribué d'Après son Organisation, Pour Servir de Base à l'Histoire Naturelle des Animaux et d'Introduction à l'Anatomie Comparée* (Vol. 2): Chez Déterville, Libraire, rue Hautefeuille, No 8 et Chez Crochard, Libraire, Cloitar Saint-Ehnoit, No 16.

Daeschler, E. B., Shubin, N. H., and Jenkins, F. A., Jr. (2006). A Devonian tetrapod-like fish and the evolution of the tetrapod body plan. *Nature,* 440(7085), 757–763.

Darwin, C. (1859). *The Origin of Species by Means of Natural Selection, or the Preservation of Favoured Races in the Struggle for Life* (1 ed.). London: John Murray.

Das, S., Campbell, P., Roy, S., Mukherjee, S., Pramanick, K., Biswas, A., and Raha, S. (2019). Cranial osteology and molecular phylogeny of *Argyrogena fasciolata* (Shaw, 1802) (Colubridae: Serpentes). *Vertebrate Zoology,* 69(3), 311–325.

Daudin, F. M. (1802). *Histoire Naturelle Générale et Particulière des Reptiles* (F. Dufarf Ed. Vol. 2). Paris.

Dawson, J. W. (1860). On a terrestrial mollusk, a chilognathous myriapod, and some new species of reptiles, from the Coal-Formation of Nova Scotia. *Quarterly Journal of the Geological Society of London,* 16(1–2), 268–277.

Daza, J. D., Diogo, R., Johnston, P., and Abdala, V. (2011). Jaw adductor muscles across lepidosaurs: a reappraisal. *The Anatomical Record,* 294(10), 1765–1782.

deBraga, M., and Reisz, R. R. (1996). The early Permian reptile *Acleistorhinus pteroticus* and its phylogenetic position. *Journal of Vertebrate Paleontology,* 16(3), 384–395.

deBraga, M., and Rieppel, O. (1997). Reptile phylogeny and the interrelationships of turtles. *Zoological Journal of the Linnean Society,* 120, 281–354.

DigiMorph Staff. (2002). *Scolecomorphus* sp. *Digital Morphology.* http://digimorph.org/specimens/Scolecomorphus_sp/ (accessed on the 12.07.2022).

Diogo, R. (2008). Comparative anatomy, homologies and evolution of mandibular, hyoid and hypobranchial muscles of bony fish and tetrapods: a new insight. *Animal Biology,* 58(2), 123–172.

Diogo, R., and Abdala, F. (2010). The Head Muscles of Dipnoans – a Review on the Homologies and Evolution of these Muscles within Vertebrates. In J. Joss and J. M. Jorgensen (Eds.), *Biology of Lungfishes* (pp. 169–218). Boca Raton: CRC Press.

Diogo, R., and Abdala, F. (2010). *Muscles of Vertebrates*. Enfield: Science Publishers.

Diogo, R., Abdala, V., Lonergan, N., and Wood, B. A. (2008). From fish to modern humans – comparative anatomy, homologies and evolution of the head and neck musculature. *Journal of Anatomy,* 213(4), 391–424.

Diogo, R., Esteve-Altava, B., Smith, C., Boughner, J. C., and Rasskin-Gutman, D. (2015). Anatomical network comparison of human upper and lower, newborn and adult, and normal and abnormal limbs, with notes on development, pathology and limb serial homology vs. homoplasy. *PLoS ONE,* 10, e0140030.

Dodick, J. T., and Modesto, S. P. (1995). The cranial anatomy of the captorhinid reptile *Labidosaurikos meachami* from the Lower Permian of Oklahoma. *Palaeontology,* 38(3), 687–711.

Dollo, L. (1884). Cinquième note sur les dinosauriens de Bernissart. *Bulletin du Musée Royal d'Histoire Naturelle de Belgique - Mededeelingen van het Koninklijk Natuurhistorisch Museum van Belgi,* 3(8), 129–146.

Dombrowski, B. (1924). Über einige Gesetzmäßigkeiten im Aufbau des schalleitenden und Kieferapparates der Tetrapoden. *Zeitschrift für Anatomie und Entwicklungsgeschichte,* 75(1–2), 69–81.

Ebel, R., Müller, J., Ramm, T., Hipsley, C., and Amson, E. (2020). First evidence of convergent lifestyle signal in reptile skull roof microanatomy. *BMC Biology,* 18, 185.

Egberts, S. (2008). *A morphological study of Captorhinus aguti using X-ray computed tomography: new insights on a well-studied species*. Paper presented at the Society of Vertebrate Paleontology, Sixty-Eighth Annual Meeting, Cleveland.

Elzanowski, A., and Mayr, G. (2018). Multiple origins of secondary temporal fenestrae and orbitozygomatic junctions in birds. *Journal of Zoological Systematics and Evolutionary Research,* 56(2), 248–269.

Erickson, G. M., Gignac, P. M., Lappin, A. K., Vliet, K. A., Brueggen, J. D., and Webb, G. J. W. (2013). A comparative analysis of ontogenetic bite-force scaling among Crocodylia. *Journal of Zoology,* 292(1), 48–55.

Escobedo-Galván, A. H., Velasco, J. A., González-Maya, J. F., and Resetar, A. (2015). Morphometric analysis of the Rio Apaporis caiman (Reptilia, Crocodylia, Alligatoridae). *Zootaxa,* 4059(3), 541–554.

Esteve-Altava, B. (2017a). Challenges in identifying and interpreting organizational modules in morphology. *Journal of Morphology,* 278(7), 960–974.

Esteve-Altava, B. (2017b). In search of morphological modules: a systematic review. *Biological Reviews,* 92(3), 1332–1347.

Esteve-Altava, B. (2017c). Network models: connecting anatomy to systems biology. *The FASEB Journal,* 31(S1), 386.382.

Esteve-Altava, B., Boughner, J. C., Diogo, R., and Rasskin-Gutman, D. (2015a). Anatomical network analysis of primate skull morphology. *The FASEB Journal,* 29, 867.863.

Esteve-Altava, B., Boughner, J. C., Diogo, R., Villmoare, B. A., and Rasskin-Gutman, D. (2015b). Anatomical network analysis shows decoupling of modular lability and complexity in the evolution of the primate skull. *PLoS ONE,* 10, e0127653.

Esteve-Altava, B., Diogo, R., Smith, C., Diego, J. C. B., and Rasskin-Gutman, D. (2015c). Anatomical networks reveal the musculoskeletal modularity of the human head. *Scientific Reports,* 5, 8298.

Esteve-Altava, B., Marugan-Lobon, J., Botella, H., Bastir, M., and Rasskin-Gutman, D. (2013a). Grist for Riedl's Mill: a network model perspective on the integration and modularity of the human skull. *Journal of Experimental Zoology (Molecular and Developmental Evolution),* 320(8), 489–500.

Esteve-Altava, B., Marugan-Lobon, J., Botella, H., and Rasskin-Gutman, D. (2011). Network models in anatomical systems. *Journal of Anthropological Sciences,* 89, 175–184.

Esteve-Altava, B., Marugan-Lobon, J., Botella, H., and Rasskin-Gutman, D. (2013b). Structural constraints in the evolution of the tetrapod skull complexity: Williston's Law revisited using network models. *Evolutionary Biology,* 40, 209–219.

Evans, S. E. (1980). The skull of a new eosuchian reptile from the Lower Jurassic of South Wales. *Zoological Journal of the Linnean Society,* 70(3), 203–264.

Evans, S. E. (2008). The skull of lizards and tuatara. In C. Gans, A. S. Gaunt, and K. Adler (Eds.), *Biology of the Reptilia* (Vol. 20, pp. 1–347): Society for the Study of Amphibians and Reptiles.

Evans, S. E., and Borsuk-Białynicka, M. (2009). A small lepidosauromorph reptile from the Early Triassic of Poland. *Palaeontologia Polonica,* 65, 179–202.

Evans, S. E., Jones, M. E., and Krause, D. W. (2008). A giant frog with South American affinities from the Late Cretaceous of Madagascar. *Proceedings of the National Academy of Sciences,* 105(8), 2951–2956.

Ezcurra, M. D., and Butler, R. J. (2015). Taxonomy of the proterosuchid archosauriforms (Diapsida: Archosauromorpha) from the earliest Triassic of South Africa, and implications for the early archosauriform radiation. *Palaeontology,* 58(1), 141–170.

Ferreira, G. S., Lautenschlager, S., Evers, S. W., Pfaff, C., Kriwet, J., Raselli, I., and Werneburg, I. (2020). Feeding biomechanics suggests progressive correlation of skull architecture and neck evolution in turtles. *Scientific Reports,* 10(1), 5505.

Ferreira, G. S., and Werneburg, I. (2019). Evolution, diversity, and development of the craniocervical system in turtles with special reference to jaw musculature. In J. M. Ziermann, R. E. Diaz Jr, and R. Diogo (Eds.), *Heads, Jaws, and Muscles - Anatomical, Functional, and Developmental Diversity in Chordate Evolution* (pp. 171–206): Springer.

Field, D. J., Gauthier, J. A., King, B. L., Pisani, D., Lyson, T. R., and Peterson, K. J. (2014). Toward consilience in reptile phylogeny: miRNAs support an archosaur, not lepidosaur, affinity for turtles. *Evolution & Development,* 16(4), 189–196.

Field, D. J., Hanson, M., Burnham, D., Wilson, L. E., Super, K., Ehret, D., Ebersole, J. A., and Bhullar, B.-A. S. (2018). Complete *Ichthyornis* skull illuminates mosaic assembly of the avian head. *Nature,* 557(7703), 96–100.

Ford, D. P. (2018). *The Evolution and Phylogeny of Early Amniotes.* (Dissertation). University of Oxford, Oxford.

Ford, D. P., and Benson, R. B. J. (2020). The phylogeny of early amniotes and the affinities of Parareptilia and Varanopidae. *Nature Ecology & Evolution,* 4(1), 57–65.

Ford, D. P., Benson, R. B. J., and Mannion, P. (2019). A redescription of *Orovenator mayorum* (Sauropsida, Diapsida) using high-resolution µCT, and the consequences for early amniote phylogeny. *Papers in Palaeontology,* 5(2), 197–239.

Fox, R. C. (1964). The adductor muscles of the jaw in some primitive reptiles. *University of Kansas Publications,* 12(15), 657–680.

Fox, R. C., and Bowman, M. C. (1966). Osteology and relationships of *Captorhinus aguti* (Cope) (Reptilia: Captorhinomorpha). *The University of Kansas Paleontological Contributions Vertebrata,* 11, 1–79.

Fracasso, M. A. (1983). *Cranial osteology, functional morphology, systematics and paleoenvironment of Limnoscelis paludis Williston.* Yale University, New Haven.

Fraser, N. C. (1988). The osteology and relationships of *Clevosaurus* (Reptilia: Sphenodontida). *Philosophical Transactions of the Royal Society of London. B, Biological Sciences,* 321(1204), 125–178.

Frazzetta, T. H. (1962). A functional consideration of cranial kinesis in lizards. *Journal of Morphology,* 111(3), 287–319.

Frazzetta, T. H. (1968). Adaptive problems and possibilities in the temporal fenestration of tetrapod skulls. *Journal of Morphology,* 125(2), 145–157.

Fuchs, H. (1909). Betrachtungen über die Schläfengegend am Schädel der Quadrupeden. *Anatomischer Anzeiger,* 35(5–7), 113–167.

Fürbringer, M. (1900). Zur vergleichenden Anatomie des Brustschulterapparates und der Schultermuskeln. *Jenaische Zeitschrift für Naturwissenschaft,* 34(4), 215–718.

Gaffney, E. S. (1979). Comparative cranial morphology of recent and fossil turtles. *Bulletin of the American Museum of Natural History,* 164(2), 65–376.

Gaffney, E. S. (1983). The cranial morphology of the extinct horned turtle, *Meiolania platyceps*, from the Pleistocene of Lord Howe Island, Australia. *Bulletin of the American Museum of Natural History,* 175(4), 361–480.

Gaffney, E. S. (1990). The comparative osteology of the Triassic turtle *Proganochelys*. *Bulletin of the American Museum of Natural History,* 194, 1–263.

Gaffney, E. S., and Jenkins, F. A., Jr. (2010). The cranial morphology of *Kayentachelys*, an Early Jurassic cryptodire, and the early history of turtles. *Acta Zoologica,* 91(3), 335–368.

Gaffney, E. S., and McKenna, M. C. (1979). A Late Permian captorhinid from Rhodesia. *American Museum Novitates,* 2688, 1–15.

Gans, C. (1960). Studies on amphisbaenids (Amphisbaenia, Reptilia) – 1. A taxonomic revision of the Trogonophinae, and a functional interpretation of the amphisbaenid adaptive pattern. *Bulletin of the American Museum of Natural History,* 119(3), 133–204.

Gaupp, E. (1895a). Ueber die Jochbogen-Bildungen am Schädel der Wirbelthiere. *Jahres-Bericht der Schlesischen Gesellschaft für vaterländische Cultur,* 72(2), 56–63.

Gaupp, E. (1895b). Beiträge zur Morphologie des Schädels. III. Zur vergleichenden Anatomie der Schläfengegend am knöchernen Wirlbelthier-Schädel. *Morphologische Arbeiten,* 4(1), 77–129.

Gauthier, J. A., and de Queiroz, K. (2020). Diapsida. In J. A. Gauthier (Ed.), *Phylonyms, a Companion to the PhyloCode* (1 ed., pp. 1033–1040). London: Taylor & Francis Group, Ltd.

Gauthier, J. A., Kluge, A. G., and Rowe, T. (1988). The early evolution of the Amniota. In M. J. Benton (Ed.), *The Phylogeny and Classification of the Tetrapods, Volume I: Amphibians, Reptiles, Birds* (Vol. 1, pp. 103–155). Oxford: Clarendon Press.

Gebauer, E. V. I. (2007). *Phylogeny and evolution of the Gorgonopsia with a special reference to the skull and skeleton of GPIT/RE/7113 ('Aelurognathus?'parringtoni).* (Dissertation). Eberhard-Karls Universität Tübingen, Tübingen.

Gee, B. M., Bevitt, J. J., Garbe, U., and Reisz, R. R. (2019). New material of the 'microsaur' *Llistrofus* from the cave deposits of Richards Spur, Oklahoma and the paleoecology of the Hapsidopareiidae. *PeerJ,* 7, e6327.

Gegenbaur, C. (1898). *Vergleichende Anatomie der Wirbelthiere mit Berücksichtigung der Wirbellosen* (Vol. 1). Leipzig: Verlag von Wilhelm Engelmann.

Gemmell, N. J., Rutherford, K., Prost, S., Tollis, M., Winter, D., Macey, J. R., . . . Ngatiwai Trust Board. (2020). The tuatara genome reveals ancient features of amniote evolution. *Nature,* 584(7821), 403–409.

Gervais, P. (1865). Description du *Mesosaurus tenuidens*, reptile fossile de l'Afrique australe. *Académie des Sciences et Lettres de Montpellier, Mémoires de la Section des Sciences,* 6(2), 169–175.

Goodrich, E. S. (1916). On the classification of the Reptilia. *Proceedings of the Royal Society of London. Series B, Containing Papers of a Biological Character,* 89(615), 261–276.

Gow, C. E. (1972). The osteology and relationships of the Millerettidae (Reptilia: Cotylosauria). *Journal of Zoology,* 167(2), 219–264.

Gow, C. E. (1997). A reassessment of *Eunotosaurus africanus* Seeley (Amniota: Parareptilia). *Palaeontologia Africana,* 34, 33–42.

Gower, D. J., Loader, S. P., Moncrieff, C. B., and Wilkinson, M. (2004). Niche separation and comparative abundance of Boulengerula boulengeri and *Scolecomorphus vittatus* (Amphibia: Gymnophiona) in an East Usambara forest, Tanzania. *African Journal of Herpetology,* 53(2), 183–190.

Gray, J. E. (1831a). Note on a particular structure in the head of an *Agama*. *The Zoological Miscellany*, 13–14.

Gray, J. E. (1831b). Characters of a new genus of freshwater tortoise from China. *Proceedings of the Zoological Society of London,* 1831, 106–107.

Gray, J. E. (1842). Description of two hitherto unrecorded species of reptiles from New Zealand; presented to the British Museum by Dr. Dieffenbach. *The Zoological Miscellany*, 72.

Gray, J. E. (1856). On some new species of freshwater tortoises from North America, Ceylon and Australia, in the collection of the British Museum. *Proceedings of the Zoological Society of London,* 1855, 197–202.

Gregory, W. K., and Adams, L. A. (1915). The temporal fossae of vertebrates in relation to the jaw muscles. *Science,* 41(1064), 763–765.

Gruntmejer, K., Konietzko-Meier, D., Marcé-Nogué, J., Bodzioch, A., and Fortuny, J. (2019). Cranial suture biomechanics in *Metoposaurus krasiejowensis* (Temnospondyli, Stereospondyli) from the Upper Triassic of Poland. *Journal of Morphology,* 280, 1850–1864.

Günther, A. (1858). *Catalogue of the Batrachia Salientia in the Collection of the British Museum*. London: Order of the Trustees.

Günther, A. (1867). Contribution to the anatomy of *Hatteria* (Rhynchocephalus, Owen). *Proceedings of the Royal Society of London,* 15(19), 595–629.

Haas, A. (2001). Mandibular arch musculature of anuran tadpoles; with comments on homologies of amphibian jaw muscles. *Journal of Morphology,* 247(1), 1–33.

Haas, A. (2003). Phylogeny of frogs as inferred from primarily larval characters (Amphibia: Anura). *Cladistics,* 19(1), 23–89.

Hall, B. K. (2005). *Bones and Cartilage – Developmental and Evolutionary Skeletal Biology*. Cambridge: Academic Press.

Hall, B. K. (2009). *The Neural Crest and Neural Crest Cells in Vertebrate Development and Evolution*. New York City: Springer.

Hall, B. K. (2014). *Bones and Cartilage – Developmental and Evolutionary Skeletal Biology* (2 ed.). London, San Diego, Waltham, Oxford: Academic Press.

Hallmann, E. (1837). *Die Vergleichende Osteologie des Schläfenbeins*. Hannover: Verlag der Hahn'schen Hofbuchhandlung.

Handschuh, S., Natchev, N., Kummer, S., Beisser, C. J., Lemell, P., Herrel, A., and Vergilov, V. (2019). Cranial kinesis in the miniaturised lizard *Ablepharus kitaibelii* (Squamata: Scincidae) *Journal of Experimental Biology,* 222(9), jeb198291.

Hanken, J., and Hall, B. K. (1993a). *The Skull. Vol. 2, Patterns of Structural and Systematic Diversity*. Chicago: The University of Chicago Press.

Hanken, J., and Hall, B. K. (1993b). *The Skull. Vol. 3, Functional and Evolutionary Mechanisms*. Chicago: The University of Chicago Press.

Haridy, Y., Macdougall, M. J., Scott, D., and Reisz, R. R. (2016). Ontogenetic change in the temporal region of the early Permian parareptile *Delorhynchus cifellii* and the implications for closure of the temporal fenestra in amniotes. *PLoS ONE,* 11(12), e0166819.

Hay, O. P. (1908). *The Fossil Turtles of North America*.

Heaton, M. J. (1979). Cranial anatomy of primitive captorhinid reptiles from the Late Pennsylvanian and Early Permian Oklahoma and Texas. *Oklahoma Geological Survey,* 127, 1–84.

Heckert, A. B., Lucas, S. G., and Spielmann, J. A. (2012). A new species of the enigmatic archosauromorph *Doswellia* from the Upper Triassic Bluewater Creek Formation, New Mexico, USA. *Palaeontology,* 55(6), 1333–1348.

Heiss, E., Aerts, P., and Van Wasserbergh, S. (2018). Aquatic–terrestrial transitions of feeding systems in vertebrates: a mechanical perspective. *Journal of Experimental Biology,* 221(8), jeb154427.

Heiss, E., and Grell, J. (2019). Same but different: aquatic prey capture in paedomorphic and metamorphic Alpine newts. *Zoological Letters,* 5(24), 1–12.

Heiss, E., Natchev, N., Gumpenberger, M., Weissenbacher, A., and van Wasserbergh, S. (2013). Biomechanics and hydrodynamics of prey capture in the Chinese giant salamander reveal a high-performance jaw-powered suction feeding mechanism. *Journal of the Royal Society Interface,* 10(82), 20121028.

Herrel, A., O'Reilly, J. C., and Richmond, A. M. (2002). Evolution of bite performance in turtles. *Journal of Evolutionary Biology,* 15(6), 1083–1094.

Herring, S. W. (1972). Sutures – a tool in functional cranial analysis. *Acta Anatomica,* 83, 222–247.

Herring, S. W. (2008). Mechanical Influences on Suture Development and Patency. In D. P. Rice (Ed.), *Craniofacial Sutures. Development, Disease and Treatment.* (pp. 41–56). Basel: Karger.

Herring, S. W., and Mucci, R. J. (1991). In vivo strain in cranial sutures: The zygomatic arch. *Journal of Morphology,* 207(3), 225–239.

Herring, S. W., Pedersen, S. C., and Huang, X. (2005). Ontogeny of bone strain: the zygomatic arch in pigs. *The Journal of Experimental Biology,* 208(23), 4509–4521.

Herring, S. W., and Teng, S. (2000). Strain in the braincase and its sutures during function. *American Journal of Physical Anthropology,* 112(4), 575–593.

Herring, S. W., Teng, S., Huang, X., Mucci, R. J., and Freeman, J. (1996). Patterns of bone strain in the zygomatic arch. *The Anatomical Record,* 246(4), 446–457.

Higashiyama, H., Koyabu, D., Hirasawa, T., Werneburg, I., Kuratani, S., and Kurihara, H. (2021). Mammalian face as an evolutionary novelty. *Proceedings of the National Academy of Sciences of the United States of America,* 118(44), e2111876118.

Hinz, J. K., Matzke, A. T., and Pfretzschner, H.-U. (2019). A new nothosaur (Sauropterygia) from the Ladinian of Vellberg-Eschenau, southern Germany. *Journal of Vertebrate Paleontology,* 39(2), e1585364.

Holliday, C. M., Porter, W. R., Vliet, K. A., and Witmer, L. M. (2020). The frontoparietal fossa and dorsotemporal fenestra of archosaurs and their significance for interpretations of vascular and muscular anatomy in dinosaurs. *The Anatomical Record,* 303(4), 1060–1074.

Holliday, C. M., and Witmer, L. M. (2007). Archosaur adductor chamber evolution: integration of musculoskeletal and topological criteria in jaw muscle homology. *Journal of Morphology,* 268(6), 457–484.

Holliday, C. M., and Witmer, L. M. (2008). Cranial kinesis in dinosaurs: intracranial joints, protractor muscles, and their significance for cranial evolution and function in diapsids. *Journal of Vertebrate Paleontology,* 28(4), 1073–1088.

Holmes, R., Cheng, Y. N., and Wu, X.-C. (2008). New information on the skull of *Keichousaurus hui* (Reptilia: Sauropterygia) with comments on sauropterygian interrelationships. *Journal of Vertebrate Paleontology,* 28(1), 76–84.

Holmes, R. B. (1984). The Carboniferous amphibian *Proterogyrinus scheelei* Romer, and the early evolution of tetrapods. *Philosophical Transactions of the Royal Society of London,* 306(1130), 431–524.

Holmes, R. B., Carroll, R. L., and Reisz, R. R. (1998). The first articulated skeleton of *Dendrerpeton acadianum* (Temnospondyli, Dendrerpetontidae) from the Lower Pennsylvanian locality of Joggins, Nova Scotia, and a review of its relationships. *Journal of Vertebrate Paleontology,* 18(1), 64–79.

Hotton, N., Olson, E. C., and Beerbower, R. (1997). The Amniote Transition and the Discovery of Herbivory. In S. Sumida and K. L. M. Martin (Eds.), *Amniote Origins – Completing the Transition to Land* (pp. 207–264). San Diego, London: Academic Press.

Hülsmann, E., and Wahlert, G. V. (1972). *Das Schädelkabinett - Eine erklärende Naturgeschichte der Wirbeltiere*. Basel: Basilius Presse.

Huxley, T. H. (1863). Description of *Anthracosaurus russelli*, a new labyrinthodont form the Lanarkshire coal field. *Quarterly Journal of the Geological Society of London,* 19, 56–68.

Hylander, W. L., and Johnson, K. R. (1997). In vivo bone strain patterns in the zygomatic arch of macaques and the significance of these patterns for functional interpretations of craniofacial form. *American Journal of Physical Anthropology,* 102(2), 203–232.

Illiger, D. (1811). *Prodromus Systematis Mammalium et Avium Additis Terminis Zoographicis Utriusque Classis, Eorumque Versione Germanica*. Berlin: Sumptibus C. Salfeld.

Iordansky, N. N. (1990). Evolution of cranial kinesis in lower tetrapods. *Netherlands Journal of Zoology,* 40(1–2), 32–54.

Iordansky, N. N. (1996). The temporal ligaments and their bearing on cranial kinesis in lizards. *Journal of Zoology,* 239(1), 167–175.

Iordansky, N. N. (2000). Cranial kinesis in the Amphibia: a review. *Zhurnal Obshchei Biologii,* 61(1), 102–118.

Iordansky, N. N. (2004). The jaw apparatus of *Lialis* (Lacertilia, Pygopodidae): patterns of intensification of cranial kinesis and the problem of the origin of snakes. *Entomological Review,* 84, S99–S109.

Iordansky, N. N. (2010). Pterygoideus muscles and other jaw adductors in amphibians and reptiles. *Biology Bulletin,* 37(9), 905–914.

Iordansky, N. N. (2011). Cranial kinesis in lizards (Lacertilia): origin, biomechanics, and evolution. *Biology Bulletin,* 38(9), 868–877.

Iordansky, N. N. (2015). Streptostyly and biological coordinations in the Jaw apparatus of lizards (Lacertilia). *Biology Bulletin,* 42(9), 784–792.

Irisarri, I., Baurain, D., Brinkmann, H., Delsuc, F., Sire, J.-Y., Kupfer, A., Petersen, J., Jarek, M., Meyer, A., Vences, M., and Philippe, H. (2017). Phylotranscriptomic consolidation of the jawed vertebrate timetree. *Nature Ecology & Evolution,* 1, 1370–1378.

Jaekel, O. (1902). Ueber *Gephyrostegus bohemicus* nov. gen. nov. sp. *Zeitschrift der Deutschen Geologischen Gesellschaft,* 54, 127–132.

Jaekel, O. (1909a). Über die Klassen der Tetrapoden. *Zoologischer Anzeiger,* 34(7–8), 193–212.

Jaekel, O. (1909b). Über das System der Reptilien. *Zoologischer Anzeiger,* 35(11), 324–341.

Jaekel, O. (1913). *Über den Bau des Schädels*. Paper presented at the Verhandlungen der Anatomischen Gesellschaft, Greifswald.

Jaekel, O. (1916). Die Wirbeltierfunde aus dem Keuper von Halberstadt. *Paläontologische Zeitschrift,* 2, 88–214.

Jaekel, O. (1922). Neues über Hemispondyla. *Paläontologische Zeitschrift,* 5(1), 1–25.

Jaekel, O. (1927). Neue Forschungen über das Primordial-Cranium und Gehirn paläozoischer Fische. *Paläontologische Zeitschrift,* 8(1), 161–184.

Jenkins, F. A., Walsh, D. M., and Carroll, R. L. (2007). Anatomy of *Eocaecilia micropodia*, a limbed caecilian of the Early Jurassic. *Bulletin of the Museum of Comparative Zoology,* 158(6), 285–365.

Jimenez-Huidobro , P., and Caldwell, M. W. (2016). Reassessment and reassignment of the early Maastrichtian mosasaur *Hainosaurus bernardi* Dollo, 1885, to *Tylosaurus* Marsh, 1872. *Journal of Vertebrate Paleontology,* 36(3), e1096275.

Johnson, M. M., Young, M. T., and Brusatte, S. L. (2020). The phylogenetics of Teleosauroidea (Crocodylomorpha, Thalattosuchia) and implications for their ecology and evolution. *PeerJ,* 8, e9808.

Johnston, P. (2010). The constrictor dorsalis musculature and basipterygoid articulation in *Sphenodon*. *Journal of Morphology,* 271(3), 280–292.

Jollie, M. T. (1957). The head skeleton of the chicken and remarks on the anatomy of this region in other birds. *Journal of Morphology,* 100(3), 389–436.

Jones, M. E. H. (2004). *Skull evolution in the Rhynchocephalia (Diapsida: Lepidosauria)*. Paper presented at the Sixty-Fourth Annual Meeting Society of Vertebrate Paleontology, Denver.

Jones, M. E. H. (2008). Skull shape and feeding strategy in *Sphenodon* and other Rhynchocephalia (Diapsida: Lepidosauria). *Journal of Morphology,* 269(8), 945–966.

Jones, M. E. H., Curtis, N., Fagan, M. J., O'Higgins, P., and Evans, S. E. (2011). Hard tissue anatomy of the cranial joints in *Sphenodon* (Rhynchocephalia): sutures, kinesis, and skull mechanics. *Palaeontologia Electronica,* 14(2), 1–92.

Jones, M. E. H., Curtis, N., O'Higgins, P., Fagan, M., and Evans, S. E. (2009). The head and neck muscles associated with feeding in *Sphenodon* (Reptilia: Lepidosauria: Rhynchocephalia). *Palaeontologia Electronica,* 12(2), 1–56.

Jones, M. E. H., Werneburg, I., Curtis, N., Penrose, R., O'Higgins, P., Fagan, M. J., and Evans, S. E. (2012). The head and neck anatomy of sea turtles (Cryptodira: Chelonioidea) and skull shape in Testudines. *PLoS ONE,* 7(11), e47852.

Jones, M. E. H., and Zikmund, T. (2012). *A functional interpretation of the cranial suture morphology in Captorhinus aguti (Reptilia)*. Paper presented at the Society of Vertebrate Paleontology, Seventy-Second Annual Meeting, Raleigh.

Joyce, W. G. (2007). Phylogenetic relationships of Mesozoic turtles. *Bulletin of the Peabody Museum of Natural History,* 48(1), 3–102.

Kammerer, C. F. (2011). Systematics of the Anteosauria (Therapsida: Dinocephalia). *Journal of Systematic Palaeontology,* 9(2), 261–304.

Kathe, W. (1995). Morphology and function of the sutures in the dermal skull roof of *Discosauriscus austriacus* Makowsky, 1876 (Seymouriamorpha; Lower Permian of Moravia) and *Onchiodon labyrinthicus* Geinitz, 1861 (Temnospondyli; Lower Permian of Germany). *Geobios,* 19(255–261).

Kathe, W. (1999). Comparative morphology and functional interpretation of the sutures in the dermal skull roof of temnospondyl amphibians. *Zoological Journal of the Linnean Society,* 126, 1–39.

Kemp, T. S. (1969). On the functional morphology of the gorgonopsid skull. *Philosophical Transactions of the Royal Society of London. B, Biological Sciences,* 256(801), 1–83.

Kemp, T. S. (1980). Origin of the mammal-like reptiles. *Nature,* 283(5745), 378–380.

Kemp, T. S. (1984). *Mammal-like Reptiles and the Origin of Mammals* (2 ed.). London: Academic Press Inc. (London) LTD.

Kerr, R. (1792). *The Animal Kingdom or Zoological System, of the Celebrated Sir Charles Linnaeus. Class I. Mammalia: Containing a Complete Systematic Description, Arrangement, and Nomenclature, of All the Known Species and Varieties of the Mammalia, or Animals which Give Suck to their Young*. Edinburgh: Gmelin, J F.

Keyser, A. W., and Gow, C. E. (1981). First complete skull of the Permian reptile *Eunotosaurus africanus* Seeley. *South African Journal of Science,* 77(9), 417–421.

Khatra, G. S. (1980). Morphology of the pars squamosa os temporale of buffalo (*Babalus bubalis*). *Journal of Research, Punjab Agricultural University,* 17(1), 92–94.

Kilias, R. (1957). Die funktionell-anatomische und systematische Bedeutung der Schläfenreduktionen bei Schildkröten. *Mitteilungen aus dem Museum für Naturkunde in Berlin,* 33(2), 307–354.

Kissel, R. A. (2010). *Morphology, Phylogeny, and Evolution of Diadectidae (Cotylosauria: Diadectomorpha).* (Dissertation). University of Toronto, Toronto.

Kissel, R. A., Dilkes, D. W., and Reisz, R. R. (2002). *Captorhinus magnus*, a new captorhinid (Amniota: Eureptilia) from the Lower Permian of Oklahoma, with new evidence on the homology of the astragalus. *Canadian Journal of Earth Sciences,* 39(9), 1363–1372.

Kleinteich, T., and Haas, A. (2011). The hyal and ventral branchial muscles in caecilian and salamander larvae: Homologies and evolution. *Journal of Morphology,* 272(5), 598–613.

Kleinteich, T., Maddin, H. C., Herzen, J., Beckmann, F., and Summers, A. P. (2012). Is solid always best? Cranial performance in solid and fenestrated caecilian skulls. *The Journal of Experimental Biology,* 215(Pt 5), 833–844.

Klembara, J. (1994). The sutural pattern of skull-roof bones in Lower Permian *Discosauriscus austriacus* from Moravia. *Lethaia,* 27(1), 85–95.

Klembara, J. (1997). The cranial anatomy of *Discosauriscus* Kuhn, a seymouriamorph tetrapod from the Lower Permian of the Boskovice Furrow (Czech Republic). *Philosophical Transactions of the Royal Society of London,* 352(1351), 257–302.

Klembara, J. (2011). The cranial anatomy, ontogeny, and relationships of *Karpinskiosaurus secundus* (Amalitzky) (Seymouriamorpha, Karpinskiosauridae) from the Upper

Permian of European Russia. *Zoological Journal of the Linnean Society,* 161(1), 184–212.

Klembara, J., Berman, D. S, Henrici, A. C., Cernansky, A., and Werneburg, R. (2006). Comparison of cranial anatomy and proportions of similarly sized *Seymouria sanjuanensis* and *Discosauriscus austriacus*. *Annals of Carnegie Museum,* 75(1), 37–49.

Klembara, J., Berman, D. S, Henrici, A. C., Čerňanský, A., Werneburg, R., and Martens, T. (2007). First description of skull of Lower Permian *Seymouria sanjuanensis* (Seymouriamorpha: Seymouriidae) at an early juvenile growth stage. *Annals of Carnegie Museum,* 76(1), 53–72.

Klembara, J., Clack, J. A., Milner, A. R., and Ruta, M. (2014). Cranial anatomy, ontogeny, and relationships of the Late Carboniferous tetrapod *Gephyrostegus bohemicus* Jaekel, 1902. *Journal of Vertebrate Paleontology,* 34(4), 774–792.

Klembara, J., Dobiašová, K., Hain, M., and Yaryhin, O. (2017). Skull anatomy and ontogeny of legless lizard *Pseudopus apodus* (Pallas, 1775): heterochronic influences on form. *The Anatomical Record,* 300(3), 460–502.

Klembara, J., Hain, M., Ruta, M., Berman, D. S, Pierce, S. E., and Henrici, A. C. (2019). Inner ear morphology of diadectomorphs and seymouriamorphs (Tetrapoda) uncovered by high-resolution X-ray microcomputed tomography, and the origin of the amniote crown group. *Palaeontology,* 63(1), 131–154.

Klembara, J., Tomasik, A., and Kathe, W. (2002). Subdivisions, fusions and extended sutural areas of dermal skull bones in *Discosauriscus* KUHN (Seymouriamorpha). *Neues Jahrbuch für Geologie und Paläontologie - Abhandlungen,* 223(3), 317–349.

Klenner, S., Witzel, U., Paris, F., and Distler, C. (2015). Structure and function of the septum nasi and the underlying tension chord in crocodylians. *Journal of Anatomy,* 228(1), 113-124.

Koyabu, D., Maier, W., and Sánchez-Villagra, M. R. (2012). Paleontological and developmental evidence resolve the homology and dual embryonic origin of a mammalian skull bone, the interparietal. *Proceedings of the National Academy of Sciences of the United States of America,* 109(35), 14075–14080.

Koyabu, D., Werneburg, I., Morimoto, N., Zollikofer, C. P. E., Forasiepi, A. M., Endo, H., Kimura, J., Ohdachi, S. D., Nguyen, T. S., and Sánchez-Villagra, M. (2014). Mammalian skull heterochrony reveals modular evolution and a link between cranial development and brain size. *Nature Communications,* 5(1), 1–9.

Kuhn, O. (1961). *Die Familien der rezenten und fossilen Amphibien und Reptilien*. Bamberg: Verlagshaus Meisenbach KG.

Kuhn-Schnyder, E. (1954). The origin of lizards. *Endevour,* 13(52), 213–219.

Kuhn-Schnyder, E. (1961). Der Schädel von *Simosaurus*. *Paläontologische Zeitschrift,* 35(3/4), 95–113.

Kuhn-Schnyder, E. (1963). Wege der Reptiliensystematik. *Paläontologische Zeitschrift,* 37(1-2), 61.

Kuhn-Schnyder, E. (1967). Das Problem der Euryapsida. *Mitteilungen aus dem Paläontologischen Institut der Universität Zurich,* 49, 335–348.

Kuhn-Schnyder, E. (1980). Observations on temporal openings of reptilian skulls and the classification of reptiles. In L. L. Jacobs (Ed.), *Aspects of Vertebrate History, Essays in Honor of Edwin Harris Colbert* (pp. 153–175). Flagstaff: Museum of Northern Arizona Press.

Lakjer, T. (1926). *Studien über die Trigeminus-versorgte Kaumuskulatur der Sauropsiden* (A. Luther & C. Wesenberg-Lund Eds.). Kopenhagen: CA Reitzel, Buchandlung.

Lakjer, T. (1927). Studien über die Gaumenregion bei Sauriern im Vergleich mit Anamniern und primitiven Sauropsiden. *Zoologische Jahrbücher,* 49, 57–356.

Lane, H. H. (1945). New mid-Pennsylvanian reptiles from Kansas. *Transactions of the Kansas Academy of Science,* 47(3), 381–390.

Lauder, G. V., and Gillis, G. B. (1997). Origin of the amniote feeding mechanism: experimental analyses of outgroup clades. In S. Sumida and K. L. M. Martin (Eds.), *Amniote Origins - Completing the Transition to Land* (pp. 169–206). San Diego, London: Academic Press.

Laurin, M. (1991). The osteology of a Lower Permian eosuchian from Texas and a review of diapsid phylogeny. *Zoological Journal of the Linnean Society,* 101(1), 59–95.

Laurin, M. (2005). Embryo retention, character optimization, and the origin of the extra-embryonic membranes of the amniotic egg. *Journal of Natural History,* 39, 3151–3161.

Laurin, M. (2010). *How Vertebrates Left the Water*. Berkeley, Los Angeles, London: University of California Press.

Laurin, M. (2020a). Stegocephali. In P. Cantino, J. A. Gauthier, and K. de Queiroz (Eds.), *Phylonyms, a Companion to the PhyloCode* (1 ed., pp. 741–745): Taylor & Francis Group, Ltd.

Laurin, M. (2020b). Tetrapoda. In P. Cantino, J. A. Gauthier, and K. de Queiroz (Eds.), *Phylonyms, a Companion to the PhyloCode* (1 ed., pp. 759–764): Taylor & Francis Group, Ltd.

Laurin, M., and Anderson, J. S. (2004). Meaning of the name Tetrapoda in the scientific literature: an exchange. *Systematic Biology,* 53(1), 68–80.

Laurin, M., Arntzen, J. W., Báez, A. M., Bauer, A. M., Damiani, R., Evans, S. E., Kupfer, A., Larson, A., Marjanović, D., Müller, H., Olsson, L., Rage, J.-C., and Walsh, D. (2020a). Amphibia. In P. Cantino, J. A. Gauthier, and K. de Queiroz (Eds.), *Phylonyms, a Companion to the PhyloCode* (1 ed., pp. 765–770): Taylor & Francis Group, Ltd.

Laurin, M., Arntzen, J. W., Báez, A. M., Bauer, A. M., Damiani, R., Evans, S. E., Kupfer, A., Larson, A., Marjanović, D., Müller, H., Olsson, L., Rage, J.-C., and Walsh, D. (2020b). Lissamphibia. In P. Cantino, J. A. Gauthier, and K. de Queiroz (Eds.), *Phylonyms, a Companion to the PhyloCode* (1 ed.): Taylor & Francis Group, Ltd.

Laurin, M., Lapauze, O., and Marjanović, D. (2019). *What do ossification sequences tell us about the origin of extant amphibians?* Peer Community in Paleontology.

Laurin, M., and Piñeiro, G. H. (2017). A reassessment of the taxonomic position of mesosaurs, and a surprising phylogeny of early amniotes. *Frontiers in Earth Science,* 5(88), 1–13.

Laurin, M., and Piñeiro, G. H. (2018). Response: commentary: a reassessment of the taxonomic position of mesosaurs, and a surprising phylogeny of early amniotes. *Frontiers in Earth Science,* 6(220), 1–9.

Laurin, M., and Reisz, R. R. (1995). A reevaluation of early amniote phylogeny. *Zoological Journal of the Linnean Society,* 113(2), 165–223.

Laurin, M., and Reisz, R. R. (1997). A new perspective on tetrapod phylogeny. In S. S. Sumida and K. L. M. Martin (Eds.), *Amniote Origins, Completing the Transition to Land* (pp. 9–59). San Diego: Academic Press.

Laurin, M., and Reisz, R. R. (2020). Synapsida. In J. A. Gauthier (Ed.), *Phylonyms, a Companion to the PhyloCode* (1 ed., pp. 811–814): Taylor & Francis Group, Ltd.

Laurin, M. P., G H. (2017). A reassessment of the taxonomic position of mesosaurs, and a surprising phylogeny of early amniotes. *Frontiers in Earth Science,* 5(88), 1–13.

Lautenschlager, S. (2015). Estimating cranial musculoskeletal constraints in theropod dinosaurs. *Royal Society Open Science,* 2(11), 150495.

Lautenschlager, S., Gill, P., Luo, Z.-X., Fagan, M. J., and Rayfield, E. J. (2017). Morphological evolution of the mammalian jaw adductor complex. *Biological Reviews,* 92(4), 1910-1940.

LeBlanc, A. R. H., MacDougall, M. J., Haridy, Y., Scott, D., and Reisz, R. R. (2018). Caudal autotomy as anti-predatory behaviour in Palaeozoic reptiles. *Scientific Reports,* 8, 3328.

Lebrun, R. (2018). *MorphoDig, an open-source 3D freeware dedicated to biology*. Paper presented at the The 5th International Palaeontological Congress, Paris.

Lee, H. W., Esteve-Altava, B., and Abzhanov, A. (2020). Evolutionary and ontogenetic changes of the anatomical organization and modularity in the skull of archosaurs. *Scientific Reports,* 10, 16138.

Lee, M. S. (1995). Historical burden in systematics and the interrelationships of ‘parareptiles’. *Biological Reviews,* 70, 459–547.

Lee, M. S. (1997). Pareiasaur phylogeny and the origin of turtles. *Zoological Journal of the Linnean Society, 120*(3), 197–280.

Lee, M. S. (2000). The Russian Pareiasaurs. In M. J. Benton, M. A. Shishkin, D. M. Unwin, and E. N. Kurochkin (Eds.), *The Age of Dinosaurs in Russia and Mongolia* (pp. 71–85). Cambridge: Cambridge University Press.

Lee, M. S. (2013). Turtle origins: insights from phylogenetic retrofitting and molecular scaffolds. *Journal of Evolutionary Biology,* 26(12), 2729–2738.

Lee, M. S., and Caldwell, M. W. (1998). Anatomy and relationships of *Pachyrhachis problematicus*, a primitive snake with hindlimbs. *Philosophical Transactions of the Royal Society of London,* 353(1375), 1521–1552.

Lee, M. S., and Spencer, P. S. (1997). Crown-clades, key characters and taxonomic stability: when is an amniote not an amniote. In S. S. Sumida and K. L. M. Martin (Eds.), *Amniote Origins, Completing the Transition to Land* (pp. 61–84). San Diego: Academic Press.

Li, C., Fraser, N. C., Rieppel, O., and Wu, X.-C. (2018). A Triassic stem turtle with an edentulous beak. *Nature,* 560, 476–479.

Li, C., Wu, X.-C., Rieppel, O., Wang, L.-T., and Zhao, L.-J. (2008). An ancestral turtle from the Late Triassic of southwestern China. *Nature,* 456(7221), 497–501.

Lichtig, A. J., and Lucas, S. G. (2021). *Chinlechelys* from the upper Triassic of New Mexico, USA, and the origin of turtles. *Palaeontologia Electronica,* 24(1), a:13.

Lucas, S. G., Rinehart, L. F., and Celeskey, M. D. (2018). The oldest specialized tetrapod herbivore: A new eupelycosaur from the Permian of New Mexico, USA. *Palaeontologia Electronica,* 21(3), 1–42.

Luo, Z.-X. (2011). Developmental patterns in Mesozoic evolution of mammal ears. *Annual Review of Ecology, Evolution, and Systematics,* 42, 355–380.

Luther, A. (1914). Über die vom N. trigeminus versorgte Muskulatur der Amphibien, mit einem vergleichenden Ausblick über den Adductor mandibulae der Gnathostomen, und einem Beitrag zum Verständnis der Organisation der Anurenlarven. *Acta Societatis Scientiarum Fennicae,* 7, 1–151.

Lyson, T. R., Bever, G. S., Bhullar, B. A., Joyce, W. G., and Gauthier, J. A. (2010). Transitional fossils and the origin of turtles. *Biology Letters,* 6(6), 830–833.

Lyson, T. R., Sperling, E. A., Heimberg, A. M., Gauthier, J. A., King, B. L., and Peterson, K. J. (2012). MicroRNAs support a turtle + lizard clade. *Biology Letters,* 8(1), 104–107.

MacDougall, M. J., Modesto, S. P., Brocklehurst, N., Verrière, A., Reisz, R. R., and Fröbisch, J. (2018). Commentary: a reassessment of the taxonomic position of mesosaurs, and a surprising phylogeny of early amniotes. *Frontiers in Earth Science,* 6(99), 1–5.

MacDougall, M. J., and Reisz, R. R. (2014). The first record of a nyctiphruretid parareptile from the Early Permian of North America, with a discussion of parareptilian temporal fenestration. *Zoological Journal of the Linnean Society,* 172(3), 616–630.

MacGregor, J. H. (1908). On *Mesosaurus brasiliensis* nov. sp. from the Permian of Brasil. In I. D. White (Ed.), *Commissao dos Estudos das Minas de Carvao de Pedra do Brasil, Parte II* (pp. 301–336). Rio de Janeiro: National Press.

Macrini, T. (2004). *Tachyglossus aculeatus*. *Digital Morphology.* http://digimorph.org/specimens/Tachyglossus_aculeatus/skull/ (accessed on the 12.07.2022).

Maddin, H. C., Jenkins, F. A., Jr, and Anderson, J. S. (2012). The braincase of *Eocaecilia micropodia* (Lissamphibia, Gymnophiona) and the origin of caecilians. *PLoS ONE,* 7(12), e50743.

Maddison, W. P., and Maddison, D. R. (2021). Mesquite: a modular system for evolutionary analysis (Version 3.7). Retrieved from http://www.mesquiteproject.org.

Maier, W. (1989). Ala Temporalis and Alisphenoid in Therian Mammals. In H. Splechtna and H. Hilgers (Eds.), *Trends in Vertebrate Morphology* (pp. 396–400). Stuttgart: Fischer Verlag.

Maier, W. (1993). Cranial Morphology of the Therian Common Ancestor, as Suggested by the Adaptation of Neonate Marsupials. In F. S. Szalay, M. J. Novacek, and M. C. McKenna (Eds.), *Mesozoic Differentiation, Multituberculates, Monotremes and Early Marsupials* (pp. 165–181). New York CIty: Springer Verlag.

Maier, W. (1999). On the evolutionary biology of early mammals – with methodological remarks on the interaction between ontogenetic adaptation and phylogenetic transformation. *Zoologischer Anzeiger,* 238(1–2), 55–74.

Maier, W. (2018). Fortpflanzungsbiologie und Ursprung der Säugetiere - Säugen als Alleinstellungsmerkmal. *Biologie in unserer Zeit*, 48(5), 301–309.

Maier, W., and Werneburg, I. (2014). Einführung: Zur Methodik der organismischen Evolutionsbiologie. In W. Maier and I. Werneburg (Eds.), *Schlüsselereignisse der organismischen Makroevolution* (pp. 11–17). Zürich: Scidinge Hall Verlag.

Maisano, J. (2003). *Cricosaura typica*. *Digital Morphology.* http://digimorph.org/specimens/Cricosaura_typica/ (accessed on the 12.07.2022).

Maisch, M. W., and Gebauer, E. V. I. (2005). Reappraisal of *Geikia locusticeps* (Therapsida: Dicynodontia) from the Upper Permian of Tanzania. *Palaeontology,* 48(2), 309–324.

Maisch, M. W., and Hungerbühler, A. (2001). New evidence for a discrete supratemporal bone in the Jurassic ichthyosaur *Temnodontosaurus*. *Historical Biology: A Journal of Paleobiology,* 15(4), 335–345.

Mann, A., Calthorpe, A. S., and Maddin, H. C. (2021). *Joermungandr bolti*, an exceptionally preserved 'microsaur' from the Mazon Creek Lagerstätte reveals patterns of integumentary evolution in Recumbirostra. *Royal Society Open Science,* 8(7), 210319.

Mann, A., Pardo, J. D., and Maddin, H. C. (2019). *Infernovenator steenae*, a new serpentine recumbirostran from the 'Mazon Creek' Lagerstätte further clarifies lysorophian origins. *Zoological Journal of the Linnean Society,* 187(2), 506–517.

Marjanović, D., and Laurin, M. (2019). Phylogeny of Paleozoic limbed vertebrates reassessed through revision and expansion of the largest published relevant data matrix. *PeerJ,* 6, e5565.

Markey, M. J., Main, R. P., and Marshall, C. D. (2006). *In vivo* cranial suture function and suture morphology in the extant fish *Polypterus*: implications for inferring skull function in living and fossil fish. *The Journal of Experimental Biology,* 209(11), 2085–2102.

Metzger, K. (2002). Cranial Kinesis in Lepidosaurs: Skulls in Motion. In P. Aerts, K. D'Août, A. Herrel, and R. Van Damme (Eds.), *Topics in Functional and Ecological Vertebrate Morphology* (pp. 15–46): Shaker Publishing.

Mezzasalma, M., Maio, N., and Guarino, F. M. (2014). To move or not to move: cranial joints in European gekkotans and lacertids, an osteological and histological perspective. *The Anatomical Record,* 297(3), 463–472.

Milner, A. C. (1993). The aïstopod amphibian from the Viséan of East Kirkton, West Lothian, Scotland. *Earth and Environmental Science Transactions of the Royal Society of Edinburgh,* 84(3–4), 363–368.

Mo, J.-Y., Xu, X., and Evans, S. E. (2010). The evolution of the lepidosaurian lower temporal bar: new perspectives from the Late Cretaceous of South China. *Proceedings of the Royal Society B: Biological Sciences,* 277, 331–336.

Moazen, M., Curtis, N., O'Higgins, P., Jones, M. E. H., Evans, S. E., and Fagan, M. (2009). Assessment of the role of sutures in a lizard skull: a computer modelling study. *Proceedings of the Royal Society B,* 276(1654), 39–46.

Modesto, S. P. (1995). The skull of the herbivorous synapsid *Edaphosaurus boanerges* from the Lower Permian of Texas. *Palaeontology,* 38(1), 213–239.

Modesto, S. P. (1998). New information on the skull of the Early Permian reptile *Captorhinus aguti*. *Paleobios,* 18(2–3), 21–35.

Modesto, S. P. (2006). The cranial skeleton of the Early Permian aquatic reptile *Mesosaurus tenuidens*: implications for relationships and palaeobiology. *Zoological Journal of the Linnean Society,* 146(3), 345–368.

Modesto, S. P., and Anderson, J. S. (2004). The phylogenetic defintion of Reptilia. *Systematic Biology,* 53(5), 815–821.

Modesto, S. P., and Reisz, R. R. (1990). A new skeleton of *Ianthasaurus hardestii*, a primitive edaphosaur (Synapsida: Pelycosauria) from the Upper Pennsylvanian of Kansas. *Canadian Journal of Earth Sciences,* 27(6), 834–844.

Modesto, S. P., and Reisz, R. R. (2003). An enigmatic new diapsid reptile from the Upper Permian of eastern Europe. *Journal of Vertebrate Paleontology,* 22(4), 851–855.

Modesto, S. P., Scott, D. M., Berman, D. S, Müller, J., and Reisz, R. R. (2007). The skull and palaeoecological significance of *Labidosaurus hamatus*, a captorhinid reptile from the Lower Permian of Texas. *Zoological Journal of the Linnean Society,* 149(2), 237–262.

Modesto, S. P., Sues, H.-D., Scott, D. M., and Reisz, R. R. (2009). A new parareptile with temporal fenestration from the Middle Permian of South Africa. *Canadian Journal of Earth Sciences,* 46(1), 9-20.

Molnar, J., Esteve-Altava, B., Rolian, C., and Diogo, R. (2017). Comparison of musculoskeletal networks of the primate forelimb. *Scientific Reports,* 7, 10520.

Mook, C. C. (1921). Skull characters of recent Crocodilia, with notes on the affinities of the recent genera. *Contributions to the Osteology, Affinities, and Distribution of the Crocodilia,* 10(13), 123–268.

Moss, M. L. (1957). Experimental alteration of sutural area morphology. *The Anatomical Record,* 127(3), 569–589.

Motani, R., Jiang, D. Y., Chen, G. B., Tintori, A., Rieppel, O., Ji, C., and Huang, J. D. (2015). A basal ichthyosauriform with a short snout from the Lower Triassic of China. *Nature,* 517(7535), 485–488.

Müller, J. (2003). Early loss and multiple return of the lower temporal arcade in diapsid reptiles. *Naturwissenschaften,* 90(10), 473–476.

Müller, J., and Reisz, R. R. (2005). An early captorhinid reptile (Amniota, Eureptilia) from the Upper Carboniferous of Hamilton, Kansas. *Journal of Vertebrate Paleontology,* 25(3), 561–568.

Müller, J., and Reisz, R. R. (2006). The phylogeny of early eureptiles: comparing parsimony and Bayesian approaches in the investigation of a basal fossil clade. *Systematic Biology,* 55(3), 503–511.

Murray, P. F. (1981). A unique jaw mechanism in the echidna, *Tachyglossus aculeatus* (Monotremata). *Australian Journal of Zoology,* 29, 1–5.

Nabavizadeh, A. (2020). Cranial musculature in herbivorous dinosaurs: a survey of reconstructed anatomical diversity and feeding mechanisms. *The Anatomical Record,* 303(4), 1104–1145.

Natchev, N., Handschuh, S., Lukanov, S., Tzankov, N., Naumov, B., and Werneburg, I. (2016). Contributions to the functional morphology of caudate skulls: kinetic and akinetic forms. *PeerJ,* 4, e2392.

Natchev, N., Tzankov, N., Werneburg, I., and Heiss, E. (2015). Feeding behaviour in a 'basal' tortoise provides insights on the transitional feeding mode at the dawn of modern land turtle evolution. *PeerJ,* 3, e1172.

Neenan, J. M., Klein, N., and Scheyer, T. M. (2013). European origin of placodont marine reptiles and the evolution of crushing dentition in Placodontia. *Nature Communications,* 4(1), 1–8.

Nesbitt, S. J. (2011). The early evolution of archosaurs: relationships and the origin of major clades. *Bulletin of the American Museum of Natural History,* 2011(352), 1–292.

Nicholls, E. L. (1999). A reexamination of *Thalattosaurus* and *Nectosaurus* and the relationships of the Thalattosauria (Reptilia: Diapsida). *Paleobios,* 19(1), 1–29.

Nick, L. (1912). Das Kopfskelett von *Dermochelys coriacea* L. *Zoologische Jahrbücher, Abteilung für Anatomie und Ontogenie der Tiere,* 33, 1–238.

Norman, D. B., Crompton, A. W., Butler, R. J., Porro, L. B., and Charig, A. J. (2011). The Lower Jurassic ornithischian dinosaur *Heterodontosaurus tucki* Crompton & Charig, 1962: cranial anatomy, functional morphology, taxonomy, and relationships. *Zoological Journal of the Linnean Society,* 163, 182–276.

Norman, D. B., and Weishampel, D. B. (1985). Ornithopod feeding mechanisms: their bearing on the evolution of herbivory. *The American Naturalist,* 126(2), 154–164.

Novacek, M. J. (1993). Patterns of Diversity in the Mammalian Skull. In J. Hanken and B. K. Hall (Eds.), *The Skull. Vol.2, Patterns of Structural and Systematic Diversity* (pp. 438–545). Chicago: University of Chicago Press.

Nussbaum, R. A. (1983). The evolution of a unique dual jaw-closing mechanism in caecilians (Amphibia: Gymnophiona) and its bearing on caecilian ancestry. *Journal of Zoology,* 199(4), 545–554.

Nyakatura, J. A., Melo, K., Horvat, T., Karakasiliotis, K., Allen, V. R., Andikfar, A., Andrada, E., Arnold, P., Laustroer, J., and Hutchinson, J. R. (2019). Reverse-engineering the locomotion of a stem amniote. *Nature,* 565(7739), 351–355.

O'Connor, J. K., and Chiappe, L. M. (2011). A revision of enantiornithine (Aves: Ornithothoraces) skull morphology. *Journal of Systematic Palaeontology,* 9(1), 135-157.

Ogushi, K. (1911). Anatomische Studien an der japanischen dreikralligen Lippenschildkrote (*Trionyx japonicus*). *Gegenbaurs Morphologisches Jahrbuch,* 43, 1–106.

Olson, E. C. (1951). Fauna of Upper Vale and Choza: 1–5. *Fieldiana Geology,* 10(11), 89–128.

Olson, E. C. (1961). Jaw mechanisms: rhipidistians, amphibians, reptiles. *American Zoologist,* 1(2), 205–215.

Olsson, L., Hoßfeld, U., and Breidbach, O. (2006). Preface: From evolutionary morphology to the modern synthesis and 'evo-devo': Historical and contemporary perspectives. In *Theory in Biosciences* (Vol. 124, pp. 259–263).

Osborn, H. F. (1903). On the primary division of the Reptilia into two sub-classes, Synapsida and Diapsida. *Science, 17*(424), 275–276.

Osborn, H. F. (1905). *Tyrannosaurus* and other Cretaceous carnivorous dinosaurs. *Bulletin of the American Museum of Natural History,* 21(14), 259–265.

Owen, R. (1876). *Descriptive and Illustrated Catalogue of the Fossil Reptilia of South Africa in the Collection of the British Museum*. London: Order of the Trustees.

Packard, M. J., and Seymour, R. S. (1997). Evolution of the amniote egg. In S. S. Sumida and K. L. M. Martin (Eds.), *Amniote Origins - Completing the Transition to Land* (pp. 265–290). San Diego, London: Academic Press.

Paluh, D. J., Stanley, E. L., and Blackburn, D. C. (2020). Evolution of hyperossification expands skull diversity in frogs. *Proceedings of the National Academy of Sciences of the United States of America,* 117(15), 8554–8562.

Panchen, A. L. (1964). The cranial anatomy of two coal measure anthracosaurs. *Philosophical Transactions of the Royal Society,,* 247(742), 593–637.

Panchen, A. L. (1972). The skull and skeleton of *Eogyrinus attheyi* Watson (Amphibia: Labyrinthodontia). *Philosophical Transactions of the Royal Society of London,* 263(851), 279–326.

Panchen, A. L. (1977). On *Anthracosaurus russelli* Huxley (Amphibia: Labyrinthodontia) and the family Anthracosauridae. *Philosophical Transactions of the Royal Society of London. B, Biological Sciences,* 279(968), 447–512.

Pardo, J. D., and Anderson, J. S. (2016). Cranial morphology of the Carboniferous-Permian tetrapod *Brachydectes newberryi* (Lepospondyli, Lysorophia): New data from microCT. *PLoS ONE,* 11(8), e0161823.

Pardo, J. D., Szostakiwskyj, M., Ahlberg, P. E., and Anderson, J. S. (2017). Hidden morphological diversity among early tetrapods. *Nature,* 546, 642–645.

Payne, S. L., Holliday, C. M., and Vickaryous, M. K. (2011). An osteological and histological investigation of cranial joints in geckos. *The Anatomical Record,* 294(3), 399–405.

Piñeiro, G. H., Ferigolo, J., Ramos, A., and Laurin, M. (2012). Cranial morphology of the early Permian mesosaurid *Mesosaurus tenuidens* and the evolution of the lower temporal fenestration reassessed. *Comptes Rendus Palevol,* 11(5), 379–391.

Piveteau, J. (1926). Paleontologie de Madagascar, XIII. Amphibiens et reptiles permiens. *Annales de Paléontologie,* 15, 53–180.

Plateau, O., and Foth, C. (2020). Birds have peramorphic skulls, too: anatomical network analyses reveal oppositional heterochronies in avian skull evolution. *Communications Biology,* 3, 195.

Poglayen-Neuwall, I. (1953). Untersuchungen der Kiefermuskulatur und deren Innervation bei Schildkröten. *Acta Zoologica,* 34(3), 241–292.

Polachowski, K. M., and Werneburg, I. (2013). Late embryos and bony skull development in *Bothropoides jararaca* (Serpentes, Viperidae). *Zoology,* 116(1), 36–63.

Porro, L. B., Rayfield, E. J., and Clack, J. A. (2015). Descriptive anatomy and three-dimensional reconstruction of the skull of the early tetrapod *Acanthostega gunnari* Jarvik, 1952. *PLoS ONE,* 10(3), e0118882.

Price, L. I. (1935). Notes on the brain case of *Captorhinus*. *Proceedings of the Boston Society of Natural History,* 40, 377–386.

Price, L. I. (1937). Two new cotylosaurs from the Permian of Texas. *New England Zoological Club,* 16, 97–102.

R Core Team (2020). *R: a language and environment for statistical computing*. Vienna: R Foundation for Statistical Computing.

Rafferty, K. L., and Herring, S. W. (1999). Craniofacial sutures: morphology, growth, and in vivo masticatory strains. *Journal of Morphology,* 242(2), 167–179.

Rafferty, K. L., Herring, S. W., and Artese, F. (2000). Three-dimensional loading and growth of the zygomatic arch. *The Journal of Experimental Biology,* 203(14), 2093–3004.

Ramirez, B. A. S., Sandoval, S., Sparks, J., Elsey, R., and Owerkowicz, T. (2022). *Do crocodilians have an air-conditioning unit in their skulls? Experimental test of purported thermoregulatory function of the dorsal temporal fenestrae in the American alligator*. Paper presented at the Experimental Biology 2022, Philadelphia.

Rasskin-Gutman, D. (2003). Boundary Constraints for the Emergence of Form. In G. B. Müller and S. A. Newman (Eds.), *Origination of Organismal Form. Beyond the Gene in Developmental and Evolutionary Biology* (pp. 305–322). Cambridge: MIT Press.

Rasskin-Gutman, D., and Esteve-Altava, B. (2014). Connecting the dots: anatomical network analysis in morphological EvoDevo. *Biological Theory,* 9, 178–193.

Rasskin-Gutman, D., and Esteve-Altava, B. (2021). Concept of Burden in Evo-Devo. In L. Nuño de la Rosa and G. B. Müller (Eds.), *Evolutionary Developmental Biology. A Reference Guide* (pp. 39–49). Berlin: Springer.

Rawson, J. R. G., Porro, L. B., Martin-Silverstone, E., and Rayfield, E. J. (2021). Osteology and digital reconstruction of the skull of the early tetrapod *Whatcheeria deltae*. *Journal of Vertebrate Paleontology*, 41(2), e1927749.

Ray, S. (2005). *Lystrosaurus* (Therapsida, Dicynodontia) from India: Taxonomy, relative growth and cranial dimorphism. *Journal of Systematic Palaeontology,* 3(2), 203–221.

Rayfield, E. J. (2005). Using finite-element analysis to investigate suture morphology: A case study using large carnivorous dinosaurs. *The Anatomical Record,* 283(A), 349–365.

Reisz, R. R. (1972). Pelycosaurian reptiles from the Middle Pennsylvanian of North America. *Bulletin of the Museum of Comparative Zoology,* 144(2), 27–62.

Reisz, R. R. (1977). *Petrolacosaurus*, the oldest known diapsid reptile. *Science,* 196(4294), 1091–1093.

Reisz, R. R. (1997). The origin and early evolutionary history of amniotes. *Trends in Ecology & Evolution,* 12(6), 218–222.

Reisz, R. R., Berman, D. S, and Scott, D. (1984). The anatomy and relationships of the lower Permian reptile *Araeoscelis*. *Journal of Vertebrate Paleontology,* 4(1), 57–67.

Reisz, R. R., and Dilkes, D. W. (2003). *Archaeovenator hamiltonensis*, a new varanopid (Synapsida: Eupelycosauria) from the Upper Carboniferous of Kansas. *Canadian Journal of Earth Sciences,* 40, 667–678.

Reisz, R. R., and Fröbisch, J. (2014). The oldest caseid synapsid from the Late Pennsylvanian of Kansas, and the evolution of herbivory in terrestrial vertebrates. *PLoS ONE,* 9(4), e94518.

Reisz, R. R., and Heaton, M. J. (1980). Matters arising: Origin of mammal-like reptiles. *Nature,* 288(5787), 193.

Reisz, R. R., Schoch, R. R., and Anderson, J. S. (2009). The armoured dissorophid *Cacops* from the early Permian of Oklahoma and the exploitation of the terrestrial realm by amphibians. *Naturwissenschaften,* 96(7), 789–796.

Rieppel, O. (1984). The upper temporal arcade of lizards: an ontogenetic problem. *Revue Suisse de Zoologie,* 91, 475–482.

Rieppel, O. (1987). The development of the trigeminal jaw adductor musculature and associated skull elements in the lizard *Podarcis sicula*. *Journal of Zoology,* 212(1), 131–150.

Rieppel, O. (1993). Patterns of Diversity in the Reptilian Skull. In J. Hanken and B. K. Hall (Eds.), *The Skull. Vol. 2, Patterns of Structural and Systematic Diversity* (pp. 344–389). Chicago: University of Chicago Press.

Rieppel, O. (2001). Cranial anatomy of *Placochelys placodonta* Jaekel, 1902, and a review of the Cyamodontoidea (Reptilia, Placodonta). *Fieldiana: Geology, N.S.,* 45, 1–104.

Rieppel, O., and deBraga, M. (1996). Turtles as diapsid reptiles. *Nature,* 384(6608), 453–455.

Rieppel, O., and Gronowski, R. W. (1981). The loss of the lower temporal arcade in diapsid reptiles. *Zoological Journal of the Linnean Society,* 72, 203–217.

RStudio Team (2019). RStudio: Integrated Development for R. Boston, MA: RStudio, PBC.

Robinson, P. L. (1973). A problematic reptile from the British Upper Trias. *Journal of the Geological Society,* 129(5), 457–479.

Roček, Z., Boistel, R., Lenoir, N., Mazurier, A., Pierce, S. E., Rage, J.-C., Smirnov, S. V., Schwermann, A. H., Valentin, X., Venczel, M., Wuttke, M., and Zikmund, T. (2015). Frontoparietal bone in extinct Palaeobatrachidae (Anura): its variation and taxonomic value. *The Anatomical Record,* 298(11), 1848–1863.

Romer, A. S. (1927). The pelvic musculature of ornithischian dinosaurs. *Acta Zoologica,* 8(2–3), 225–275.

Romer, A. S. (1946). The primitive reptile *Limnoscelis* restudied. *American Journal of Science,* 244(3), 149–188.

Romer, A. S. (1956). *Osteology of the Reptiles*. Chicago: University of Chicago Press.

Romer, A. S. (1956). A Typical Reptilian Skull Pattern – the Captorhinomorph Skull. In *Osteology of the Reptiles* (pp. 69–73). Malabar: Krieger Publishing Company. (Reprinted from: 1997).

Romer, A. S., and Price, L. I. (1940). Review of the Pelycosauria. *Special Paper – Geological Society of America,* 28, 1–538.

Sawin, H. J. (1941). The cranial anatomy of *Eryops megacephalus*. *Bulletin of the Museum of Comparative Zoology,* 88(5), 407–463.

Schlegel, H. (1850). Description of a new genus of batrachians from Swan River. *Proceedings of the Zoological Society of London,* 18, 9–10.

Schoch, R. R. (2014a). *Amphibian Evolution, the Life of Early Land Vertebrates*. New York: Wiley-Blackwell.

Schoch, R. R. (2014b). Amphibian skull evolution: The developmental and functional context of simplification, bone loss and heterotopy. *Journal of Experimental Zoology (Molecular and Developmental Evolution),* 322(B), 619–630.

Schoch, R. R., and Sues, H.-D. (2015). A Middle Triassic stem-turtle and the evolution of the turtle body plan. *Nature,* 523(7562), 584–587.

Schoch, R. R., and Sues, H.-D. (2017). Osteology of the Middle Triassic stem-turtle *Pappochelys rosinae* and the early evolution of the turtle skeleton. *Journal of Systematic Palaeontology,* 16(11), 927–965.

Schumacher, G. H. (1956). Über die Fascien des Kopfes der Schildkröten nebst einigen Bemerkungen zu der Arbeit von Lakjer, 1926. *Zoologischer Anzeiger,* 156, 35–34.

Schumacher, G. H. (1972). *Die Kopf- und Halsregion der Lederschildkröte Dermochelys coriacea (Linnaeus 1766) - Anatomische Untersuchungen im Vergleich zu anderen rezenten Schildkröten - Mit 7 Figuren im Text und 31 Tafeln*. Berlin: Akademie-Verlag.

Schumacher, G. H. (1973). The Head Muscles and Hyolaryngeal Skeleton of Turtles and Crocodilians. In C. Gans and T. S. Parsons (Eds.), *Biology of the Reptilia.* (Vol. Volume 4. Morphology D, pp. 101–199). London, New York: Academic Press.

Seeley, H. G. (1892). On a new reptile from Welte Vreden (Beaufort West), *Eunotosaurus africanus* (Seeley). *Quarterly Journal of the Geological Society of London,* 48(1–4), 583–585.

Sherratt, E., Gow, C. E., Klingenberg, C. P., and Wilkinson, M. (2014). Evolution of cranial shape in caecilians (Amphibia: Gymnophiona). *Evolutionary Biology,* 41, 528–545.

Sigurdsen, T., and Bolt, J. R. (2010). The lower Permian amphibamid *Doleserpeton* (Temnospondyli: Dissorophoidea), the interrelationships of amphibamids, and the origin of modern amphibians. *Journal of Vertebrate Paleontology,* 30(5), 1360–1377.

Silva, R. R., Ferigolo, J., Bajder, P., and Piñeiro, G. H. (2017). The feeding habits of Mesosauridae. *Frontiers in Earth Science,* 5(23), 1–18.

Smith, H. M., Chiszar, D., and Frey, M. J. (1983). The terminology of amniote temporal vacuities. *Transactions of the Kansas Academy of Science,* 86(1), 48–54.

Smith-Paredes, D., Núñez-León, D., Soto-Acuña, S., O'Connor, J., Botelho, J. F., and Vargas, A. O. (2018). Dinosaur ossification centres in embryonic birds uncover developmental evolution of the skull. *Nature Ecology & Evolution,* 2, 1966–1973.

Smithson, T. R. (1985). The morphology and relationships of the Carboniferous amphibian *Eoherpeton watsoni* Panchen. *Zoological Journal of the Linnean Society,* 85, 317–410.

Sookias, R. B., Dilkes, D. W., Sobral, G., Smith, R. M. H., Wolvaardt, F. P., Arucci, A. B., Bhullar, B.-A., and Werneburg, I. (2020). The craniomandibular anatomy of the early archosauriform *Euparkeria capensis* and the dawn of the archosaur skull. *Royal Society Open Science,* 7, 200116.

Spindler, F., Werneburg, R., Schneider, J. W., Luthardt, L., Annacker, V., and Rößler, R. (2018). First arboreal 'pelycosaurs' (Synapsida: Varanopidae) from the early Permian Chemnitz Fossil Lagerstätte, SE Germany, with a review of varanopid phylogeny. *Paläontologische Zeitschrift,* 92(2), 315–364.

Starck, D. (1995). *5. Teil: Säugetiere. 5/1: Allgemeines, Ordo 1–9*. Jena: Gustav Fischer Verlag.

Strand, E. (1928). Miscellanea nomenclatorica zoologica et palaeontologica: I–II. *Archiv für Naturgeschichte,* 92, 41–68.

Sues, H.-D. (1986). The skull and dentition of two tritylodontid synapsids from the Lower Jurassic of western North America. *Bulletin of the Museum of Comparative Zoology,* 151(4), 217–268.

Sues, H.-D. (1987). On the skull of *Placodus gigas* and the relationships of the Placodontia. *Journal of Vertebrate Paleontology,* 7(2), 138-144.

Sues, H.-D., and Reisz, R. R. (1988). Origins and early evolution of herbivory in tetrapods. *Trends in Ecology & Evolution,* 13(4), 141–145.

Sulej, T. (2005). A new rauisuchian reptile (Diapsida: Archosauria) from the Late Triassic of Poland. *Journal of Vertebrate Paleontology,* 25(1), 78–86.

Sullivan, C., and Reisz, R. R. (2005). Cranial anatomy and taxonomy of the Late Permian dicynodont *Diictodon*. *Annals of Carnegie Museum,* 74(1), 45–75.

Sumida, S. S. (1997). Locomotor features of taxa spanning the origin of amniotes. In S. Sumida and K. L. M. Martin (Eds.), *Amniote Origins - Completing the Transition to Land* (pp. 353–398). San Diego, London: Academic Press.

Sumida, S. S., Lombard, R. E., and Berman, D. S (1992). Morphology of the atlas-axis complex of the late Palaeozoic tetrapod suborders Diadectomorpha and Seymouriamorpha. *Philosophical Transactions of the Royal Society of London. B, Biological Sciences,* 336, 259–273.

Sumida, S. S., and Martin, K. L. M. (1997). *Amniote Origins: Completing the Transition to Land*. San Diego: Academic Press.

Sushkin, P. P. (1928). Contributions to the cranial morphology of *Captorhinus* Cope (Reptilia, Cotylosauria, Captorhinidae). *Palaeobiologica,* 1, 263–280.

Swinton, W. E. (1939). A new Triassic rhynchocephalian from Gloucestershire. *Annals and Magazines of Natural History: Zoology, Botany, and Geology,* 4(24), 591–594.

Tarsitano, S. F. (1983). A case for the diapsid origin of ichthyosaurs. *Neues Jahrbuch für Geologie und Paläontologie - Abhandlungen,* 205(1), 111–127.

Tarsitano, S. F., Oelofsen, B., Frey, E., and Riess, J. (2001). The origin of temporal fenestrae. *South African Journal of Science,* 97(7–8), 334–336.

Tassy, P. (2011). Trees before and after Darwin. *Journal of Zoological Systematics and Evolutionary Research,* 49(2), 89–101.

Thomson, K. S. (1967). Mechanisms of intracranial kinetics in fossil rhipidistian fishes (Crossopterygii) and their relatives. *Zoological Journal of the Linnean Society,* 46(310), 223–253.

Tokita, M., Chaeychomsri, W., and Siruntawineti, J. (2013). Skeletal gene expression in the temporal region of the reptilian embryos: implications for the evolution of reptilian skull morphology. *SpringerPlus,* 2(336), 1–20.

Tsuji, L. A. (2006). Cranial anatomy and phylogenetic affinities of the Permian parareptile *Macroleter poezicus*. *Journal of Vertebrate Paleontology,* 26(4), 849-865.

Tsuji, L. A., and Müller, J. (2009). Assembling the history of the Parareptilia: Phylogeny, diversification, and a new definition of the clade. *Fossil Record,* 12(1), 71–81.

Tsuji, L. A., Müller, J., and Reisz, R. R. (2010). *Microleter mckinzieorum* gen. et sp. nov. from the lower Permian of Oklahoma: The basalmost parareptile from Laurasia. *Journal of Systematic Palaeontology,* 8(2), 245–255.

Tsuji, L. A., Müller, J., and Reisz, R. R. (2012). Anatomy of *Emeroleter levis* and the phylogeny of the nycteroleter parareptiles. *Journal of Vertebrate Paleontology,* 32(1), 45–67.

van den Heuvel, W. F. (1992). Kinetics of the skull in the chicken (*Gallus gallus domesticus*). *Netherlands Journal of Zoology,* 42(4), 561–582.

Versluys, J. (1910). Streptostylie bei Dinosauriern, nebst Bemerkungen über die Verwandtschaft der Vögel und Dinosaurier. *Zoologische Jahrbücher, Abteilung für Anatomie und Ontogenie der Tiere,* 30, 177–260.

Versluys, J. (1912). Das Streptostylie-Problem und die Bewegungen im Schädel der Sauropsiden. *Zoologische Jahrbücher,* 15, 545–702.

Versluys, J. (1919). Über die Phylogenie der Schläfengruben und Jochbogen bei den Reptilia. *Sitzungsberichte der Heidelberger Akademie der Wissenschaften, Stiftung Heinrich Lanz, Mathematisch-naturwissenschaftliche Klasse Abteilung B. Biologische Wissenschaften,* 13, 3–29.

von Huene, F. (1912). Die Cotylosaurier der Trias. *Palaeontographica,* 59(1-2), 69–102.

von Huene, F. (1941). Osteologie und Systematische Stellung von *Mesosaurus*. *Palaeontographica,* 92, 6–58.

von Huene, F. (1954). Die natürliche Art grundlegender Stammesentwicklung der Tetrapoden. *Paläontologische Zeitschrift,* 28(3–4), 178–188.

von Huene, F. (1956). Grundsätzliches zur Stammesgeschichte der Tetrapoden. *Paläontologische Zeitschrift,* 30(1-2), 26–29.

Vorobyeva, E. I. (2007). The morphofunctional approach in paleontology. *Paleontological Journal,* 41(4), 347–359.

Wagler, J. (1830). *Natürliches System der Amphibien: mit vorangehender Classification der Säugethiere und Vögel: ein Beitrag zur vergleichenden Zoologie*. Munich, Stuttgart, Tübingen: J. G. Cotta'sche Buchhandlung.

Wake, M. H., and Donnelly, M. (2012). *Caecilita iwokramae*. *Digital Morphology.* http://digimorph.org/specimens/Caecilita_iwokramae/ (accessed on the 12.07.2022).

Waldman, M., and Evans, S. E. (1994). Lepidosauromorph reptiles from the Middle Jurassic of Skye. *Zoological Journal of the Linnean Society,* 112(1–2), 135–150.

Warren, J. W. (1961). The basicranial articulation of the Early Permian cotylosaur, *Captorhinus*. *Journal of Paleontology,* 35(3), 561–563.

Watson, D. M. S. (1914). *Eunotosaurus africanus* Seeley, and the ancestry of the Chelonia. *Proceedings of the Zoological Society of London,* 84(4), 1011–1020.

Weinbaum, J. C. (2011). The skull of *Postosuchus kirkpatricki* (Archosauria: Paracrocodyliformes) from the Upper Triassic of the United States. *Paleobios,* 30(1). 18–44.

Weishampel, D. B. (1996). Herbivory and reptiles. *Lethaia,* 29(3), 224–224.

Werneburg, I. (2011). The cranial musculature of turtles. *Palaeontologia Electronica,* 14(2), 14.2.15A.

Werneburg, I. (2012). Temporal bone arrangements in turtles: an overview. *Journal of Experimental Zoology Part B: Molecular and Developmental Evolution,* 318(4), 235–249.

Werneburg, I. (2013a). Jaw musculature during the dawn of turtle evolution. *Organisms Diversity & Evolution,* 13(2), 225–254.

Werneburg, I. (2013b). The tendinous framework in the temporal skull region of turtles and considerations about its morphological implications in amniotes: a review. *Zoological Science,* 30(3), 141–153.

Werneburg, I. (2015). Neck motion in turtles and its relation to the shape of the temporal skull region. *Comptes Rendus Palevol,* 14(6–7), 527–548.

Werneburg, I. (2019). Morphofunctional categories and ontogenetic origin of temporal skull openings in amniotes. *Frontiers in Earth Science,* 7(13), 1–7.

Werneburg, I. (2020). Konsequenzen der Panzer-Produktion auf die Radkettenmechanik und deren Wirkung auf terminale Greifarm-Effizienz bei Schildkröten. In I. Werneburg and O. Betz (Eds.), *Phylogenie, Funktionsmorphologie und Bionik. Schriften zum 60. Phylogenetischen Symposium in Tübingen* (pp. 227–316). Tübingen: Scidinge Hall.

Werneburg, I., and Abel, P. (2022). Modeling skull network integrity at the dawn of amniote diversification with considerations on functional morphology and fossil jaw muscle reconstructions. *Frontiers in Ecology and Evolution,* 9, 799637.

Werneburg, I., Esteve-Altava, B., Bruno, J., Torres Ladeira, M., and Diogo, R. (2019). Unique skull network complexity of *Tyrannosaurus rex* among land vertebrates. *Scientific Reports,* 9, 1520.

Werneburg, I., Evers, S. W., and Ferreira, G. S. (2021). On the “cartilaginous rider” in the endocasts of turtle brain cavities. *Vertebrate Zoology,* 71, 403–418.

Werneburg, I., Hinz, J.-K., Gumpenberger, M., Volpato, V., Natchev, N., and Joyce, W. G. (2015a). Modeling neck mobility in fossil turtles. *Journal of Experimental Zoology (Molecular and Developmental Evolution),* 324(B3), 230–243.

Werneburg, I., and Maier, W. (2019). Diverging development of akinetic skulls in cryptodire and pleurodire turtles: an ontogenetic and phylogenetic study. *Vertebrate Zoology,* 69(2), 113–143.

Werneburg, I., Polachowski, K. M., and Hutchinson, M. (2015b). Bony skull development in the Argus monitor (Squamata, Varanidae, *Varanus panoptes*) with comments on developmental timing and adult anatomy. *Zoology,* 118(4), 225–280.

Werneburg, I., Wilson, L. A. B., Parr, W. C. H., and Joyce, W. G. (2015c). Evolution of neck vertebral shape and neck retraction at the transition to modern turtles: an integrated geometric morphometric approach. *Systematic Biology,* 64(2), 187–204.

Werneburg, I., and Yaryhin, O. (2019). Character definition and tempus optimum in comparative chondrocranial research. *Acta Zoologica,* 100(4), 376–388.

Westphal, F. (1962). Die Krokodilier des deutschen und englischen oberen Lias. *Palaeontographica Abteilung A,* 118(1–3), 23–118.

Whiteside, D. I. (1986). The head skeleton of the Rhaetian sphenodontid *Diphydontosaurus avonis* gen. et sp.nov. and the modernizing of a living fossil. *Philosophical Transactions of the Royal Society of London. B, Biological Sciences,* 312(1156), 379–430.

Wible, J. R., Novacek, M. J., and Rougier, G. W. (2004). New data on the skull and dentition in the Mongolian Late Cretaceous eutherian mammal *Zalambdalestes*. *Bulletin of the American Museum of Natural History,* 2004(281), 1–144.

Wied-Neuwied, M. A. P. (1824). Verzeichnis der Amphibien welche in zweiten Bande der Naturgeschichte Brasiliens von Prinz Max von Neuwied werden beschreiben werden. *Isis von Oken,* 14, 661–673.

Wild, E. R. (1997). Description of the adult skeleton and developmental osteology of the hyperossified horned frog, *Ceratophrys cornuta* (Anura: Leptodactylidae). *Journal of Morphology,* 232(2), 169–206.

Wilken, A. T., Middleton, K. M., Sellers, K. C., Cost, I. N., and Holliday, C. M. (2019). The roles of joint tissues and jaw muscles in palatal biomechanics of the savannah monitor (*Varanus exanthematicus*) and their significance for cranial kinesis. *Journal of Experimental Biology,* 222(18), jeb201459.

Williston, S. W. (1904). The temporal arches of the Reptilia. *The Biological Bulletin,* 7(4), 175–192.

Williston, S. W. (1909). New or little known Permian vertebrates. Pariotichus. *The Biological Bulletin,* 17(3), 241–255.

Williston, S. W. (1910). New Permian reptiles: rhachitomous vertebrae. *The Journal of Geology,* 18(7), 585–600.

Williston, S. W. (1911). A new family of reptiles from the Permian of New Mexico. *The American Journal of Science,* 4(185), 378–398.

Williston, S. W. (1912). *American Permian Vertebrates*. Chicago: The University of Chicago Press.

Williston, S. W. (1914). *Water Reptiles of the Past and Present*. Chicago: The University of Chicago Press.

Williston, S. W. (1917). The phylogeny and classification of reptiles. *The Journal of Geology, 25*(5), 411-421.

Williston, S. W. (1925). *The Osteology of the Reptiles* (W. Gregory Ed.). Cambridge: Harvard University Press.

Wittorski, A., Losos, J. B., and Herrel, A. (2016). Proximate determinants of bite force in *Anolis* lizards. *Journal of Anatomy,* 228(1), 85–95.

Witzmann, F., and Schoch, R. R. (2018). Skull and postcranium of the bystrowianid *Bystrowiella schumanni* from the Middle Triassic of Germany, and the position of chroniosuchians within Tetrapoda. *Journal of Systematic Palaeontology,* 16(9), 711–739.

Witzmann, F., and Werneburg, I. (2017). The palatal interpterygoid vacuities of temnospondyls and the implications for the associated eye-and jaw musculature. *The Anatomical Record,* 300(7), 1240–1269.

Woodhead, J., Reisz, R. R., Fox, D., Drysdale, R., Hellstrom, J., Maas, R., Hai, C., and Edwards, R. L. (2010). Speleothem climate records from deep time? Exploring the potential with an example from the Permian. *Geology,* 38(5), 455–458.

Yaryhin, O., and Werneburg, I. (2019). The origin of orbitotemporal diversity in lepidosaurs: insights from tuatara chondrocranial anatomy. *Vertebrate Zoology,* 69(2), 169–181.

Young, M. T., Brusatte, S. L., Ruta, M., and de Andrade, M. B. (2010). The evolution of Metriorhynchoidea (Mesoeucrocodylia, Thalattosuchia): an integrated approach using geometric morphometrics, analysis of disparity, and biomechanics. *Zoological Journal of the Linnean Society,* 158, 801–859.

Young, M. T., Hua, S., Steel, L., Foffa, D., Brusatte, S. L., Thüring, S., Mateus, O., Ruiz-Omeñaca, J. I., Havlik, P., Lepage, Y., and De Andrade, M. B. (2014). Revision of the Late Jurassic teleosaurid genus *Machimosaurus* (Crocodylomorpha, Thalattosuchia). *Royal Society Open Science,* 1(2), 140222.

Zaher, M., Coram, R. A., and Benton, M. J. (2019). The Middle Triassic procolophonid *Kapes bentoni*: computed tomography of the skull and skeleton. *Papers in Palaeontology,* 5(1), 111–138.

Zdansky, O. (1923–1925). Über die Temporalregion des Schildkrötenschädels. *Bulletin of the Geological Instituion of the University of Upsala,* 19, 89–114.

Zepf, F. (2021). *Ontogenetic changes in the skull of the Early Jurassic marine crocodyle* Macrospondylus bollensis *with focus on the temporal region.* (Bachelor). Tübingen.

Zhou, M., Jiang, D.-Y., Motani, R., Tintori, A., Ji, C., Sun, Z.-Y., Ni, P.-G., and Lu, H. (2017). The cranial osteology revealed by three-dimensionally preserved skulls of the Early Triassic ichthyosauriform *Chaohusaurus chaoxianensis* (Reptilia: Ichthyosauromorpha) from Anhui, China. *Journal of Vertebrate Paleontology,* 37(4).

Ziermann, J. M. (2019). Diversity of Heads, Jaws, and Cephalic Muscles in Amphibians. In J. M. Ziermann, R. E. Diaz Jr, and R. Diogo (Eds.), *Heads, Jaws, and Muscles - Anatomical, Functional, and Developmental Diversity in Chordate Evolution* (pp. 143–170): Springer.

Ziermann, J. M., Clement, A. M., Ericsson, R., and Olsson, L. (2018). Cephalic muscle development in the Australian lungfish, *Neoceratodus forsteri*. *Journal of Morphology,* 279, 494–516.

Ziermann, J. M., Diaz Jr, R. E., and Diogo, R. (2019). *Heads, Jaws, and Muscles: Anatomical, Functional, and Developmental Diversity in Chordate Evolution*. Cham: Springer.

Zusi, R. L. (1993). Patterns of Diversity in the Avian Skull. In J. Hanken and B. K. Hall (Eds.), *The Skull. Vol. 2, Patterns of Structural and Systematic Diversity* (pp. 391–437). Chicago: University of Chicago Press.

7. Supplementary

The supplementary contains the following materials:

- **Suppl. Tab. 1**; overview on the preserved articulations of the dermatocranium of OMNH 44816.
- **Suppl. Tab. 2**; suture thickness along the articulations of the dermatocranium in OMNH 44816.
- **Suppl. Tab. 3**; R-script used for Chapter 4.
- **Suppl. Tab. 4**; binary coded matrix of the skull network of *Captorhinus aguti*.
- **Suppl. Tab. 5**; the same as Suppl. Tab. 4. but modified to simulate an infrafenestral skull as in Fig. 31B.
- **Suppl. Tab. 6**; the same as Suppl. Tab. 4. but modified to simulate an infrafenestral skull as in Fig. 31C.
- **Suppl. Tab. 7**; the same as Suppl. Tab. 4. but modified to simulate an infrafossal skull as in Fig. 31D.
- **Suppl. Tab. 8**; the same as Suppl. Tab. 4. but modified to simulate a suprafenestral skull as in Fig. 31E.
- **Suppl. Tab. 9**; the same as Suppl. Tab. 4. but modified to simulate a suprafossal skull as in Fig. 31F.
- **Suppl. Tab. 10**; the same as Suppl. Tab. 4. but modified to simulate a bifenestral skull as in Fig. 31G.
- **Suppl. Tab. 11**; the same as Suppl. Tab. 4. but modified to simulate a bifenestral skull as in Fig. 31H.
- **Suppl. Tab. 12**; the same as Suppl. Tab. 4. but modified to simulate a bifossal skull as in Fig. 31I.
- **Suppl. Tab. 13**; the same as Suppl. Tab. 4. but modified to simulate a fossafenestral skull as in Fig. 31J.
- **Suppl. Tab. 14**; the same as Suppl. Tab. 4. but modified to simulate a fossafenestral skull as in Fig. 31K.

Suppl. Tab. 1. Overview on the preserved articulations in the dermatocranium of OMNH 44816. Colors and numbers refer to the suture types as described in Fig. 24. A digital version can be obtained from Abel et al. (2022*a*; Suppl Tab. 1).

	Dentary_left	Dentary_right	Splenial_left	Splenial_right	Coronoid_left	Coronoid_right	Angular_left	Angular_right	Surangular_left	Surangular_right	Prearticular_left	Prearticular_right	Septomaxilla_left	Maxilla_left	Maxilla_right	Lacrimal_left	Lacrimal_right	Nasal_right	Prefrontal_left	Prefrontal_right	Frontal_left	Frontal_right	Postfrontal_left	Postfrontal_right	Jugal_right	Postorbital_left	Postorbital_right	Squamosal_left	Squamosal_right	Quadratojugal_left	Quadratojugal_right	Parietal_left	Parietal_right	Postparietal_left	Postparietal_right	Vomer_left	Vomer_right	Palatine_left	Palatine_right	Pterygoid_left	Pterygoid_right
Dentary_left	0	1	7	0	7	0	5	0	5	0	1	0	0	0	0	0	0	0	0	0	0	0	0	0	0	0	0	0	0	0	0	0	0	0	0	0	0	0	0	0	0
Dentary_right	1	0	0	7	0	7	0	5	0	5	0	1	0	0	0	0	0	0	0	0	0	0	0	0	0	0	0	0	0	0	0	0	0	0	0	0	0	0	0	0	0
Splenial_left	7	0	0	1	7	0	1	0	0	0	7	0	0	0	0	0	0	0	0	0	0	0	0	0	0	0	0	0	0	0	0	0	0	0	0	0	0	0	0	0	0
Splenial_right	0	7	1	0	0	7	0	1	0	0	0	7	0	0	0	0	0	0	0	0	0	0	0	0	0	0	0	0	0	0	0	0	0	0	0	0	0	0	0	0	0
Coronoid_left	7	0	7	0	0	0	0	0	4	0	1	0	0	0	0	0	0	0	0	0	0	0	0	0	0	0	0	0	0	0	0	0	0	0	0	0	0	0	0	0	0
Coronoid_right	0	7	0	7	0	0	0	0	0	4	0	1	0	0	0	0	0	0	0	0	0	0	0	0	0	0	0	0	0	0	0	0	0	0	0	0	0	0	0	0	0
Angular_left	5	0	1	0	0	0	0	0	7	0	0	0	0	0	0	0	0	0	0	0	0	0	0	0	0	0	0	0	0	0	0	0	0	0	0	0	0	0	0	0	0
Angular_right	0	5	0	1	0	0	0	0	0	7	0	0	0	0	0	0	0	0	0	0	0	0	0	0	0	0	0	0	0	0	0	0	0	0	0	0	0	0	0	0	0
Surangular_left	5	0	0	0	4	0	7	0	0	0	1	0	0	0	0	0	0	0	0	0	0	0	0	0	0	0	0	0	0	0	0	0	0	0	0	0	0	0	0	0	0
Surangular_right	0	5	0	0	0	4	0	7	0	0	0	1	0	0	0	0	0	0	0	0	0	0	0	0	0	0	0	0	0	0	0	0	0	0	0	0	0	0	0	0	0
Prearticular_left	1	0	7	0	1	0	0	0	1	0	0	0	0	0	0	0	0	0	0	0	0	0	0	0	0	0	0	0	0	0	0	0	0	0	0	0	0	0	0	0	0
Prearticular_right	0	1	0	7	0	1	0	0	0	1	0	0	0	0	0	0	0	0	0	0	0	0	0	0	0	0	0	0	0	0	0	0	0	0	0	0	0	0	0	0	0
Septomaxilla_left	0	0	0	0	0	0	0	0	0	0	0	0	0	?	0	7	0	0	0	0	0	0	0	0	0	0	0	0	0	0	0	0	0	0	0	0	0	0	0	0	0
Maxilla_left	0	0	0	0	0	0	0	0	0	0	0	0	?	0	0	2	0	0	0	0	0	0	0	0	0	0	0	0	0	0	0	0	0	0	0	0	0	3	0	0	0
Maxilla_right	0	0	0	0	0	0	0	0	0	0	0	0	0	0	0	0	2	0	0	0	0	0	0	0	7	0	0	0	0	0	0	0	0	0	0	0	0	0	3	0	0
Lacrimal_left	0	0	0	0	0	0	0	0	0	0	0	0	7	2	0	0	0	0	8	0	0	0	0	0	0	0	0	0	0	0	0	0	0	0	0	0	0	3	0	0	0
Lacrimal_right	0	0	0	0	0	0	0	0	0	0	0	0	0	0	2	0	0	8	0	8	0	0	0	0	7	0	0	0	0	0	0	0	0	0	0	0	0	0	3	0	0
Nasal_right	0	0	0	0	0	0	0	0	0	0	0	0	0	0	0	0	8	0	0	8	0	8	0	0	0	0	0	0	0	0	0	0	0	0	0	0	0	0	0	0	0
Prefrontal_left	0	0	0	0	0	0	0	0	0	0	0	0	0	0	0	8	0	0	0	0	1	0	0	0	0	0	0	0	0	0	0	0	0	0	0	0	0	0	0	0	0
Prefrontal_right	0	0	0	0	0	0	0	0	0	0	0	0	0	0	0	0	8	8	0	0	0	1	0	0	0	0	0	0	0	0	0	0	0	0	0	0	0	0	0	0	0
Frontal_left	0	0	0	0	0	0	0	0	0	0	0	0	0	0	0	0	0	0	1	0	0	6	5	0	0	0	0	0	0	0	0	8	0	0	0	0	0	0	0	0	0
Frontal_right	0	0	0	0	0	0	0	0	0	0	0	0	0	0	0	0	0	8	0	1	6	0	0	5	0	0	0	0	0	0	0	0	8	0	0	0	0	0	0	0	0
Postfrontal_left	0	0	0	0	0	0	0	0	0	0	0	0	0	0	0	0	0	0	0	0	5	0	0	0	0	7	0	0	0	0	0	8	0	0	0	0	0	0	0	0	0
Postfrontal_right	0	0	0	0	0	0	0	0	0	0	0	0	0	0	0	0	0	0	0	0	0	5	0	0	0	0	7	0	0	0	0	0	8	0	0	0	0	0	0	0	0
Jugal_right	0	0	0	0	0	0	0	0	0	0	0	0	0	0	7	0	7	0	0	0	0	0	0	0	0	0	7	0	8	0	8	0	0	0	0	0	0	0	0	0	?
Postorbital_left	0	0	0	0	0	0	0	0	0	0	0	0	0	0	0	0	0	0	0	0	0	0	7	0	0	0	0	8	0	0	0	1	0	0	0	0	0	0	0	0	0
Postorbital_right	0	0	0	0	0	0	0	0	0	0	0	0	0	0	0	0	0	0	0	0	0	0	0	7	7	0	0	0	8	0	0	0	1	0	0	0	0	0	0	0	0
Squamosal_left	0	0	0	0	0	0	0	0	0	0	0	0	0	0	0	0	0	0	0	0	0	0	0	0	0	8	0	0	0	7	0	7	0	?	0	0	0	0	0	0	0
Squamosal_right	0	0	0	0	0	0	0	0	0	0	0	0	0	0	0	0	0	0	0	0	0	0	0	0	8	0	8	0	0	0	7	0	7	0	?	0	0	0	0	0	0
Quadratojugal_left	0	0	0	0	0	0	0	0	0	0	0	0	0	0	0	0	0	0	0	0	0	0	0	0	0	0	0	7	0	0	0	0	0	0	0	0	0	0	0	0	0
Quadratojugal_right	0	0	0	0	0	0	0	0	0	0	0	0	0	0	0	0	0	0	0	0	0	0	0	0	8	0	0	0	7	0	0	0	0	0	0	0	0	0	0	0	0
Parietal_left	0	0	0	0	0	0	0	0	0	0	0	0	0	0	0	0	0	0	0	0	8	0	8	0	0	1	0	7	0	0	0	0	1	7	0	0	0	0	0	0	0
Parietal_right	0	0	0	0	0	0	0	0	0	0	0	0	0	0	0	0	0	0	0	0	0	8	0	8	0	0	1	0	7	0	0	1	0	0	7	0	0	0	0	0	0
Postparietal_left	0	0	0	0	0	0	0	0	0	0	0	0	0	0	0	0	0	0	0	0	0	0	0	0	0	0	0	?	0	0	0	7	0	0	1	0	0	0	0	0	0
Postparietal_right	0	0	0	0	0	0	0	0	0	0	0	0	0	0	0	0	0	0	0	0	0	0	0	0	0	0	0	0	?	0	0	0	7	1	0	0	0	0	0	0	0
Vomer_left	0	0	0	0	0	0	0	0	0	0	0	0	0	0	0	0	0	0	0	0	0	0	0	0	0	0	0	0	0	0	0	0	0	0	0	0	1	6	0	1	0
Vomer_right	0	0	0	0	0	0	0	0	0	0	0	0	0	0	0	0	0	0	0	0	0	0	0	0	0	0	0	0	0	0	0	0	0	0	0	1	0	0	6	0	1
Palatine_left	0	0	0	0	0	0	0	0	0	0	0	0	0	3	0	3	0	0	0	0	0	0	0	0	0	0	0	0	0	0	0	0	0	0	0	6	0	0	0	6	0
Palatine_right	0	0	0	0	0	0	0	0	0	0	0	0	0	0	3	0	3	0	0	0	0	0	0	0	0	0	0	0	0	0	0	0	0	0	0	0	6	0	0	0	6
Pterygoid_left	0	0	0	0	0	0	0	0	0	0	0	0	0	0	0	0	0	0	0	0	0	0	0	0	0	0	0	0	0	0	0	0	0	0	0	1	0	6	0	0	1
Pterygoid_right	0	0	0	0	0	0	0	0	0	0	0	0	0	0	0	0	0	0	0	0	0	0	0	0	?	0	0	0	0	0	0	0	0	0	0	0	1	0	6	1	0

Suppl. Tab. 2. Suture thickness along the articulations of the dermatocranium in OMNH 44816. Points of measurement are indicated in Fig. 25. All values are in millimeters. A digital version can be obtained from Abel et al. (2022*a*; Suppl Tab. 2).

Skull region	Suture	Direction of measurement	Point 1	Point 2	Point 3	Point 4	Point 5	Mean
Preorbital region	nasal-nasal	posterior-anterior	0.93	0.92	0.79	0.87	1.02	0.91
	lacrimal-nasal	posterior-anterior	0.78	0.99	1.12	0.92	0.92	0.94
	prefrontal-lacrimal	posterior-anterior	1.14	1.04	0.99	1.02	1.14	1.07
	prefrontal-nasal	posterior-anterior	1.16	1.09	1.09	1.04	1.07	1.09
	lacrimal-jugal	posterior-anterior	1.33	1.30	1.10	1.08	1.00	1.16
	frontal-nasal	medial-lateral	1.00	1.26	1.62	1.50	1.37	1.35
	frontal-prefrontal	posterior-anterior	2.60	1.59	1.35	1.09	1.07	1.54
	frontal-frontal	posterior-anterior	1.93	2.21	1.70	1.44	1.31	1.72
	jugal-maxilla	posterior-anterior	2.27	2.93	2.60	1.61	1.11	2.10
	lacrimal-maxilla	posterior-anterior	1.73	2.40	2.43	2.66	1.88	2.22
Palatal region	palatine-pterygoid	posterior-anterior	0.52	0.76	0.55	0.68	0.55	0.61
	palatine-vomer	posterior-anterior	0.75	0.65	0.68	0.79	0.71	0.72
	palatine-maxilla	posterior-anterior	1.12	1.28	0.87	1.08	0.98	1.06
	vomer-pterygoid	posterior-anterior	1.40	1.66	1.83	2.17	1.56	1.72
	vomer-vomer	posterior-anterior	1.29	1.50	1.87	2.31	2.04	1.80
	palatine-lacrimal	posterior-anterior	0.82	1.25	1.43	3.28	3.55	2.07
	pterygoid-pterygoid	posterior-anterior	2.24	2.32	2.20	2.02	2.12	2.18
Temporal region	jugal-squamosal	medial-lateral	0.46	0.52	0.88	0.71	1.00	0.72
	parietal-parietal	posterior-anterior	0.83	0.88	0.36	0.86	1.34	0.85
	postfrontal-parietal	medial-lateral	1.13	1.07	0.54	0.83	0.91	0.90
	postorbital-parietal	medial-lateral	0.97	1.23	1.44	1.26	1.17	1.21
	quadratojugal-squamosal	posterior-anterior	1.21	1.85	1.28	1.27	0.93	1.31
	postorbital-squamosal	medial-lateral	1.43	1.40	1.45	1.34	1.02	1.33
	parietal-squamosal	posterior-anterior	1.67	1.41	1.35	1.43	1.44	1.46
	jugal-quadratojugal	medial-lateral	1.30	1.52	1.56	1.60	1.35	1.47
	frontal-parietal	medial-lateral	1.63	1.62	1.76	1.49	1.08	1.51
	frontal-postfrontal	posterior-anterior	2.05	1.78	2.03	1.42	1.14	1.68
	postorbital-jugal	posterior-anterior	1.33	1.79	2.10	2.38	2.56	2.03
	postfrontal-postorbital	medial-lateral	1.35	1.87	2.36	3.56	3.35	2.50

Suppl. Tab. 3. R-script used for Chapter 4. To run an R-script, download R from https://cran.r-project.org/bin/.
You may also download RStudio from https://www.rstudio.com/products/rstudio/download/. Instructions below are based on the RStudio interface. A digital version can be obtained from Werneburg & Abel (2022; Suppl Tab. 1).

```
########################################

#To run a command line, select it and press Ctrl+enter or click on the "Run" button in the top right corner.
#Before running the analysis, make sure that the package(s) below are activated ('library'). If you use this R script on another PC, you might have to install the packages first.
#To install packages, run 'install.packages("package name")' here or below in the Console window (if you want to run commands in the console window, you just have to click the enter key)
#Packages have to be installed only once on each PC. The 'library' command below has to be run every time you restart RStudio.

install.packages("igraph") #only mandatory for the first time you use the igraph package on your PC
library(igraph) #this package is needed to perform network analyses

########################################

#######################################
#Import data
#######################################

#this imports an excel file, where the first row and first column are assigned to be names, so only the cells with 0 and 1 are considered for the analysis
#make sure, that your excel table is saved as a CSV file that is separated by semicolons, otherwise it will not work!
#make also sure, that your CSV files are in the same folder as your R script/R project,

sheet.capto <- read.csv("network_sheet.csv", header=T, row.names=1, sep=";")

#This transforms the imported CSV file into an adjacency matrix. This is needed to get the igraph object below

mx.capto <- data.matrix(sheet.capto, rownames.force=T)

#This transforms the matrix into an igraph object. igraph objects are needed to perform a network analysis with the "igraph" package.

net.capto <-graph_from_adjacency_matrix(mx.capto, mode="undirected")

plot(net.capto)  #not mandatory. Just use it to take a preliminary look at your network


#####################################
# First parameters
#####################################

#You can already determine some parameters that are independent of potential modules
#gives you D, number of observed links relative to the possible number of links

edge_density(net.capto, loops=F)

#gives you C, average clustering coefficient

transitivity(net.capto, type="average")
```

```
#gives you K, number of links

sum(degree(net.capto, mode="in"))

#gives you L, average shortest path length

mean_distance(net.capto)

#############################################
#Modules
#############################################

#There are several alogrithms to calculate modules. We're using here a heuristic walk-trap algorithm.
#Use the following line to find modules. "Steps" is the length of random walks to perform.

mod.capto <- cluster_walktrap(net.capto, steps=3)

#Use these two lines together to get the dendrogram. You can change the values in 'mar' (i.e. the
margin) to adjust the format of the plot

par(mar=c(2,7,0.1,7))
plot(as.dendrogram(mod.capto), horiz=T)

#To get a table with the module membership for each bone/muscle, run the following sets of lines

m.capto <- as.data.frame(sort(membership(mod.capto)))
names(m.capto)[names(m.capto) == "sort(membership(mod.capto))"] <- "Membership"
member.capto <- tibble::rownames_to_column(m.capto, "Bones")
View(member.capto)

############################################
#Q parameter
############################################

#Run the "mod.capto" object below
#In the first line of the output, you will find the number of modules ("groups"), and the modularity/Q
parameter ("mod")

mod.capto

#Alternatively, to get only the modularity, you can also use the following version

modularity(mod.capto)

###########################################
#Skull models
###########################################

#Repeat the procedure above for the respective skull models
#infrafenestral 1
sheet.LTF <- read.csv("network_sheet_LTF.csv", header=T, row.names=1, sep=";")
mx.LTF <- data.matrix(sheet.LTF, rownames.force=T)
net.LTF <-graph_from_adjacency_matrix(mx.LTF, mode="undirected")

plot(net.LTF)

edge_density(net.LTF, loops=F)
transitivity(net.LTF, type="average")
sum(degree(net.LTF, mode="in"))
mean_distance(net.LTF)
```

```
mod.LTF <- cluster_walktrap(net.LTF, steps=3)
par(mar=c(2,7,0.1,7))
plot(as.dendrogram(mod.LTF), horiz=T)

mLTF <- as.data.frame(sort(membership(mod.LTF)))
names(mLTF)[names(mLTF) == "sort(membership(mod.LTF))"] <- "Membership"
member.LTF <- tibble::rownames_to_column(mLTF, "Bones")
View(member.LTF)

mod.LTF
modularity(mod.LTF)

#infrafenestral 2
sheet.thera <- read.csv("network_sheet_therapsid.csv", header=T, row.names=1, sep=";")
mx.thera <- data.matrix(sheet.thera, rownames.force=T)
net.thera <-graph_from_adjacency_matrix(mx.thera, mode="undirected")

plot(net.thera)

edge_density(net.thera, loops=F)
transitivity(net.thera, type="average")
sum(degree(net.thera, mode="in"))
mean_distance(net.thera)

mod.thera <- cluster_walktrap(net.thera, steps=3)
par(mar=c(2,7,0.1,7))
plot(as.dendrogram(mod.thera), horiz=T)

m.thera <- as.data.frame(sort(membership(mod.thera)))
names(m.thera)[names(m.thera) == "sort(membership(mod.thera))"] <- "Membership"
member.thera <- tibble::rownames_to_column(m.thera, "Bones")
View(member.thera)

mod.thera
modularity(mod.thera)

#infrafossal
sheet.infra <- read.csv("network_sheet_infrafossal.csv", header=T, row.names=1, sep=";")
mx.infra <- data.matrix(sheet.infra, rownames.force=T)
net.infra <-graph_from_adjacency_matrix(mx.infra, mode="undirected")

plot(net.infra)

edge_density(net.infra, loops=F)
transitivity(net.infra, type="average")
sum(degree(net.infra, mode="in"))
mean_distance(net.infra)

mod.infra <- cluster_walktrap(net.infra, steps=3)
par(mar=c(2,7,0.1,7))
plot(as.dendrogram(mod.infra), horiz=T)

m.infra <- as.data.frame(sort(membership(mod.infra)))
names(m.infra)[names(m.infra) == "sort(membership(mod.infra))"] <- "Membership"
member.infra <- tibble::rownames_to_column(m.infra, "Bones")
View(member.infra)

mod.infra
modularity(mod.infra)

#suprafenestral
```

```
sheet.UTF <- read.csv("network_sheet_UTF.csv", header=T, row.names=1, sep=";")
mx.UTF <- data.matrix(sheet.UTF, rownames.force=T)
net.UTF <-graph_from_adjacency_matrix(mx.UTF, mode="undirected")

plot(net.UTF)

edge_density(net.UTF, loops=F)
transitivity(net.UTF, type="average")
sum(degree(net.UTF, mode="in"))
mean_distance(net.UTF)

mod.UTF <- cluster_walktrap(net.UTF, steps=3)
par(mar=c(2,7,0.1,7))
plot(as.dendrogram(mod.UTF), horiz=T)

m.UTF <- as.data.frame(sort(membership(mod.UTF)))
names(m.UTF)[names(m.UTF) == "sort(membership(mod.UTF))"] <- "Membership"
member.UTF <- tibble::rownames_to_column(m.UTF, "Bones")
View(member.UTF)

mod.UTF
modularity(mod.UTF)

#suprafossal
sheet.supra <- read.csv("network_sheet_suprafossal.csv", header=T, row.names=1, sep=";")
mx.supra <- data.matrix(sheet.supra, rownames.force=T)
net.supra <-graph_from_adjacency_matrix(mx.supra, mode="undirected")

plot(net.supra)

edge_density(net.supra, loops=F)
transitivity(net.supra, type="average")
sum(degree(net.supra, mode="in"))
mean_distance(net.supra)

mod.supra <- cluster_walktrap(net.supra, steps=3)
par(mar=c(2,7,0.1,7))
plot(as.dendrogram(mod.supra), horiz=T)

m.supra <- as.data.frame(sort(membership(mod.supra)))
names(m.supra)[names(m.supra) == "sort(membership(mod.supra))"] <- "Membership"
member.supra <- tibble::rownames_to_column(m.supra, "Bones")
View(member.supra)

mod.supra
modularity(mod.supra)

#bifenestral 1
sheet.dia <- read.csv("network_sheet_diapsid.csv", header=T, row.names=1, sep=";")
mx.dia <- data.matrix(sheet.dia, rownames.force=T)
net.dia <-graph_from_adjacency_matrix(mx.dia, mode="undirected")

plot(net.dia)

edge_density(net.dia, loops=F)
transitivity(net.dia, type="average")
sum(degree(net.dia, mode="in"))
mean_distance(net.dia)

mod.dia <- cluster_walktrap(net.dia, steps=3)
par(mar=c(2,7,0.1,7))
```

```
plot(as.dendrogram(mod.dia), horiz=T)

m.dia <- as.data.frame(sort(membership(mod.dia)))
names(m.dia)[names(m.dia) == "sort(membership(mod.dia))"] <- "Membership"
member.dia <- tibble::rownames_to_column(m.dia, "Bones")
View(member.dia)

mod.dia
modularity(mod.dia)

#bifenestral 2
sheet.neo <- read.csv("network_sheet_neodiapsida1.csv", header=T, row.names=1, sep=";")
mx.neo <- data.matrix(sheet.neo, rownames.force=T)
net.neo <-graph_from_adjacency_matrix(mx.neo, mode="undirected")

plot(net.neo)

edge_density(net.neo, loops=F)
transitivity(net.neo, type="average")
sum(degree(net.neo, mode="in"))
mean_distance(net.neo)

mod.neo <- cluster_walktrap(net.neo, steps=3)
par(mar=c(2,7,0.1,7))
plot(as.dendrogram(mod.neo), horiz=T)

m.neo <- as.data.frame(sort(membership(mod.neo)))
names(m.neo)[names(m.neo) == "sort(membership(mod.neo))"] <- "Membership"
member.neo <- tibble::rownames_to_column(m.neo, "Bones")
View(member.neo)

mod.neo
modularity(mod.neo)

#bifossal
sheet.bi <- read.csv("network_sheet_bifossal.csv", header=T, row.names=1, sep=";")
mx.bi <- data.matrix(sheet.bi, rownames.force=T)
net.bi <-graph_from_adjacency_matrix(mx.bi, mode="undirected")

plot(net.bi)

edge_density(net.bi, loops=F)
transitivity(net.bi, type="average")
sum(degree(net.bi, mode="in"))
mean_distance(net.bi)

mod.bi <- cluster_walktrap(net.bi, steps=3)
par(mar=c(2,7,0.1,7))
plot(as.dendrogram(mod.bi), horiz=T)

m.bi <- as.data.frame(sort(membership(mod.bi)))
names(m.bi)[names(m.bi) == "sort(membership(mod.bi))"] <- "Membership"
member.bi <- tibble::rownames_to_column(m.bi, "Bones")
View(member.bi)

mod.bi
modularity(mod.bi)

#fossafenestral 1
sheet.fo <- read.csv("network_sheet_neodiapsida2.csv", header=T, row.names=1, sep=";")
mx.fo <- data.matrix(sheet.fo, rownames.force=T)
```

```
net.fo <-graph_from_adjacency_matrix(mx.fo, mode="undirected")

plot(net.fo)

edge_density(net.fo, loops=F)
transitivity(net.fo, type="average")
sum(degree(net.fo, mode="in"))
mean_distance(net.fo)

mod.fo <- cluster_walktrap(net.fo, steps=3)
par(mar=c(2,7,0.1,7))
plot(as.dendrogram(mod.fo), horiz=T)

m.fo <- as.data.frame(sort(membership(mod.fo)))
names(m.fo)[names(m.fo) == "sort(membership(mod.fo))"] <- "Membership"
member.fo <- tibble::rownames_to_column(m.fo, "Bones")
View(member.fo)

mod.fo
modularity(mod.fo)

#fossafenestral 2
sheet.kata <- read.csv("network_sheet_kata.csv", header=T, row.names=1, sep=";")
mx.kata <- data.matrix(sheet.kata, rownames.force=T)
net.kata <-graph_from_adjacency_matrix(mx.kata, mode="undirected")

plot(net.kata)

edge_density(net.kata, loops=F)
transitivity(net.kata, type="average")
sum(degree(net.kata, mode="in"))
mean_distance(net.kata)

mod.kata <- cluster_walktrap(net.kata, steps=3)
par(mar=c(2,7,0.1,7))
plot(as.dendrogram(mod.kata), horiz=T)

m.kata <- as.data.frame(sort(membership(mod.kata)))
names(m.kata)[names(m.kata) == "sort(membership(mod.kata))"] <- "Membership"
member.kata <- tibble::rownames_to_column(m.kata, "Bones")
View(member.kata)

mod.kata
modularity(mod.kata)
```

Suppl. Tab. 4. Binary coded matrix of the skull network of *Captorhinus aguti*, see also Tab. 3. A CSV file with labeled lines and columns can be obtained from Werneburg & Abel (2022; Data sheet 2\network_sheet).

```
00100001000000000000000000000000000000000000000000001000000001000
00010000100000000000000000000000000000000000000000000100000000100
10000000000000000000000000000000000000100000000010000000000001000
01000000000000000000000000000000000000010000000001000000000000100
00000000000110000000000110010000000000000000000000000000111000000
00000001000000000000000000000000000000100000000000001000000001000
00000000100000000000000000000000000000010000000000000100000000100
10000100100000000000000000000000000000100000000000001000000001000
01000011000000000000000000000000000000010000000000000100000000100
00000000000000000000000000010000000000000000100000000000000000000
00000000000000000000000000010000000000000000010000000000000000000
00001000000000000000000100000000000000000000000000000000001000000
00001000000000000000000010000000000000000000000000000000001000000
00000000000000100000010000001010000000100000000000000000000000000
00000000000001000000001000000101000000010000000000000000000000000
00000000000000000101000000000000100000000000100010000010000000000
00000000000000000010100000000000000000000000010001000001000000000
00000000000000010001010001000000000000100000000000100000000000000
00000000000000001000101000100000000000010000000000010000000000000
00000000000000010100000000010000000000001000000000100000000000000
00000000000000001010000000001000000000000100000000010000000000000
00000000000001000100001000000000000000001010000000001000000000000
00000000000000100010010000000000000000000101000000000100000000000
00001000000100000000000000000000000000000010000000000000101010000000
```

```
00000000000000001000000000000101000000000000000000000001000000000
00000000000000000000000000001000000100000000000000000010001100000
00000000000000000000000000000100001000000000000000000000100101000
00100101000000000000000000000000000000000000000000001000000001000
00010010100000000000000000000000000000000000000000000100000000100
00000000000001000100010000000000000000000000000000000000000000000
00000000000000100010001000000000000000000000000000000000000000000
00000000000000000001010000000000000000000100000000000000000000010
00000000000000000000101000000000000000001000000000000000000000001
00000000000000000000000100010000000000000000000000000000101000000
00000000000000000000000010010000000000000000000000000000011000000
00000000010000010000000001000000000000000000011000000000100000010
00000000001000001000000000100000000000000000100100000000010000001
00100000000000000000000000000000000000000000100010000010100000000
00010000000000000000000000000000000000000000010001000001010000000
00000000000000010000000000000000000000000000001000000010000000000
00000000000000001000000000000000000000000000000100000001000000000
00000000000000000101010000000000000000000000000000000000000000000
00000000000000000010101000000000000000000000000000000000000000000
10000101000000000000000000000000000010000000000000000100000000000
01000010100000000000000000000000000001000000000000001000000000000
00000000000000010000000100001000101000000000001010000000000100000
00000000000000001000000010000100010100000000000101000000000010000
00001000000000000000000100010000000000101010000000000000000010000000
00001000000000000000000010010000000000000001010100000000000100000000
00001000000110000000000110001100001100000011000000000000011000000
00000000000000000000000000001000001000000000000000000010000000000
00000000000000000000000000000100000100000000000000000001000000000
10100101000000000000000000000000000010000000000000000000000000000
01010010100000000000000000000000000001000000000000000000000000000
00000000000000000000000001000000000000001000100000000000000000001
00000000000000000000000000100000000000000100010000000000000000010
```

Suppl. Tab. 5. Binary coded matrix of the skull network of *Captorhinus aguti*, modified to simulate an infrafenestral skull as in Fig. 31B. A CSV file with labeled lines and columns can be obtained from Werneburg & Abel (2022; Data sheet 2\network_sheet_LTF).

01101010101000000000000000000000000000000000000000000000000000000

10010101010100000000000000000000000000000000000000000000000000000

10011010001000000000000000000000000000000000000000000000000000000

01100101000100000000000000000000000000000000000000000000000000000

10100000101000000000000000000000000000000000000000000000000000000

01010000010100000000000000000000000000000000000000000000000000000

10100000100010000000000000000000000000000000000000000000000000000

01010000010001000000000000000000000000000000000000000000000000000

10001010001010000000000000000000000000000000000000000000000000000

01000101000101000000000000000000000000000000000000000000000000000

10101000100010000000000000000000000000000000000000000000000000000

01010100010001000000000000000000000000000000000000000000000000000

00000010101000000000000000000000000000000000000000000000000000010

00000001010100000000000000000000000000000000000000000000000000001

00000000000000000010101000000000000000000000000000000000000000000

00000000000000000001010100000000000000000000000000000000000000000

00000000000000000110001000000000000000000000100000000000000000000

00000000000000001001000100000000000000000000010000000000000000000

00000000000000101000100000000010000000000000001000000000000000000

00000000000000010100010000000001000000000000000100000000000000000

00000000000000100010001010000010000000000000001000000000000000000

00000000000000010001000101000001000000000000000100000000000000000

00000000000000101000100110100000000000000000000000000000000000000

00000000000000010100011001010000000000000000000000000000000000000

00000000000000000000101000100000000000000000000000000000000000000

00000000000000000000010100010000000000000000000000000000000000000

00000000000000000000001010011000000000100000000000000000000000000

00000000000000000000000101100100000000010000000000000000000000000

00000000000000000000000000100000100000010000000000000000000000000

00000000000000000000000000010000010000001000000000000000000000000

00000000000000000010100000000000100010000000000010000000000000000

00000000000000000001010000000000000001000000000001000000000000000

00000000000000000000000000001010001000100000000000000000000000000

```
00000000000000000000000000000101000100010000000000000000000000000
00000000000000000000000000000000100010101010000000000000000100010
00000000000000000000000000000000010001010101000000000000000010001
00000000000000000000000000000010001000000000000000000000000000010
00000000000000000000000000000001000100000000000000000000000000001
00000000000000000000000000101000101000011010000000000100000000000
00000000000000000000000000010100010100100101000000000100000000000
00000000000000000000000000000000001000100010000000000000000000000
00000000000000000000000000000000000100010001000000000000000000000
00000000000000000000000000000000001000101001000000000100000000000
00000000000000000000000000000000000100010110000000000100000000000
00000000000000001000000000000000000000000000011010000000000000000
00000000000000000100000000000000000000000000100101000000000000000
00000000000000000010100000000000000000000000100010000000000000000
00000000000000000001010000000000000000000000010001000000000000000
00000000000000000000000000000010000000000000101001100000010000010
00000000000000000000000000000001000000000000010110010000001000001
00000000000000000000000000000000000000000000000010001000000000000
00000000000000000000000000000000000000000000000001001000000000000
00000000000000000000000000000000000000000000000000110010011001100
00000000000000000000000000000000000000110011000000000011111111100
00000000000000000000000000000000000000000000000000001101111110000
00000000000000000000000000000000000000000000000000000110000100000
00000000000000000000000000000000000000000000000000000110000010000
00000000000000000000000000000000000000000000000010001110000101010
00000000000000000000000000000000000000000000000001001110000010101
00000000000000000000000000000000001000000000000000000111010001000
00000000000000000000000000000000000100000000000000000110101000100
00000000000000000000000000000000000000000000000000001100010100000
00000000000000000000000000000000000000000000000000001100001010000
00000000000010000000000000000000001010000000000001000000010000000
00000000000001000000000000000000000101000000000000100000001000000
```

Suppl. Tab. 6. Binary coded matrix of the skull network of *Captorhinus aguti*, modified to simulate an infrafenestral skull as in Fig. 31C. A CSV file with labeled lines and columns can be obtained from Werneburg & Abel (2022; Data sheet 2\network_sheet_therapsid).

```
01101010101000000000000000000000000000000000000000000000000000000
10010101010100000000000000000000000000000000000000000000000000000
10011010001000000000000000000000000000000000000000000000000000000
01100101000100000000000000000000000000000000000000000000000000000
10100000101000000000000000000000000000000000000000000000000000000
01010000010100000000000000000000000000000000000000000000000000000
10100000100010000000000000000000000000000000000000000000000000000
01010000010001000000000000000000000000000000000000000000000000000
10001010001010000000000000000000000000000000000000000000000000000
01000101000101000000000000000000000000000000000000000000000000000
10101000100010000000000000000000000000000000000000000000000000000
01010100010001000000000000000000000000000000000000000000000000000
00000010101000000000000000000000000000000000000000000000000000010
00000001010100000000000000000000000000000000000000000000000000001
00000000000000000010101000000000000000000000000000000000000000000
00000000000000000001010100000000000000000000000000000000000000000
00000000000000000110001000000000000000000000100000000000000000000
00000000000000001001000100000000000000000000010000000000000000000
00000000000000101000100000000010000000000000001000000000000000000
00000000000000010100010000000001000000000000000100000000000000000
00000000000000100010001010000010000000000000001000000000000000000
00000000000000010001000101000001000000000000000100000000000000000
00000000000000101000100110100000000000000000000000000000000000000
00000000000000010100011001010000000000000000000000000000000000000
00000000000000000000101000100000000000000000000000000000000000000
00000000000000000000010100010000000000000000000000000000000000000
00000000000000000000001010011000000000100000000000000000000000000
00000000000000000000000101100100000000010000000000000000000000000
00000000000000000000000000100000100000100000000000000000000000000
00000000000000000000000000010000010000010000000000000000000000000
00000000000000000010100000000000101000000000000010000000000000000
00000000000000000001010000000000000100000000000001000000000000000
00000000000000000000000000001010000000100000000000000000000000000
```

```
00000000000000000000000000000101000000010000000000000000000000000
00000000000000000000000000000010000010101010000000000000000100010
00000000000000000000000000000001000001010101000000000000000010001
00000000000000000000000000000000001000000000000000000000000000010
00000000000000000000000000000000000100000000000000000000000000001
00000000000000000000000000101000101000011010000000000100000000000
00000000000000000000000000010100010100100101000000000100000000000
00000000000000000000000000000000001000100010000000000000000000000
00000000000000000000000000000000000100010001000000000000000000000
00000000000000000000000000000000001000101001000000000100000000000
00000000000000000000000000000000000100010110000000000100000000000
00000000000000001000000000000000000000000000001101000000000000000
00000000000000000100000000000000000000000000100101000000000000000
00000000000000000010100000000000000000000000010001000000000000000
00000000000000000001010000000000000000000000001000100000000000000
00000000000000000000000000000010000000000000101001100000010000010
00000000000000000000000000000001000000000000010110010000001000001
00000000000000000000000000000000000000000000000010001000000000000
00000000000000000000000000000000000000000000000001001000000000000
00000000000000000000000000000000000000000000000000110010011001100
00000000000000000000000000000000000000110011000000000001111111100
00000000000000000000000000000000000000000000000000001101111110000
00000000000000000000000000000000000000000000000000000110000100000
00000000000000000000000000000000000000000000000000000110000010000
00000000000000000000000000000000000000000000000010001110000101010
00000000000000000000000000000000000000000000000001001110000010101
00000000000000000000000000000000001000000000000000000111010001000
00000000000000000000000000000000000100000000000000000110101000100
00000000000000000000000000000000000000000000000000001100010100000
00000000000000000000000000000000000000000000000000001100001010000
00000000000010000000000000000000001010000000000010000000010000000
00000000000001000000000000000000000101000000000001000000001000000
```

Suppl. Tab. 7. Binary coded matrix of the skull network of *Captorhinus aguti*, modified to simulate an infrafossal skull as in Fig. 31D. A CSV file with labeled lines and columns can be obtained from Werneburg & Abel (2022; Data sheet 2\network_sheet_infrafossal).

01101010101000000000000000000000000000000000000000000000000000000

10010101010100000000000000000000000000000000000000000000000000000

10011010001000000000000000000000000000000000000000000000000000000

01100101000100000000000000000000000000000000000000000000000000000

10100000101000000000000000000000000000000000000000000000000000000

01010000010100000000000000000000000000000000000000000000000000000

10100000100010000000000000000000000000000000000000000000000000000

01010000010001000000000000000000000000000000000000000000000000000

10001010001010000000000000000000000000000000000000000000000000000

01000101000101000000000000000000000000000000000000000000000000000

10101000100010000000000000000000000000000000000000000000000000000

01010100010001000000000000000000000000000000000000000000000000000

00000010101000000000000000000000000000000000000000000000000000010

00000001010100000000000000000000000000000000000000000000000000001

00000000000000000010101000000000000000000000000000000000000000000

00000000000000000001010100000000000000000000000000000000000000000

00000000000000000110001000000000000000000000100000000000000000000

00000000000000001001000100000000000000000000010000000000000000000

00000000000000101000100000000010000000000000001000000000000000000

00000000000000010100010000000001000000000000000100000000000000000

00000000000000100010001010000010000000000000001000000000000000000

00000000000000010001000101000001000000000000000100000000000000000

00000000000000101000100110100000000000000000000000000000000000000

00000000000000010100011001010000000000000000000000000000000000000

00000000000000000000101000100000000000000000000000000000000000000

00000000000000000000010100010000000000000000000000000000000000000

00000000000000000000001010011000000000100000000000000000000000000

00000000000000000000000101100100000000010000000000000000000000000

00000000000000000000000000100000100000100000000000000000000000000

00000000000000000000000000010000010000010000000000000000000000000

00000000000000000010100000000000100000000000000010000000000000000

00000000000000000001010000000000000000000000000001000000000000000

00000000000000000000000000001010001000100000000000000000000000000

00000000000000000000000000000101000100010000000000000000000000000

00000000000000000000000000000000100010101010000000000000000100010

00000000000000000000000000000000010001010101000000000000000010001

00000000000000000000000000000000001000000000000000000000000000010

00000000000000000000000000000000000100000000000000000000000000001

00000000000000000000000000101000101000011010000000000100000000000

00000000000000000000000000010100010100100101000000000100000000000

00000000000000000000000000000000001000100010000000000000000000000

00000000000000000000000000000000000100010001000000000000000000000

00000000000000000000000000000000001000101001000000000100000000000

00000000000000000000000000000000000100010110000000000100000000000

00000000000000001000000000000000000000000000011010000000000000000

00000000000000000100000000000000000000000000100101000000000000000

00000000000000000010100000000000000000000000100010000000000000000

00000000000000000001010000000000000000000000010001000000000000000

00000000000000000000000000000010000000000000010100110000001000010

00000000000000000000000000000001000000000000010110010000001000001

00000000000000000000000000000000000000000000000010001000000000000

00000000000000000000000000000000000000000000000001001000000000000

00000000000000000000000000000000000000000000000000110010011001100

00000000000000000000000000000000000000110011000000000011111111100

00000000000000000000000000000000000000000000000000001101111110000

00000000000000000000000000000000000000000000000000000110000100000

00000000000000000000000000000000000000000000000000000110000010000

00000000000000000000000000000000000000000000000010001110000101010

00000000000000000000000000000000000000000000000001001110000010101

00000000000000000000000000000000001000000000000000000111010001000

00000000000000000000000000000000000100000000000000000110101000100

00000000000000000000000000000000000000000000000000001100010100000

00000000000000000000000000000000000000000000000000001100001010000

00000000000010000000000000000000001010000000000001000000000100000

00000000000001000000000000000000000101000000000000100000000010000

Suppl. Tab. 8. Binary coded matrix of the skull network of *Captorhinus aguti*, modified to simulate a suprafenestral skull as in Fig. 31E. A CSV file with labeled lines and columns can be obtained from Werneburg & Abel (2022; Data sheet 2\network_sheet_UTF).

```
01101010101000000000000000000000000000000000000000000000000000000
10010101010100000000000000000000000000000000000000000000000000000
10011010001000000000000000000000000000000000000000000000000000000
01100101000100000000000000000000000000000000000000000000000000000
10100000101000000000000000000000000000000000000000000000000000000
01010000010100000000000000000000000000000000000000000000000000000
10100000100010000000000000000000000000000000000000000000000000000
01010000010001000000000000000000000000000000000000000000000000000
10001010001010000000000000000000000000000000000000000000000000000
01000101000101000000000000000000000000000000000000000000000000000
10101000100010000000000000000000000000000000000000000000000000000
01010100010001000000000000000000000000000000000000000000000000000
00000010101000000000000000000000000000000000000000000000000000010
00000001010100000000000000000000000000000000000000000000000000001
00000000000000000010101000000000000000000000000000000000000000000
00000000000000000001010100000000000000000000000000000000000000000
00000000000000000110001000000000000000000000100000000000000000000
00000000000000001001000100000000000000000000010000000000000000000
00000000000000101000100000000010000000000000001000000000000000000
00000000000000010100010000000001000000000000000100000000000000000
00000000000000100010001010000010000000000000001000000000000000000
00000000000000010001000101000001000000000000000100000000000000000
00000000000000101000100110100000000000000000000000000000000000000
00000000000000010100011001010000000000000000000000000000000000000
00000000000000000000101000100000000000000000000000000000000000000
00000000000000000000010100010000000000000000000000000000000000000
00000000000000000000001010011000000000100000000000000000000000000
00000000000000000000000101100100000000010000000000000000000000000
00000000000000000000000000100000100000100000000000000000000000000
00000000000000000000000000010000010000010000000000000000000000000
00000000000000000010100000000000101010000000000010000000000000000
00000000000000000001010000000000000001000000000001000000000000000
00000000000000000000000000001010001000000000000000000000000000000
```

```
00000000000000000000000000000101000100000000000000000000000000000
00000000000000000000000000000010100010101010000000000000000100010
00000000000000000000000000000001010001010101000000000000000010001
00000000000000000000000000000010001000000000000000000000000000010
00000000000000000000000000000001000100000000000000000000000000001
00000000000000000000000000101000001000011010000000000100000000000
00000000000000000000000000010100000100100101000000000100000000000
00000000000000000000000000000000001000100010000000000000000000000
00000000000000000000000000000000000100010001000000000000000000000
00000000000000000000000000000000001000101001000000000100000000000
00000000000000000000000000000000001000101100000000000100000000000
00000000000000001000000000000000000000000000001101000000000000000
00000000000000000100000000000000000000000000100101000000000000000
00000000000000000010100000000000000000000000100010000000000000000
00000000000000000001010000000000000000000000010001000000000000000
00000000000000000000000000000010000000000000101001100000010000010
00000000000000000000000000000001000000000000010110010000001000001
00000000000000000000000000000000000000000000000010001000000000000
00000000000000000000000000000000000000000000000001001000000000000
00000000000000000000000000000000000000000000000000110010011001100
00000000000000000000000000000000000000110011000000000011111111100
00000000000000000000000000000000000000000000000000001101111110000
00000000000000000000000000000000000000000000000000000110000100000
00000000000000000000000000000000000000000000000000000110000010000
00000000000000000000000000000000000000000000000010001110000101010
00000000000000000000000000000000000000000000000001001110000010101
00000000000000000000000000000000001000000000000000000111010001000
00000000000000000000000000000000000100000000000000000110101000100
00000000000000000000000000000000000000000000000000001100010100000
00000000000000000000000000000000000000000000000000001100001010000
00000000000010000000000000000000001010000000000010000000010000000
00000000000001000000000000000000000101000000000001000000001000000
```

Suppl. Tab. 9. Binary coded matrix of the skull network of *Captorhinus aguti*, modified to simulate a suprafossal skull as in Fig. 31F. A CSV file with labeled lines and columns can be obtained from Werneburg & Abel (2022; Data sheet 2\network_sheet_suprafossal).

```
01101010101000000000000000000000000000000000000000000000000000000
10010101010100000000000000000000000000000000000000000000000000000
10011010001000000000000000000000000000000000000000000000000000000
01100101000100000000000000000000000000000000000000000000000000000
10100000101000000000000000000000000000000000000000000000000000000
01010000010100000000000000000000000000000000000000000000000000000
10100000100010000000000000000000000000000000000000000000000000000
01010000010001000000000000000000000000000000000000000000000000000
10001010001010000000000000000000000000000000000000000000000000000
01000101000101000000000000000000000000000000000000000000000000000
10101000100010000000000000000000000000000000000000000000000000000
01010100010001000000000000000000000000000000000000000000000000000
00000010101000000000000000000000000000000000000000000000000000010
00000001010100000000000000000000000000000000000000000000000000001
00000000000000000010101000000000000000000000000000000000000000000
00000000000000000001010100000000000000000000000000000000000000000
00000000000000000110001000000000000000000000100000000000000000000
00000000000000001001000100000000000000000000010000000000000000000
00000000000000101000100000000010000000000000001000000000000000000
00000000000000010100010000000001000000000000000100000000000000000
00000000000000100010001010000010000000000000001000000000000000000
00000000000000010001000101000001000000000000000100000000000000000
00000000000000101000100110100000000000000000000000000000000000000
00000000000000010100011001010000000000000000000000000000000000000
00000000000000000000101000100000000000000000000000000000000000000
00000000000000000000010100010000000000000000000000000000000000000
00000000000000000000001010011000000000100000000000000000000000000
00000000000000000000000101100100000000010000000000000000000000000
00000000000000000000000000100000100000100000000000000000000000000
00000000000000000000000000010000010000010000000000000000000000000
00000000000000000010100000000000101010000000000010000000000000000
00000000000000000001010000000000000101000000000001000000000000000
00000000000000000000000000001010001000100000000000000000000000000
```

```
00000000000000000000000000000101000100010000000000000000000000000
00000000000000000000000000000010100010001010000000000000000100010
00000000000000000000000000000001010001000101000000000000000010001
00000000000000000000000000000010001000000000000000000000000000010
00000000000000000000000000000001000100000000000000000000000000001
00000000000000000000000000101000100000010010000000000100000000000
00000000000000000000000000010100010000100001000000000010000000000
00000000000000000000000000000000001000000010000000000000000000000
00000000000000000000000000000000000100000001000000000000000000000
00000000000000000000000000000000001000101001000000000010000000000
00000000000000000000000000000000000100010110000000000010000000000
00000000000000001000000000000000000000000000011010000000000000000
00000000000000000100000000000000000000000000100101000000000000000
00000000000000000010100000000000000000000000100010000000000000000
00000000000000000001010000000000000000000000010001000000000000000
00000000000000000000000000000010000000000000010100110000001000010
00000000000000000000000000000001000000000000010110010000001000001
00000000000000000000000000000000000000000000000010001000000000000
00000000000000000000000000000000000000000000000001001000000000000
00000000000000000000000000000000000000000000000000110010011001100
00000000000000000000000000000000000000110011000000000011111111100
00000000000000000000000000000000000000000000000000001101111110000
00000000000000000000000000000000000000000000000000000110000100000
00000000000000000000000000000000000000000000000000000110000010000
00000000000000000000000000000000000000000000000010001110000101010
00000000000000000000000000000000000000000000000001001110000010101
00000000000000000000000000000000001000000000000000000111010001000
00000000000000000000000000000000000100000000000000000110101000100
00000000000000000000000000000000000000000000000000001100010100000
00000000000000000000000000000000000000000000000000001100001010000
00000000000010000000000000000000001010000000000010000000010000000
00000000000001000000000000000000000101000000000001000000000100000
```

Suppl. Tab. 10. Binary coded matrix of the skull network of *Captorhinus aguti*, modified to simulate a bifenestral skull as in Fig. 31G. A CSV file with labeled lines and columns can be obtained from Werneburg & Abel (2022; Data sheet 2\network_sheet_diapsid).

01101010101000000000000000000000000000000000000000000000000000000

10010101010100000000000000000000000000000000000000000000000000000

10011010001000000000000000000000000000000000000000000000000000000

01100101000100000000000000000000000000000000000000000000000000000

10100000101000000000000000000000000000000000000000000000000000000

01010000010100000000000000000000000000000000000000000000000000000

10100000100010000000000000000000000000000000000000000000000000000

01010000010001000000000000000000000000000000000000000000000000000

10001010001010000000000000000000000000000000000000000000000000000

01000101000101000000000000000000000000000000000000000000000000000

10101000100010000000000000000000000000000000000000000000000000000

01010100010001000000000000000000000000000000000000000000000000000

00000010101000000000000000000000000000000000000000000000000000010

00000001010100000000000000000000000000000000000000000000000000001

00000000000000000010101000000000000000000000000000000000000000000

00000000000000000001010100000000000000000000000000000000000000000

00000000000000000110001000000000000000000000100000000000000000000

00000000000000001001000100000000000000000000010000000000000000000

00000000000000101000100000000010000000000000001000000000000000000

00000000000000010100010000000001000000000000000100000000000000000

00000000000000100010001010000010000000000000001000000000000000000

00000000000000010001000101000001000000000000000100000000000000000

00000000000000101000100110100000000000000000000000000000000000000

00000000000000010100011001010000000000000000000000000000000000000

00000000000000000000101000100000000000000000000000000000000000000

00000000000000000000010100010000000000000000000000000000000000000

00000000000000000000001010011000000000100000000000000000000000000

00000000000000000000000101100100000000010000000000000000000000000

00000000000000000000000000100000100000100000000000000000000000000

00000000000000000000000000010000010000010000000000000000000000000

00000000000000000010100000000000100010000000000000100000000000000

00000000000000000001010000000000000001000000000000010000000000000

00000000000000000000000000001010001000000000000000000000000000000

```
00000000000000000000000000000101000100000000000000000000000000000
00000000000000000000000000000000100010101010000000000000000100010
00000000000000000000000000000000010001010101000000000000000010001
00000000000000000000000000000010001000000000000000000000000000010
00000000000000000000000000000001000100000000000000000000000000001
00000000000000000000000000101000001000011010000000000100000000000
00000000000000000000000000010100000100100101000000000100000000000
00000000000000000000000000000000001000100010000000000000000000000
00000000000000000000000000000000000100010001000000000000000000000
00000000000000000000000000000000001000101001000000000100000000000
00000000000000000000000000000000000100010110000000000100000000000
00000000000000001000000000000000000000000000011010000000000000000
00000000000000000100000000000000000000000000100101000000000000000
00000000000000000010100000000000000000000000100010000000000000000
00000000000000000001010000000000000000000000010001000000000000000
00000000000000000000000000000010000000000000101001100000010000010
00000000000000000000000000000001000000000000010110010000001000001
00000000000000000000000000000000000000000000000010001000000000000
00000000000000000000000000000000000000000000000001001000000000000
00000000000000000000000000000000000000000000000000110010011001100
00000000000000000000000000000000000000110011000000000011111111100
00000000000000000000000000000000000000000000000000001101111110000
00000000000000000000000000000000000000000000000000000110000100000
00000000000000000000000000000000000000000000000000000110000010000
00000000000000000000000000000000000000000000000010001110000101010
00000000000000000000000000000000000000000000000001001110000010101
00000000000000000000000000000000001000000000000000000111010001000
00000000000000000000000000000000000100000000000000000110101000100
00000000000000000000000000000000000000000000000000001100010100000
00000000000000000000000000000000000000000000000000001100001010000
00000000000010000000000000000000001010000000000010000000001000000
00000000000001000000000000000000000101000000000001000000000100000
```

Suppl. Tab. 11. Binary coded matrix of the skull network of *Captorhinus aguti*, modified to simulate a bifenestral skull as in Fig. 31H. A CSV file with labeled lines and columns can be obtained from Werneburg & Abel (2022; Data sheet 2\network_sheet_neodiapsida1).

```
01101010101000000000000000000000000000000000000000000000000000

10010101010100000000000000000000000000000000000000000000000000

10011010001000000000000000000000000000000000000000000000000000

01100101000100000000000000000000000000000000000000000000000000

10100000101000000000000000000000000000000000000000000000000000

01010000010100000000000000000000000000000000000000000000000000

10100000100010000000000000000000000000000000000000000000000000

01010000010001000000000000000000000000000000000000000000000000

10001010001010000000000000000000000000000000000000000000000000

01000101000101000000000000000000000000000000000000000000000000

10101000100010000000000000000000000000000000000000000000000000

01010100010001000000000000000000000000000000000000000000000000

00000010101000000000000000000000000000000000000000000000000010

00000001010100000000000000000000000000000000000000000000000001

00000000000000000010101000000000000000000000000000000000000000

00000000000000000001010100000000000000000000000000000000000000

00000000000000000110001000000000000000000001000000000000000000

00000000000000001001000100000000000000000000100000000000000000

00000000000000101000100000000010000000000000010000000000000000

00000000000000010100010000000001000000000000001000000000000000

00000000000000100010001010000010000000000000010000000000000000

00000000000000010001000101000001000000000000001000000000000000

00000000000000101000100110100000000000000000000000000000000000

00000000000000010100011001010000000000000000000000000000000000

00000000000000000000101000100000000000000000000000000000000000

00000000000000000000010100010000000000000000000000000000000000

00000000000000000000001010011000000001000000000000000000000000

00000000000000000000000101100100000000100000000000000000000000

00000000000000000000000000100000100000000000000000000000000000

00000000000000000000000000010000010000000000000000000000000000

00000000000000000010100000000000100010000000000100000000000000

00000000000000000001010000000000000000010000000000100000000000

00000000000000000000000000001010001000000000000000000000000000
```

```
00000000000000000000000000000101000100000000000000000000000000000
00000000000000000000000000000000100010101010000000000000000100010
00000000000000000000000000000000010001010101000000000000000010001
00000000000000000000000000000010001000000000000000000000000000010
00000000000000000000000000000001000100000000000000000000000000001
00000000000000000000000000100000001000011010000000000100000000000
00000000000000000000000000010000000100100101000000000100000000000
00000000000000000000000000000000001000100010000000000000000000000
00000000000000000000000000000000000100010001000000000000000000000
00000000000000000000000000000000001000101001000000000100000000000
00000000000000000000000000000000000100010110000000000100000000000
00000000000000001000000000000000000000000000011010000000000000000
00000000000000000100000000000000000000000000100101000000000000000
00000000000000000010100000000000000000000000100010000000000000000
00000000000000000001010000000000000000000000010001000000000000000
00000000000000000000000000000010000000000000101001100000010000010
00000000000000000000000000000001000000000000010110010000001000001
00000000000000000000000000000000000000000000000010001000000000000
00000000000000000000000000000000000000000000000001001000000000000
00000000000000000000000000000000000000000000000000110010011001100
00000000000000000000000000000000000011001100000000000111111111100
00000000000000000000000000000000000000000000000000001101111110000
00000000000000000000000000000000000000000000000000000110000100000
00000000000000000000000000000000000000000000000000000110000010000
00000000000000000000000000000000000000000000000010001110000101010
00000000000000000000000000000000000000000000000001001110000010101
00000000000000000000000000000000001000000000000000000111010001000
00000000000000000000000000000000000100000000000000000110101000100
00000000000000000000000000000000000000000000000000001100010100000
00000000000000000000000000000000000000000000000000001100001010000
00000000000010000000000000000000001010000000000010000000010000000
00000000000001000000000000000000000101000000000001000000001000000
```

Suppl. Tab. 12. Binary coded matrix of the skull network of *Captorhinus aguti*, modified to simulate a bifossal skull as in Fig. 31I. A CSV file with labeled lines and columns can be obtained from Werneburg & Abel (2022; Data sheet 2\network_sheet_bifossal).

0110101010100000000000000000000000000000000000000000000000000000

1001010101010000000000000000000000000000000000000000000000000000

1001101000100000000000000000000000000000000000000000000000000000

0110010100010000000000000000000000000000000000000000000000000000

1010000010100000000000000000000000000000000000000000000000000000

0101000001010000000000000000000000000000000000000000000000000000

1010000010001000000000000000000000000000000000000000000000000000

0101000001000100000000000000000000000000000000000000000000000000

1000101000101000000000000000000000000000000000000000000000000000

0100010100010100000000000000000000000000000000000000000000000000

1010100010001000000000000000000000000000000000000000000000000000

0101010001000100000000000000000000000000000000000000000000000000

0000001010100000000000000000000000000000000000000000000000000010

0000000101010000000000000000000000000000000000000000000000000001

0000000000000000001010100000000000000000000000000000000000000000

0000000000000000000101010000000000000000000000000000000000000000

0000000000000000011000100000000000000000000010000000000000000000

0000000000000000100100010000000000000000000001000000000000000000

0000000000000010100010000000001000000000000000100000000000000000

0000000000000001010001000000000100000000000000010000000000000000

0000000000000010001000101000001000000000000000100000000000000000

0000000000000001000100010100000100000000000000010000000000000000

0000000000000010100010011010000000000000000000000000000000000000

0000000000000001010001100101000000000000000000000000000000000000

0000000000000000000010100010000000000000000000000000000000000000

0000000000000000000001010001000000000000000000000000000000000000

0000000000000000000000101001100000000010000000000000000000000000

0000000000000000000000010110010000000001000000000000000000000000

0000000000000000000000000010000010000010000000000000000000000000

0000000000000000000000000001000001000001000000000000000000000000

0000000000000000001010000000000010000000000000100000000000000000

0000000000000000000101000000000000000000000000010000000000000000

0000000000000000000000000000101000100010000000000000000000000000

0000000000000000000000000000101000100010000000000000000000000000

0000000000000000000000000000000100010001010000000000000000100010

0000000000000000000000000000000010001000101000000000000000010001

0000000000000000000000000000000001000000000000000000000000000010

0000000000000000000000000000000000100000000000000000000000000001

0000000000000000000000000101000100000010010000000000100000000000

0000000000000000000000000010100010000100001000000000100000000000

0000000000000000000000000000000001000000010000000000000000000000

0000000000000000000000000000000000100000001000000000000000000000

0000000000000000000000000000000001000101001000000000100000000000

0000000000000000000000000000000001000101100000000000100000000000

0000000000000001000000000000000000000000000011010000000000000000

0000000000000000100000000000000000000000000100101000000000000000

0000000000000000010100000000000000000000000100010000000000000000

0000000000000000001010000000000000000000000010001000000000000000

0000000000000000000000000000010000000000000101001100000010000010

0000000000000000000000000000001000000000000010110010000001000001

0000000000000000000000000000000000000000000000010001000000000000

0000000000000000000000000000000000000000000000001001000000000000

0000000000000000000000000000000000000000000000000110010011001100

0000000000000000000000000000000000000110011000000000001111111100

0000000000000000000000000000000000000000000000000001101111110000

0000000000000000000000000000000000000000000000000000110000100000

0000000000000000000000000000000000000000000000000000110000010000

0000000000000000000000000000000000000000000000010001110000101010

0000000000000000000000000000000000000000000000001001110000010101

0000000000000000000000000000000001000000000000000000111010001000

0000000000000000000000000000000000100000000000000000110101000100

0000000000000000000000000000000000000000000000000001100010100000

0000000000000000000000000000000000000000000000000001100001010000

0000000000001000000000000000000000101000000000001000000001000000

0000000000000100000000000000000000010100000000000100000000100000

Suppl. Tab. 13. Binary coded matrix of the skull network of *Captorhinus aguti*, modified to simulate a fossafenestral skull as in Fig. 31J. A CSV file with labeled lines and columns can be obtained from Werneburg & Abel (2022; Data sheet 2\network_sheet_kata).

```
01101010101000000000000000000000000000000000000000000000000000000
10010101010100000000000000000000000000000000000000000000000000000
10011010001000000000000000000000000000000000000000000000000000000
01100101000100000000000000000000000000000000000000000000000000000
10100000101000000000000000000000000000000000000000000000000000000
01010000010100000000000000000000000000000000000000000000000000000
10100000100010000000000000000000000000000000000000000000000000000
01010000010001000000000000000000000000000000000000000000000000000
10001010001010000000000000000000000000000000000000000000000000000
01000101000101000000000000000000000000000000000000000000000000000
10101000100010000000000000000000000000000000000000000000000000000
01010100010001000000000000000000000000000000000000000000000000000
00000010101000000000000000000000000000000000000000000000000000010
00000001010100000000000000000000000000000000000000000000000000001
00000000000000000010101000000000000000000000000000000000000000000
00000000000000000001010100000000000000000000000000000000000000000
00000000000000000110001000000000000000000000100000000000000000000
00000000000000001001000100000000000000000000010000000000000000000
00000000000000101000100000000010000000000000001000000000000000000
00000000000000010100010000000001000000000000000100000000000000000
00000000000000100010001010000010000000000000001000000000000000000
00000000000000010001000101000001000000000000000100000000000000000
00000000000000101000100110100000000000000000000000000000000000000
00000000000000010100011001010000000000000000000000000000000000000
00000000000000000000101000100000000000000000000000000000000000000
00000000000000000000010100010000000000000000000000000000000000000
00000000000000000000001010011000000000100000000000000000000000000
00000000000000000000000101100100000000010000000000000000000000000
00000000000000000000000000100000100000000000000000000000000000000
00000000000000000000000000010000010000000000000000000000000000000
00000000000000000010100000000000100000000000000010000000000000000
00000000000000000001010000000000000000000000000001000000000000000
00000000000000000000000000001010001000000000000000000000000000000
```

```
0000000000000000000000000000101000100000000000000000000000000000
0000000000000000000000000000000100010101010000000000000000100010
0000000000000000000000000000000010001010101000000000000000010001
0000000000000000000000000000000001000000000000000000000000000010
0000000000000000000000000000000000100000000000000000000000000001
0000000000000000000000000100000001000011010000000000100000000000
0000000000000000000000000010000000100100101000000000100000000000
0000000000000000000000000000000000000100010000000000000000000000
0000000000000000000000000000000000000010001000000000000000000000
0000000000000000000000000000000001000101001000000000100000000000
0000000000000000000000000000000000100010110000000000100000000000
0000000000000000100000000000000000000000000011010000000000000000
0000000000000000010000000000000000000000000100101000000000000000
0000000000000000001010000000000000000000000100010000000000000000
0000000000000000000101000000000000000000000010001000000000000000
0000000000000000000000000000100000000000000101001100000010000010
0000000000000000000000000000010000000000000010110010000001000001
0000000000000000000000000000000000000000000000010001000000000000
0000000000000000000000000000000000000000000000001001000000000000
0000000000000000000000000000000000000000000000000110010011001100
0000000000000000000000000000000000000110011000000000011111111100
0000000000000000000000000000000000000000000000000001101111110000
0000000000000000000000000000000000000000000000000000110000100000
0000000000000000000000000000000000000000000000000000110000010000
0000000000000000000000000000000000000000000000010001110000101010
0000000000000000000000000000000000000000000000001001110000010101
0000000000000000000000000000000001000000000000000000111010001000
0000000000000000000000000000000000100000000000000000110101000100
0000000000000000000000000000000000000000000000000001100010100000
0000000000000000000000000000000000000000000000000001100001010000
0000000000001000000000000000000000101000000000001000000001000000
0000000000000100000000000000000000010100000000000100000000100000
```

Suppl. Tab. 14. Binary coded matrix of the skull network of *Captorhinus aguti*, modified to simulate a fossafenestral skull as in Fig. 31K. A CSV file with labeled lines and columns can be obtained from Werneburg & Abel (2022; Data sheet 2\network_sheet_neodiapsida2).

```
01101010101000000000000000000000000000000000000000000000000000000
10010101010100000000000000000000000000000000000000000000000000000
10011010001000000000000000000000000000000000000000000000000000000
01100101000100000000000000000000000000000000000000000000000000000
10100000101000000000000000000000000000000000000000000000000000000
01010000010100000000000000000000000000000000000000000000000000000
10100000100010000000000000000000000000000000000000000000000000000
01010000010001000000000000000000000000000000000000000000000000000
10001010001010000000000000000000000000000000000000000000000000000
01000101000101000000000000000000000000000000000000000000000000000
10101000100010000000000000000000000000000000000000000000000000000
01010100010001000000000000000000000000000000000000000000000000000
00000010101000000000000000000000000000000000000000000000000000010
00000001010100000000000000000000000000000000000000000000000000001
00000000000000000010101000000000000000000000000000000000000000000
00000000000000000001010100000000000000000000000000000000000000000
00000000000000000110001000000000000000000000100000000000000000000
00000000000000001001000100000000000000000000010000000000000000000
00000000000000101000100000000000100000000000001000000000000000000
00000000000000010100010000000000010000000000000100000000000000000
00000000000000100010001010000000100000000000001000000000000000000
00000000000000010001000101000000010000000000000100000000000000000
00000000000000101000100110100000000000000000000000000000000000000
00000000000000010100011001010000000000000000000000000000000000000
00000000000000000000101000100000000000000000000000000000000000000
00000000000000000000010100010000000000000000000000000000000000000
00000000000000000000001010011000000000100000000000000000000000000
00000000000000000000000101100100000000010000000000000000000000000
00000000000000000000000000100000100000100000000000000000000000000
00000000000000000000000000010000010000010000000000000000000000000
00000000000000000010100000000000100000000000000010000000000000000
00000000000000000001010000000000000000000000000001000000000000000
00000000000000000000000000001010001000000000000000000000000000000
```

```
0000000000000000000000000001010001000000000000000000000000000000
0000000000000000000000000000000100010101010000000000000000100010
0000000000000000000000000000000010001010101000000000000000010001
0000000000000000000000000000000001000000000000000000000000000010
0000000000000000000000000000000000100000000000000000000000000001
0000000000000000000000000101000001000011010000000000100000000000
0000000000000000000000000010100000100100101000000000100000000000
0000000000000000000000000000000001000100010000000000000000000000
0000000000000000000000000000000000100010001000000000000000000000
0000000000000000000000000000000001000101001000000000100000000000
0000000000000000000000000000000000100010110000000000100000000000
0000000000000000100000000000000000000000000011010000000000000000
0000000000000000010000000000000000000000000100101000000000000000
0000000000000000001010000000000000000000000100010000000000000000
0000000000000000000101000000000000000000000010001000000000000000
0000000000000000000000000000010000000000000101001100000010000010
0000000000000000000000000000001000000000000010110010000001000001
0000000000000000000000000000000000000000000000010001000000000000
0000000000000000000000000000000000000000000000001001000000000000
0000000000000000000000000000000000000000000000000110010011001100
0000000000000000000000000000000000000110011000000000011111111100
0000000000000000000000000000000000000000000000000001101111110000
0000000000000000000000000000000000000000000000000000110000100000
0000000000000000000000000000000000000000000000000000110000010000
0000000000000000000000000000000000000000000000010001110000101010
0000000000000000000000000000000000000000000000001001110000010101
0000000000000000000000000000000001000000000000000000111010001000
0000000000000000000000000000000000100000000000000000110101000100
0000000000000000000000000000000000000000000000000001100010100000
0000000000000000000000000000000000000000000000000001100001010000
0000000000001000000000000000000001010000000000010000000010000000
0000000000000100000000000000000000101000000000001000000001000000
```

Pascal Abel, M.Sc.

Born 3rd April 1994 in Gunzenhausen. He obtained his B.Sc. degree in Geoscience at the University of Erlangen-Nuremberg in 2016, where he described an Upper Jurassic marine crocodile from Bavaria under the supervision of Prof. Dr. Wolfgang Kiessling. He received his M.Sc. degree at the same institute in 2019. He was supervised by Prof. Dr. Manuel Steinbauer and Prof. Dr. Kenneth De Baets for an analysis of macroecological patterns in Paleozoic ammonoids.

List of publications:

- **Abel, P.** (2016). Taxonomic analysis of an Upper Jurassic marine reptile from the northern Franconian Alb (Bavaria, Germany). *87th Annual Meeting of the Paläontologische Gesellschaft*.
- **Abel, P.** (2021). 1907: *Tylosaurus* – der Leviathan aus Kansas, in: Aus der Tiefenzeit – Die Paläontologische Sammlung der Universität Tübingen (eds. Seidl, E., Bierende, E., and Werneburg, I.). Tübingen: Museum der Universität Tübingen MUT, 358–365.
- **Abel, P.** (2021). Vor 1955: *Macrospondylus bollensis* – Puzzle eines Meereskrokodils, in: Aus der Tiefenzeit – Die Paläontologische Sammlung der Universität Tübingen (eds. Seidl, E., Bierende, E., and Werneburg, I.). Tübingen: Museum der Universität Tübingen MUT, 456–467.
- **Abel, P.**, Blanco, M.V.F., Johnson, M.M., Zepf, F., Bona, P., and Werneburg, I. (2023). The temporal region of the first aquatic crocodylomorphs and a comparison with extant crocodylians. *International Congress of Vertebrate Morphology (ICVM)*.
- **Abel, P.**, De Baets, K., and Steinbauer, M. (2018). Macroecological patterns in Paleozoic ammonoids. *GeoBonn 2018 Living Earth Abstracts*, 230.
- **Abel, P.**, De Baets, K., Korn, D., and Steinbauer, M. (2019). Macroecological patterns in the extinct cephalopod subclass Ammonoidea. *macro 2019 – Bridging local patterns and global challenges*, 57.
- **Abel, P.**, Hornung, J.J., Kear, B.P., and Sachs, S. (2019). Reassesment of the enigmatic pterosaur "*Ornithocheirus*" *wiedenrothi* from the Lower Cretaceous of Northern Germany. *International Congress of Vertebrate Morphology (ICVM) Abstract Issue 2019. Journal of Morphology*, Supplement 280, S73–S74.
- **Abel, P.**, Hornung, J.J., Kear, B.P., and Sachs, S. (2019). A possible anhangueran pterosaur mandible from the Lower Cretaceous of Germany. *Program and abstracts. XVII Conference of the EAVP – Brussels, Belgium 2–6 July 2019*, 7.
- **Abel, P.**, Hornung, J.J., Kear, B.P., and Sachs, S. (2021). An anhanguerian pterodactyloid mandible from the lower Valanginian of Northern Germany, and the German record of Cretaceous pterosaurs. *Acta Palaeontologica Polonica* 66(3), S5–S12.
- **Abel, P.**, Koyabu, D., and Werneburg, I. (2019). Evolution of the temporal region in the early amniote skull. *Paleo & Life Abstracts of the 90th Annual Meeting of the Paläontologische Gesellschaft, Munich 2019*, 7.
- **Abel, P.**, and Pommery, Y. (2023). Fragmentary remains of a metriorhynchid crocodylomorph from the middle Oxfordian of France — the oldest known rhacheosaurin? *4th Palaeontological Virtual Congress*, 248.
- **Abel, P.**, Pommery, Y., Ford, D.P., Koyabu, D., and Werneburg, I. (2021). Sutures and skull mechanics in the 'anapsid' *Captorhinus aguti* – what are their implications for early amniote evolution?. *XVIII Conference of the European Association of Vertebrate Palaeontologists*, 19.
- **Abel, P.**, Pommery, Y., Ford, D.P., Koyabu, D., and Werneburg, I. (2022). Skull sutures and cranial mechanics in the Permian reptile *Captorhinus aguti* and the evolution of the temporal region in early amniotes. *Frontiers in Ecology and Evolution* 10, 841784.

- **Abel, P.**, Pommery, Y., Ford, D.P., Koyabu, D., and Werneburg, I. (2022). 3D models related to the publication: Skull sutures and cranial mechanics in the Permian reptile *Captorhinus aguti* and the evolution of the temporal region in early amniotes. *MorphoMuseuM* 8(167), 2 pp.
- **Abel, P.**, Sachs, S., and Young, M.T. (2018). Thalattosuchian remains from the late Aalenian Eisensandstein Formation of Baden-Württemberg, southwestern Germany. *GeoBonn 2018 Living Earth Abstracts*, 223.
- **Abel, P.**, Sachs, S., and Young, M.T. (2020). Metriorhynchid crocodylomorphs from the lower Kimmeridgian of Southern Germany: evidence for a new large-bodied geosaurin lineage in Europe. *Alcheringa: An Australasian Journal of Palaeontology* 44(2), 312–326.
- **Abel, P.**, Sachs, S., and Young, M.T. (2021). Das Drügendorfer Krokodil: ein fränkischer Riese mit europaweiter Verwandtschaft. *fossilien – Erdgeschichte erleben* 38(5), 24–31.
- **Abel, P.**, and Werneburg, I. (2021). Morphology of the temporal skull region in tetrapods: research history, functional explanations, and a new comprehensive classification scheme. Biological Reviews 96, 2229–2257.
- **Abel, P.**, and Werneburg, I. (2024). The temporal region of the tetrapod skull: a textbook example on integrative morphology. *Revue de Paléobiologie*.
- Blanco, M.V.F., **Abel, P.**, Johnson, M.M., Zepf, F., Bona, P., and Werneburg, I. (2023). The temporal region of the first aquatic crocodylomorphs and a comparison with extant crocodylians. ICVM 2023.
- Sachs, S., **Abel, P.**, and Madzia, D. (2023). A 'long-forgotten' plesiosaur provides evidence of large-bodied rhomaleosaurids in the Middle Jurassic of Germany. *Journal of Vertebrate Paleontology* 42(5), e2205456.
- Sachs, S., **Abel, P.**, and Madzia, D. (2023). Unusual plesiosaur vertebrae from the Lower Jurassic Posidonia Shale of Germany. *Historical Biology*.
- Sachs, S., Johnson, M.M., Young, M.T., and **Abel, P.** (2019). The mystery of *Mystriosaurus*: redescribing the poorly known Early Jurassic teleosauroid thalattosuchians *Mystriosaurus laurillardi* and *Steneosaurus brevior*. *Acta Palaeontologica Polonica* 64(3), 565–579.
- Sachs, S., Young, M.T., **Abel, P.**, and Mallison, H. (2019). A new species of the metriorhynchid crocodylomorph *Cricosaurus* from the Upper Jurassic of southern Germany. *Acta Palaeontologica Polonica* 64(2), 343–356.
- Sachs, S., Young, M.T., **Abel, P.**, and Mallison, H. (2021). A new species of *Cricosaurus* (Thalattosuchia, Metriorhynchidae) based upon a remarkably well-preserved skeleton from the Upper Jurassic of Germany. *Palaeontologia Electronica* 24(2), a24.
- Werneburg, I., and **Abel, P.** (2022). Modelling skull network integrity at the dawn of amniote diversification with considerations on functional morphology and fossil jaw muscle reconstructions. *Frontiers in Ecology and Evolution* 9, 799637.
- Young, M.T., Sachs, S., and **Abel, P.** (2018). Fossil Focus: Thalattosuchia. *Palaeontology Online* 8(5), 1–13.
- Young, M.T., Sachs, S., and **Abel, P.** (2018). Einblicke in die Evolution der Thalattosuchier – Meereskrokodile des Mesozoikums. *fossilien – Erdgeschichte erleben* 2018(3), 16–23.
- Young, M.T., Sachs, S., **Abel, P.**, Foffa, D., Herrera, Y., and Kitson, J.J.N. (2020). Convergent evolution and possible constraint in the posterodorsal retraction of the external nares in pelagic crocodylomorphs. *Zoological Journal of the Linnean Society* 189(29), 494–520.

- Young, M.T., Wilberg, E.W., Johnson, M.M., Herrera, Y., De Andrade, M.B., Brignon, A., Sachs, S., **Abel, P.**, Foffa, D., Fernández, M., Vignaud, P., Cowgill, T., and Brusatte, S. (in press). The history, systematics, and nomenclature of Thalattosuchia (Archosauria: Crocodylomorpha). *Zoological Journal of the Linnean Society*.